A Methodology to Link Cost and Reliability for Launch Vehicle Design

A Thesis
Presented to
The Academic Faculty

by

Zachary C. Krevor

In Partial Fulfillment
of the Requirements for the Degree
Doctor of Philosophy

School of Aerospace Engineering
Georgia Institute of Technology
August 2007

A Methodology to Link Cost and Reliability for Launch Vehicle Design

Approved by:

Dr. Alan Wilhite, Advisor
National Institute of Aerospace
Georgia Institute of Technology

Dr. Robert Braun
School of Aerospace Engineering
Georgia Institute of Technology

Dr. Daniel Schrage
School of Aerospace Engineering
Georgia Institute of Technology

Dr. Trina Chytka
Vehicle Analysis Branch
Langley Research Center
National Aeronautics and Space Administration

Dr. Vitali Volovoi
School of Aerospace Engineering
Georgia Institute of Technology

Date Approved: August 2007

ACKNOWLEDGEMENTS

There are a number of people who have helped me throughout my academic career. First, I would like to thank my advisor and chairman Dr. Alan Wilhite for supporting a student he had never met prior to becoming his advisor. I would also like to thank Dr. Wilhite for his guidance and the effort he put forth in making this dissertation possible. Dr. Wilhite has provided many wonderful opportunities to grow and learn within the aerospace industry and I thank him for those occasions. I would like to thank Dr. Robert Braun for his advice and insight during our time together at Georgia Tech. I would also like to thank the remaining members of my committee, Dr. Daniel Schrage, Dr. Vitali Volovoi, and Dr. Trina Chytka, for their support and patience over the past two years. I would like to thank Dr. Dimitri Mavris and Dr. John Olds for accepting me into their respective graduate laboratories.

I would also like to thank my friends and fellow students in the Space Systems Design Laboratory. I thank them for their help and I have enjoyed my time with them in Atlanta and at the Georgia Institute of Technology.

I would like to thank my family and friends back in California. I would like to thank my parents for pushing my brothers' and I to achieve academic excellence. I would also like to thank my grandparents, both paternal and maternal, for providing a standard in life that I hope to reach. I would also like to thank my extended family and friends for their continued support and encouragement.

Finally, I would like to thank my wife Leilani. I was able to finish my academic career because of her constant encouragement, support, cajoling, and love. I thank her for always being there for me and I only hope I can provide the same support for her. I am looking forward to the next step in our lives sweetheart!

TABLE OF CONTENTS

ACKNOWLEDGEMENTS . . . . . **iii**

LIST OF TABLES . . . . . **viii**

LIST OF FIGURES . . . . . **xi**

LIST OF SYMBOLS OR ABBREVIATIONS . . . . . **xv**

SUMMARY . . . . . **xviii**

I INTRODUCTION **1**

1.1 Thesis Goals and Objectives 1

1.2 Motivation 3

1.3 Methodology Outline 6

1.4 Summary 12

II BACKGROUND **13**

2.1 Systems Engineering 13

2.1.1 Design Phases 18

2.2 Historical Launch Vehicle Design 20

2.2.1 Saturn V 20

2.2.2 Space Transportation System 23

2.2.3 Cargo Launch Vehicle 26

2.2.4 Apollo and ESAS Comparison 29

2.2.5 Methodology Utility 32

2.3 Launch Vehicle Design Literature 34

2.3.1 Integrated Launch Vehicle Design 36

2.4 Related Aerospace System Studies 44

2.5 Alternate Design Approaches to Couple Cost and Reliability 47

2.6 Summary of Techniques 50

2.7 Research Questions 51

III METHODOLOGY 53

3.1 Performance Disciplines 53

3.1.1 Launch Vehicle Description 54

3.1.2 Mission Constraints 55

3.1.3 Mass Estimates 55

3.1.4 Propulsion 56

3.1.5 Trajectory Analysis 57

3.1.6 Performance Parameters 58

3.1.7 Completing the Sizing Process 64

3.1.8 Integrating the Performance Disciplines 67

3.2 Present Method for Evaluating Launch Vehicle Performance 70

3.3 Reliability Modeling 73

3.3.1 Reliability Breakdown Structure 76

3.3.2 Calculating Component and Subsystem Reliability 78

3.3.3 Reliability Analysis Techniques 80

3.3.4 Reliability Growth Modeling 95

3.3.5 Techniques for Improving System Reliability 96

3.4 Present Method for Calculating System Reliability 102

3.4.1 Engine Modeling 103

3.4.2 Redundant Subsystems 111

3.4.3 Uncertainty Analysis 112

3.4.4 System Reliability Calculation 114

3.4.5 Reliability Growth Model 118

3.4.6 Reliability Summary 120

3.5 Cost Analysis 121

3.5.1 Cost Calculation Techniques 123

3.5.2 Calculating Cost for Space Applications 125

3.6 Current Cost Estimation 126

3.6.1 Cost and Redundancy 130

3.6.2 Uncertainty Analysis . . . 131
3.6.3 Summary of Cost Estimation . . . 132
3.7 Optimization . . . 133
3.7.1 Genetic Algorithm . . . 136
3.7.2 Optimization Application . . . 138
3.8 Integrated Model . . . 139
3.8.1 Design Process . . . 139
3.9 Research Hypotheses . . . 144
3.10 Methodology Enhancements . . . 145
3.10.1 Additional Metrics . . . 146
3.10.2 Operations Costs . . . 148
3.10.3 Methodology Limitations . . . 148
IV RESULTS . . . 151
4.1 Saturn V . . . 152
4.1.1 Model Validation . . . 155
4.1.2 RSE Validation . . . 158
4.1.3 Saturn V Results . . . 159
4.1.4 Optimal Configurations . . . 161
4.1.5 Reliability Results . . . 164
4.1.6 Cost Results . . . 166
4.1.7 Additional Results . . . 170
4.1.8 Results Summary . . . 172
4.1.9 Optimal Design Point Validation . . . 173
4.1.10 Saturn V Reliability Growth . . . 174
4.2 Cargo Launch Vehicle . . . 177
4.2.1 CaLV Model Validation . . . 179
4.2.2 CaLV RSE Validation . . . 181
4.2.3 CaLV Results . . . 182

4.2.4 CaLV Optimal Configurations 184
4.2.5 CaLV Reliability Results 187
4.2.6 CaLV Cost Results 189
4.2.7 CaLV Additional Results 194
4.2.8 CaLV Results Summary 195
4.2.9 CaLV Optimal Design Point Validation 196
4.2.10 CaLV Reliability Growth 197

V CONCLUSION AND FUTURE WORK 200

5.1 Conclusion 200
5.2 Future Work 205

APPENDIX A — S-IC SUBSYSTEM RELIABILITY AND RELIABILITY UNCERTAINTY RANGES 209

APPENDIX B — RELIABILITY MODEL VALIDATION 211

APPENDIX C — RELIABILITY TECHNIQUE COMPARISON 213

APPENDIX D — RELIABILITY GROWTH DATA 216

APPENDIX E — VEHICLE WBS 217

APPENDIX F — RSE VALIDATION 219

APPENDIX G — COST TABLES 224

APPENDIX H — MASS TABLES 226

APPENDIX I — TRAJECTORY AND ENGINE DATA 228

APPENDIX J — DEVELOPMENT COST PROFILES 233

REFERENCES 238

VITA 245

LIST OF TABLES

3-1 S-II Reliability Comparison. 58

3-2 Saturn V Mass Sensitivity. 63

3-3 DOE Run Comparison. 69

3-4 90% Confidence Interval Comparison of MFBF. 100

3-5 Confidence Level for Saturn V Reliability Estimate. 101

3-6 S-II Engine Out Model Unreliability Comparison. 110

3-7 S-II GNC Redundancy Comparison. 112

3-8 S-II Subsystem Reliability Estimates. 116

3-9 S-IVB Subsystem Reliability Estimates. 116

3-10 CaLV Baseline Reliability Estimates. 117

3-11 Growth Rate Parameter. 118

3-12 Development Cost Comparison. 128

3-13 Full Subsystem Redundancy Notional Cost Comparison. 130

3-14 Generic Launch Vehicle Design Variables. 140

4-1 Saturn V Design Variables. 153

4-2 Reliability Validation for Component Redundancy. 155

4-3 Dry Mass Comparison for Saturn V Stages[lb]. 156

4-4 Gross Mass Comparison for Saturn V Stages[lb]. 156

4-5 Design Variable Settings for the Saturn V Pareto Frontier. 163

4-6 Design 3 Reliability Importance. 164

4-7 Design 3 Stage Engine Out Comparison. 165

4-8 Minimum Cost Comparison. 166

4-9 Engine Cost Comparison for Minimum Cost Configurations [$M FY '04]. 167

4-10 Peak Funding Comparison. 170

4-11 β Sensitivity Study. 172

4-12 Optimal Design Validation. 174

4-13 Saturn V Reliability Growth Configurations. 175

4-14 CaLV Design Variables. 177
4-15 CaLV Mass Comparison Between ESAS and Young [lb]. 179
4-16 Design Variable Settings for the CaLV Pareto Frontier. 186
4-17 CaLV Design 2 Reliability Trade Study. 188
4-18 CaLV Minimum Cost Comparison. 189
4-19 Engine Cost Comparison for CaLV Minimum Cost Configurations [$M FY '04]. 191
4-20 CaLV Peak Funding Comparison. 193
4-21 CaLV β Sensitivity Study. 195
4-22 CaLV Design Nine Validation. 197
4-23 CaLV Reliability Growth Configurations. 197
A-1 S-IC Subsystem Reliability Estimates. 209
A-2 Saturn V MCS Reliability Ranges. 209
A-3 CaLV MCS Reliability Ranges. 210
C-1 Analysis Comparison for 5 Engine Configuration with Engine Out (E.O.).214
E-1 Saturn V WBS. 217
E-2 CaLV WBS. 218
F-1 Saturn V SIC Mass Ratio RSE Data. 219
F-2 Saturn V SIC Burn Time RSE Data. 219
F-3 Saturn V SII Mass Ratio RSE Data. 219
F-4 Saturn V SII Burn Time RSE Data. 220
F-5 Saturn V SIVB Mass Ratio RSE Data. 220
F-6 Saturn V SIVB Burn Time RSE Data. 220
F-7 Saturn V T/W_{eng} RSE Validation. 221
F-8 Saturn V Mass Ratio & Burn Time RSE Validation. 221
F-9 CaLV Booster Mass Ratio RSE Data. 221
F-10 CaLV Booster Burn Time RSE Data. 222
F-11 CaLV EDS Mass Ratio RSE Data. 222
F-12 CaLV EDS Burn Time RSE Data. 222

F-13 CaLV T/W_{eng} RSE Validation. 222
F-14 CaLV Mass Ratio & Burn Time RSE Validation. 223
G-1 Saturn V Design Configuration Cost Comparison [$M FY '04]. 224
G-2 CaLV SRB Assumption. 225
G-3 CaLV Design Configuration Cost Comparison [$M FY '04]. 225
H-1 Saturn V Design Mass Comparison. 226
H-2 CaLV Design Mass Comparison. 227
I-1 Saturn V POST Assumptions. 228
I-2 CaLV POST Assumptions. 228
I-3 Engine Characteristics. 229
J-1 Saturn V Development Cost Profile with 40 Percent Assumption [$M FY '04]. 234
J-2 Saturn V Development Cost Profile with Constant Assumption [$M FY '04]. 234
J-3 Saturn V Development Cost Profile with 60 Percent Assumption [$M FY '04]. 235
J-4 Saturn V Development Cost Profile with 70 Percent Assumption [$M FY '04]. 235
J-5 CaLV Development Cost Profile with 40 Percent Assumption [$M FY '04]. 236
J-6 CaLV Development Cost Profile with Constant Assumption [$M FY '04]. 236
J-7 CaLV Development Cost Profile with 60 Percent Assumption [$M FY '04]. 237
J-8 CaLV Development Cost Profile with 70 Percent Assumption [$M FY '04]. 237

LIST OF FIGURES

2-1 DoD Systems Engineering Process [14]. 14
2-2 System Life-Cycle Elements [14]. 15
2-3 IPPD at the Georgia Institute of Technology [86]. 16
2-4 Traditional Design versus Concurrent Engineering [86]. 17
2-5 Design Paradigm Shift [51]. 17
2-6 NASA Design Phases [62]. 18
2-7 Saturn V. 21
2-8 Space Transportation System. 23
2-9 Cargo Launch Vehicle [66]. 26
2-10 ESAS Human Missions to the Moon [66]. 27
2-11 Apollo Mission Mode Comparison [58]. 30
2-12 Loss of Mission Architecture Comparison [66]. 30
2-13 CaLV Design Candidates [66]. 31
2-14 CaLV FOM Comparison [66]. 31
2-15 Block Diagram of Computer Application [69]. 48
3-1 REDTOP-2 User Interface. 57
3-2 Effects on Delta V of Increasing the Mass Ratio. 60
3-3 Saturn V Trajectory Comparison. 61
3-4 Saturn V Velocity Comparison. 62
3-5 Closing a Launch Vehicle Design. 65
3-6 Design Structure Matrix for the Performance Disciplines. 67
3-7 Engine Mass as a function of Engine Thrust. 71
3-8 Vacuum Isp as a Function of Thrust for the J-2 Engine [74]. 72
3-9 Gravity Losses as a Function of EDS Thrust-to-Weight Ratio [66]. . . 74
3-10 TLI Burn Time for Varying EDS thrust-to-weight ratio [66]. 75
3-11 Bathtub Curve Created by Multiple Weibull Distributions [87]. 79
3-12 FMECA Worksheet [18]. 82

3-13 Series Reliability Block Diagram. 83
3-14 Parallel Block Diagram. 84
3-15 CCF Impacts of Different Component Configurations [73]. 86
3-16 Notional Fault Tree Diagram. 89
3-17 Notional Event Sequence Diagram. 92
3-18 Shuttle Event Tree [23]. 92
3-19 SPN Example Problem [93]. 94
3-20 Atlas Launch Vehicle Reliability Growth. 96
3-21 S-II Subsystem Unreliability Contribution [59]. 103
3-22 CaLV Booster Unreliability Contribution [66]. 104
3-23 Engine Out Failure Model. 106
3-24 Trajectory Comparison Between a Nominal Saturn V and Apollo 13. 108
3-25 SPN Catastrophic Failure Model. 109
3-26 Engine Out Model. 110
3-27 SIVB Reliability Calculation with Uncertainty Analysis. 113
3-28 SII Stage Representation with No Subsystem Redundancy. 114
3-29 SII Stage Representation with Power and Avionics Redundancy. . . . 114
3-30 Saturn V Reliability Calculation. 115
3-31 DoD LCC Categories [15]. 121
3-32 Engine Costs as a function of Engine Thrust. 124
3-33 NAFCOM Visual Example. 126
3-34 Learning Curve Example. 129
3-35 Mass Margin. 131
3-36 Cost Uncertainty Analysis. 132
3-37 GA Process. 136
3-38 Methodology Design Structure Matrix. 141
4-1 Saturn V Design Structure Matrix. 154
4-2 Trajectory Comparison for the Saturn V. 156
4-3 Inertial Velocity Comparison for the Saturn V. 157

4-4 Acceleration Comparison for the Saturn V. 158
4-5 System Cost versus Reliability for the Saturn V. 160
4-6 System Cost versus MFBF for the Saturn V. 161
4-7 Saturn V Pareto Frontier. 162
4-8 S-II DDT&E Cost Breakdown. 167
4-9 Alternative Design Cost Comparison. 168
4-10 Optimal Configuration Peak Funding Comparison. 169
4-11 Pareto Frontier with Uncertainty. 171
4-12 Saturn V Reliability Growth with $\alpha = 0.2006$ [Atlas]. 175
4-13 Saturn V Reliability Growth with $\alpha = 0.0669$ [Delta]. 176
4-14 CaLV Design Structure Matrix. 178
4-15 Trajectory Comparison for CaLV. 180
4-16 Inertial Velocity Comparison for CaLV. 180
4-17 Acceleration Comparison for CaLV. 181
4-18 CaLV Design Space. 183
4-19 CaLV Cost versus MFBF. 184
4-20 CaLV Pareto Frontier. 185
4-21 CaLV DDT&E Subsystem Cost Percentage. 190
4-22 CaLV TFU Subsystem Cost Percentage. 190
4-23 CaLV Minimum Cost Configurations. 192
4-24 CaLV Optimal Configuration Peak Funding Comparison. 193
4-25 CaLV Pareto Frontier with Uncertainty. 194
4-26 CaLV Reliability Growth with $\alpha = 0.2006$ [Atlas]. 198
4-27 CaLV Reliability Growth with $\alpha = 0.0669$ [Delta]. 198
B-1 RELEX Component Redundancy Model. 211
B-2 RELEX Engine Out Failure Model. 212
D-1 Titan Launch Vehicle Reliability Growth. 216
D-2 Delta Launch Vehicle Reliability Growth. 216
I-1 Trajectory Results for Saturn V Configurations. 229

I-2 Velocity Comparison for Saturn V Configurations. 230
I-3 Acceleration Comparison for Saturn V Configurations. 230
I-4 Trajectory Results for Optimal CaLV Configurations. 231
I-5 Velocity Comparison for Optimal CaLV Configurations. 231
I-6 Acceleration Comparison for Optimal CaLV Configurations. 232

LIST OF SYMBOLS OR ABBREVIATIONS

AATe	Architectural Assessment Tool - enhanced.
AEE	Advanced Engineering Environment.
CaLV	Cargo Launch Vehicle.
CCD	Central Composite Design.
CCF	Common Cause Failure.
CER	Cost Estimating Relationship.
CEV	Crew Exploration Vehicle.
CLV	Crew Launch Vehicle.
COMET	Conceptual Operations Manpower Estimating Tool.
DoD	Department of Defense.
DOE	Design of Experiment.
EDS	Earth Departure Stage.
ELV	Expendable Launch Vehicle.
ESAS	Exploration System Architecture Study.
ESD	Event Sequence Diagram.
FIRST	Flight-oriented Integrated Reliability and Safety Tool.
FMEA	Failure Mode and Effect Analysis.
FMECA	Failure Modes, Effects, and Criticality Analysis.
FOM	Figures of Merit.
FTA	Fault Tree Analysis.
GA	Genetic Algorithm.
GASP	General Aviation Synthesis Program.
HAVOC	Hypersonic Vehicle Optimization Code.
IPPD	Integrated Product & Process Development.
IPT	Integrated Product Teams.

KSC Kennedy Space Center.

LaRC Langley Research Center.

LCC Life-Cycle Cost.

LEO Low Earth Orbit.

LM Lunar Module.

LOR Lunar Orbit Rendezvous.

MCS Monte Carlo Simulation.

MER Mass Estimating Relationship.

MFBF Mean Flights Between Failure.

MGL Multiple Greek Letter.

MLD Master Logic Diagram.

MSFC Marshall Space Flight Center.

MTTF Mean Time To Failure.

NAFCOM NASA/Air Force Costing Model.

NASA National Aeronautics and Space Administration.

NPV Net Present Value.

OCM Operations Cost Model.

OEC Overall Evaluation Criteria.

POST Program to Optimize Simulated Trajectories.

PRA Probabilistic Risk Assessment.

QRAS Quantitative Risk Assessment System.

RBD Reliability Block Diagram.

REDTOP-2 Rocket Engine Design Tool for Optimal Performance - 2.

ROPOT risk oriented program optimization tool.

RSE Response Surface Equation.

RSM Response Surface Methodology.

SPST Space Propulsion Synergy Team.

SSME	Space Shuttle Main Engine.
STS	Space Transportation System.
TLI	Trans-Lunar Injection.
WBS	Work Breakdown Structure.

SUMMARY

The emphasis on performance, cost, and reliability has changed for NASA launch vehicles over the history of manned space flight. In the 1960's, Apollo was initially designed to meet the President's requirements of "...landing a man on the [M]oon and returning him safely to [E]arth"; however, the final design was based on performance and schedule while reliability was not considered as important. In the 1970's, the Shuttle was initially designed for high flight rates and low production/operations cost, but was finally restrained by the peak yearly funding that severely compromised both operations cost and reliability. In 2005, the Exploration Systems Architecture Study for future launch vehicles and in-space transportation systems took a balanced figure of merit approach of performance, affordability, reliability/safety, extensibility, and programmatic risk. Performance, cost, and reliability were evaluated quantitatively while extensibility and risk were evaluated qualitatively.

This dissertation is focused on the quantitative metrics of performance, cost, and reliability for future launch vehicles. Methods are developed that hold performance constant for a required mission and payload so that cost and reliability can be traded. Reliability strategies such as reducing the number of engines, increasing the thrust-to-weight ratio, and adding redundant subsystems all increase launch vehicle reliability for a fixed performance. However, there are few references that illustrate the cost of increasing launch vehicle reliability in a disciplined, integrated approach.

For launch vehicle design, integrated performance, cost, and reliability disciplines are required to show the sensitivity of cost to different reliability strategies. A methodology is presented that demonstrates how to create the necessary launch vehicle reliability models and integrate them with the performance and cost disciplines. An

integrated environment is developed for conceptual design that can rapidly assess thousands of launch vehicle configurations. The design process begins with a feasible launch vehicle configuration and its mission objectives. The performance disciplines, such as trajectory analysis, propulsion, and mass estimation are modeled to include the effects of using different reliability strategies. Reliability models are created based upon the launch vehicle configuration. Engine reliability receives additional attention because engines are historically one of the leading causes of launch vehicle failure. Additionally, the reliability of the propulsion subsystem changes dynamically when a launch vehicle design includes engine out capability. Cost estimating techniques which use parametric models are employed to capture the dependencies on system cost of increasing launch vehicle reliability. Uncertainty analysis is included within the cost and reliability disciplines because of the limited historical database for launch vehicles. Optimization is applied within the integrated design environment to find the best launch vehicle configuration based upon a particular weighting of cost and reliability. Limitations of this methodology, such as the focus on space hardware, are also are discussed.

The Saturn V is used as a demonstration problem to show the capability of this methodology and validate the models with existing historical data. Various reliability models are compared to validate the basis of the present reliability model. An integrated environment combining the performance, cost, and reliability disciplines is used to show the sensitivity of various system metrics, such as gross mass, system cost, and reliability, to changes in reliability strategies such as the number of engines and redundancy.

The results show that both the Apollo and the ESAS launch vehicles could be optimized to be significantly cheaper, be more reliable, or have a compromise solution by illustrating how cost and reliability are coupled with vehicle configuration changes.

CHAPTER I

INTRODUCTION

1.1 Thesis Goals and Objectives

The objective of this dissertation is to create a methodology that links system cost and reliability for launch vehicle design. The result of using this design process is a set of optimal launch vehicle configurations based upon different weightings of system cost and reliability. Uncertainty analysis is also included to show the range of cost and reliability estimates. The set of optimal configurations can assist the process of selecting a final vehicle configuration by showing the sensitivity of a launch vehicle's cost to increases in reliability.

Another objective of this dissertation is to increase the amount of information available to a top-level decision maker. There are scenarios during conceptual design where certain launch vehicle configurations may not be evaluated quantitatively; this reduces the amount of available information about a launch vehicle concept. While the reasons for eliminating a concept may be validated when the concept is evaluated quantitatively, the eliminated concept may lead to other configurations that were not previously considered. Therefore, the choice of whether or not to quantitatively evaluate certain launch vehicle configurations can be eliminated by implementing this methodology.

Another goal is improving the efficiency of the launch vehicle design process. An integrated environment for considering the performance, cost, and reliability disciplines can be created by using the methodology outlined in this dissertation. Thousands of vehicle configurations can be studied in a matter of hours and the process is automated to allow system designers the time to analyze the results.

Reliability is defined as "the probability that an item (component, subsystem, system) will perform a required function under stated conditions for a stated period of time."[81] The reliability of a launch vehicle is the probability that the vehicle will complete its mission successfully. This metric can also be referred to as the probability of loss of mission by subtracting the success probability from one.

A cost metric is important for launch vehicle design because sustainable programs are generally created by minimizing system cost. The National Aeronautics and Space Administration (NASA) is constrained by the budget approved by Congress and only a subset of those resources can be devoted to programs such as launch vehicle development. Therefore, optimizing a launch vehicle configuration for cost as well as its reliability will enable NASA to pursue the vehicle's development and the missions that require the launch vehicle.

The methodology created in this dissertation will be used to explore the design space of a baseline launch vehicle configuration created by a top-level system designer. The mission objectives and constraints of the launch vehicle will be constant. Additionally, some of the engine parameters, such as the cycle type and chamber pressure, will be constant. The performance disciplines, such as trajectory analysis, propulsion, and mass estimating, will be modeled to couple cost and reliability. Configuration changes, such as reducing the number of engines or adding another power subsystem, will be used to increase system reliability. The corresponding system costs are calculated using the subsystem and component mass estimates. Uncertainty is included in both the cost and reliability disciplines to create confidence bounds and show the range of possible cost and reliability values. Optimization is applied in the design process to find the best combination of design variables for a weighted value function of cost and reliability. The steps for implementing this methodology are discussed in Section 1.3 and Chapter 3 reveals the details for creating the necessary models.

A set of design variables are used to change the configuration of a baseline launch

vehicle with the goal of increasing its reliability. To determine the design variables, the question of how to increase system reliability must be answered. Research is presented to explain the different strategies that can be used to increase launch vehicle reliability. Within this research, the primary drivers of launch vehicle reliability are revealed. Once the primary drivers are known along with the techniques for increasing system reliability, design variables can be determined for use in studying how vehicle configuration changes can increase system reliability. The configuration changes will be fully integrated with the performance and cost disciplines to examine how they are affected by increasing vehicle reliability.

A more detailed goal of this methodology is to examine the system effects of increasing reliability on both cost and performance. The cost of increasing system reliability may vary depending on the baseline vehicle configuration. Another goal is to calculate the cost of using a specific reliability strategy. There remains a question about the most cost effective manner to increase system reliability and if one reliability strategy is more cost effective than another. While system cost is one of the metrics, the performance disciplines will also be affected by increasing launch vehicle reliability.

Another goal of this methodology is to examine how increasing the system reliability will affect the performance of a vehicle. The launch vehicle gross mass and trajectory will change as system reliability is increased, but uncertainty exists about the magnitude of those changes. Accomplishing all of these goals will create a process that can provide additional information to make more informed decisions during the conceptual design phase.

1.2 Motivation

In January of 2004, President George W. Bush announced his "Vision for Space Exploration." [6] Within this statement, the President outlined a mission for the human return to the Moon. To enable the mission to the Moon, a new heavy lift

launch vehicle is required. With a set budget for NASA, the new launch vehicle must be designed for minimum cost. However, the launch vehicle must also be designed to perform the mission and to do so reliably. There are dire consequences, such as additional cost or program cancellation, if a vehicle must be redesigned to perform its mission or to improve its reliability. Thus, future space transportation systems must consider cost and reliability when selecting a final design.

The Exploration System Architecture Study (ESAS) created the foundation for accomplishing the Vision for Space Exploration [66]. ESAS is reviewed in more detail in Section 2.2.3. In this study, NASA engineers examined a wide variety of lunar architectures to determine which plan would best enable the United States to return to the Moon. Within each architecture, different vehicle models were created to calculate the various Figures of Merit (FOM) used for architecture comparison. The launch vehicles were evaluated across a set of quantitative and qualitative metrics. The quantitative FOMs were safety/mission success, effectiveness/performance, and affordability; the qualitative FOMs were extensibility/flexibility and programmatic risk. This dissertation will focus on the quantitative FOMs. Mission success and system reliability will be synonymous in this dissertation. System cost will only include design, development, testing, evaluation, and total production; operations cost is neglected.

The Exploration System Architecture Study was given a time constraint of 90 days to develop an architecture and recommend a final solution. Due to this time constraint, a number of launch vehicle configurations were not included in the study. A decision was made to only evaluate launch vehicles that use existing hardware [66], with a focus on using existing engines. Therefore, thousands of launch vehicle configurations were eliminated from the design process without being evaluated for their quantitative system metrics.

There is an opportunity to improve the efficiency of evaluating thousands of permutations of a launch vehicle configuration. Without evaluating a launch vehicle design quantitatively, it is uncertain how an updated configuration will compare to the baseline concept. Additionally, evaluating an alternative launch vehicle configuration without restrictions could lead to another concept that may fit the original constraints. Inspiration comes from the optimization community where many techniques approach an optimal solution from the infeasible region [92]. By using current computing resources, every advantage should be taken to create additional information about a launch vehicle concept for use in deciding the final vehicle selection.

An example of a configuration in ESAS that showed reason for future study was a vehicle with engine out capability on the Earth Departure Stage (EDS). An engine out scenario is where a vehicle can operate when one engine fails in a benign manner. "For upper stages, results indicate that engine-out is a preferred capability" [66]. Due to the restricted study time, concepts like the EDS engine out case were not included in any of the final design solutions. These concepts were left to consider during the preliminary design phase.

Few references exist about the sensitivity of a launch vehicle's cost to its reliability. The ESAS report showed changes to reliability and cost for a few selected concepts [66]. However, there was not a direct linkage between cost and reliability. The effectiveness of increasing a system's reliability by using different reliability strategies, such as engine out, is not well defined. Uncertainty exists about the most cost effective method for increasing system reliability and if one approach is consistently favored over another. An integrated environment can be used to complete trade studies that show the effects of using different reliability strategies. The results reveal which design variables deserve further study because they are the significant parameters for determining a vehicle's cost and reliability. An integrated environment is beneficial because the process can be automated and additional work can be

completed in a given amount of time.

The primary goal of this methodology is to create additional information to assist with selecting the final launch vehicle design. Time constraint concerns will be reduced because this process can evaluate thousands of launch vehicle configurations in a matter of hours while maintaining a comparable level of fidelity to past conceptual design studies. The sensitivity of cost to increases in system reliability can be determined by using this design process. Resources within the space community are limited and moving along an incorrect path could result in unnecessary expenditure and/or program cancellation. Therefore, the methodology created in this dissertation is beneficial for launch vehicle design because the results provide additional information to make a more informed decision.

1.3 Methodology Outline

A series of steps are required to complete this methodology. This section will briefly outline the steps to link system cost and reliability for launch vehicle design. The detailed modeling is discussed in Chapter 3 for the performance, cost, and reliability disciplines.

- **Step 1:** Obtain top-level performance requirements about the launch vehicle configuration under study.
  - The trajectory requirements:
    - The final orbit conditions, such as altitude and velocity.
    - The payload requirement. If the final stage is used to provide an in-space burn, then the in-space velocity requirement is needed.
    - Any mission constraints, such as a maximum acceleration or maximum dynamic pressure.
  - Engine characteristics:

        * Engine cycle type, which leads to the vacuum Isp.
        * Chamber pressure.
        * Expansion ratio.
    - Reliability failure rates for each subsystem and component.

- **Step 2:** Create the performance models.
    - Determine the range of parameters for performance analysis.
        * Parameters may include stage thrust-to-weight ratio, the number of engines, engine thrust-to-weight ratio, etc.
    - Create response surface equations to improve design efficiency.
        * Response surface equations are discussed in Section 3.1.8.1.
        * Determine the cases to run for the response surface equations.
    - Use response surface equations to replace the propulsion discipline.
        * The independent parameter is the thrust level and the dependent parameter is the engine thrust-to-weight ratio.
    - Utilize response surface equations to replace the trajectory analysis.
        * The independent variable is the stage thrust-to-weight ratio and the dependent parameter is the stage mass ratio.
        * Find the lowest stage thrust-to-weight ratio that closes the vehicle as a minimum bound. Use previous knowledge and experience gained from this process to find an upper bound.
        * Create another response surface to calculate the operating time of each stage. The independent parameter is the stage thrust-to-weight ratio and the dependent parameter is the stage burn time.
    - Create a mass estimating model.

    - Determine the mass breakdown structure.
    - Use Mass Estimating Relationships (MERs) to calculate subsystem mass based upon vehicle characteristics. MERs are reviewed in Section 3.1.3.
    - The inputs to the mass discipline are the stage thrust-to-weight ratios, stage mass ratios, and the reliability strategies that affect the mass, such as engine out.
    - The mass estimating model must be created in a manner to include reliability strategies such as engine out and power subsystem redundancy.
    - Include the response surface equations from the trajectory and propulsion disciplines.
    - Use iteration, such as the SOLVER routine in EXCEL, to close a vehicle. Closing a launch vehicle can be accomplished by changing the stage propellant mass to match the stage thrust-to-weight ratio with the correct stage mass ratio.
  - Validate the integrated performance models against existing models or flight data.

- **Step 3**: Create the reliability models.
  - Reliability Block Diagrams (RBDs) and Fault Tree Analysis (FTA) are recommended for use as the reliability modeling technique. They are discussed in Section 3.3.3.2 and Section 3.3.3.5, respectively.
  - Reliability modeling should be performed at the subsystem indenture level. Indenture levels are discussed in Section 3.3.1. Recommendations are made to separate the engine from the propulsion subsystem and model the engine at the component level.

- Create reliability models with the capability to analyze different configurations. Dynamically updating fault tree analysis is recommended to capture the effects of changing configurations, such as adding engine out capability. An example of dynamic fault tree analysis is shown in Section 3.4.4.
- Redundancy models using common cause failure must be created when using identical components. Common cause failure is discussed in Section 3.3.3.3.
- Create engine out modeling capability as discussed in Section 3.4.1.
- Create launch vehicle stage and system reliability models. The stage reliability models are created by combining reliability estimates from the subsystem and component models. The vehicle reliability model is created by combining the stage reliability estimates. Stage and system reliability modeling is discussed in Section 3.4.4.
- Validate the present model with existing software and existing launch vehicle reliability models.
- Research historical failure rates of subsystems and components for use in reliability uncertainty analysis. Section 3.4.3 lists references that can provide historical reliability estimates.
- Create a reliability growth model for use in comparing the initial reliability of various launch vehicle configurations. The Department of Defense has compiled a list of general reliability growth models [11].

- **Step 4:** Create the cost model.
  - Determine system cost breakdown structure.
    * Use the mass breakdown structure as a guide and calculate cost at the same indenture level.

    - Calculate the Design, Development, Testing, and Evaluation (DDT&E) cost.
    - Calculate the Theoretical First Unit (TFU) cost.
  - Determine the subsystem technology levels to select analogous relationships.
  - Use cost estimating relationships from an established cost model for subsystem and component cost estimates or develop a cost estimating tool and validate the tool with an accepted software package.
  - Ensure that the cost model can incorporate different reliability strategies, such as using two sets of power components to provide redundancy.
  - Combine the subsystem and component cost estimates into a stage and a vehicle cost estimate.
  - Use established procedures for estimating uncertainty based upon the cost estimates.

- **Step 5:** Create an integrated design environment.
  - Create an Overall Evaluation Criterion (OEC) for use in optimization. The OEC is a combination of the system Figures of Merit and is discussed in Section 3.7.2.
  - Link the performance, cost, and reliability disciplines by passing the appropriate variables from one discipline to another.
  - The system design variables will be the stage thrust-to-weight ratio and any reliability strategies, such as changing the number of engines and using engine out capability.
  - Use an optimization technique that can incorporate discrete design variables, such as a genetic algorithm. The genetic algorithm optimization

technique is described in Section 3.7.

    * The applications in this methodology require at least 12 iterations with no change in the objective function to ensure an optimal design is found.

    * Other characteristics of the genetic algorithm include tournament selection with two participants, a 70 percent crossover rate, and a 20 percent mutation rate.

  - Optimize the configuration for a specific weighting of the Figures of Merit.

  - Repeat the optimization for as many different weightings as desired. A script can be written to automate this process.

- **Step 6:** Post-processing of the results.

  - Compile the optimal solutions into a plot showing the pareto frontier. A 70 percent confidence level was used as the optimal value for system cost and reliability.

  - Use the 10 percent and 90 percent confidence levels to illustrate uncertainty bands.

  - Compile the design settings for the optimal configurations into a results table.

  - Examine the results and draw conclusions.

The process outlined above will change the configuration of a launch vehicle based upon a set of design variables while constraining the system performance. The goal of changing the configuration is to increase system reliability while meeting the original mission objectives. An integrated model of the design disciplines is used to examine the sensitivity of increasing system reliability on the cost and performance metrics.

1.4 Summary

Two applications of this methodology are presented. The first problem examines the Saturn V launch vehicle from the Apollo program. The objective is to show a variety of optimal Saturn V configurations based upon a weighting of system cost and reliability. The Saturn V was chosen because the vehicle was flown twelve times during the Apollo program and data exists to validate the discipline models. Once validation of the Saturn V system is shown, the figures in the results section illustrate how the Saturn V reliability could have been increased by changing the design configuration. Potential design changes include varying the stage thrust-to-weight ratio, the number of engines on each stage, and adding engine out capability on each stage. The option of using redundancy on additional subsystems, such as the power and avionics subsystems, is also considered.

The second application is for the Cargo Launch Vehicle (CaLV) proposed by the Exploration Systems Architecture Study to perform the heavy lift capability needed for missions to the Moon [66]. This application was selected to demonstrate how the methodology could benefit conceptual design studies such as ESAS. The results will reveal a set of configurations that can be used to increase CaLV reliability and the corresponding system cost. The CaLV baseline used existing engines, which affects the system cost and is reflected in the results.

The next chapter of this dissertation will review systems engineering and how it applies to the design process. Additional literature review is provided to describe past approaches for completing launch vehicle design. Non-aerospace methods are also considered for coupling system cost and reliability. Chapter 3 will reveal the details of modeling the performance, cost, and reliability disciplines. Chapter 4 will show the results of applying this methodology to the Saturn V and the Cargo Launch Vehicle and the conclusions and future work will be described in Chapter 5.

CHAPTER II

BACKGROUND

There are a variety of approaches to engineering design. Systems analysis considers all phases of a concept's life-cycle during the conceptual design phase. This chapter begins by reviewing the principles of systems engineering and explaining why it should be applied during the design phase. The next section discusses the different approaches used for launch vehicle design.

Within launch vehicle design, there are a variety of methods for implementing the systems engineering process. Many of the recent techniques include optimization to find the best combination of design variables for a system metric. This chapter includes a review of different launch vehicle design approaches along with a review of other aerospace design methods. Outside of the aerospace industry, reliability allocation techniques can be used to link cost and reliability; some of those approaches are also discussed. This chapter concludes with a set of research questions that this dissertation will attempt to answer.

2.1 Systems Engineering

Systems engineering is a process that can be used to aid in selecting an engineering design. The Department of Defense (DoD) defines systems engineering as:

"... a comprehensive, iterative and recursive problem solving process, applied sequentially top-down by integrated teams. [Systems Engineering] transforms needs and requirements into a set of system product and process descriptions, generates information for decision makers, and provides input for the next level of development." [14]

The DoD refers to integrated teams as Integrated Product Teams (IPTs), which include interdisciplinary experts from each area of the product life-cycle [14]. IPTs consist of management, technical discipline experts, specialty areas such as quality assurance, and business analysts who have knowledge of financial and contracting issues.

Figure 2-1 illustrates the systems engineering process. A set of requirements, such as the mission objectives and constraints, are passed on to the engineers, who use engineering principles to create a design that satisfies the requirements. The process of creating a design occurs within the oval in Figure 2-1.

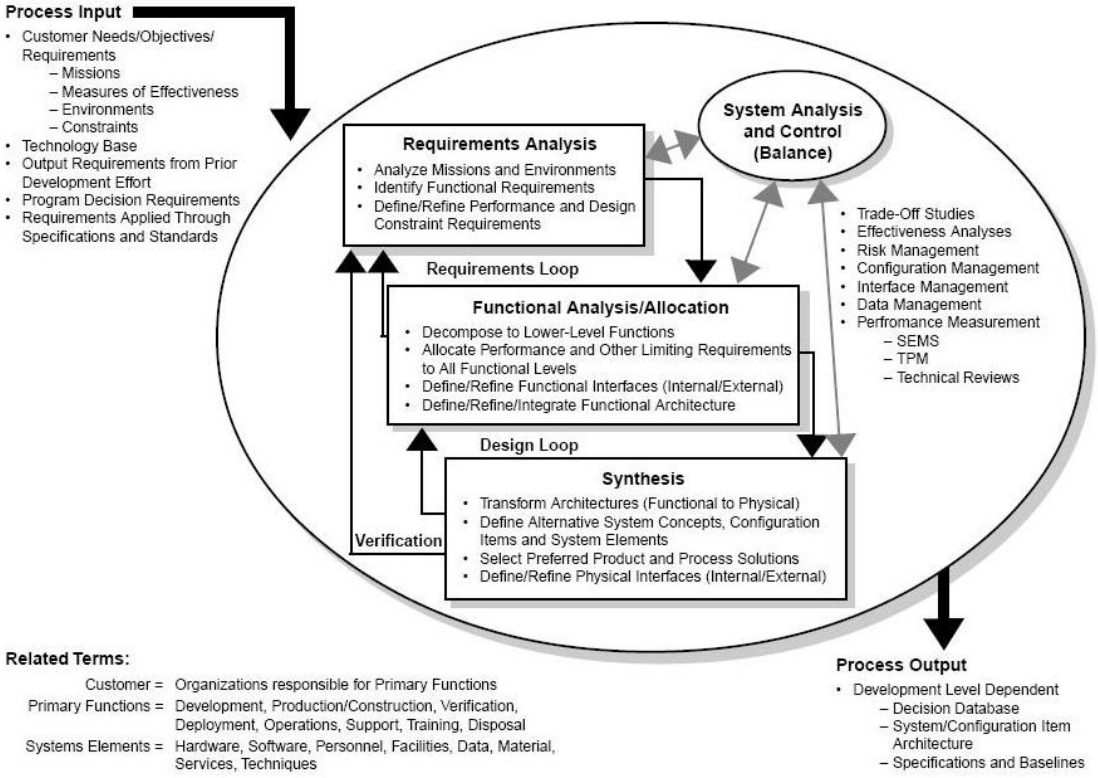

Figure 2-1: DoD Systems Engineering Process [14].

To execute the process outlined in Figure 2-1, systems engineering practices recommend integrated development to ensure that all aspects of the life-cycle are considered. Figure 2-2 illustrates the different elements of a system life-cycle [14].

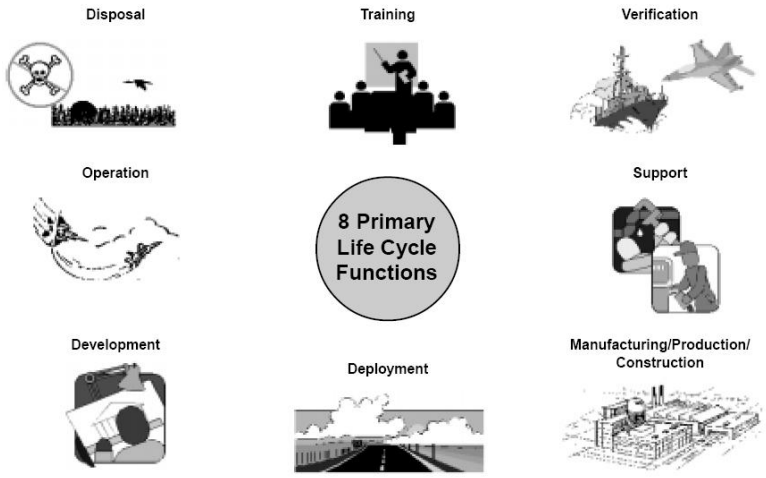

Figure 2-2: System Life-Cycle Elements [14].

The DoD refers to integrated development as "Integrated Product and Process Development (IPPD)" [14]. IPPD is defined as "...a management methodology that incorporates a systematic approach to the early integration and concurrent application of all the disciplines that play a part throughout a systems life cycle." [40] The Georgia Institute of Technology has developed a design process utilizing the fundamentals of IPPD [86]. Figure 2-3 illustrates the IPPD process at the Georgia Institute of Technology.

By considering all aspects of a system's life-cycle, additional knowledge is introduced during the design phase that has traditionally been omitted from the early system definition. This is one reason why systems engineering is recommended over the traditional design approach.

"The conventional way of doing product design has been to carry out all of the steps serially...these serial functions have been carried out in distinct and separate organizations with little interaction between them. Thus, it is easy to see how the design team will make decisions, many of which can be changed only at great cost in time and money, without adequate knowledge of the manufacturing process." [13]

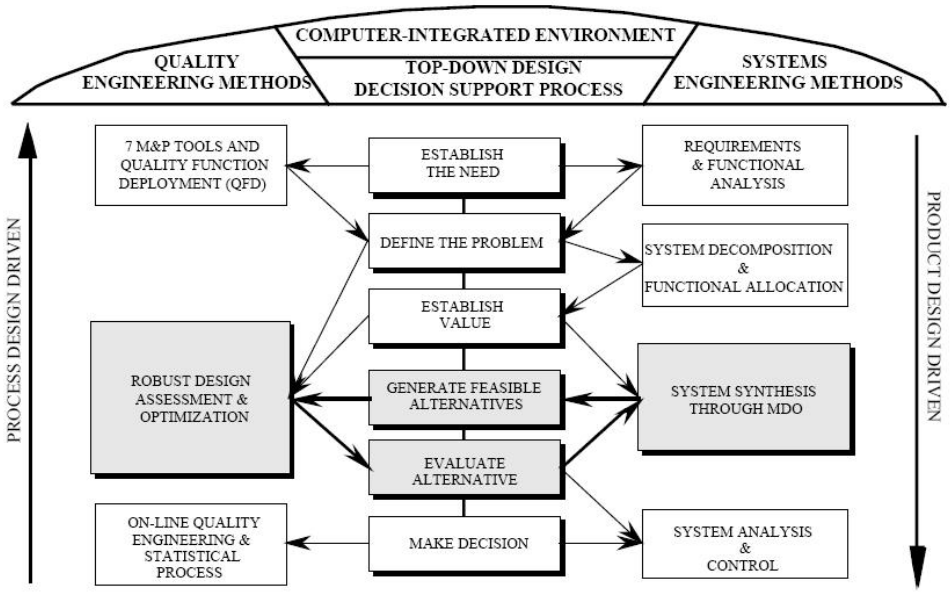

Figure 2-3: IPPD at the Georgia Institute of Technology [86].

The costs of a system are determined early in the design phase as decisions are made about the system definition. "...[T]he design process consists of the accumulation of many decisions that result in design commitments that affect about 70 to 80 percent of the manufactured cost of the product." [13] In the traditional design approach, problems that occur during the manufacturing phase are very costly to fix because redesign effort cascades through a complex system. "If the design proves to be faulty just before the product goes to market, it will cost a great deal of money to correct the problem." [13] Figure 2-4 illustrates a notional cost comparison between the traditional manner of design and using a concurrent approach.

During the design phase, systems engineering and IPPD are used to bring all the disciplines together to eliminate faulty designs before they reach the manufacturing phase. Figure 2-5 illustrates the concept of introducing knowledge earlier in the design by using integrated development. The additional knowledge gained from evaluating the complete life-cycle during the conceptual design phase will lead to better decisions about the final configuration.

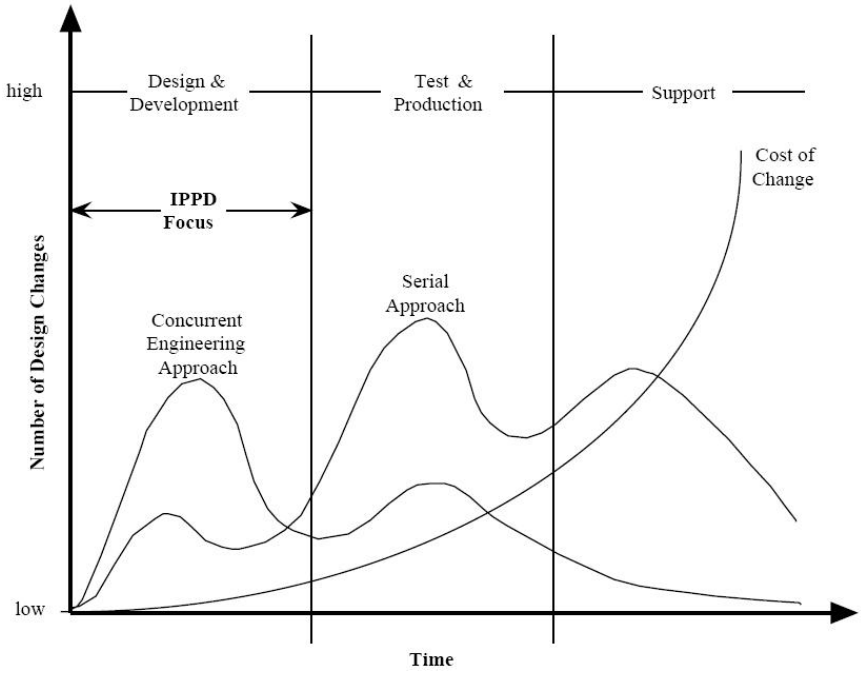

Figure 2-4: Traditional Design versus Concurrent Engineering [86].

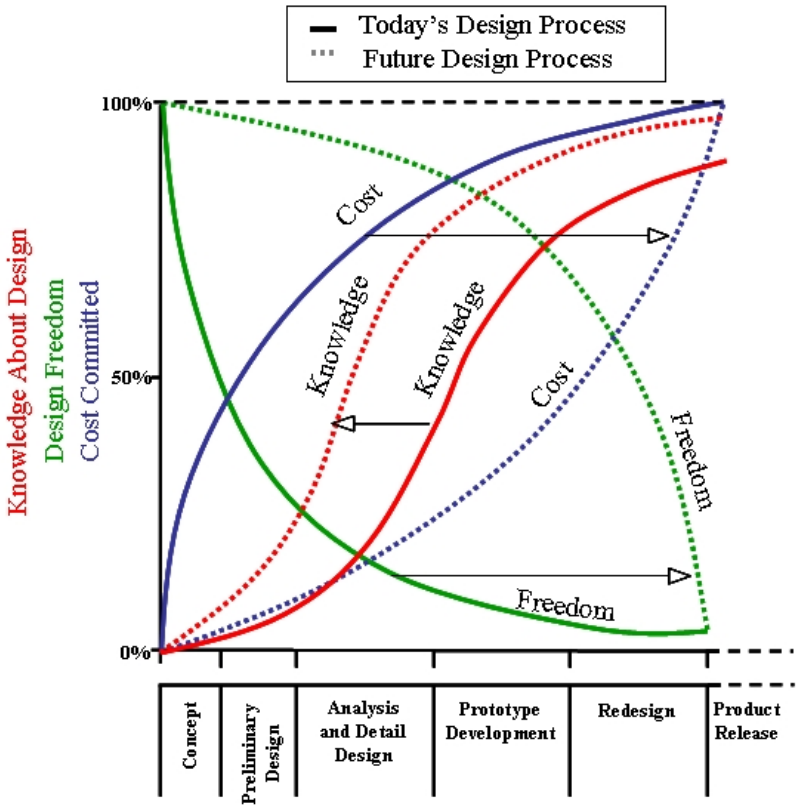

Figure 2-5: Design Paradigm Shift [51].

The methodology created in this dissertation aims to fill a small role in the overall systems engineering process by providing a means to perform integrated launch vehicle design. The process outlined in Chapter 3 will fit in the Synthesis and Systems Analysis areas of Figure 2-1. Using this methodology will lead to creation of an integrated framework that can be used to perform rapid studies. This methodology could be applied during the conceptual design phase, where very few design choices have been made. The design phases are discussed further in Section 2.1.1.

Many of the references discussed earlier provide an excellent guide for the overall systems engineering process. The references review the major tasks that should be completed to ensure a system's life-cycle elements are considered. However, these references do not provide in-depth details about how to accomplish some of the tasks, such as Synthesis and Systems Analysis.

Additional references, which are reviewed in Section 2.3, provide the technical foundation for completing segments of the Synthesis and Systems Analysis portion of Figure 2-1. Other literature reveals how to create an integrated environment for launch vehicle design and is examined in Section 2.3.1.

2.1.1 Design Phases

The methodology is created for use during the conceptual design phase, which is the design phase where much of the vehicle configuration has yet to be determined. Figure 2-6 is a diagram illustrating the design phases according to the NASA Systems Engineering Handbook [62].

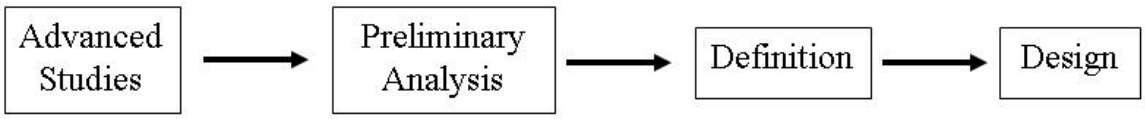

Figure 2-6: NASA Design Phases [62].

Each design phase is described in greater detail below. The conceptual design phase in this dissertation is equivalent to the preliminary analysis in Figure 2-6.

- **Pre-Phase A: Advanced Studies**

  The goal of this design phase is to create ideas and initial concepts for various missions. These missions will be based on opportunity and the current need within the science community.

- **Phase A: Preliminary Analysis**

  In the preliminary analysis phase, the mission is studied in more detail to examine its feasibility. Feasibility assessments are completed by performing trade studies. A study is also completed to ensure that the mission fits within NASA's overall objectives. Two other tasks completed during the preliminary analysis phase are establishing the "[t]op-level requirements" and identifying the system FOMs [62].

- **Phase B: Definition**

  In the definition phase, a baseline design that will satisfy the mission objectives is established. The "initial configuration management" and the baseline system requirements are defined during this phase. Other products that are completed during the definition phase are a project plan, including the schedule, and the concept of operations. This design phase is referred to as detail design throughout the remainder of the dissertation.

- **Phase C: Design**

  In the final design phase, a complete design of the system is created. This includes all of the lower level requirements for the subsystems. After the end of the final design phase, system manufacturing begins. The subsystems are created first and then integrated together to create the final product. All qualification and acceptance level testing is completed on the subsystems prior to system integration. However, some decisions are re-evaluated based upon the

results of certification testing. The next step is to complete the launch vehicle and deploy a payload in orbit. Once the launch vehicle flies successfully, the operations phase of the system life-cycle will begin.

2.2 Historical Launch Vehicle Design

This section will review three different launch vehicles and explore how their design was developed. The goal is to learn from existing methods and try to improve upon the design process by using systems engineering principles. The launch vehicles under review are the Saturn V, the Space Transportation System (STS), and the as yet to be manufactured Cargo Launch Vehicle (CaLV).

The Saturn V and CaLV are elements of a larger mission that involves multiple vehicles. A conflict appears to occur between using integrated design and designing the launch vehicles as their own entity. However, this conflict is removed by requirements analysis, as shown in Figure 2-1, which considers all of the other vehicle needs in the mission before determining the launch vehicle requirements. Once the requirements are determined, this methodology is used to evaluate alternative configurations of a launch vehicle. Thus, the review will focus on the launch vehicle design even though the launch vehicle is one element of a larger mission.

2.2.1 Saturn V

The Saturn V was developed for the Apollo program, which sent United States astronauts to the Moon in a series of missions from 1969 to 1972 [85]. The Apollo program began as a follow up to the Mercury program, which launched the first American into space. However, NASA did not receive the full go-ahead to try for a lunar landing until President John F. Kennedy delivered a speech to Congress in 1961. "...I believe that this nation should commit itself to achieving the goal, before this decade is out, of landing a man on the [M]oon and returning him safely to [E]arth." [43]

The Saturn V was a three stage launch vehicle and is illustrated in Figure 2-7.

The first stage of the Saturn V is called the S-IC, the second stage is the S-II, and the third stage is the S-IVB. The first stage used five F-1 engines; the propellant was liquid oxygen and a refined form of kerosene known as RP-1. The F-1 engine cycle was a gas generator. The second stage used five J-2 engines, which also employed a gas generator engine cycle. The propellants were liquid oxygen and liquid hydrogen. The third stage used a single J-2 engine.

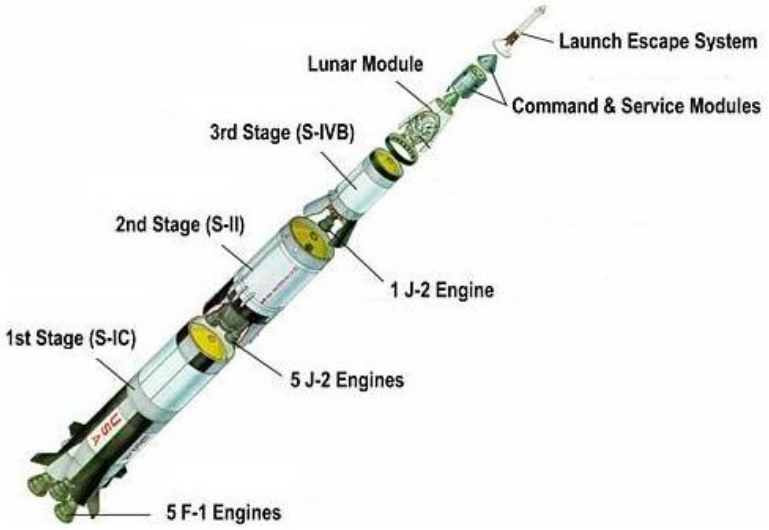

Figure 2-7: Saturn V.

The Apollo program chose between four different lunar architectures to satisfy the mission objectives [58]. Each architecture had its own set of vehicles which were designed together to meet the total mission objectives. Once Lunar Orbit Rendezvous (LOR) was selected, the Saturn V became the launch vehicle responsible for launching the Apollo missions to the Moon.

With very little heritage, NASA engineers focused on satisfying the performance objectives to ensure that the mission could occur. Therefore, very few trade studies for evaluating different Saturn V configurations were completed. One trade was completed to decide between using four and five engines on the S-IC. Five engines were selected to add design margin due to uncertainty about the final mass of the vehicles launched on top of the Saturn V [5].

The Saturn V reliability was based on comparisons with launch vehicles used for the Mercury program and various missile systems [58]. Different models were created that evaluated the system reliability of various configurations, such as the number of engines on each stage and the use of engine out capability on the S-II stage. However, the reliability models produced mission success probabilities that were so low that NASA moved away from using quantitative methods to calculate system reliability [70], [22].

Early cost estimates were not conducive for use in trade studies. During the early Apollo program, cost estimates were created by using "...analogies, intuition and guesses..." [33]. The cost estimates were developed by the design engineer responsible for a particular subsystem or component. Thus, integrated cost models did not exist to determine how the configuration would affect system cost.

Time is another reason why few trade studies for the Saturn V design were completed. The first United States manned space flight, which did not orbit the Earth, occurred in May of 1961 and NASA engineers were expected to land on the Moon by the end of the decade. Additionally, computers were still in the infancy stages during the Apollo era, and engineers did not have the tools and capability of the current space flight program. In fact, many of the "computers" of the Apollo era were women who performed the needed analytical calculations on mechanical calculators and slide rules [57].

The methods for completing conceptual design in the space industry have been greatly upgraded over the past four decades. These methods can provide additional information to make more informed decisions that should result in less redesign and costly changes later in the program's development. The Space Transportation System (commonly referred to as the Shuttle) capitalized on some of the lessons learned regarding conceptual design but there was still room for improvement.

2.2.2 Space Transportation System

The Space Transportation System (STS) followed the Apollo program. During Apollo, Vice-President Spiro Agnew led an effort to determine the next direction for the United States space program [60]. President Richard Nixon then made the decision to pursue a strategy for expanding into Low Earth Orbit (LEO) based on projected cost [3]. The STS was originally rejected until NASA obtained support from other agencies, such as the DoD and the Air Force, and also guaranteed "...that the Shuttle would be the only launch vehicle developed in the 1980's." [3] The Shuttle had its first flight on April 12, 1981.

Figure 2-8 illustrates the Space Transportation System. The STS was built to carry astronauts and payloads to Low Earth Orbit and is a partially reusable system.

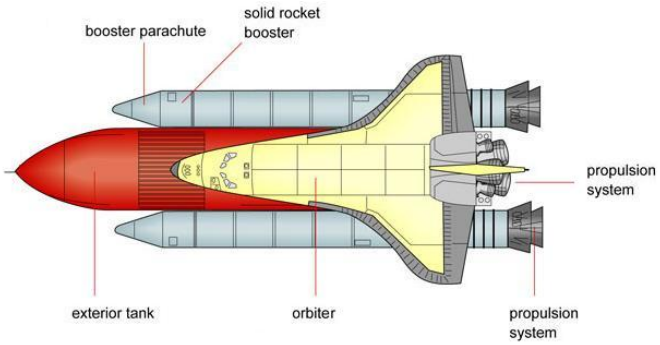

Figure 2-8: Space Transportation System.

There are four main elements that compose the STS:

1. **Orbiter:** This element carries the astronauts to and from space. Any science payloads, such as telescopes or satellites are carried inside the orbiter's payload bay. This element is reused after each flight.

2. **External Tank:** This segment stores propellant for use by the orbiter propulsion system during vehicle ascent. The External Tank is discarded after every flight.

3. **Space Shuttle Main Engines (SSMEs):** These are the engines on the orbiter that help power the STS to orbit. The engines use a staged-combustion engine cycle and the propellants are liquid oxygen and liquid hydrogen. The engines are also reused after every flight.

4. **Solid Rocket Boosters:** The two boosters also provide thrust for the STS to reach orbit. They burn for approximately 120 seconds and then drop off the vehicle. The boosters land in the Atlantic Ocean and are retrieved for additional use.

The Shuttle design was influenced by payload requirements from NASA, the DoD, and the Air Force [3]. The desired concept was a fully reusable system that would reduce operations cost compared to the existing expendable launch vehicles. Thus, performance and operations were the initial significant figures of merit for the preliminary Shuttle design.

During the early 1970s, the Shuttle development became constrained by the budget. While the life-cycle cost of the desired system was predicted to be lower than the selected concept, the peak year funding was too great for NASA's budget [3]. Thus, NASA was forced to move away from its desired concept: a fully reusable system with fly back boosters [96]. The partially reusable system was predicted to cost more during the operational phase but would have a lower development cost. Later in the design phase the booster stages were changed from liquid to solid propellants, as illustrated in Figure 2-8, to reduce the development cost even further. However, the engineers knew that the solid rocket boosters would result in a higher operational cost.

During the design, NASA completed trade studies to compare the cost of different concepts. Performance modeling was becoming more sophisticated as computers gained more power. The cost discipline also became more refined after the Apollo era. The Air Force had developed a "Space Planner's Guide" which devoted a chapter

to mass based Cost Estimating Relationships (CERs) to be used in projecting space vehicle costs [33]. These CERs were parametric equations that depended on the mass of the vehicle and are discussed in more detail in Section 3.5.

Cost estimates for the STS were created using the cost estimating relationships and analogies to other systems, such as winged-body aircraft, when the CERs did not exist. However, these cost estimates were calculated after the designs were created because the traditional serial approach was still used for design. Additionally, with the focus on development cost, life-cycle cost was sacrificed in order to ensure the Shuttle was built.

The reliability for the initial Shuttle designs relied upon qualitative techniques such as Failure Modes and Effect Analysis (FMEA). FMEA is discussed in greater detail in Section 3.3.3. These qualitative techniques were not conducive to trade studies during conceptual design because they relied upon expert opinion. When quantitative reliability analysis was performed, estimates were quoted "...without any formal systems analysis to support such..." [70] results. Thus, reliability was not a primary figure of merit for design decisions.

The Shuttle initially focused on full reusability and low operations cost but because of yearly budget constraints, the focus became the development cost. The result is a system with high operating costs and two accidents during its lifetime. The STS provides an excellent lesson learned about the pitfalls of neglecting the total life cycle and quantitative reliability analysis during conceptual design. These lessons learned were demonstrated during NASA's Exploration Systems Architecture Study and its Cargo Launch Vehicle that was created considering all aspects of the system's life-cycle.

2.2.3 Cargo Launch Vehicle

In 2004, President George W. Bush announced his Vision for Space Exploration [6] which includes the objective of returning to the Moon no later than 2020. In response to the Vision, NASA carried out the Exploration Systems Architecture Study (ESAS) with the goal to select the vehicles that would carry American astronauts back to the Moon [66].

Figure 2-9: Cargo Launch Vehicle [66].

One of the vehicles studied during ESAS was a Cargo Launch Vehicle (CaLV) and the selected concept is illustrated in Figure 2-9 [66]. The CaLV is designed to carry a lunar lander to Low Earth Orbit (LEO). The second stage of the CaLV, the Earth Departure Stage (EDS), continues the launch to LEO, will rendezvous with the crew capsule and service module, and boost all three elements to the Moon. Figure 2-10 illustrates the concept of operations for human missions to the Moon [66].

The CaLV is composed of the Solid Rocket Boosters, the lower booster stage, and the previously mentioned Earth Departure Stage. The Solid Rocket Boosters are 5-segment boosters derived from the Space Transportation System but with an additional segment. The booster, or core, stage uses five SSMEs from the Shuttle which are modified for use on the CaLV. The Earth Departure Stage uses two J-2S

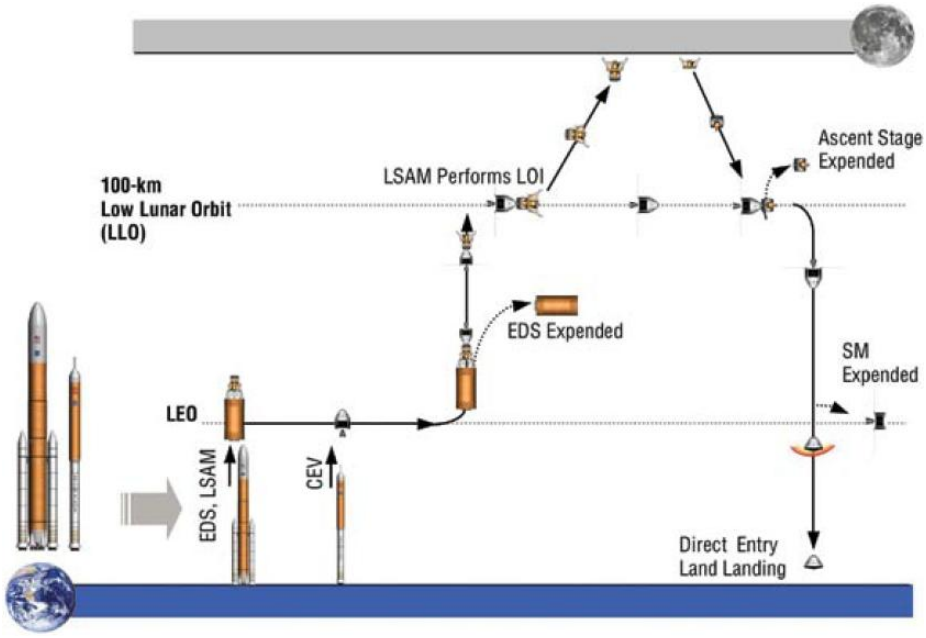

Figure 2-10: ESAS Human Missions to the Moon [66].

engines, which are a derivative engine of the J-2 used on the Saturn V. The J-2S was an engine in development during the Apollo era but the program was canceled before the J-2S had an opportunity to fly [77]. Like the original J-2 engine, the J-2S is a gas generator engine that uses liquid oxygen and liquid hydrogen as its propellants.

The ESAS evaluated many different Cargo Launch Vehicle concepts before selecting the final design. Each launch vehicle was evaluated for many different metrics, once the feasibility of the design was established. Figures of Merit (FOMs) included safety, reliability, extensibility, effectiveness, risk, and life-cycle cost [66]. Extensibility and risk were evaluated qualitatively by a "consensus of discipline experts." [66] Effectiveness was partly evaluated at the architecture level for metrics such as cargo delivered to and returned from the lunar surface. Effectiveness also included system availability and system operability which could be evaluated at the vehicle level.

In order to compare each of the different concepts, an integrated process was used that combined experts from all of the life-cycle elements. Concepts were created by using"...parametric sizing and structural analysis..." while vehicle lift capability

was determined with: "...the generation of three-Degrees-of-Freedom point-mass trajectory designs anchored by the sizing, structural, and subsystem assessment work. Output of the vehicle concept development work was forwarded to the operations, cost, and reliability/safety groups for use in their analysis." [66]

The reliability of each CaLV concept was assessed with a quantitative technique. NASA had learned from the Challenger accident that quantitative reliability assessments were needed [70]. The launch vehicle reliability modeling in ESAS was completed by using different analysis tools, such as the Flight-oriented Integrated Reliability and Safety Tool (FIRST) and the Space Shuttle Quantitative Risk Assessment System (QRAS). The launch vehicle reliability focused on the propulsion subsystem; detailed estimates of the propulsion subsystem were created by examining parts and assemblies such as engines, feed lines, and auxiliary power units. The Solid Rocket Boosters, separation systems, payload shroud, and the thermal control system were other elements included in the CaLV reliability estimates. The reliability modeling, which included uncertainty analysis, was used to evaluate various CaLV concepts to provide a range of system reliability estimates. Trade studies were performed on the type of engine, number of engines, engine out capability, and the overall CaLV configuration, such as whether the vehicle had a side mount or included Solid Rocket Boosters.

The cost modeling used the NASA/Air Force Cost Model, which is based on parametric cost estimating relationships, to calculate development cost. Parametric cost modeling and NAFCOM are discussed in greater detail in Section 3.5 and Section 3.6. The operations and support costs were prepared by NASA Kennedy Space Center experts [66].

The ESAS made a number of high-level assumptions that guided their vehicle designs. The decision was made to avoid "clean-sheet" designs because of "high development costs...and lengthy development schedules..." [66]. Additionally, "...ESAS

management directed the team members to use existing LV elements, particular engines...New design elements were acceptable where absolutely necessary, but had to be clearly superior in safety, cost, and performance to be accepted." [66]

The Exploration Systems Architecture Study demonstrated how systems engineering can be used to select a final vehicle design. As recommended by the earlier references, all aspects of the vehicle's life-cycle were considered. Due to the short study time, the ESAS relied on expert judgment for selecting key trade areas and the final selection of a launch vehicle concept. The ESAS did not have time to use an integrated design environment to determine the "optimal" architecture or the "best" launch vehicle concept for cost and reliability.

2.2.4 Apollo and ESAS Comparison

While Apollo tried to use systems engineering processes for conceptual launch vehicle design, the methods and tools were not advanced enough to provide detailed results. As discussed earlier, design variables were changed one at a time and performance margin was used as a solution for uncertainty about the final mass. Many different trade studies could not be completed due to the time constraint and the modeling capability.

Figure 2-11 is a chart that compares the Figures of Merit for the four lunar architectures that were under consideration during the Apollo era [58]. However, because the Apollo engineers did not have the advanced tools and methods practiced today, it is unknown if the architectures compared in Figure 2-11 were optimal solutions for their metrics. It is uncertain if the launch vehicle used to enable each of the architectures is the optimal configuration for the given mission constraints. Furthermore, each architecture was sized for a different performance level, thus making cost comparison difficult. Figure 2-11 also reveals the low levels of probability of success on

	PERFORMANCE CM+EM (H.E. RETURN) LBS.	PROBABILITY OF SUCCESS ON FIRST ATTEMPT%	TIME TO FIRST SUCCESSFUL LANDING 90% PROBABILITY	PROBABILITY OF CREW LOSS ON FIRST ATTEMPT-%	R&D COST MILLIONS	OPERATIONAL COST TO FIRST SUCCESS (90% PROBABILITY) MILLIONS	SIZE OF LUNAR BASE (NUMBER OF PERSONNEL) 1976	LUNAR MAN-YEAR AVERAGE COST (1970-1979) MILLIONS	CRITICAL DEVELOPMENT PROBLEM AREAS
EOR	15,300	14.5 (W/SPARE)	AUG. 69	18.2	$6490	$1240	12	$88.4	a. EARTH ORBIT RENDEZVOUS b. PROPELLANT TRANSFER c. C-5 LAUNCH VEHICLE d. STANDARD APOLLO CAPSULE
LOR	12,600 5,000 LEM	19.1	FEB. 69	16.1 (CM) 22.0 (LEM)	$5840	$620	10*	$77.4*	a. LUNAR ORBIT RENDEZVOUS b. LEM AND PERSONNEL TRANSFER c. C-5 LAUNCH VEHICLE d. STANDARD APOLLO CAPSULE
C-5 DIRECT	9,210	21.9	OCT. 68	16.7	$5690	$510	12	$61.4	a. HIGH ENERGY RETURN b. LIGHT WEIGHT CAPSULE c. C-5 LAUNCH VEHICLE
NOVA DIRECT	15,300	25.3	MAY 70	18.0	$6160	$630	15	$55.4	a. NOVA LAUNCH VEHICLE b. STANDARD APOLLO CAPSULE

Figure 2-11: Apollo Mission Mode Comparison [58].

first flight. Without a common analysis for each option, the uncertainty in the evaluation, and a lack of overall evaluation criterion, the Lunar Orbit Rendezvous (LOR) architecture was driven by political compromise between the centers and qualitative risk assessment from the decision makers [58].

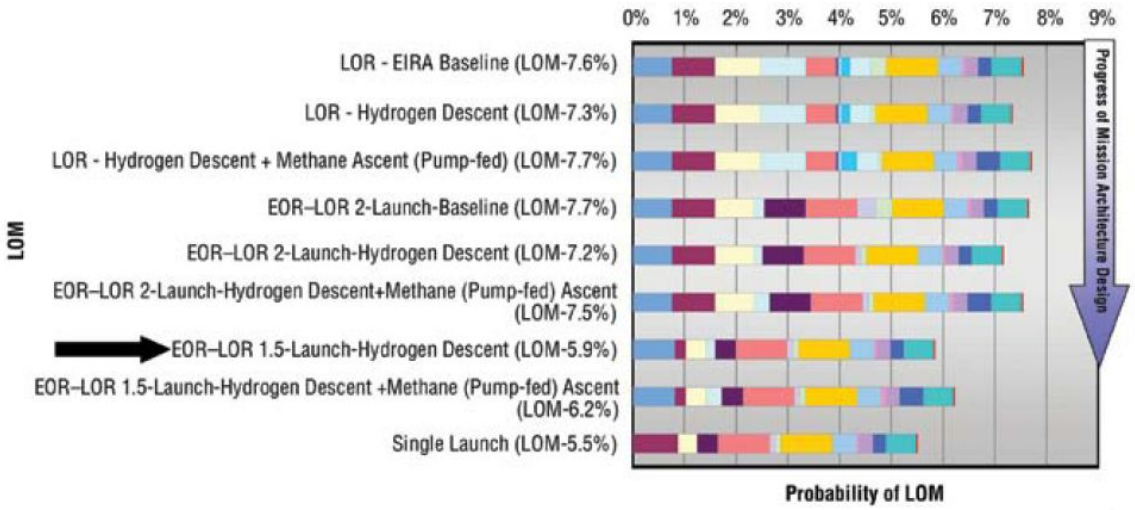

Figure 2-12: Loss of Mission Architecture Comparison [66].

The Exploration System Architecture Study was able to evaluate numerous architectures using systems engineering processes and tools. Figure 2-12 shows a comparison of the different architectures and their probability of loss of mission. As mentioned earlier, many different Figures of Merit were used to evaluate each architecture created during ESAS.

A variety of launch vehicle concepts were also evaluated for a given set of mission constraints. Figure 2-13 is a small representation of the different Cargo Launch Vehicles assessed for their use in the lunar campaign.

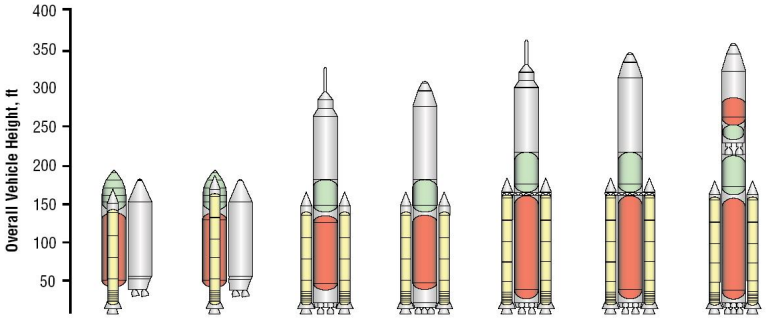

Figure 2-13: CaLV Design Candidates [66].

		Shuttle-derived CaLV				
		4-Segment RSRB Side-mount Cargo	5-Segment RSRB Side-mount Cargo	4-Segment RSRB In-line SDV Cargo	5-Segment RSRB/4 SSME Core In-line SDV Cargo	5-Segment RSRB/5 SSME Core In-line SDV Cargo Variant
	LV	20	21	24/25	26/27	27.3/13.1
FOMs	Probability of LOC	N/A	N/A	1 in 1170	1 in 915	1 in 2,021
	Probability of LOM	1 in 173	1 in 172	1 in 176	1 in 133	1 in 124
	Lunar Mission Flexibility					
	Mars Mission Extensibility					
	Commercial Extensibiity	N/A	N/A	N/A	N/A	N/A
	National Security Extensibility	N/A	N/A	N/A	N/A	N/A
	Cost Risk					
	Schedule Risk	N/A	N/A	N/A	N/A	N/A
	Political Risk					
	DDT&E Cost (family)	.85	1.03	.83	0.98	1.00
	Facilities Cost (family)	N/A	N/A	N/A	1.00	1.00

Figure 2-14: CaLV FOM Comparison [66].

As mentioned earlier, each CaLV concept was evaluated by six primary Figures of Merit (FOMs). An example of the FOMs for shuttle derived CaLV concepts is shown

in Figure 2-14. Due to the current computing capability and refinement of systems engineering processes, various CaLV designs were evaluated within a few months.

The Exploration System Architecture Study had a 90 day time constraint and thousands of alternative launch vehicle configurations were not considered. The present methodology aims to fill that information gap by creating the capability to quantitatively evaluate thousands of launch vehicle designs in a rapid manner. Additionally, ESAS used an integrated manual process of passing information from one discipline group to another for design. The design process can be improved with an integrated environment that can take advantage of numerical techniques to find an optimal solution. The next section further explains how this methodology could be used during the conceptual design process.

2.2.5 Methodology Utility

The methodology created in this dissertation will attempt to add to the information generated in ESAS by examining configurations that are "clean-sheet" launch vehicles. This methodology will begin with a configuration like the selected CaLV and re-open its design space by changing design variables, such as the number of engines and stage thrust-to-weight ratio. The goal is to examine which design options could be included on the CaLV to increase its reliability and how those design options affect the system cost. In order to make a fair comparison, the launch vehicle must meet the same mission objectives and constraints as the CaLV.

While ESAS used an integrated process, they did not create an integrated environment for launch vehicle design. Concepts were created that satisfied the mission constraints and then passed along to the reliability and cost disciplines. By using an integrated environment, the sensitivity of each launch vehicle configuration to different design parameters can be determined. Optimization can be included in an integrated environment to provide a mathematical foundation for selecting a concept

based on its system metrics. However, creating and using an integrated environment does have disadvantages compared to the process used in ESAS.

Using an integrated environment typically requires creation of parametric models for each discipline in a launch vehicle, which could reduce the fidelity of the design process. Furthermore, system experts may be removed from the design process with an automated environment, which also removes a level of fidelity. When using optimization, only quantifiable system metrics can be included. Qualitative system metrics, such as risk, must be evaluated after a vehicle design is completed. Therefore, optimization may find an optimal configuration that is later eliminated because of its development risk or flexibility.

The process created in this dissertation will attempt to remove some of the concerns regarding the use of an integrated environment for launch vehicle design. The fidelity of the models created for use in this dissertation will be comparable to the fidelity of the models used during ESAS. Additionally, while only system cost and reliability are chosen as the metrics to compare launch vehicle configurations, other quantifiable metrics can be included because of the manner in which this methodology was created. A key assumption during ESAS was the use of existing engines and the results shown in Section 4.2.4 include a comparison of a CaLV concept that relies upon the SSME and J-2S engines.

The benefits of using an integrated environment include rapid assessment of launch vehicle concepts and the finding of the significant parameters that drive the system metrics. Another benefit is using optimization to automate the process of finding the best combination of design variables for the system metrics. The time constraint of previous studies may be eliminated because thousands of different launch vehicle configurations can be evaluated within a few hours. The caveat is that the environment must be developed first. Finding the significant parameters should lead to further

study regarding these variables with the goal of providing additional information before any final decisions are made. The goal of this methodology is to create additional information and further assist a decision maker with selecting a final launch vehicle configuration.

2.3 Launch Vehicle Design Literature

There are a few books that have been written about conceptual launch vehicle design [31], [94], [38], [20]. Many of these references advocate using systems engineering principles and describe how to create models for each of the different disciplines. The mass estimates are completed using parametric equations; these equations calculate mass based upon system characteristics and are discussed in Section 3.1.3. Physics based modeling is recommended for the trajectory and propulsion disciplines and these books give excellent detail about how to create these models.

None of these books describe how to create an integrated environment that incorporates all of the disciplines required for launch vehicle design. A designer would have to use their own approach for integrating each of the disciplines when using the references discussed above. No guidance is given about which variables should pass from one discipline to another to enable integrated launch vehicle design. Additionally, very little is discussed about using optimization to find the best vehicle design. However, there is a book that outlines the conceptual design process for launch vehicles and explains how optimization can be included.

Reference [34] depicts an approach used for conceptual launch vehicle sizing at NASA's Langley Research Center (LaRC). The different tools used in the process are described and a flow diagram illustrates which discipline passes information to another discipline. Hammond also emphasizes the importance of introducing knowledge earlier in the design phase by using trade studies and sensitivity analysis. A similar figure to Figure 2-5 is shown, which describes how a paradigm shift is needed to better control

costs. Hammond reinforces the argument that costs are set by decisions made during the conceptual design phase.

An integrated environment for modeling hypersonic vehicles called "HOLIST" is discussed in Reference [34]. "[HOLIST] is used for design, analysis, and optimization of airbreathing hypersonic vehicles...HOLIST helps eliminate disconnects among disciplines, enable rapid multidisciplinary parametrics, allows the evaluation of design sensitivities, and enables optimization of the vehicle design and trajectory." [34] However, HOLIST does not include cost or reliability.

Hammond also reviews optimization techniques including how to incorporate existing analysis tools. Collaborative optimization is examined because this technique does not require modification of present analysis tools; the modules can be used as they currently exist. Additionally, these analysis modules can be run in parallel; thus, the analysis module that requires the longest operating time also determines the concept design time.

A collaborative missile design environment is also reviewed by Hammond. "This system provides analyses of missile system and subsystem performance in all the fundamental engineering disciplines including cost modeling, solid modeling, propulsion modeling, [etc.]..." [34]. A knowledge-based system then moves through the design environment to create a missile concept that matches the desired missile performance while satisfying the constraints. If the performance cannot be matched then "...the knowledge-based system will assist the user in determining which requirements and constraints should be eased to arrive at a viable design." [34]

Like many of the previously researched references, the details of implementing these approaches are left to be determined. In the approach used for sizing a conceptual launch vehicle, the reference mentions only point designs and it is unclear if the design tools are fully integrated.

2.3.1 Integrated Launch Vehicle Design

An early design process that nearly integrated the launch vehicle disciplines is discussed in Reference [90]. The authors present the design process used to create a fully reusable two stage launch vehicle. The traditional aerospace disciplines are incorporated, such as trajectory and propulsion, and trade studies are performed to determine different design characteristics, such as the staging point. The trade studies were completed one at a time with vehicle point designs created for each single variation in design variable. Quantitative cost and reliability models are not included, but they are discussed qualitatively; certain design options are favored because they are believed to increase reliability or reduce costs.

Reference [67] is one of the earliest approaches for creating an integrated environment for launch vehicle design. Olds combines the technical disciplines for the design of a rocket-based combined cycle concept into one framework and used optimization to find the minimum dry weight. The technical disciplines were represented by different analysis tools but neither reliability nor cost was included. A surrogate for cost, the dry mass, was used as the objective function and the optimization techniques minimized the dry mass.

While Olds showed that the performance disciplines could be integrated into a framework for launch vehicle design, there were some drawbacks to the approach. For each iteration of the design process, it was not guaranteed that a feasible launch vehicle would be created using the combination of design variables. Each cycle through the analysis modules required "four to eight hours" and a design usually needed three iterations before it was completed. Therefore, infeasible designs were being created with a process that could last up to a day. The acknowledgment is made that the computing power of today is orders of magnitude better compared to the computing power used in Reference [67]. However, the percentage of infeasible designs for one study was 33 percent which is a high percentage of designs that do not benefit the

conceptual design process. Finally, it was unclear how easily the reliability and cost disciplines could be added to the integrated environment. Adding extra variables would increase the run time but it was unknown how much additional time would be required.

Another early integrated design environment was created for hypersonic launch vehicles at the NASA Ames Research Center [83]. The Hypersonic Vehicle Optimization Code (HAVOC) integrates different performance disciplines, such as aerodynamics, trajectory, and propulsion, into a single monolithic design code. Various subroutines are used to represent each of the disciplines and a complete run of HAVOC results in a single point design.

While HAVOC represents another approach for creating an integrated launch vehicle design environment, the program has some drawbacks. First, HAVOC is limited by its focus on hypersonic launch vehicles. Additionally, HAVOC does not include the cost or reliability disciplines in its analysis. The subroutines must also be updated as higher fidelity modeling techniques become available as opposed to using presently developed discipline tools.

Another design approach was proposed by Unal and et al. that used Response Surface Methodology (RSM) and optimization for launch vehicle design [91]. A set of design variables was chosen for study and Design of Experiments (DOE) techniques were used to create a series of design runs with the input parameters. Each design run was evaluated by the disciplines to create a vehicle concept. Dry mass was used as the response variable and the parameter to minimize in the optimization scheme. A second order polynomial equation, also known as a response surface equation, was created using regression and calculated the dry mass of the launch vehicle based on the input parameter settings. The equation was used in an optimization scheme to determine the design variable settings that resulted in the lowest vehicle dry mass.

One disadvantage to using the RSM approach is that the process is limited by

the number of design variables. Reliability and cost were not included in this study and the number of design variables would grow in order to include those disciplines. The number of runs required to create a response surface equation increases quickly with the addition of more design variables. Furthermore, this process is limited by the range of the design variables. If the range is too large, then the response surface will produce a poor fit of the launch vehicle design process.

Braun and et al. applied collaborative optimization to integrated launch vehicle design and optimized a vehicle configuration for the lowest cost [4]. The cost considered technology applications and subsystem cost. The disciplines were represented with "stand-alone" analysis tools and were integrated into a single framework for optimization. The optimization problem contained 95 input parameters and 15 constraints.

The process used in Reference [4] was a good approach because it integrated heritage design tools. Additionally, the problem used a large number of design variables to optimize the launch vehicle. However, using collaborative optimization typically requires calculating gradients of the objective function. Using gradients is not conducive to problems with discrete variables, such as the number of engines. Braun and et al. were able to work around this by imposing constraints that corresponded to the discrete variables. However, the appearance is given that complete "clean-sheet" launch vehicles cannot be studied with this process because a discrete variable was imposing a specific constraint. In this case, the number of engines imposed a constraint on vehicle thrust-to-weight ratio, but these two variables can be decoupled in launch vehicle design.

Considerable time was also required in the process used by Braun and et al. [4] While computing power has increased by orders of magnitude since the study, the number of function calls was in the thousands. One of the benefits of using collaborative optimization is the process can be distributed among different computers.

Therefore, the time required for one cycle through the analysis process is equal to the time required for the longest discipline analysis. Yet, if the longest discipline requires a significant amount of time to run, then the complete process will also require significant amounts of time.

Collaborative optimization was also used in another integrated design environment to study the effects of technology on launch vehicle design [56]. In Reference [56], a set of technology scenarios were applied to a single stage to orbit launch vehicle with the goal of minimizing system cost. The system cost is a combination of the vehicle development and technology costs. Each technology scenario determined the total technology resources and the optimizer finds the best combination of technologies to minimize the total cost for a fixed performance level.

Moore and et al. [56] are subject to the same constraints as discussed in Reference [4]. Collaborative optimization requires gradient calculations; therefore, using discrete design variables such as the number of engines on a stage is not possible. The optimizer requires knowledge about the cost of technology to reach certain thresholds. Therefore, discipline experts must be involved in the design process to estimate how the performance and system cost is affected by various technologies. Additionally, there is no quantitative reliability model; therefore, design options may beneficial for reducing cost but could also lower vehicle reliability.

Reference [79] reviews a survey of multidisciplinary analysis techniques and their application to launch vehicle design. Rowell and et al. [79] discuss the disciplines typically required for launch vehicle design and the areas where an increase in model fidelity is needed. Specific areas which need an improvement in model fidelity include operations analysis, cost estimation, and reliability. The authors compare and contrast using a monolithic synthesis code, such as HAVOC, for launch vehicle design with an environment where discipline specific tools are integrated together. A higher level of fidelity is typically achieved for launch vehicle design by using more specific

discipline tools [79]. The authors finish with a review of optimization techniques and a vision for future launch vehicle design environments.

Monell and et al. [55] discussed an integrated design environment used for the Next Generation Launch Technology program. The Advanced Engineering Environment (AEE) was used for evaluating reusable launch vehicles and integrated the performance, cost, and reliability disciplines. The AEE also attempted to address data management with the creation of a database environment for storing previous design cases.

The AEE did have some disadvantages. The reliability discipline was recognized as one of the least mature disciplines within the environment. Additionally, it was unclear if the reliability varied as different design options were considered. There was also no optimization within the design environment. The authors discuss problems with tool maturity since they relied upon discipline experts to develop the analysis modules [55]. There was a lack of collaboration which led to various integration challenges. Once the environment was created, six weeks were required to complete 129 designs.

Reference [25] reviewed a reliability and safety tool created for application within an integrated environment for conceptual space vehicle design. The tool focused on second generation Shuttle concepts and other reusable space vehicles. Analogies are drawn from previous Shuttle reliability analyses [25] to provide the baseline reliability estimates in the risk oriented program optimization tool (ROPOT). The tool compares a functional breakdown of a new design with the Shuttle to make determinations about the system reliability and safety. Scenarios are examined where the reliability of certain components within the new concept is increased to examine the effects on system reliability. The results illustrate how specific component reliability thresholds can be reached and further increasing component reliability does not provide a large system reliability benefit. The design options that enable the component reliability

to reach those thresholds are also discussed.

Another study using ROPOT was completed the following year [27]. In this study, different reusable space vehicle concepts were examined for their reliability and safety metrics. The reusable concepts had different performance levels and required different launch vehicles to perform the orbit insertion. A cost model was included that calculated the development and operations cost of each design. While the application focused on the reusable space vehicle, the reliability and safety metrics were also influenced by the choice of launch vehicle used to boost the reusable concept. Various mission scenarios were created and the reusable concepts were evaluated across a set of reliability and safety metrics.

While the approach in Reference [25] and [27] provides a comparison of different reusable concepts, the use of optimization is unclear. There is little discussion about optimizing the design variables to provide a minimum cost solution with high system reliability and safety. Furthermore, the integration into a larger environment with the traditional performance disciplines is not discussed in great detail. The authors do not reveal the level of difficulty for modifying the baseline reliability estimates as more data becomes available. Finally, the comparison of space vehicles with different performance levels makes the selection of a final concept more challenging because the capability of each concept is different.

A more recent publication provided a comprehensive review of launch vehicle design methods, including optimization, for use in an integrated environment [80]. Rowell and Korte discuss the needs for future launch vehicle design, such as higher fidelity modeling, continued advances in optimization, and the creation of integration frameworks. The authors discuss how the integration framework used for coupling the discipline tools may determine the optimization technique for launch vehicle design. Ideally, the process of selecting an optimization technique for a design process

should be decoupled from the integration framework, but for some commercial software packages, the optimization technique is in fact determined by the framework employed.

Each of the technical disciplines is reviewed along with their corresponding design variables in Reference [80]. Rowell and Korte mention that the fidelity of some disciplines, such as operations analysis, reliability, and cost estimation do not have the same fidelity as the more traditional aerospace disciplines. Different optimization techniques and the use of uncertainty analysis are also discussed for their application to launch vehicle design. Rowell and Korte review different studies that used integrated launch vehicle design and then make recommendations about the capabilities needed to further this area of research.

Rowell and Korte discuss uncertainty analysis, which is not used in most past studies [80]. Uncertainty analysis is important during conceptual design because some of the disciplines, such as mass estimates and cost, rely upon historical data to forecast future values. Using uncertainty analysis enables a design engineer to examine the range of possible results during the launch vehicle design process.

McCormick created a process for the optimization of launch vehicles using an integrated environment and including uncertainty analysis [52]. A launch vehicle design was optimized for minimum dry mass while including uncertainty from three different disciplines. Reference [52] focused more on determining how to include uncertainty analysis and the best method for performing uncertainty analysis. A comparison was made between different uncertainty techniques such as Monte Carlo Simulation and Discrete Probability Optimal Matching Distribution. Another important component of Reference [52] was the capability to distribute the analysis among multiple networks.

While McCormick provided a good reference for how to use uncertainty in an

integrated framework for launch vehicle design, there is still an opportunity for additional enhancements. The optimization process involved only three disciplines and did not include cost and reliability. Furthermore, the optimization technique used a gradient based method; an approach for including discrete design variables is not included. Finally, the variable ranges are left to be determined by the engineer with little information about where to find uncertainty ranges.

In summary, there have been numerous launch vehicle design studies that implement a wide range of approaches. Some rely upon optimization of the analysis disciplines while others use approximations to speed up the design process. In most studies, the reliability and cost disciplines are not included and the ease at which they can be added is unknown to the outside reader. Having a flexible process that can include additional models based on the design engineer's preferences is an advantage because there are many different ways to approach launch vehicle design. In many of these studies, uncertainty analysis is not included. Uncertainty analysis is another tool that can be used in launch vehicle design to provide additional information by revealing the range of the system metrics.

The methodology outlined in this dissertation will attempt to improve upon the design processes outlined in the literature. The contribution of this methodology would be a process that can be used to rapidly assess thousands of launch vehicle configurations in a matter of hours while including uncertainty analysis and the reliability discipline. While the focus is evaluating designs for their cost and reliability, the methodology is flexible enough to include additional quantitative system metrics. The result of using this methodology is increased knowledge about a launch vehicle design for making more informed decisions during the conceptual design phase.

2.4 Related Aerospace System Studies

Reference [24] uses heritage data to forecast future launch vehicle reliability. Fragola and Collins examine the Saturn, Jupiter, Juno, and Redstone launch vehicle families to predict the Saturn V reliability if the number of Saturn V flights was increased beyond twelve. The authors use operational anomalies along with mission success rates to forecast their reliability estimates. The inclusion of launch anomalies reveals that the Saturn V may have been closer to failure than previously realized; the anomalies show a more consistent reliability pattern with the other launch vehicles of the Apollo era.

The authors discuss how including heritage data is important because traditional reliability analysis may be too optimistic. In this methodology, the historical reliability analysis of launch vehicles is considered and results are presented for both the Saturn V and CaLV application. In the approach discussed in Reference [24], it is not clear how a conceptual launch vehicle design could use the data beyond a first order analysis. Specifically, launch vehicle reliability will change with configuration changes, but it was unclear how these configuration changes would affect the reliability forecast in Reference [24].

A detailed reliability analysis was performed for the Crew Launch Vehicle (CLV), which will carry the astronauts to orbit once the Shuttle is retired [26]. Fragola and et al. [26] evaluated the probability of mission success and the probability of loss of crew for the CLV. The study includes detailed failure analysis using high fidelity modeling such as finite element analysis. The detailed failure analysis leads to a rigorous safety examination for all phases of operational flight.

The approach used in Reference [26] may be difficult to apply during the conceptual design phase. Engineering judgment is relied on to provide some reliability estimates; therefore, discipline experts would have to be involved with the conceptual design process to use this detailed approach. Additionally, it was unclear how

changing the configuration, such as using engine out, would affect the reliability calculations. Rapid reliability estimates may not be possible by the approach detailed in Reference [26] because altering the configuration may change the detailed failure models. While Reference [26] is a higher fidelity reliability analysis compared to this methodology, the significant reliability drivers are still revealed in the current methodology because of the reliance on the baseline launch vehicle reliability estimates.

Other aerospace sectors have completed integrated design studies. One of the earliest examples is an aircraft design synthesis code created by Galloway and et al. [29] The General Aviation Synthesis Program (GASP) performed parametric design studies for aircraft during the conceptual design phase. GASP was a monolithic design code with subroutines representing the various performance disciplines. Within GASP, an aircraft design was created and then evaluated for its cost metrics. There was no reliability or optimization within this design environment.

As mentioned earlier, Reference [34] reviews an integrated missile design process that employs a knowledge-based system to create a concept. In another study, collaborative optimization was studied for the conceptual design of aircraft [44]. The study was completed by some of the same authors who published the application of collaborative optimization to launch vehicle design. The collaborative optimization of an aircraft is similar to a launch vehicle because the disciplines are evaluated using parallel computing and gradient based techniques are used to find the optimal configuration.

Another paper reviewed many of the aircraft design processes that have been employed [53]. McMasters and Cummings showed that aircraft conceptual design relies upon many of the same techniques used in launch vehicle design. For example, aircraft design uses analysis modules for each of the disciplines in an integrated framework with optimization. Multidisciplinary optimization techniques were reviewed in Reference [53] including how they were applied to the aircraft design process. Finally,

the authors highlighted many of the same challenges faced during conceptual launch vehicle design: the fidelity of models during the conceptual design phase and the need for advancing optimization techniques.

Rotorcraft design also faces many of the same problems incurred by both the launch vehicle and aircraft design communities. A comprehensive survey paper showed that a comparable approach to launch vehicle design could be used for rotorcraft design [30]. A set of analysis modules are integrated together in one environment and optimization is used to find the best rotorcraft design. Again, model fidelity is a large concern because of errors caused by using low fidelity modeling to enable vehicle optimization. Aeroelastic analysis is specifically cited because of the large errors that occur when comparing an optimized design with a higher fidelity aeroelastic model. The computational time when using the higher fidelity aeroelastic analysis is extremely high and nearly prohibitive for rotorcraft optimization. However, optimization in rotorcraft design has been shown to lead to better solutions; therefore, optimization may be better used as a guide to find improved concepts [30].

In summary, other aerospace industries may use similar approaches for performing design. Many of the problems that plague launch vehicle designers, such as computational time and model fidelity, are also faced by other aerospace system engineers. However, system engineers are able to achieve similar goals during the conceptual design phase, which are to determine the driving parameters and move toward an optimal design. There are still other approaches to system design, especially when considering cost and reliability. Value based methods and reliability allocation techniques are two alternative approaches that may be useful for design.

2.5 Alternate Design Approaches to Couple Cost and Reliability

One area which examines linking reliability and cost discusses relating the cost of reliability to a financial concept known as Net Present Value (NPV). NPV is a calculation used for determining the future net cash flow while accounting for the time value of money. In Saleh and Marais [82], the authors' goal is to determine the optimum level of reliability by finding the maximum value of NPV, which would result in a positive cash flow. Different levels of redundancy are discussed and the NPV of each design is compared with an example satellite application.

The authors begin by demonstrating how current estimates of NPV over-estimate the system value since reliability is not incorporated. A different calculation for NPV, which includes reliability, is then used to compare the NPV of a theoretical system with 100% reliability. This comparison establishes the cost benefit of improved reliability. The value of redundancy is then incorporated by using a new failure rate in the calculation of NPV to determine the NPV of a system with a specific level of redundancy. This calculation becomes the basis for the cost of increasing system reliability. For these calculations, a cash flow model has been created using assumptions regarding the currency generated when the system is in operation. Finally, the cost of using different levels of redundancy is calculated by multiplying the additional components by their individual cost. An optimizer is used to determine the design with the largest difference between its cost for increased reliability in the development phase and the operational value added by using increased reliability.

Saleh and Marais [82] is a well developed model for determining the level of reliability while incorporating cost. This model could be applied to the area of human space transportation if the value of exploration could be established. The cost of unreliability could be quantified by using the cost of investigations when failure occurs. However, establishing the value of exploration is extremely difficult. The methodology

proposed in this body of work further differs because it integrates the performance, cost, and reliability into one integrated design environment. The design engineer can examine the sensitivities of vehicle mass and system cost to increasing system reliability.

One of the most interesting aspects of Saleh and Marais work [82] is the quantification of using component redundancy. This calculation is put into units easily understood by system managers without relying upon assumptions used by current cost estimating tools in the space industry. Therefore, further study is needed to combine the best practices of both methodologies.

An additional study applied a genetic algorithm to optimize a system's reliability with a budget constraint [69]. Uncertainty analysis was included by using distributions for the component failure rates instead of single point values. The methodology application was a personal computer and the goal was to find the optimal configuration by using redundancy to increase system reliability while considering a hard cost constraint. Each design was run 200 times and the 5^{th} percentile of the system reliability was considered that design's objective function evaluation. Figure 2-15 illustrates the baseline configuration used in the study.

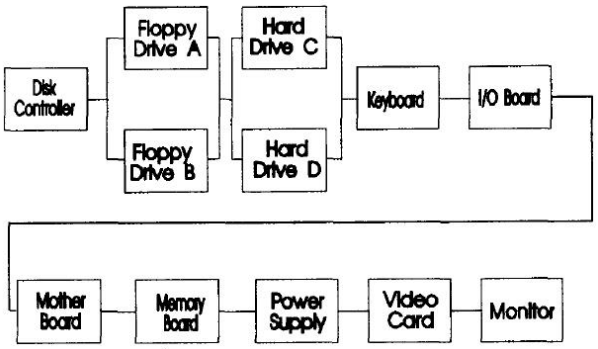

Figure 2-15: Block Diagram of Computer Application [69].

The approach in Reference [69] provides a baseline that can be improved upon for application to launch vehicle design. While only redundancy options were included

in Reference [69], reducing the operating time of a launch vehicle is another way to improve its reliability if the failure rates are constant. Additionally, changing the configuration of the computer only affected cost and reliability. For launch vehicle design, adding subsystem redundancy or using engine out requires re-sizing the vehicle to meet the payload requirement. Therefore, selecting different combinations of redundancy may result in infeasible configurations. However, the study showed that the reliability model of a configuration can be changed dynamically during the design process, which is important when studying the different configurations of a launch vehicle.

Another study also used genetic algorithms to solve a reliability optimization problem [7]. The goal was to determine the optimum level of redundancy for each subsystem in a series of subsystems. The subsystems had multiple component choices that could be used to provide redundancy. Each of the component choices had a given mass, cost, and reliability. The genetic algorithm then selects the best combination of component choices for each subsystem that maximized the reliability of the complete system.

The approach described in Reference [7] may be too simplistic for launch vehicle design. Selecting different reliability strategies for a launch vehicle cannot be based on a known mass, reliability, or cost effect because the problem is coupled. Using engine out for a three engine configuration will produce a very different result compared to using engine out on a five engine configuration. Additionally, the problem discussed in Reference [7] was deterministic and did not include any uncertainty in the mass, reliability, or cost estimates. Therefore, a design engineer could not evaluate the range of system metrics for the optimized design.

Many different studies have been dedicated to solving the reliability allocation problem, which is the problem of finding the most cost effective solution for high system reliability. A design process that attempts to find the optimal balance of

reliability and cost for a launch vehicle is essentially the same type of problem. Different strategies are applied to increase system reliability while studying the penalties imposed on the concept for using those reliability strategies. The difference occurs because of the manner in which the system metrics are evaluated. For launch vehicles, every change in configuration which increases system reliability must go through the complete design cycle before the system metrics can be measured. As mentioned earlier, different configurations will respond differently to the same reliability strategy. Yet, there are lessons learned from examining reliability allocation techniques which are included in this methodology.

2.6 Summary of Techniques

The goal of systems engineering and its principles are to evaluate all aspects of a design's life-cycle in order to select a final design, as shown in Figure 2-1. The elements of a system's life-cycle were illustrated in Figure 2-2. Considering the elements of a system's life-cycle is important because the cost is largely determined by the decisions that are made during the design, as shown in Figure 2-5.

Cost is not the only metric for comparing alternative design configurations. While the majority of the Section 2.1 was focused on making decisions to minimize Life-Cycle Cost (LCC), design engineers may want to include other metrics, such as reliability, when evaluating different concepts. A minimum cost design may have a much lower reliability compared to an alternative configuration with a higher cost. The process outlined in this dissertation includes both system cost and reliability, and is flexible enough to add other quantifiable system metrics.

A variety of design processes exist for both launch vehicle design and linking cost and reliability. Many of the launch vehicle design studies integrated their design disciplines into one framework and used optimization to find the best solution; however, few incorporated cost and reliability into the design environment. Additionally, few

studies were found which used uncertainty analysis in the design of launch vehicles. This methodology will try to close some of the missing gaps while including the best practices from previous work.

This dissertation fills a void by outlining a detailed process explaining how to create an integrated environment for use in launch vehicle design. Major elements of the launch vehicle's life-cycle are considered in order to evaluate many different configurations with a specific set of mission objectives. The fidelity of launch vehicle reliability analysis is increased compared to previous design environments. The fidelity of the performance and cost analyses will still be comparable to current launch vehicle design approaches; however, as with other design studies, the cost discipline would benefit from using higher fidelity analysis techniques. Additionally, the efficiency of the launch vehicle design process is improved compared to previous design studies because thousands of launch vehicle configurations can be quantitatively evaluated within a few hours; this efficiency has not been demonstrated by any of the previous design studies.

The parameters that have the largest effect on the system metrics of a launch vehicle can be determined by using this methodology. The significant parameters are important because their settings will heavily influence the system cost. Additionally, information is created which explains how system cost is affected by increases in launch vehicle reliability. The creation of the integrated environment provides the capability to perform rapid launch vehicle assessment and increase the amount of information that can be introduced during the conceptual design phase.

2.7 Research Questions

The methodology outlined in this dissertation will be used to solve a series of research questions. These research questions are derived from the literature and experience with launch vehicle design. A set of hypotheses answering the research questions is

presented in Section 3.9.

1. How is launch vehicle reliability increased?
    - What techniques exist for increasing launch vehicle reliability?
    - Are any techniques favored over another (such as engine out versus adding power subsystem redundancy)?
2. What improvements can be made to the launch vehicle design process?
    - How can reliability be included in launch vehicle design?
    - What tools should be included within the conceptual design framework?
    - What design variables should be passed among the different disciplines?
    - What time improvements can be made over the previously cited research?
3. How is the system affected by configuration changes?
    - How much is system reliability affected by including (1) subsystem redundancy such as dual power subsystems, (2) engine out, and/or (3) reducing flight time?
    - What are the performance effects of using (1) subsystem redundancy, (2) engine out, and/or (3) reducing operating time?
    - How is cost affected by the various reliability strategies?
4. How can the launch vehicle design process include uncertainty analysis?
    - Which disciplines should include uncertainty analysis?
    - How are the uncertainty ranges determined?

CHAPTER III

METHODOLOGY

The methodology for linking system cost and reliability is developed in this chapter by revealing the details of how to create the necessary performance, cost, and reliability models. Launch vehicle sizing is discussed in this chapter to provide a foundation for why certain disciplines are included in the launch vehicle design process. An examination of different reliability techniques is also included in this chapter along with the present method for calculating launch vehicle reliability. Various cost estimation procedures are reviewed and the approach for calculating system cost is presented. Optimization techniques are considered and a justification is made for using a genetic algorithm. The final sections of this chapter show how the integrated environment is created using the performance, cost, and reliability models developed in this dissertation.

3.1 Performance Disciplines

The methodology for linking cost and reliability relies upon performance models to complete the sizing of a launch vehicle. The effects of improving reliability through the use of engine out or adding full subsystem redundancy will not be known unless the performance aspects are also included. This section describes one method for creating and integrating the performance models of a launch vehicle. The goal of integrating the performance models is to calculate vehicle characteristics, such as the subsystem masses and stage burn time, for use in the cost and reliability disciplines.

3.1.1 Launch Vehicle Description

The goal of a launch vehicle is to launch a specific mass, the payload, into a specific orbit. For example, the Falcon 1 launch vehicle advertises the ability to launch a payload weighing 1,590 pounds to a 108 nautical mile circular orbit [19] while the Space Transportation System (STS) can reach a circular orbit of 110 nautical mile with a 63,500 pound payload [41]. The payload mass and final orbit requirements for a launch vehicle may vary depending on the requirements of the mission. For example, the STS can reach a 320 nautical mile orbit if the maximum payload is reduced to 40,600 pounds [41].

A launch vehicle will use a series of stages to accomplish its mission. These stages are stacked on top of each other to form the vehicle, as shown in Figure 2-7 for the Saturn V. The Saturn V was a three stage launch vehicle responsible for launching the Lunar Module, and the Command and Service Module (CSM) to the Moon. Each stage in Figure 2-7 fired sequentially beginning with the lowest stage. Each stage relied upon its own set of subsystems for successful operation. For example, the S-IC stage in Figure 2-7 had its own set of engines, avionics, power, and other subsystems that were all integrated within the stage. Once the S-IC stage performed its mission, the S-IC stage would drop off the vehicle and the S-II stage would begin its mission. A successful launch occurs when all stages had completed their individual missions.

Decisions about launch vehicle characteristics, such as the number of stages, are made during the conceptual design phase. These decisions are made by creating the different launch vehicle configurations and calculating the vehicle's system metrics. The performance metrics typically include the vehicle's mass, its thrust to weight ratio, the trajectory a vehicle will fly, and the required engine performance. A number of different analysis modules are evaluated to calculate the performance metrics during conceptual design. The analysis modules used to evaluate the performance metrics are discussed in this section.

3.1.2 Mission Constraints

When evaluating a series of launch vehicle configurations, the mission constraints should remain constant for a fair comparison. The payload and the final orbit are examples of two mission constraints. The payload is the specific mass that must reach a particular orbit. Additional mission constraints may exist, such as maximum dynamic pressure (max q) and maximum acceleration (max gs). These constraints will lead to a trajectory that requires more propellant for the launch vehicle when compared to a trajectory without the maximum dynamic pressure and/or maximum acceleration constraint. The explanation for requiring additional propellant mass when there are trajectory constraints is discussed in Section 3.1.6.

The mission constraints for the Saturn V and Cargo Launch Vehicle (CaLV) applications are listed in Appendix I. These constraints are the same mission constraints as the original launch vehicles. For the Saturn V, the final orbit parameters were calculated from mission performance [84], while the mission objectives for the CaLV were found within the Exploration System Architecture Study [66].

3.1.3 Mass Estimates

The mass estimates of a launch vehicle are determined by using Mass Estimating Relationships (MER). An MER is an equation developed from regression of historical databases that uses vehicle characteristics to estimate the mass of a subsystem or component. Since a launch vehicle is a one of a kind system, there is some error when using MERs because of the reliance upon historical space systems to forecast future subsystem masses.

The MERs used in the application of the methodology are from Rohrschneider [78]. An example MER is shown in Equation 3-1. This equation estimates the mass of the crew cabin from the number of crew. The values “2347” and “0.5” are estimated using a regression analysis of the historical database.

$$M_{CrewCabin}[lb] = 2347 * N_{crew}^{0.5} \tag{3-1}$$

The Work Breakdown Structure (WBS) for the Saturn V is listed in Appendix E. Each of the subsystems listed in Appendix E has an associated MER used to estimate the mass of that subsystem. A comparison with the actual Saturn V [95] is also listed in Appendix E. The CaLV WBS is listed in Appendix E with a comparison between ESAS [66] and the model used in this dissertation. For the CaLV, the models created from previous work by Young and et al. [99] were built upon for application of this methodology.

3.1.4 Propulsion

Another analysis area used to complete a launch vehicle design is the propulsion discipline. The propulsion model calculates the required engine characteristics based upon the design configuration. Using a conceptual design tool, engine characteristics such as the engine thrust, engine thrust-to-weight ratio, and Isp are determined.

The engine thrust provides the vehicle's acceleration, while the engine thrust-to-weight ratio provides a higher fidelity method for calculating engine mass when compared with MERs. Engine Isp is a measure of efficiency for a rocket engine, similar to the miles per gallon rating in an automotive motor. Isp measures how much thrust can be provided compared to the rate of the propellant burned; Isp units are in seconds. Equation 3-2 illustrates how to calculate Isp, where 'T' is the thrust and $\dot{m}_{prop}$ is the propellant mass flow rate.

$$Isp[s] = \frac{T}{g_0 * \dot{m}_{prop}} \tag{3-2}$$

Since the thrust varies depending on the ambient pressure, the Isp will also vary depending on this pressure. A high vacuum Isp value for an engine that uses liquid propellants is 450 seconds. The Solid Rocket Boosters on the Space Transportation

System have a vacuum Isp of around 266 seconds; solid rockets are less efficient than liquid engines.

A conceptual powerhead design code called Rocket Engine Design Tool for Optimal Performance - 2 (REDTOP-2) [74] is used for the analysis in this methodology. Figure 3-1 illustrates the user interface for REDTOP-2. REDTOP-2 requires a user to set a number of design parameters such as the engine thrust level, chamber pressure, and cycle type to calculate the desired output variables. The output variables in this methodology are Isp and engine thrust-to-weight ratio which have excellent agreement with all relevant rockets that have been produced.

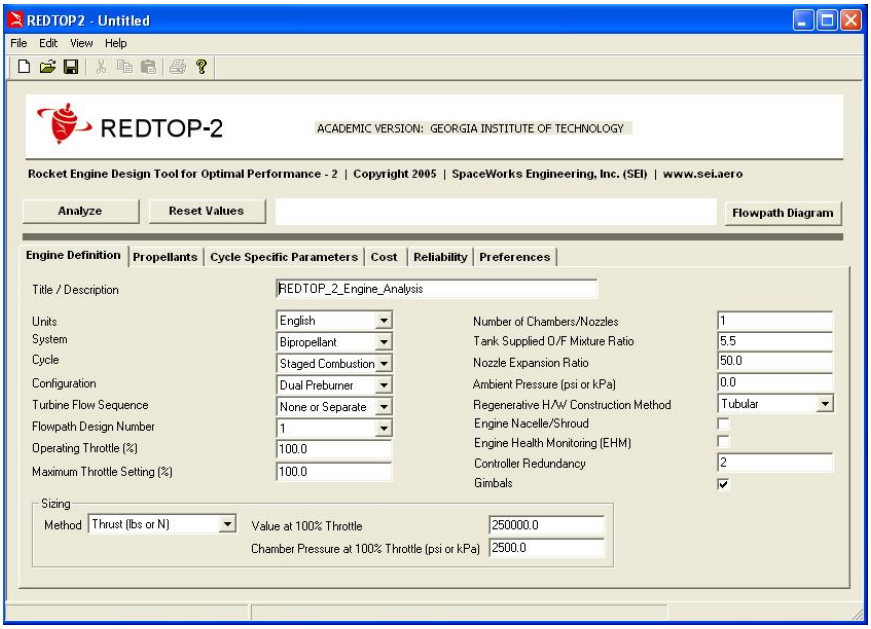

Figure 3-1: REDTOP-2 User Interface.

3.1.5 Trajectory Analysis

To finish sizing a launch vehicle, the propellant mass is required which can be calculated using trajectory analysis. The trajectory discipline depends upon the mission constraints, such as those discussed in Section 3.1.2, along with a set of input variables. These input variables include the vehicle thrust-to-weight ratio, the dry mass of each stage, and the Isp of the engine on each stage.

The trajectory analysis in this methodology is completed by using the Program to Optimize Simulated Trajectories (POST) [71], which is a three degree of freedom trajectory simulation widely used at NASA. The trajectory is solved by integrating the equations of motion over time for a specific set of mission objectives. POST can be used to find a trajectory that minimizes the amount of propellant required. The vehicle mass will decrease because the mass of the tanks and supporting structure is reduced when the propellant mass decreases. Additionally, graphs such as the launch vehicle position versus time and the acceleration versus time can be created once the trajectory analysis is completed.

Another parameter calculated with trajectory analysis is the burn time of each stage on the launch vehicle. The burn time is important for the reliability analysis because the burn time will dictate how long each subsystem needs to operate. Table 3-1 is a first order reliability comparison of the S-II stage of the Saturn V. As the burn time increases on the S-II stage, the reliability decreases. This occurs because of the governing failure distribution that is used to calculate reliability which is discussed in Section 3.3.2. Table 3-1 demonstrates how the trajectory and reliability disciplines are coupled.

Table 3-1: S-II Reliability Comparison.

Burn Time [s]	**Stage Reliability**
371	0.893
680	0.813

3.1.6 Performance Parameters

Creating a conceptual launch vehicle design requires iteration of certain parameters between the trajectory, mass, and propulsion disciplines. The iteration process is discussed in more detail in Section 3.1.7. A few of the iteration parameters are in the rocket equation, shown in Equation 3-3.

$$\int_i^f \delta V = g_0 \int_f^i Isp(\frac{dm}{M}) - \int_i^f (\frac{D}{m})dt - \int_i^f g * (sin\gamma)dt - TVC_{losses} \tag{3-3}$$

The rocket equation is used to determine the amount of velocity boost to a payload provided by its launch vehicle; the velocity boost is referred to as "delta-V". A payload has been defined as the mass needed at a specified position and velocity. The first parameter in Equation 3-3 is gravity and the second parameter, Isp, was discussed earlier in Section 3.1.4.

The next term in Equation 3-3, $\frac{dm}{M}$, is the natural logarithm of the mass ratio after completing the integration. Mass ratio is defined as the initial mass of the vehicle divided by the final mass of the vehicle; Equation 3-4 illustrates this relationship.

$$MR = \frac{M_{initial}}{M_{final}} \tag{3-4}$$

The initial mass is equivalent to the gross lift-off mass for a launch vehicle while the final mass is the used propellant mass subtracted from the gross lift-off mass. The final mass is also equivalent to the dry mass of the vehicle plus any residual propellants. The dry mass of a vehicle is all of the hardware, such as the propulsion and avionics subsystems, needed to create a launch vehicle. The additional terms in Equation 3-3 will be discussed later.

The mass ratio reveals the effectiveness of the vehicle for providing additional velocity. A higher mass ratio leads to a higher velocity change provided by the propulsive vehicle. Figure 3-2 is a notional example that shows how the delta-V increases with an increasing mass ratio. The analysis for Figure 3-2 included no losses and an Isp of 450 seconds. For reference, the CaLV used later in this dissertation has a baseline mass ratio of 3.5 for the first stage and 4.2 for the second stage.

An infinite mass ratio is impossible to achieve because increasing the propellant mass increases the tank mass. As a result, the vehicle gross mass will increase and

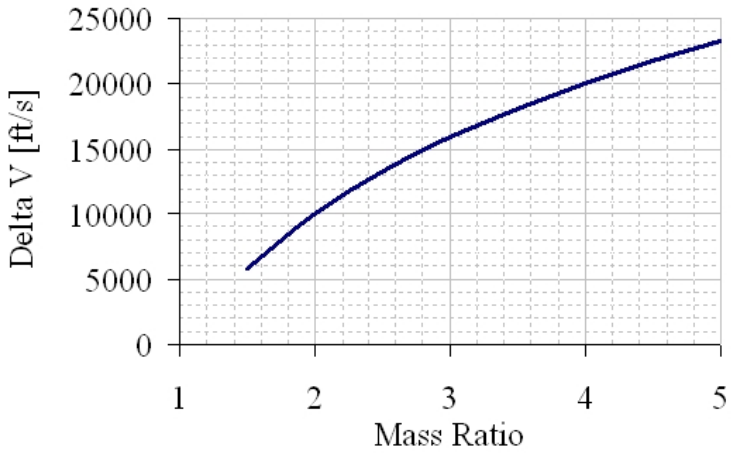

Figure 3-2: Effects on Delta V of Increasing the Mass Ratio.

the thrust of the engine must be increased in order to maintain a constant vehicle thrust-to-weight ratio, which is important for the trajectory. Therefore, increasing the gross mass by increasing the propellant mass can cause the required engine thrust to reach an infeasible level.

The thrust-to-weight ratio of the vehicle is important due to the remaining terms in Equation 3-3 because they determine the time of flight. These terms are the losses that occur while the vehicle is performing its propulsive maneuvers. The $\frac{D}{m}$ term is the velocity loss due to drag since the vehicle is flying in the atmosphere; if the vehicle is already in orbit then this term is negligible. The next term, $g * (sin\gamma)$, is the velocity loss due to gravity. This loss occurs because the vehicle is partly thrusting in the same direction as the gravity force. For example, a launch vehicle begins its trajectory with the thrust vector aligned in the opposite direction of gravity. Therefore, the vehicle is ascending to orbit while overcoming gravity. As the vehicle begins to pitch over toward its final flight path angle, the gravity losses lessen because the acceleration vector is no longer in the complete opposite direction as the gravity vector. The flight path angle is defined as the angle between the velocity vector and the local horizon; the local horizon is defined as a perpendicular line to the position

vector [32]. The final loss in Equation 3-3 is the thrust vector loss which occurs because the acceleration and position vector are not aligned. These vectors are not aligned because the vehicle is changing position while thrusting.

The vehicle thrust-to-weight ratio determines the trajectory that is flown by the vehicle. With a higher thrust-to-weight ratio, a launch vehicle can quickly escape the dense part of the atmosphere and attempt to minimize drag losses. Additionally, the vehicle can begin to pitch over to minimize gravity losses after escaping the dense atmosphere. However, there is a "sweet spot" for minimizing losses because of the interaction between the propellant mass and the dry mass of the vehicle. As the thrust-to-weight ratio increases, the required dry mass may increase, which increases the system cost. However, if the thrust-to-weight ratio is too low, then velocity losses increase, which increases the required propellant mass, which then increases the required dry mass.

Figure 3-3 is a comparison between two POST trajectories delivering the same payload to orbit. The trajectories have been optimized for a minimum propellant mass solution. The trajectories differ because of their different vehicle thrust-to-weight ratios. The solid line trajectory is the original Saturn V, while the dashed line trajectory is a Saturn V configuration with engine out on the S-II stage.

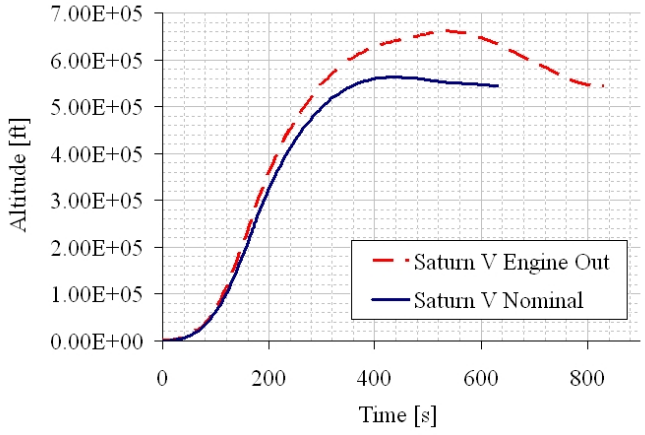

Figure 3-3: Saturn V Trajectory Comparison.

The vehicle thrust-to-weight ratio of the dashed line trajectory is lower than the nominal Saturn V; this can be seen in Figure 3-4 where the vehicle with the solid line trajectory reaches a higher velocity at 400 seconds compared to the vehicle with the dashed line trajectory. The vehicle with the dashed line trajectory will not reach its orbital velocity until much later in the flight, which increases its required propellant mass compared to the nominal Saturn V.

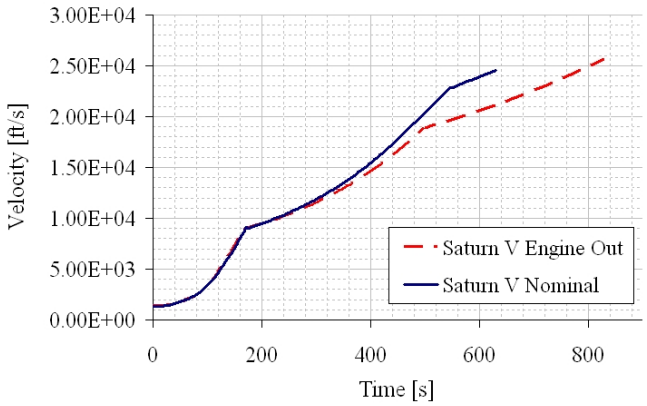

Figure 3-4: Saturn V Velocity Comparison.

The vehicle with the dashed line trajectory is exhibiting a behavior called lofting, where a vehicle reaches a higher than necessary altitude because it does not have the proper velocity at the required altitude. Therefore, the vehicle with the dashed line trajectory must continue to burn until it reaches the required orbital velocity; this increases the propellant mass compared to the nominal Saturn V trajectory. In Figure 3-3, the vehicle represented by the dashed line trajectory must have a higher mass ratio than the nominal Saturn V because the vehicle with the dashed line trajectory is overcoming more losses.

While a minimum propellant mass trajectory will minimize the dry mass of a launch vehicle, it is unknown if a minimum dry mass configuration is an optimal design with regard to cost and reliability. Figure 3-32 will show that the engine cost increases with engine thrust. Therefore, while minimizing the propellant mass will

lead to a lower dry mass, the thrust required to achieve this trajectory may result in a higher vehicle cost compared to a configuration that does not use the optimal trajectory. Only an integrated model will be able to determine the full effects on the system cost and reliability of changing the thrust-to-weight ratio.

The vehicle thrust-to-weight ratio can change due to a number of parameters. A decrease in engine thrust will lead to a lower vehicle thrust-to-weight ratio and may increase the required propellant mass to provide the velocity boost. Adding subsystem redundancy by using multiple subsystems will decrease the vehicle thrust-to-weight ratio because the dry mass will increase with additional subsystem mass. Mass sensitivity ratio is the sensitivity of vehicle mass to changes in the vehicle configuration. Equation 3-5 illustrates the mass sensitivity ratio used to examine the sensitivity of the Saturn V launch vehicle to changes in mass.

$$MassSensitivityRatio_{Mass} = \frac{MassGrowth_{Element}}{AddedMass_{Element}} \tag{3-5}$$

To calculate Equation 3-5, mass is added to a stage, such as the S-IVB. The entire vehicle grows in size to account for the additional mass and this change in mass from the original configuration is divided by the added mass. Table 3-2 lists how the mass sensitivity ratio changes as mass is increased on different stages of the Saturn V.

Table 3-2: Saturn V Mass Sensitivity.

Element	**S-IVB**	**S-II**	**S-IC**
Added Mass [lb]	+1000	+1000	+1000
S-IVB	3200	0	0
S-II	7700	3500	0
S-IC	35000	11400	4400
Saturn V (total)	45700	14900	4400
Element	**Mass Multiplier**	**Mass Multiplier**	**Mass Multiplier**
Saturn V	45.7	14.9	4.4

In Table 3-2, the gross mass of the Saturn V does not change significantly when

1000 pounds is added to the S-IC stage in column four. The S-IC stage is the first stage of the launch vehicle and therefore adding mass only affects the initial vehicle thrust-to-weight ratio. However, the gross mass changes significantly when 1000 pounds is added to the S-IVB stage in column two. The S-IVB stage must provide both the propellant for the final burn to Low Earth Orbit (LEO) and the Trans-Lunar Injection (TLI) burn. Therefore, any changes in S-IVB mass must also increase the propellant for both S-IVB burns in order to keep the mass ratio constant. Additionally, as discussed earlier, when the propellant mass is increased, the dry mass will increase. The S-IVB engine thrust must increase to maintain a constant stage thrust-to-weight ratio to fly the same trajectory. These changes on the S-IVB stage cascade to the S-II stage, where the S-II engines must also increase their thrust level to use the same trajectory. The S-IVB and S-II changes cascade to the Saturn V. As a result the Saturn V must grow in size to maintain a constant mass ratio and vehicle-thrust-to-weight ratio. Thus, any changes on the S-IVB will have a large impact on the whole vehicle, as seen in Table 3-2.

In Table 3-2, the mission objectives were constant. However, as discussed earlier, the question remains about whether a minimum propellant mass trajectory leads to an optimal solution with regard to system reliability and production cost. Therefore, a wide range of trajectories are explored within the integrated model to find the best vehicle configuration for a combination of cost and reliability.

3.1.7 Completing the Sizing Process

The vehicle sizing process is completed by using the mass estimates from the MERs in conjunction with the trajectory and propulsion discipline to create a vehicle design. In this methodology an aerodynamics analysis is completed based on the baseline launch vehicle configuration and it is assumed that the aerodynamic results will not vary by a large amount based upon design changes. Iteration is required within the

trajectory, mass, and propulsion disciplines because the MERs cannot create mass estimates of the vehicle without the propellant mass, but the trajectory analysis requires a payload and dry mass for operation. The iteration process is referred to as "closing" a vehicle design and is illustrated in Figure 3-5.

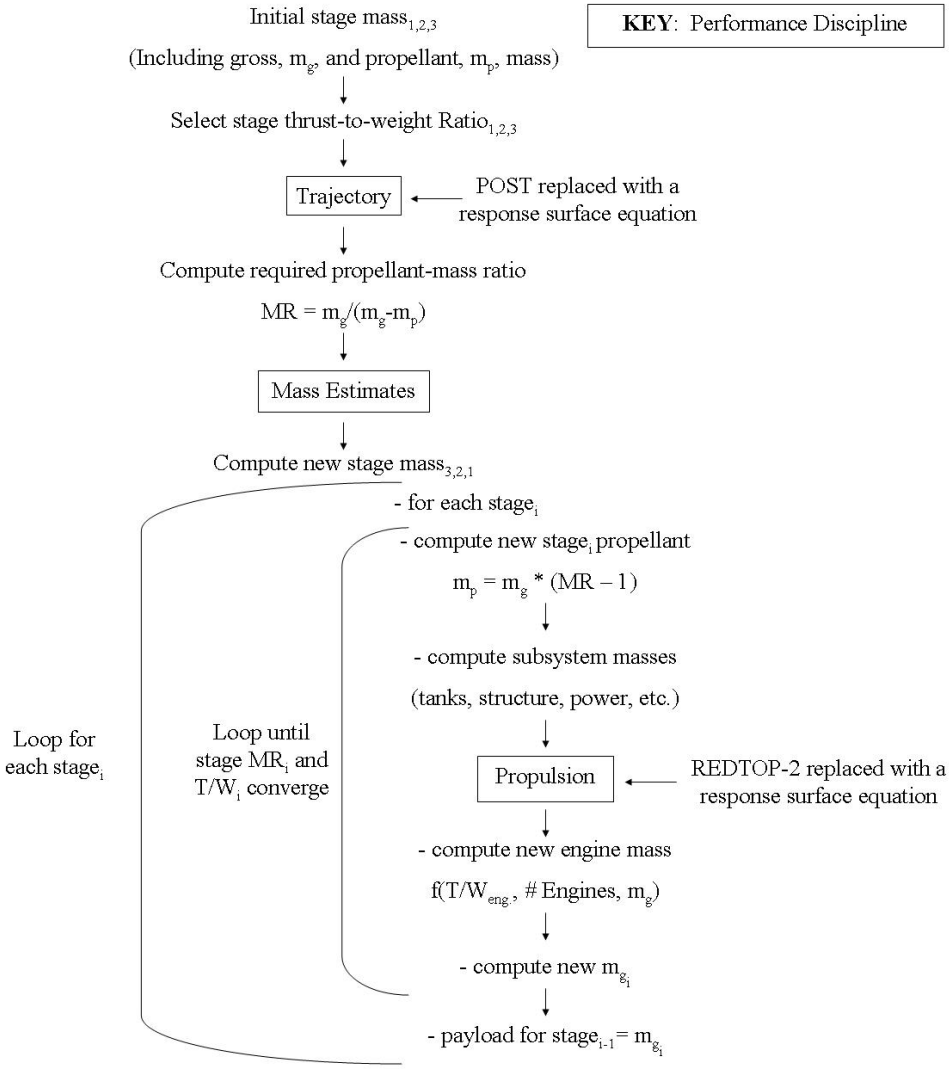

Figure 3-5: Closing a Launch Vehicle Design.

Figure 3-5 illustrates closing a three stage launch vehicle as completed in this methodology. A design engineer selects a stage thrust-to-weight ratio and uses trajectory analysis to determine the required mass ratio. In this methodology, response

surface equations replace the trajectory analysis and are discussed further in Section 3.1.8.1. The stage thrust-to-weight ratio and stage mass ratio are used to compute the subsystem masses in the mass estimation tool. The stage propellant mass is calculated first within the mass discipline, and then the supporting structure and subsystem masses are computed. The stage thrust-to-weight ratio, gross mass, and number of engines are used to calculate the engine thrust; the engine thrust is passed to the propulsion discipline. Another response surface equation replaces the propulsion discipline and is used to calculate the engine thrust-to-weight ratio based upon the engine thrust. The engine mass is computed using the engine thrust-to-weight ratio and engine thrust. A new gross mass is calculated with the updated engine mass.

Iteration may occur because the stage thrust-to-weight ratio and stage mass ratio do not match their initial values. Therefore, the subsystem masses are calculated in a loop that runs until the stage thrust-to-weight ratio and stage mass ratio equal their initial values.

The iteration process occurs one stage at a time. The subsystem masses of the top stage are computed first because this stage is the payload for the second stage. In turn, the second stage is the payload for the first stage. Once all of the stages have converged on their respective thrust-to-weight ratios and mass ratios, the launch vehicle is considered closed.

There is the possibility that the chosen thrust-to-weight ratio cannot complete the mission. If the thrust-to-weight ratio is too low, the iteration loop will never converge and the thrust-to-weight ratio must be increased to close a vehicle design. The minimum thrust-to-weight ratios for the Saturn V and CaLV applications were found by finding a ratio that would barely close the vehicle design. If the thrust-to-weight ratio is too high, then the vehicle masses become prohibitive for closing the launch vehicle concept.

The process illustrated in Figure 3-5 is one reason why Response Surface Equations (RSEs) were used for the trajectory and propulsion discipline. A range of thrust-to-weight ratios for each stage on the Saturn V and CaLV were closed with POST and REDTOP-2 prior to creating an integrated model. Therefore, the efficiency of closing a launch design, as shown in Figure 3-5, is improved because the intensive computational programs, such as POST and REDTOP-2, are subsequently removed from the design process.

3.1.8 Integrating the Performance Disciplines

Figure 3-6 is a design structure matrix for the performance analysis modules and illustrates how the disciplines are integrated together to create a launch vehicle design. The black dots in Figure 3-6 indicate which parameters are used as inputs and outputs for each discipline. The design engineer controls the thrust-to-weight ratio of each stage, the number of engines per stage, and other reliability options that are discussed further in Section 3.4. Based on the configuration selections, the subsystem masses of the launch vehicle are calculated with the process shown in Figure 3-6.

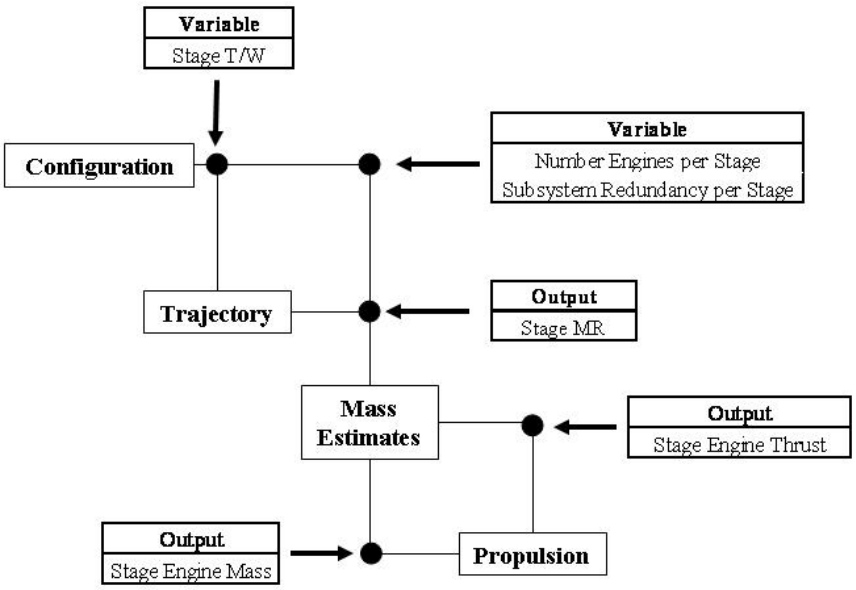

Figure 3-6: Design Structure Matrix for the Performance Disciplines.

The iteration process discussed in Section 3.1.7 has been eliminated through the use of Response Surface Equations (RSEs). RSEs are polynomial equations that can be used in place of an original analysis module. RSEs are used for both the trajectory and propulsion disciplines in Figure 3-6. The trajectory RSEs use the stage thrust-to-weight ratio to calculate the stage mass ratio and burn time while the propulsion RSE uses the engine thrust to calculate the engine thrust-to-weight ratio. The process of creating RSEs is explained in the next section.

3.1.8.1 Response Surface Methodology

Response Surface Methodology (RSM) can be used to create meta-models that speed up the design process [18]. Meta-models are polynomial equations, also called Response Surface Equations (RSEs), and can be used in place of an analysis module. RSEs introduce error but techniques can be used to minimize the error introduced into the design process. Additionally, the time saved by using an RSE instead of an analysis module may be considerable.

RSEs use a set of independent variables to model the analysis behavior. These independent variables are chosen due to their large effect on the desired response of the original analysis module. An example of an RSE is shown in Equation 3-6.

$$R = b_o + \sum_{i=1}^{k} b_i x_i + \sum_{i=1}^{k} b_{ii} x_i^2 + \sum_{i=1}^{k-1} \sum_{j=i+1}^{k} b_{ij} x_i x_j \tag{3-6}$$

'R' is the desired response, the 'b' values are the coefficients and the 'x' variables represent the design choices. During the RSE creation process, the user will determine the order of the equation by examining how well the meta-model fits the original analysis. The width of the design variable ranges also affects how closely the RSE represents the original analysis module. Once the ranges are determined, a series of case studies are created to generate the response data needed for completion of the RSE.

The number of analysis runs can be determined by a variety of methods. A full factorial will evaluate every design variable combination and lead to the best fit, provided that the analysis module is capable of being approximated with polynomial equations. However, using every design variable combination may be prohibitive because of time considerations. Therefore, techniques such as a Design of Experiments (DOE) can be used to accelerate the process of data collection [18]. DOEs are statistical methods for determining the optimum number of cases to run through the analysis module to fit a RSE. The number of runs is determined by how many design variables are in use and the number of levels for these design variables. A DOE such as a Central Composite Design (CCD) requires only 15 runs for a three variable, three level study while a full factorial design requires 27 runs.

Table 3-3: DOE Run Comparison.

DOE Type	**3 Vars.**	**7 Vars.**	**12 Vars.**
Full Factorial	27	2,187	531,441
CCD	15	143	4,121
Box Behnken	15	62	2,187

Table 3-3 lists a comparison of the number of analysis runs needed by each DOE technique to generate an RSE for three different sets of variables. Once a DOE technique is selected, a table is populated with the design variables and the analysis module is run an appropriate number of times.

Once the data set is generated by the analysis module, regression is used to fit the data to a RSE. Regression is an optimization technique that attempts to minimize the difference between the predicted value of the RSE and the actual value of the analysis module [35]. This optimization scheme will change the RSE coefficients until the error is minimized. The exact process of performing regression will vary depending on the number of variables [35]. The regression technique may result in a poor fit of the analysis module and additional steps must be taken to increase the goodness of fit.

The quality of fit for a response surface equation is important because the RSE is representing a required analysis module. A measure of goodness of fit is R^2, which measures the proportion of variation due to the design variables. A high R^2, such as 0.98, is desired when representing analysis modules with RSEs. Another measure of fit quality is $R^2 - adjusted$, which measures the same variation except by excluding every data point in the table of cases. Likewise, a high value on the order of 0.98 is desired when using RSEs. If these values are not achieved, then higher order terms can be used. For example, if an RSE is a quadratic equation, cubic terms can be included in an attempt to increase the goodness of fit. However, the addition of higher order terms artificially increases both the R^2 and $R^2 - adjusted$ terms [35].

Another method for increasing the fit quality is to include more analysis runs in the RSE generation. Decreasing the ranges of the design variables will also increase the goodness of fit. Transforming the variables is another technique for increasing the goodness of fit. The responses and/or the design variables can be transformed with a logarithmic function. Once a good fit of the RSE is established, the user can substitute the RSE for the analysis module and accelerate the design process.

3.2 Present Method for Evaluating Launch Vehicle Performance

In order to improve the computational time of the integrated environment, the two computationally intensive programs, REDTOP-2 (propulsion) and POST (trajectory) are replaced with response surface equations. Both POST and REDTOP-2 can take minutes to run whereas an RSE is instantaneous. As mentioned earlier, the independent variable of the propulsion RSE is the engine thrust and the dependent variable is the engine thrust-to-weight ratio. Two RSEs are used over a range of thrust levels for the J-2 application to increase the accuracy of the RSEs. The high thrust RSE, with thrust levels up to 400,000 pounds, is shown in Equation 3-7. The RSE ranges

and the goodness of fit statistics, such as the R^2 value, are listed in Appendix F. An RSE is used because the J-2 engine thrust-to-weight ratio changes as engine thrust varies; additionally, the RSE is much faster than REDTOP-2.

$$\frac{T}{W}_{eng.} = 72.12 + (-1.34E-5) * Thrust + 9.03E-11 * Thrust^2 + (-1.12E-16) * Thrust^3 \quad (3\text{-}7)$$

Figure 3-7 illustrates how the engine mass changes with engine thrust. While Figure 3-7 appears linear, the engine thrust-to-weight ratio is actually increasing slightly as engine thrust increases. For a low thrust engine, such as a 100,000 pound thrust level, the engine thrust-to-weight ratio is 69. A high thrust engine, on the order of 400,000 pounds, has an engine thrust-to-weight ratio of 74. The engine thrust-to-weight ratio increases because some components within the engine, such as the controllers and avionics boxes, do not increase in mass with increasing thrust levels.

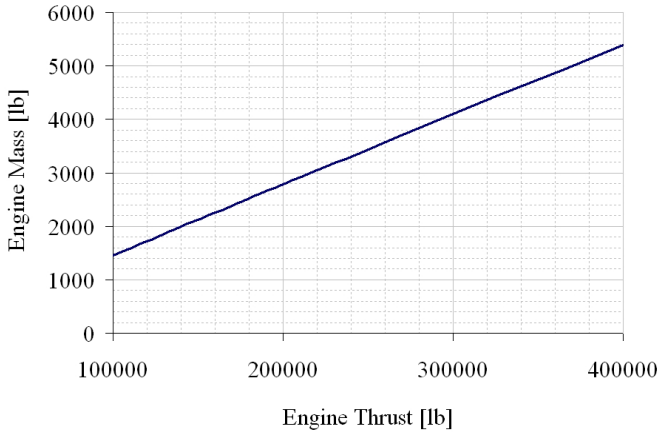

Figure 3-7: Engine Mass as a function of Engine Thrust.

An assumption is made that the vacuum Isp value is constant over the range of vacuum thrust levels. Figure 3-8 is created using REDTOP-2 [74] and plots vacuum Isp as a function of thrust for the J-2 engine.

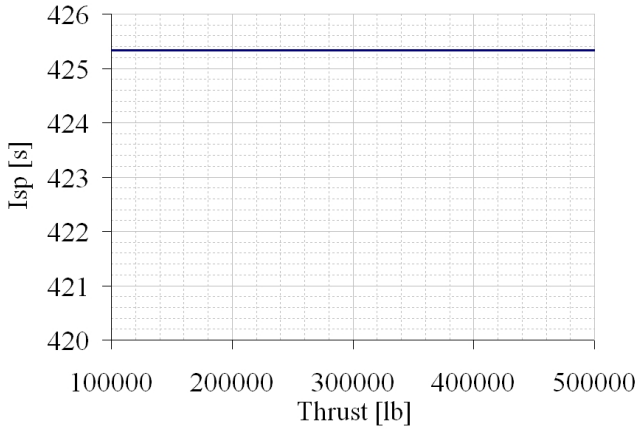

Figure 3-8: Vacuum Isp as a Function of Thrust for the J-2 Engine [74].

For trajectory analysis, POST requires additional time and the program can be difficult to solve depending upon the input parameters. Therefore, a set of RSEs have been created to replace the trajectory discipline in Figure 3-6. The independent parameter for the RSE is the stage thrust-to-weight ratio and the dependent parameter is the stage mass ratio. Equation 3-8 is the RSE for the S-II stage of the Saturn V.

$$MR_{stage} = 5.19 + (-6.28) * \frac{T}{W}_{stage} + 5.57 * \frac{T}{W}^{2}_{stage} + (-1.67) * \frac{T}{W}^{3}_{stage} \tag{3-8}$$

Each stage has its own RSE based upon the stage thrust-to-weight ratio. For example, both the booster and Earth Departure Stage of the Cargo Launch Vehicle have their own trajectory RSEs. All of the RSEs were created as a step prior to creating the integrated design environment. The RSE ranges and the goodness of fit statistics are listed in Appendix F. The constraints for the trajectory analysis are listed in Appendix I.

Response surface equations were also created to calculate the burn time of each stage based on the stage thrust-to-weight ratio. Equation 3-9 shows the RSE for calculating the Earth Departure Stage burn time based upon its thrust-to-weight ratio. The burn time for the injection to the Moon has also been captured with an

RSE based upon Figure 3-10. All of the statistics pertaining to the burn time RSEs are listed in Appendix F.

$$BT_{stage} = 1676.8 + (-4523.6) * \frac{T}{W}_{stage} + 4805.9 * \frac{T}{W}^{2}_{stage} + (-1768.7) * \frac{T}{W}^{3}_{stage} \quad (3\text{-}9)$$

When using RSEs, validation is important in order to show that the RSEs can approximate the original analysis module accurately. Validation of both the propulsion and trajectory RSEs are shown in Chapter 4 when the results are discussed.

The stage burn time is an important parameter for the reliability discipline and is calculated by the trajectory analysis. The burn time provides an operating time for each subsystem and greatly affects the reliability estimate of the stage, as seen in Table 3-1. The next section discusses why reliability and time are coupled. The next section also reviews various reliability analysis techniques and the modeling used in this methodology.

3.3 Reliability Modeling

Reliability was defined earlier as "the probability that an item (component, subsystem, system) will perform a required function under stated conditions for a stated period of time." [81] For launch vehicles, the reliability is the probability of successfully completing its mission. A launch vehicle reliability estimate can be converted into another metric, called the Mean Flights Between Failure (MFBF), which estimates an average number of flights between launch vehicle failures and is discussed in more detail in Section 3.3.2.

Reliability can be modeled using failure rates and the operating time for each subsystem in a launch vehicle. The operating time is a function of the launch vehicle's trajectory and is the same for each subsystem on a particular stage.

A first order example is used to illustrate the relationship existing between the performance, cost, and reliability disciplines. The thrust-to-weight ratio for the Earth Departure Stage (EDS), the second stage of the Cargo Launch Vehicle, was partially selected by examining the gravity losses for the trans-lunar trajectory. Figure 3-9 illustrates how the gravity losses are a function of the EDS thrust-to-weight ratio.

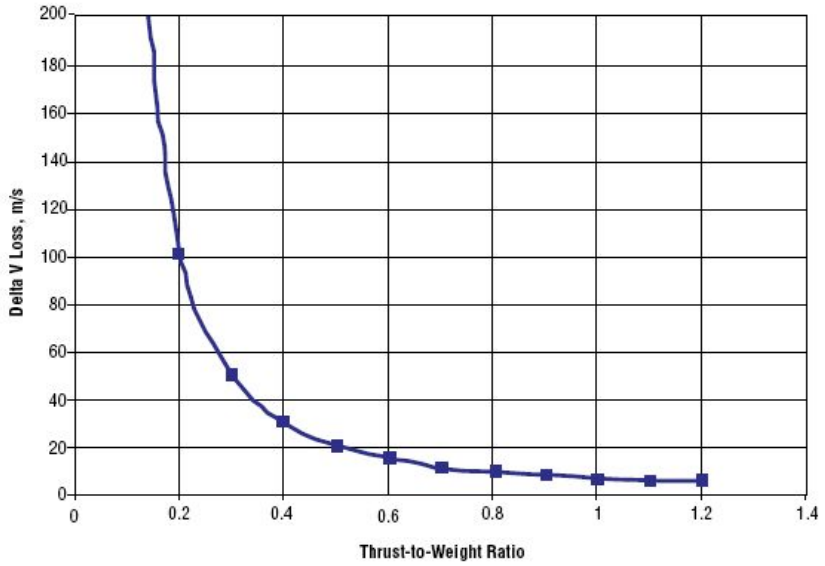

Figure 3-9: Gravity Losses as a Function of EDS Thrust-to-Weight Ratio [66].

If the EDS is assumed to weigh 350,000 pounds at the time of the burn to the Moon, then there is an EDS thrust difference of over 150,000 pounds for the range of thrust-to-weight ratios. A first order calculation of the corresponding engine development cost shows that the difference in engine cost could be between 500 million dollars [FY '04] and 700 million dollars [FY '04], in addition to the difference in production cost per engine. Additionally, the difference in EDS mass from selecting between two thrust-to-weight ratios will cascade down to the booster stage and cause large differences in required engine thrust for a set booster thrust-to-weight ratio. The booster engine development cost is then affected by the wide range of booster engine thrust. Furthermore, reliability conflicts with cost because a higher stage thrust-to-weight ratio reduces the burn time which can increase the system reliability.

Figure 3-10 illustrates how the burn time decreases with vehicle thrust-to-weight ratio. While the difference of 400 seconds may appear small, the difference in reliability on a vehicle such as the Cargo Launch Vehicle (CaLV) is almost 50 percent using the estimates shown later in this dissertation. A first order calculation shows the mean flights between failures can increase from 150 flights to 230 flights for the CaLV when varying the EDS thrust-to-weight ratio between 0.4 and 1.0. Therefore, while decreasing the EDS thrust-to-weight ratio will benefit the cost discipline, a lower EDS thrust-to-weight ratio also decreases the system reliability. An integrated environment can rapidly assess the effects of changing a design variable, such as stage thrust-to-weight ratio or engine out capability, to find an optimal launch vehicle configuration for a given weighting of cost and reliability.

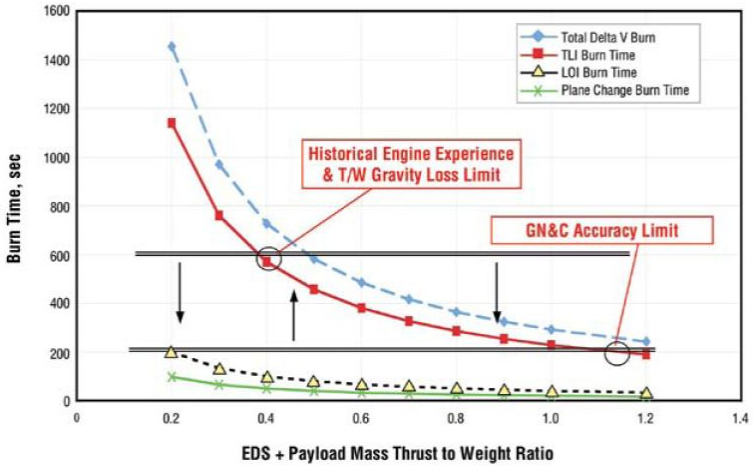

Figure 3-10: TLI Burn Time for Varying EDS thrust-to-weight ratio [66].

In this section, various methods for analyzing system reliability are discussed along with their advantages and disadvantages. The concept of reliability growth is reviewed and an approach to incorporate reliability growth into the methodology is presented. Different techniques for improving reliability are presented in this section. The section concludes with a detailed description of the method used for calculating launch vehicle reliability.

3.3.1 Reliability Breakdown Structure

Reliability can be calculated at many different indenture levels of a launch vehicle to produce the system reliability estimate. An indenture level is a plane on which all of the subsystems, components, assemblies, or parts are of the same complexity [12]. The indenture levels of a launch vehicle are similar to the Work Breakdown Structure in Appendix E. The lowest possible indenture level would be the individual parts making up an assembly, such as the bolts, nuts and structure. A description of each indenture level relevant to this methodology is listed below.

1. **Architecture**

   A reliability calculation at the architecture level results in a complete mission estimate. For example, multiplying the reliability of every element in the Apollo missions, such as the Command and Service Module, the Lunar Module, the Saturn V, etc., would result in the probability of success for a lunar mission.

   - **Element/System**

     The reliability calculation at the element/system level is the reliability of a single vehicle, such as the Saturn V. First order reliability analysis can be conducted at this indenture level, such as the example in Table 3-1, or the element/system reliability can be calculated by including the reliability estimates of the lower indenture levels. The launch vehicle reliability calculation in this methodology will be completed by using the reliability estimates of the lower indenture levels.

     – **Stage**

       A launch vehicle is composed of stages (with the exception of a single stage to orbit launch vehicle). The stage reliability estimate is calculated using the subsystem reliability estimates, which are calculated on the next indenture level. The stage reliability estimates are

then combined to calculate the system reliability estimate, which is the preceding indenture level.

* **Subsystem**

  The majority of the reliability analysis in this methodology will occur at the subsystem level. The subsystem level is the indenture level of the power, avionics, and other subsystems within a launch vehicle. This indenture level is equivalent to many of the levels in the WBS in Appendix G.

  - **Component**

    Some reliability analysis used in calculating launch vehicle reliability can occur at the component level. Examples of items at the component level are the engines, feed system, and other components that are within the propulsion subsystem. Engine reliability is a significant parameter of launch vehicle reliability; therefore, in this investigation, the engines are separated from the propulsion subsystem and the engine reliability is calculated at the component level.

Additional indenture levels could include objects such as assemblies and parts. Assemblies are items that make up a component, such as an engine turbine, while parts are the items, such as turbine blades, that make up assemblies. Reliability assessment at the assembly or parts level is generally performed in Phase C, the detailed design phase. For conceptual design, reliability analysis down to the component level will suffice for calculating launch vehicle reliability. While the detailed engine components, such as the feed lines and controllers are not modeled explicitly, the single engine reliability includes their effects. The significant subsystems and components will be revealed by applying this methodology even though a level of fidelity in the engine reliability analysis has been sacrificed.

3.3.2 Calculating Component and Subsystem Reliability

Reliability at the component level can be calculated using the survivor function of a governing failure distribution. The survivor function calculates the probability of successful operation at any given time [47]. An example of a survivor function is the exponential distribution shown in Equation 3-10.

$$R_i(t) = e^{-\lambda_i t} \tag{3-10}$$

Equation 3-10 is the formula for calculating the reliability of a component or subsystem with an exponential distribution as the governing failure distribution. In Equation 3-10, λ is the failure rate associated with the component and t is the time of operation. The units of the failure rate are failures per unit time. The unreliability of a system is equal to one minus the reliability.

The failure rate is determined by the hazard function, which is shown in Equation 3-11 for the exponential distribution. The hazard function is the probability that an item will fail at precisely time t.

$$h_i(t) = \lambda_i \tag{3-11}$$

The inverse of the failure rate is the Mean Time To Failure (MTTF), which is an average measure of the amount of time that will elapse before a component fails. For launch vehicles, MTTF is equivalent to MFBF when the exponential distribution is used and the units of MTTF are failures per mission.

From Equation 3-10, there are two methods for improving reliability. One approach is to decrease the failure rate shown in Equation 3-11. The other method for increasing reliability is to reduce the operating time. For launch vehicles, increasing the thrust-to-weight ratio will decrease the time to orbit. As the time decreases in Equation 3-10, the reliability will increase, as shown in Table 3-1.

An exponential function is a special form of the Weibull distribution and is important because the distribution has a constant failure rate with time. The exponential distribution exhibits the memoryless property, which means that the probability of failure in the next instant of time is the same as when the component began operating.

The Weibull distribution is another common failure distribution. A familiar example of the Weibull distribution is the failure rate curve, also known as the bathtub curve, exhibited by electronic components. The curve is illustrated in Figure 3-11. Figure 3-11 is the compilation of three Weibull distributions pieced together. The curve represents the burn in period where (I) the failure rate is initially high but decreases, (II) a period of constant failure rate, and (III) a period of degradation as the failure rate increases again.

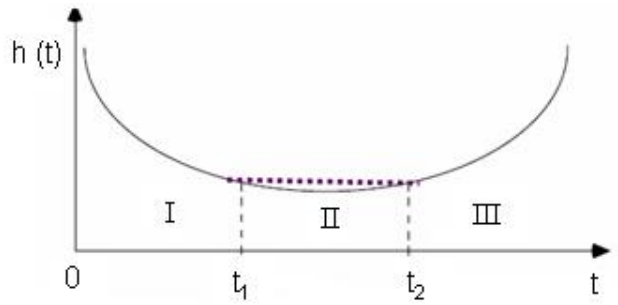

Figure 3-11: Bathtub Curve Created by Multiple Weibull Distributions [87].

The formulas for the reliability and the failure rate of the Weibull distribution are given by Equation 3-12 and Equation 3-13, respectively. The shape parameter is denoted by the symbol κ and the scale parameter is denoted by the symbol λ. The exponential distribution is a special case of the Weibull distribution where κ is equal to one. By using a Weibull distribution with a shape parameter larger than one, a degrading component can be modeled. The component's failure rate will increase with time signifying the component's degradation.

$$R_i(t) = e^{-\lambda_i t^{\kappa}} \tag{3-12}$$

$$h_i(t) = \kappa \lambda_i^{\kappa} t^{\kappa-1} \tag{3-13}$$

In summary, different failure distributions can be used to calculate the reliability of a part, assembly, component, or subsystem. For expendable launch vehicles, the failure distribution is typically the exponential distribution [59], [23] because of the relatively short lifetime of the vehicles. Therefore, in this analysis, all component and subsystem reliability calculations will use the exponential distribution as the governing failure distribution. In addition to a variety of distributions that can be used to calculate single component reliability, there are a number of different techniques when using the component reliability estimates to calculate the system reliability. A review of the different methods for analyzing the system reliability is the focus of the next section.

3.3.3 Reliability Analysis Techniques

There are a number of techniques that can be used to complete a system reliability analysis. Some of the more common practices include Reliability Block Diagrams (RBDs), Fault Tree Analysis (FTA), and Failure Mode and Effects Analysis (FMEA). A more rigorous analysis is a Probabilistic Risk Assessment (PRA), which combines Master Logic Diagrams (MLDs) with event trees and FTA. Other reliability analysis techniques include Petri nets and Markov chains. This section will discuss a few of the common reliability practices. By understanding how to quantify system reliability, techniques can be applied to increase the vehicle's reliability.

3.3.3.1 Failure Mode and Effect Analysis

Failure Mode and Effect Analysis (FMEA) is a qualitative analysis with the goal of identifying all failure modes and their consequences in a system. "FMEA analysis attempts to predict possible sequences of events that lead to system failure, determine

their consequences, and devise methods to minimize their occurrence or re occurrence [54]." Since many industries use FMEAs, the Government has established the military standard MIL-STD-1629A [12].

There are two different approaches to performing a FMEA: hardware and functional. The hardware approach begins with identifying each of the parts in the system. A part was defined previously as a lower level object that comprises assemblies, such as a turbine blade. The hardware method should be used when all objects of the same indenture level are known.

A functional approach should be used when all of the system levels cannot be identified. A functional FMEA defines the system into specific functions as opposed to hardware. The functional FMEA is still effective in identifying problem areas but should be replaced with a hardware scheme as additional knowledge becomes available. A FMEA is most effective when hardware is used in the analysis.

The first task in FMEA is to "define the system [12]." An initial step is to create a functional block diagram of the system and then identify the elements within the functions to the lowest indenture level. This task will be incomplete if the items for completing a function are still unknown.

The next step is to ascertain all of the failure modes for each of these objects or functions if the hardware is unknown. Failure modes are identified such as premature operation, intermittent action, failure to stop working and degradation of performance [12]. Once the failure modes have been pinpointed, their consequences must be established: a local effect, a higher abstract effect, and an end effect. The local effect is how the failure directly affects the item itself. The abstract effect details how the failure affects the next higher level, like an assembly or a subsystem to which the component belongs. The end effect is the result of the failure on the highest level of propagation. In addition to identifying the effects of a failure, the type of failure is classified. These grades range from category I for a catastrophic failure to category

IV for a minor failure. The failure mode must be classified by the worst possible outcome. These categories are listed in reference [12]. Categories I and II are identified as the most critical because they lead directly to loss of vehicle and loss of mission, respectively.

The next step in FMEA is describing the failure detection and preventative measures. Any corrective actions that reduce the risk after failure should be identified. All backup systems, redundancy, and alternative modes of operation must also be clarified for each failure mode. Finally, the effects of these backup systems and/or corrective actions must be defined.

Throughout the FMEA process various documents should be created. A standard worksheet has been established to help with the FMEA process and an example worksheet is shown in Figure 3-12 [18]. The worksheet can also be used for a slightly more rigorous process that includes the criticality modes and is called Failure Modes, Effects, and Criticality Analysis (FMECA).

FMEA NO: _____ PROJECT NO.: _____ SUBSYSTEM NO.: _____ SYSTEM NO.: _____ PROB. INTERVAL: _____	**FAILURE MODES, EFFECTS, AND CRITICALITY ANALYSIS WORKSHEET**					SHEET ___ OF ___ DATE _____ PREPARED BY: _____ REVIEWED BY: _____ APPROVED BY: _____			
TARGET CODE: P -- PERSONNEL / E -- EQUIPMENT / T -- DOWNTIME / R - PRODUCTS / D -DATA / V --ENVIRONMENT									
Id. No.	Item/ Functional Ident.	Failure Mode	Failure Cause	Failure Event	Target	Risk Assessment			Action Required/ Comments
						Sev	Prob	Risk	

Figure 3-12: FMECA Worksheet [18].

In addition to the worksheet, a list of all category I and II failure modes must be created. The information on this list should include design features that will minimize the occurrence the category I and II failure modes. Another file to create is a critical item list, which is a record of all single point failures. A single failure point is a

breakdown that results in system failure without any type of backup or redundancy.

FMEAs may not be an appropriate reliability analysis technique during the conceptual design phase because they are most effective when they are hardware based. However, FMEAs can be useful for conceptual design by identifying category I and II failure modes. These modes are especially important because failure in these areas may have severe consequences. If the failure modes are recognized early enough in the design, then a different configuration or design strategy can be used to eliminate or reduce a critical failure mode. Additionally, all single point failures must be addressed to ensure a more reliable system. The Apollo engineers used FMEA to list multiple failure modes of their components. To perform the quantitative analysis, the engineers used Reliability Block Diagrams.

3.3.3.2 Reliability Block Diagrams

Reliability Block Diagrams (RBDs) are a quantitative technique that can be used for reliability analysis. Early spacecraft reliability analysis was completed using RBDs, as seen in Hershkowitz, and et al. [36] for the Apollo vehicles. RBDs follow the physical layout of the system and use a block representation. The block representation begins at the top level by decomposing the system into its hardware subsystems. Within these subsystems, block representations of the components are created. These blocks are strung together to represent how each component must operate in the system for success. The manner in which these blocks are constructed determines how the calculations are performed.

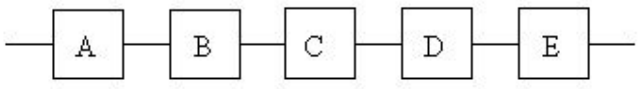

Figure 3-13: Series Reliability Block Diagram.

In a series system, top level success is achieved when every component in the

series operates successfully. A diagram of a series system is shown in Figure 3-13. Components A through E must function properly for the complete system to perform its task.

$$R_s(t) = \prod_{i}^{n} R_i(t) \tag{3-14}$$

The formula for calculating a series system is Equation 3-14; the component reliabilities are represented by R_i and the system reliability is R_s. The component reliabilities could be calculated using Equation 3-10 if the governing failure distribution is the exponential distribution. Since reliability never equals unity, system reliability will decrease with each additional series component. Improving subsystems with the lowest reliability causes the biggest improvement in system reliability for elements in series. Techniques for increasing subsystem and component reliability are discussed in Section 3.3.5.

In a parallel system, there are multiple paths to achieve success. Parallel systems are used to represent redundant components. Full redundancy is a scenario where only one component out of a set of components is required to operate for system success. An illustration of a parallel system is shown in Figure 3-14 where only one of three components must be functioning for the system to operate properly.

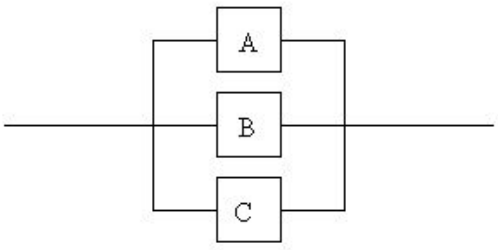

Figure 3-14: Parallel Block Diagram.

The formula for calculating the reliability of fully redundant components is shown in Equation 3-15. The component reliabilities are represented by R_i and the system

reliability is R_s. Again, the component reliability can be calculated with Equation 3-10. Using parallel configurations will increase the system reliability because only one of a set of components is required to work for system success.

$$R_s(t) = 1 - \prod_{i}^{n}(1 - R_i(t)) \tag{3-15}$$

Using identical components when only one is required will lessen the probability that a single component failure will lead to system failure. There are two primary disadvantages to using identical components to provide redundancy. First, mass and maintenance time increase when any redundancy is used. The second disadvantage is due to Common Cause Failures (CCFs). CCFs can bypass component redundancy completely if, for example, a manufacturing defect is present in all redundant components.

3.3.3.3 Common Cause Failure

Common Cause Failures (CCFs) can bypass redundancy that uses identical components by causing these components to fail because of something inherent in all of the components. One example of CCF could be a manufacturing defect that invaded all components in a particular batch.

When using identical components to provide redundancy, common cause failure effects should be included because the reliability benefit is not as large compared to redundancy calculations that do not include CCF. Upon component failure, an identical component will exhibit a 10 percent CCF rate; that is, 10 percent of the time that a component fails, its identical component will also fail [73]. For three components of the same type, the percentage grows to 75 percent for the third component failure; in other words, if the first two components fail, the third component will also fail 75 percent of the time due to CCF.

Common cause failure can be included in any system reliability analysis by using

the Multiple Greek Letter (MGL) method [54]. In this methodology, a reduced version of the MGL method known as the "Beta" (β) model is used. The full MGL model is shown in Equation 3-16.

$$Q_k = \frac{1}{\binom{m-1}{k-1}}(1-\rho_{k+1})(\prod_{i=1}^{k}\rho_i)Q_t \tag{3-16}$$

Within this dissertation, only dual components (i.e. a one out of two system) are used for redundancy. This strategy was chosen because a triple redundant system (i.e. one out of three) is almost as likely to fail as a dual redundant system because of common cause failure [72]. Figure 3-15 illustrates why the benefit from using triple redundancy is minimal [73].

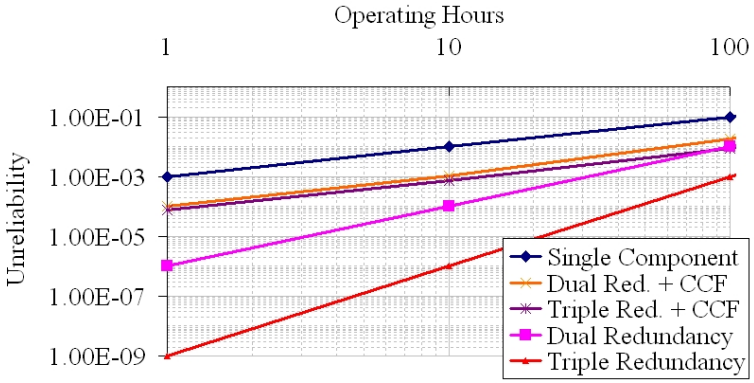

Figure 3-15: CCF Impacts of Different Component Configurations [73].

The governing failure distribution in Figure 3-15 is the exponential distribution; the failure rate for a single component is 5.5E-5. The unreliability of a single component is illustrated by the top line in Figure 3-15. The bottom two lines, the pink and brown lines, show the benefits of redundancy without considering common cause failure. However, once CCF is considered, as represented by the middle two lines in Figure 3-15, the reliability benefits of using identical components in a parallel configuration are significantly reduced.

Figure 3-15 is heavily dependent on the common cause failure probabilities along with the component failure rate, but the graph exhibits the same characteristics until

the failure rate for a single component becomes unreasonably high. One mention should be made about the STS-9 mission, which utilized a triple redundant APU system. During the landing phase, two APUs caught on fire but the orbiter was able to land safely because it had one additional APU [88].

3.3.3.4 Complex Reliability Block Diagrams

RBDs can also be more complex, such as when they are used to represent a shared load. A shared load is when each of the components performs a fraction of the work necessary to make the subsystem function. The operating requirement of each component is less because there are multiple components to help perform the total function. Yet, when there is a component failure, the remaining components have to match the increased burden required to make the subsystem operate. An example of a shared load subsystem is the propulsion subsystem of a Boeing 777 with its two aircraft engines. FAA regulations mandate that a passenger aircraft have the capability to take off with one engine out; the single engine is performing the workload of two engines. An example applicable to space systems is engine out capability.

Engine out can be referred to as an 'm' out of 'n' set of components. An 'm' out of 'n' set of components is one where if 'm' components are working, then the subsystem is operating. The equation for calculating the reliability of this type of subsystem with RBDs is shown in Equation 3-17. The component reliabilities are represented by R_i and the subsystem reliability is R_s. While an 'm' out of 'n' system is not a fully redundant scenario and does not provide the same reliability benefit, it is an improvement over a series system.

$$R_s(t) = 1 - \prod_{i=m}^{n} \binom{n}{i} R_i(t)[1 - R_i(t)]^{n-i} \tag{3-17}$$

Calculating the system reliability using reliability block diagrams requires that all of the components be combined into the proper system configuration. Many

components will be combined in a series configuration because these components are required to function for successful system operation. The Apollo engineers created a large reliability block diagram for the Command and Service Module, the Lunar Module, and the Saturn V [36]. Each of the components were combined into their subsystems and the subsystem reliabilities were combined using Equation 3-14 to calculate the system level reliability.

RBDs do have their limitations. Both the diagram and number of calculations are substantial for complex applications, as seen in the Apollo reference [36]. Additionally, RBDs cannot be used for varying failure conditions where the failure rate may change during the operation time. An example of a varying failure rate could be a shared load scenario, where the component failure rate changes when its workload increases.

3.3.3.5 Fault Tree Analysis

Fault trees are a common technique for performing reliability analysis in complex aerospace systems. Fault Tree Analysis (FTA) is used to determine the probability of a top level event. A top level event is an undesirable occurrence such as loss of mission. All sub-levels are either gates or events that are responsible for the top level event occurring. The fault tree's lowest levels are individual components that make up the system.

For the same system, reliability block diagrams and fault tree analysis will calculate the same result. The difference between the two approaches is Fault Tree Analysis calculates unreliability, which is one minus the reliability. Therefore, either technique can be used to achieve the desired result.

FTA begins with identifying a top level undesirable event. Depending on the application, the set of elements, subsystems, or components that affect the top level event must be compiled. These items are organized within the fault tree to reflect whether they are redundant, singular, or part of an 'm' out of 'n' system. A fault

tree example is shown in Figure 3-16.

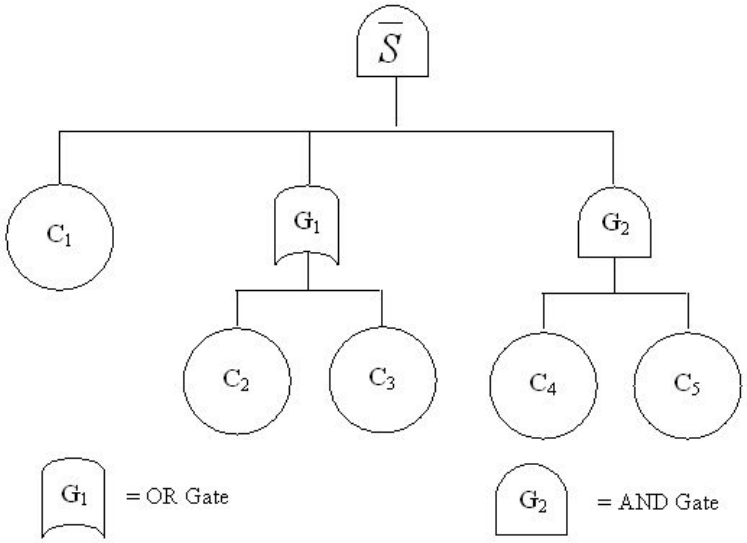

Figure 3-16: Notional Fault Tree Diagram.

A fault tree diagram uses specific terminology to represent the system [54]. The symbols represent one of three basic objects: an event, a gate or a transfer gate. An event is a component with a probability of failure. A gate illustrates redundancy or series systems with "OR" and "AND" type gates. An "AND" gate indicates that all components listed below the gate must fail before failure occurs. In Figure 3-16, objects C_4 and C_5 must fail before G_2 will fail.

An "OR" gate signifies that only one of the components listed below the gate must fail before a breakdown happens. In Figure 3-16, G_1 will fail if either objects C_2 or C_3 fail. There are also variations on both "OR" and "AND" gates such as a voting gate, which represents the 'm' out of 'n' scenario. Transfer gates are used for complex systems when the complete fault tree becomes large.

The calculation methods are very similar to the RBD analysis method, except failure probabilities are calculated instead of success probabilities. For components in series, such as C_2 and C_3 in Figure 3-16, the probability of failure (or unreliability) is calculated with Equation 3-18. UnR_s is the probability of failure while R_i is the

single component reliability.

$$UnR_s(t) = 1 - \prod_{i}^{n} R_i \tag{3-18}$$

For fully redundant components, Equation 3-19 is used to calculate the probability of failure. Again, UnR_s is the probability of failure while R_i represents the single component reliability.

$$UnR_s(t) = 1 - \prod_{i}^{n} (1 - R_i) \tag{3-19}$$

There are a variety of software packages available for calculating system reliability with fault tree analysis. One software package, RELEX [75], will be used to verify some of the reliability models needed in the application of this methodology. An example of a reliability model with the RELEX software is shown in Figure 3-23.

The main disadvantage of using a fault tree is for large complex systems. As with Reliability Block Diagrams (RBDs), fault trees can become very large and challenging to calculate for complex systems. Additionally, the underlying failure rate cannot be varied during the analysis. Therefore, fault trees have the same problems with dynamic analysis that RBDs encounter.

3.3.3.6 Probabilistic Risk Assessment

Probabilistic Risk Assessment (PRA) is a rigorous method of reliability analysis that incorporates multiple reliability techniques. Familiarization with the system is the first task in PRA and is important because the system must be decomposed into great detail for an effective PRA. Additionally, this familiarization will help with determining the quantitative reliability techniques to use in the PRA.

The next task is to compile a list of initiating events. These events begin scenarios that lead directly to an undesirable end state, such as loss of vehicle. Typically these scenarios are a string of multiple events that must occur in order to reach a specific

end state. There are exceptions where an initiating event will lead directly to a hazardous end state. All analysis will be based on the list of initiating events.

FMEA is one technique that can be used to identify initiating events. If a FMEA is already complete, then using this analysis as a reference is one way to locate the initiating events. If a previous FMEA does not exist, then the system should be broken down into a functional block diagram. The top level functions that are critical for success are noted, and all other sub-functions, subsystems, and components will be decomposed from these top level blocks. Another technique for use in identifying initiating events is a Master Logic Diagram (MLD). MLDs are a hierarchical representation of the system by functional categories [45]. A benefit of using MLDs is that the initiating events are more easily identified because analysts can visualize what functions are critical for mission success. Once all of the initiating events have been identified, event sequence diagrams can be created.

Event sequence diagrams (ESDs) are block representations of scenarios that happen once an initiating event has occurred. There may be multiple scenarios depending on the number of mitigating strategies. If there is only one safety feature, then the event sequence diagram will only have one block with two possible results: a favorable and an unfavorable end state.

An example of an ESD is shown in Figure 3-17. This diagram has three possible outcomes. After the initiating event occurs, two outcomes are favorable and one outcome is undesirable.

The next step in Probabilistic Risk Assessment is to convert Figure 3-17 into an event tree. Event trees use Boolean algebra to calculate the probability of an initiating event. A Space Shuttle Main Engine (SSME) event tree is shown in Figure 3-18. Each ending branch of the tree represents a different scenario; probabilities of scenario occurrence are located to the right of the branch end [23]. To compute the likelihood of failure from the initiating event, the probability of occurrence of the

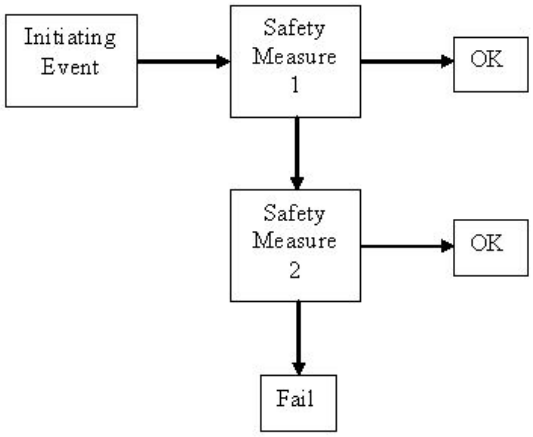

Figure 3-17: Notional Event Sequence Diagram.

singular events in the tree must be calculated. The singular events are calculated with fault tree analysis and combined to determine the total probability.

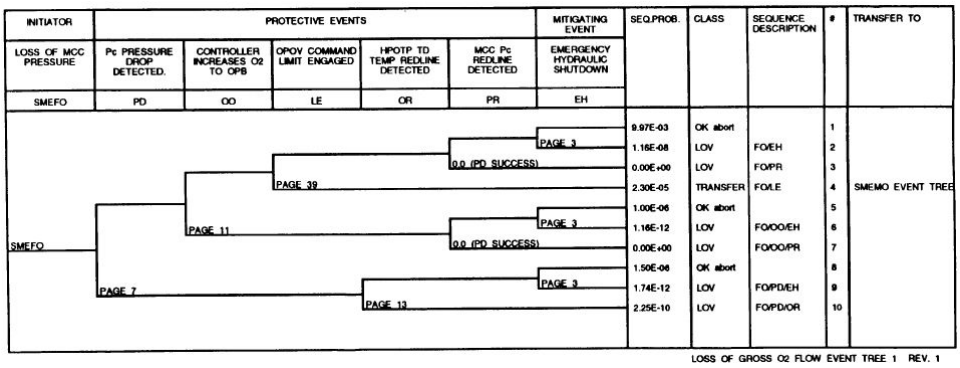

Figure 3-18: Shuttle Event Tree [23].

Probabilistic risk assessment was completed for the Space Transportation System [23]. The PRA created a rigorous definition of the system and calculated the loss of vehicle and loss of crew probabilities. The study referenced was completed before the Columbia accident and estimated the mean loss of vehicle to be one per 131 missions. The Shuttle Orbiter and the Space Shuttle Main Engine (SSME) are the two main elements that lead to loss of vehicle. Within the SSME, turbomachinery is the biggest cause of failure, while the auxiliary power units are the leading risk contributor on the orbiter.

PRA originated in the nuclear industry [54] and the nuclear industry uses different quantitative reliability techniques to assess system safety. Methods such as cause consequence diagrams, Markov analysis, and block diagrams are used for determining the safety level at nuclear power plants [39]. There are many ways to complete a PRA and the application will determine which quantitative reliability methods are most appropriate.

The limitations of PRA are defined by the methods for calculating the top level event probability. The STS PRA used fault trees and event trees and was limited by their capability. The STS PRA also assumed an exponential distribution which may not be appropriate for a reusable system with a long lifetime. Since the components of the STS will degrade over time, the Weibull distribution may have been a more appropriate failure distribution. One example of degrading components is the shuttle wiring system, which has been in the vehicle since its development. Using an exponential distribution for the wire failure rate does not reveal how hazardous the wires have become [87]. A relatively new technique called Stochastic Petri Nets (SPNs) is attempting to address the aging concern in a more rigorous manner by incorporating the ability to use dynamically changing failure distributions for single component reliability analysis.

3.3.3.7 Stochastic Petri Nets

Stochastic Petri Nets are a state space tool built on the Petri Net foundation. SPNs have the same goal of all other quantitative reliability techniques: to calculate system reliability [50]. The most important aspect about SPNs is the ability to model dynamic scenarios such as a varying failure rate like the one mentioned in the shared load problem. Another use for SPNs is the application of redundancy. Many times redundant components are switched on when the initial component fails; the second component is known as a cold spare. The failure rates of both components are

assumed to be the same even though the redundant component has not been used. SPNs can model this scenario properly and treat the redundant component as a brand new part. Figure 3-19 illustrates a shared load example from Reference [93].

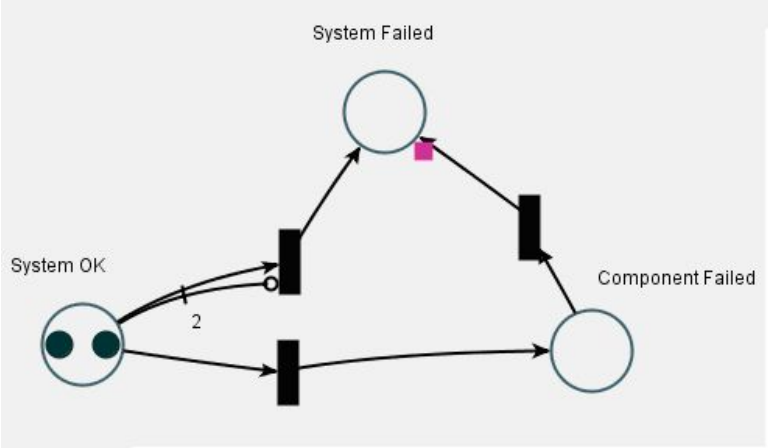

Figure 3-19: SPN Example Problem [93].

In Figure 3-19, there is a state that represents system operating (i.e. "system ok"), a state for single component failure, and another state for system failure. The tokens (i.e. black circles) in Figure 3-19 move throughout the diagram to represent each of the different states. A token in system failure will represent a failed mission. The black boxes are transitions and are associated with governing failure distributions, such as the exponential distribution. Thus, the transitions will dictate the manner in which tokens move between the different system states. The arrows illustrate the direction of token movement. In Figure 3-19 an inhibitor is represented by the line with a circle at the end and marked with a "2" in the middle. Due to the inhibitor, the tokens in Figure 3-19 cannot move directly to the failure state until one component fails. When a component fails, a token will move to the component failed state. Since only one component is operating, the second token is exposed to a higher failure rate. System failure is now more likely than the initial component failure because of a higher failure rate.

Stochastic Petri Nets use Monte Carlo Simulation (MCS) to calculate system

reliability [93] by counting the number of times a token enters the system failed state during the total simulation. If one run of the Monte Carlo simulation ends before a token reaches the failed state, the mission occurred successfully. If a token enters the failed state before the end of one MCS, the system has failed. The simulation uses thousands of runs to ensure the true failure probability is calculated.

Another state space technique for reliability analysis is called Markov chains. Markov chains are similar to SPNs because Markov chains also use different system states to calculate an overall reliability estimate. However, SPNs are more rigorous than Markov chains because Markov chains can only use the exponential distribution [87]. SPNs can use a variety of distributions to model failure rates and can be configured to represent the bathtub curve exhibited by electronics.

Stochastic Petri Nets can represent a higher fidelity model of a complex system with respect to reliability analysis. The opportunity to use varying failure rates enhances its capability over the more traditional reliability tools. In the current software package, the failure distribution parameters are single point values, making uncertainty analysis difficult. Uncertainty analysis is an important part of reliability since many failure rate parameters are assumed or derived from similar components. Therefore, the reliability analysis technique used in this dissertation will combine the best attributes of both SPNs and FTA to incorporate uncertainty analysis.

3.3.4 Reliability Growth Modeling

As a system's operating life increases, the reliability of a system may increase. The increase in reliability over time is defined as reliability growth and was shown to exist empirically by Duane [17]. Reliability growth occurs because engineers are correcting design defects throughout the system's lifetime [48]. There are a variety of models that can be used to forecast the reliability growth of a new system [11].

One reliability growth model is the Duane model which is shown in Equation 3-20 [17]. The number of failures per total test time is λ, 'K' is a constant, 'T' is the total test time, and α is the reliability growth constant. The Duane model is a power law formulation that depends on α to determine the rate of growth.

$$\lambda = KT^{-\alpha} \tag{3-20}$$

For launch vehicles, reliability growth occurs as the number of flights increases. Figure 3-20 shows the reliability, or mission success, history of the Atlas launch vehicles [41], [21], [89]. As the number of flights increases, the probability of mission success for the Atlas launch vehicle also increases, demonstrating the reliability growth of the Atlas program.

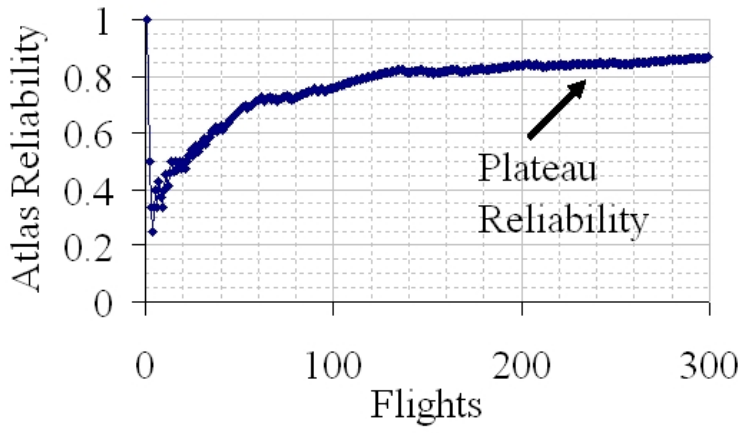

Figure 3-20: Atlas Launch Vehicle Reliability Growth.

3.3.5 Techniques for Improving System Reliability

A number of different techniques exist for improving system reliability which including: (1) increasing component reliability, (2) decreasing operating time, (3) increasing subsystem reliability through the use of redundancy, and (4) performing validation and verification tests. There are advantages and disadvantages to each method.

3.3.5.1 Increasing Component Reliability

Increasing component reliability within the space industry can be completed through a few different strategies. Building in larger design and environmental margins [31] are two recommendations for increasing component reliability. Higher component reliability can also be attained by carefully controlling the manufacturing process with tight tolerances. However, adding margin or using tighter manufacturing tolerances may increase system cost as the design effort becomes more labor-intensive.

One advantage to increasing component reliability is a potentially lower parts count. With fewer components in the system, processing and turnaround times will decrease [76]. While this is not as important for expendable launch vehicles, reusable vehicles such as the proposed Crew Exploration Vehicle (CEV) would benefit from using fewer components. A possible cost decrease from a reduction in processing time may offset the increased cost of using higher reliability components. However, little information is found about quantifying the cost of increasing component reliability within the space industry. The future work section will explain how to incorporate a model for calculating the cost of increasing component reliability within this methodology.

3.3.5.2 Time

When using an exponential function as the governing failure distribution, as shown in Equation 3-10, reducing the operating time will increase the system reliability. The operating time can be reduced by increasing the stage thrust-to-weight ratio as discussed in Section 3.1.5. The example at the beginning of the reliability section calculated a possible decrease in the mean flights between failure when the operating time is reduced. Table 3-1 also provided an example of how decreasing the operating time will increase the probability of mission success.

The assumption of the exponential distribution is important because the reliability

of a different failure distribution, such as the Weibull distribution, may not increase as time decreases. If subsystem reliability was governed by a Weibull distribution with a decreasing failure rate, such as region I in Figure 3-11, then decreasing operating time will decrease reliability.

3.3.5.3 Redundancy

System reliability can also be increased by using redundancy. Redundant components are a set of components in a configuration where only one component is required to operate for success. Redundancy was discussed in Section 3.3.3.2 and Equation 3-15 is used to calculate the reliability of parallel components.

The reliability of a subsystem can be increased by using multiple components of the same type even though only one component is necessary. For example, a power subsystem may require only one battery for successful operation but two batteries are included in the final design. If one battery fails, the power subsystem can continue operating because of the second battery.

Another type of redundancy is functional redundancy, where two different systems are used to perform the same function. One example of functional redundancy is using batteries and fuel cells for the power subsystem when only batteries are needed. Another example is using two different manufacturers to produce two batteries when only one is required. A famous example of functional redundancy is the ill-fated Apollo 13 mission. When the CSM lost its power and oxygen due to an explosion in the oxygen tanks, the crew was able to use the Lunar Module (LM) for life support until re-entry [31]. Functional redundancy is not as susceptible to common cause failure since an inherent flaw in one component may not exist in a separate component. Therefore, functional redundancy will generally provide a higher system reliability benefit compared to using identical components in a parallel configuration.

Any type of redundancy will increase mass and processing time, and may increase

overall cost. There is a debate about the amount of redundancy to include on a vehicle. The work completed by the Space Propulsion Synergy Team (SPST), headquartered at the Kennedy Space Center (KSC), advocates using as little redundancy as possible [76]. The SPST believes that the penalties on processing time are too great to justify using multiple components. The SPST advocates increasing the component reliability in order to use single components within each subsystem. On the other hand, companies such as Space X have advertised the engine out capability on their larger launch vehicles [19]. Increasing component reliability to levels high enough where only single components are necessary may be challenging. Thus, some redundancy may be beneficial, and this dissertation will attempt to quantify the cost of adding that extra advantage. Redundancy will be split into two types: using identical components and employing functional redundancy.

3.3.5.4 Validation and Verification

Another technique for improving reliability is validation and verification, which is accomplished through component, subsystem, and system testing. Testing does not increase reliability unless changes are made after the tests. The increase in system reliability through flight testing is called reliability growth and was discussed in Section 3.3.4.

Classical statistical approaches can be used to understand the impact of testing at all indenture levels. Confidence intervals are one method for examining the impact of testing using classical statistics. A confidence interval represents the range of possible values for a parameter such as the Mean Flights Between Failure. As the number of tests increases, the confidence interval decreases around the reliability estimate.

$$\mu \in \left(\frac{2n\bar{t}}{\chi^2_{2n,\ \alpha/2}}, \frac{2n\bar{t}}{\chi^2_{2n,\ 1-\alpha/2}}\right) \tag{3-21}$$

The formula for a 1-α confidence interval is shown in Equation 3-21 [35]. This

formula is based on using the exponential distribution as the governing failure equation. Equation 3-21 is used to calculate an upper and lower bound for the MFBF value, denoted by μ. The chi-square distribution with 2n degrees of freedom is used and the number of tests is the value n. Degrees of freedom refer to the number of independent values that are used in the estimation [10]. The $\bar{t}$ symbol represents the average MFBF generated from the test runs.

A confidence interval can be created once testing has occurred. As the number of tests increase, the confidence interval will decrease around the most likely estimate. An example of using a confidence interval is listed in Table 3-4 for the Saturn V launch vehicle.

Table 3-4: 90% Confidence Interval Comparison of MFBF.

Number of Flights	**Lower Bound**	**Upper Bound**
1	1.57	71.5
5	2.53	9.76
12	2.94	6.83
112	3.67	4.81

The reliability of the Saturn V was estimated at 76 percent [59], which is equivalent to 1 failure per 4.16 missions. The confidence interval is 90 percent, which means that 90 percent of all sets of test flights will have a MFBF value between the upper and lower bounds. After the first flight, the confidence interval is still very wide. After the fifth flight, the confidence interval has decreased significantly. However, many more flights are required before the confidence interval begins to center around the mean. There is one important assumption for this example: the confidence interval is highly dependent on the average MFBF. Therefore, if the Saturn V program had 112 flights, a failure would have to occur every 4.16 flights, on average, for Table 3-4 to be valid.

A statistical approach based on the number of tests and using Bayes success run

theorem can be employed to state the confidence in a reliability estimate [49]. Equation 3-22 illustrates the relationship between a reliability estimate and a confidence level. A key assumption in Equation 3-22 is the system has never failed [49].

$$C = 1 - (R_c)^{n+1} \tag{3-22}$$

In Equation 3-22, the confidence level is C and the reliability estimate is R_c. The number of flights is the variable n. In Equation 3-22, the analyst is X percent confident that the reliability value is at least the input estimate or greater. Table 3-5 lists an example of how the confidence estimate in the reliability value grows with the number of flights.

Table 3-5: Confidence Level for Saturn V Reliability Estimate.

Number of Flights	**Confidence Level**
2	56.10%
5	80.73%
12	97.18%

Table 3-5 reveals that by the end of the Apollo program, engineers could be 97.18 percent confident that the Saturn V reliability was at least 76 percent. Furthermore, if sets of 12 flights were repeated, 97.18 percent of them would have a reliability of at least 76 percent. When the initial reliability value is higher than the example in Table 3-5, the confidence level will grow more slowly with the number of tests. The use of Bayesian statistics results in an increasing confidence level with every successful flight.

The effects of testing will be shown through the use of reliability growth. Only complete system flights will be used to demonstrate how launch vehicle reliability increases; the system reliability will increase as a function of flight number. It is assumed that the cost modeling, discussed in Section 3.5, will account for the cost

of testing required to certify hardware at indenture levels below the element level. An acknowledgment is made that additional testing at the component and subsystem level may increase the reliability of the components or subsystems, but a method for quantifying the cost of additional testing is not proposed. Discussion in the future work section will show how a model that quantifies the cost of additional testing at indenture levels below the system level could be incorporated into the methodology.

3.4 Present Method for Calculating System Reliability

Reliability modeling in this methodology will be completed at the subsystem and component level. Section 3.3.1 described the indenture levels used within this dissertation. Engine reliability is a significant driver of launch vehicle reliability [1]; therefore, engine reliability analysis is calculated at the component level.

The reliability discipline in this methodology relies upon fault trees, reliability block diagrams, and uncertainty analysis to calculate the system reliability. The system reliability is calculated by combining the subsystem and component level reliability estimates. The subsystem and component level reliability is calculated by using the exponential distribution shown in Equation 3-10. Uncertainty analysis is included by using triangular distributions for the failure rate, or λ in Equation 3-10, at the subsystem and component level. The ranges for the triangular distributions are determined from historical launch vehicle reliability.

The following section will describe in greater detail how the present method computes system reliability. Special attention is given to the largest driver of system reliability [1]: engine reliability and engine out. The following section also details how full subsystem redundancy is treated for the two different types considered in this methodology. Illustrations will show how uncertainty analysis is used at the

subsystem and component level. Fault tree diagrams are used to show how the subsystem and component reliability estimates are combined to calculate the system reliability. The section will conclude with an explanation of how reliability growth is incorporated into the methodology.

3.4.1 Engine Modeling

Since the engine is such a significant driver of launch vehicle reliability, it must be separated from the propulsion subsystem and calculated at the component level. Throughout the history of launch vehicles, engines have been one of the leading causes of launch vehicle failure [1]. Figure 3-21 shows the leading subsystem and component contributors to unreliability of the S-II stage [59]. Engine unreliability is the leading cause of unreliability for the S-II stage [59]. Figure 3-22 shows that engine unreliability is expected to be the largest contributor to the first stage of the Cargo Launch Vehicle [66].

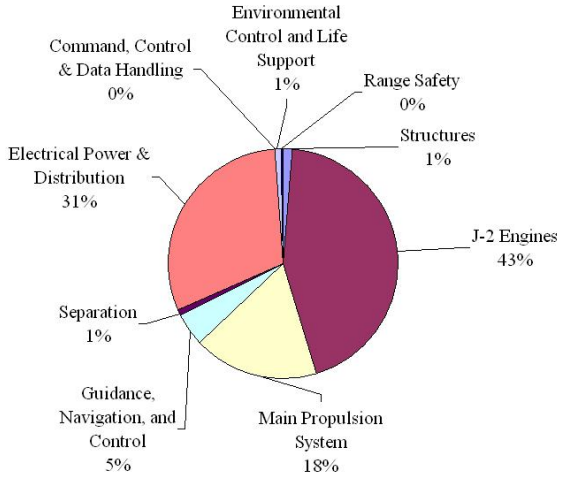

Figure 3-21: S-II Subsystem Unreliability Contribution [59].

In Figure 3-21, the reliability of the propulsion subsystem is determined from the total engine reliability and the main propulsion subsystem. The main propulsion subsystem consists of all other components within the propulsion subsystem, such as the feed lines and thrust vector control components. When engine out is not

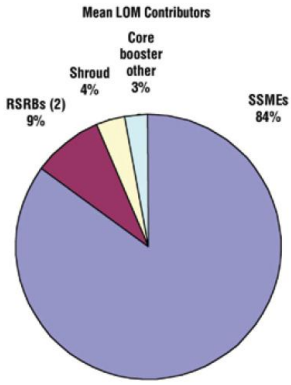

Figure 3-22: CaLV Booster Unreliability Contribution [66].

considered, the total engine reliability is calculated with the series equation shown in Equation 3-14. The total engine reliability is combined with the other components of the propulsion subsystem, using Equation 3-14, to calculate the propulsion subsystem reliability. Engine out modeling requires a different model because engine out is a dynamic scenario.

3.4.1.1 Catastrophic Engine Model

An engine out scenario is a partially redundant system where two engines must fail before the vehicle will fail. Therefore, a basic engine out model could use Equation 3-17 to calculate the total engine reliability. However, Equation 3-17 would ignore the common cause failure contribution from using identical components along with a catastrophic failure mode exhibited by engines.

A catastrophic engine failure is an "uncontained" failure that will lead directly to system failure. An example would be an engine explosion that destroys the launch vehicle. The benefits of engine out are reduced because of a catastrophic failure mode, similar to how the reliability benefit of using identical components for redundancy is reduced by common cause failure. However, a catastrophic failure is different from CCF because the catastrophic failure mode only affects one engine but causes the complete system to fail.

For this methodology, engine out modeling builds upon an 'm' out of 'n' fault tree with catastrophic failure modes that was proposed by Huang and et al. [37]. Huang and et al. [37] propose the percentage of catastrophic failures is between 20 and 40 percent based on historical data. In the model created by Huang and et al. [37], common cause failure was not a consideration. This dissertation has further modified the model to include CCF with the Beta (β) model [54] based upon the assumptions stated earlier regarding CCF. The modified model using the failure rate and CCF was derived in conjunction with the work completed by Young [97]. A fault tree representation of this new catastrophic failure model is shown in Figure 3-23.

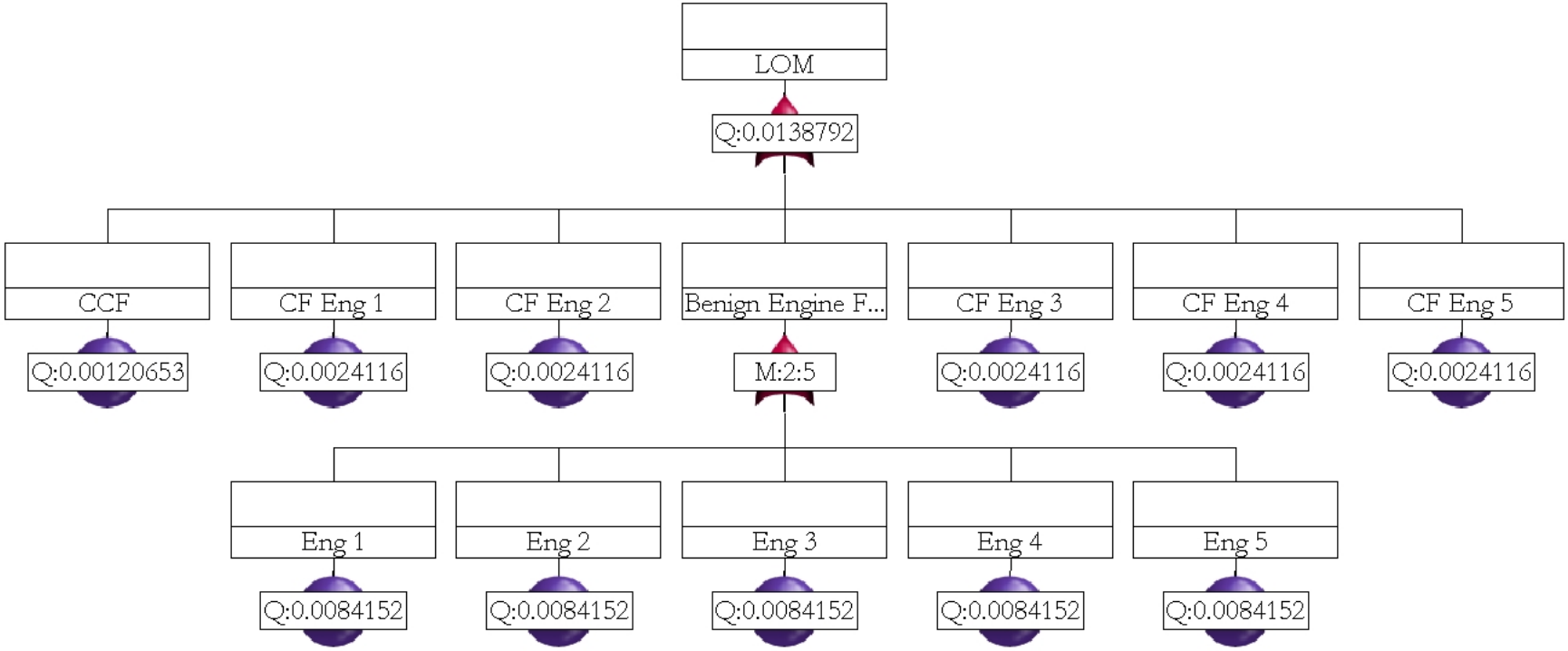

Figure 3-23: Engine Out Failure Model.

The top calculation in Figure 3-23 is the unreliability of a five engine configuration with engine out. The model is the S-II propulsion subsystem with a 20 percent catastrophic failure percentage and 10 percent β value for CCF. The single engine reliability for the J-2 is 0.988 from Reference [59]. The middle 'OR' gate signifies a benign engine failure mode where at least two engines must fail before the system will fail. On the same level as the benign engine failure mode are the failure modes that cause immediate system failure: a common cause failure and the catastrophic failure probability for each engine in the configuration.

Equation 3-23 shows how the engine out reliability is calculated using Figure 3-23. N is the number of engines and λ is the original engine failure rate. The catastrophic failure percentage is C.F. and CCF is represented by β. This engine out model is the baseline for all engine out reliability calculations.

$$R_{EO} = (e^{-\beta * \lambda_{eng} t}) * (e^{-C.F. * \lambda_{eng} t})^N * [N * (e^{-(1-\beta-C.F.)\lambda_{eng} t})^{N-1} * (1 - e^{-(1-\beta-C.F.)\lambda_{eng} t})] \quad (3\text{-}23)$$

The catastrophic failure model incorporates both common cause failure and the catastrophic failure mode, but the model does not account for the additional burn time that occurs when an engine fails. When an engine fails, the vehicle thrust-to-weight ratio decreases and the burn time to reach orbit will increase. Additional operating time will decrease the single engine reliability, as seen in Equation 3-10. While fault tree analysis cannot include the effects of additional burn time, stochastic petri nets can model the change in reliability.

3.4.1.2 Stochastic Petri Nets and Engine Out Modeling

Apollo 13, in addition to its notorious in-space accident, had a center engine shutdown two minutes prior to the scheduled cut-off. The engine shutdown because of pogo oscillations and the remaining four engines had to burn longer for the payload to

reach orbit [2]. Figure 3-24 is a comparison between the nominal Saturn V trajectory and the Apollo 13 trajectory which illustrates the additional burn time to orbit for the Apollo 13 mission.

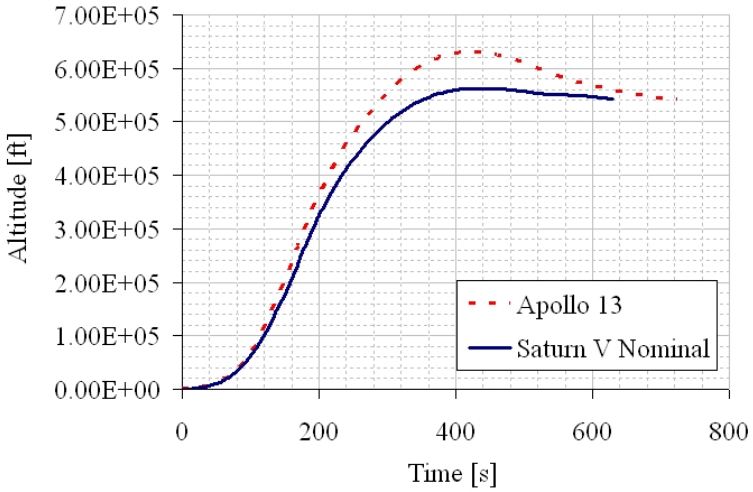

Figure 3-24: Trajectory Comparison Between a Nominal Saturn V and Apollo 13.

Stochastic petri nets are created for dynamic modeling, such as a propulsion subsystem with engine out capability. The stochastic petri net model used in this analysis is illustrated in Figure 3-25 which is a higher fidelity version of the catastrophic failure model shown in Figure 3-23. Common cause failure is represented with the "CCF" state, the catastrophic failure mode is represented by the "Catastrophic Failure" state, and the benign failure modes are represented by the "Benign Engine Failure" state.

For the reliability analysis using stochastic petri nets and the model shown in Figure 3-25, system failure occurs once a token reaches the "System Failure" state. System failure can occur if a token moves from either the CCF or catastrophic failure state. If a benign engine failure occurs, the remaining four tokens move to the "System Degraded" state. If another benign failure occurs, then an inhibitor will open and the system will fail. An inhibitor is placed on the catastrophic failure state to stop this failure mode once a benign engine failure occurs. The next engine failure will cause loss of mission, so the catastrophic mode does not need to be singled out.

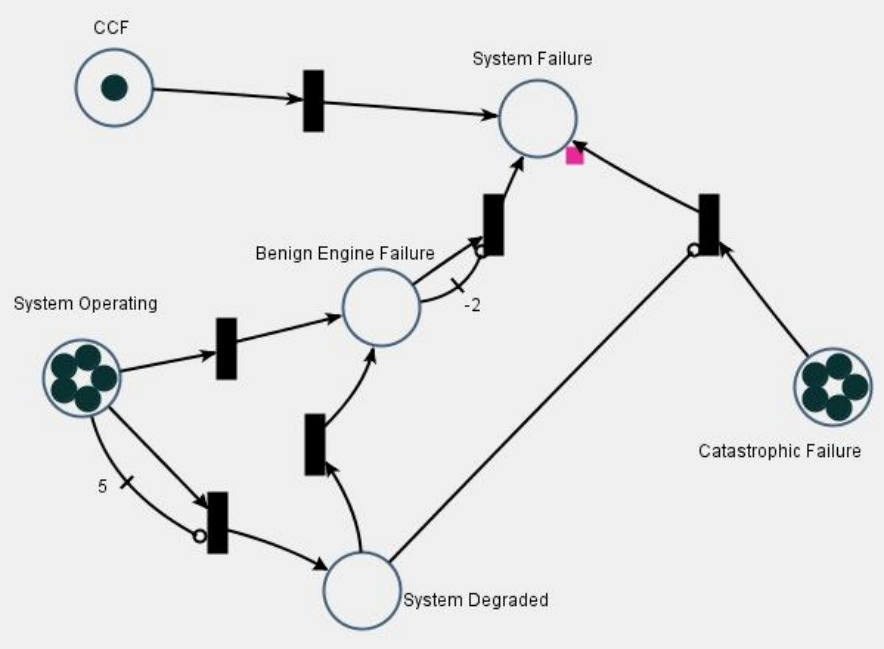

Figure 3-25: SPN Catastrophic Failure Model.

Once a benign engine failure occurs, the four remaining engines move to the "System Degraded" state so the failure distribution can be changed. The "System Degraded" failure rate is higher compared to the "System Operating" stage in order to account for the increased burn time. It is assumed that because the system has been designed for engine out capability, the failure rate does not degrade even though the remaining engines must perform the work of having one additional engine.

As mentioned earlier, the stochastic petri net software package is not conducive to making automated changes such as the number of engines on a stage. Therefore, the updated burn time from the trajectory analysis is combined with the catastrophic engine failure model to capture the effects of using the SPNs. Uncertainty analysis is also included by using triangular distributions in place of a single failure rate for each individual engine reliability calculation. A uniform distribution is used for the catastrophic failure percentage instead of using a single value. Figure 3-26 illustrates the engine out model used in this dissertation. In Figure 3-26, triangular distributions replace the deterministic engine failure rates illustrated in Figure 3-23.

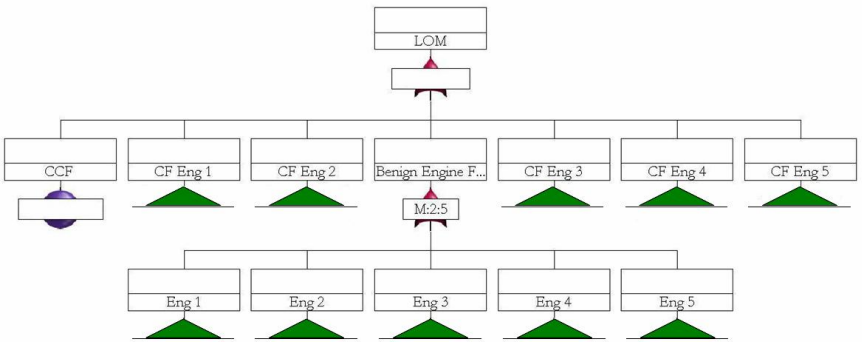

Figure 3-26: Engine Out Model.

Table 3-6 lists a comparison of the engine out unreliability calculations between the catastrophic engine failure model with the correct burn time and the stochastic petri net model. Unreliability is used since unreliability is the value calculated by the SPNs. The J-2 engine is used for the comparison in Table 3-6 and its characteristics are listed in Appendix F.

Table 3-6: S-II Engine Out Model Unreliability Comparison.

Eng. Configuration	**SPN**	**C.F. Eng. Model**	**% Diff.**
4 Engines w/ Eng. Out	0.0210	0.0203	3.18
5 Engines w/ Eng. Out	0.0257	0.0252	2.19
6 Engines w/ Eng. Out	0.0307	0.0301	2.08

In Table 3-6, three different S-II engine configurations are compared. By using the engine out burn time with the engine failure rate in the catastrophic engine failure model, the effect of an increasing burn time has been captured as shown by the good agreement of the unreliability results in Table 3-6. Since the updated catastrophic engine failure model produces a result similar to SPN with a faster calculation, the catastrophic engine failure model is used in this methodology. A stochastic petri net model will validate the optimal design point to ensure that using this lower fidelity analysis is acceptable. A more detailed comparison between different reliability techniques is listed in Appendix C.

3.4.2 Redundant Subsystems

While the engine is a leading driver of vehicle unreliability, other subsystems are also drivers of unreliability. Figure 3-21 showed that the power and avionics subsystems on the S-II stage are significant drivers of unreliability. Therefore, this methodology will examine the effects of using full subsystem redundancy, or a one out of two subsystem configuration, for the power and avionics subsystems on each stage of the Saturn V and the Cargo Launch Vehicle.

Two different types of fully redundant subsystems will be studied. A fully redundant subsystem is when two sets of subsystem components are included on the vehicle but only one is required (i.e. a one out of two subsystem configuration). The first type of one out of two subsystem redundancy is when identical sets of components are used. For example, two identical sets of components can be combined into a one out of two configuration to provide redundancy for the power subsystem. This type of redundancy is susceptible to common cause failure; therefore, the Multiple Greek Letter model shown in Equation 3-16 is combined with Equation 3-15 to calculate the subsystem reliability.

The other type of full subsystem redundancy is called functional redundancy and was discussed in Section 3.3.5.3. It is assumed that common cause failure will not affect subsystems that use functional redundancy although the cost of using two separate subsystems will be greater and is discussed in Section 3.6.1. The common cause failure assumption implies two different methods are used for satisfying the subsystem requirements, such as batteries and fuel cells for the power subsystem. Therefore, Equation 3-15 is used to calculate the reliability of a subsystem that employs functional redundancy.

Table 3-7 lists a reliability comparison for a one out of two subsystem configuration for the GNC subsystem on the S-II stage. Row one lists the subsystem reliability when functional redundancy is used for full subsystem redundancy. Row two lists

the subsystem reliability when two identical components are arranged in a one out of two redundancy configuration. The reliability is higher with functional redundancy because it is assumed that common cause failure does not exist. The mass of each subsystem is also affected when either type of full subsystem redundancy is selected.

Table 3-7: S-II GNC Redundancy Comparison.

Redundancy Type	**Reliability**	**MFBF**
Functional	0.998	561
Identical Components	0.994	176

When full subsystem redundancy is used for a subsystem, the mass of the subsystem is doubled. For example, if full subsystem redundancy is selected for the power subsystem, the mass of the power subsystem is doubled. This assumption is accurate when two identical sets of components are used to provide full subsystem redundancy, but, when using functionally redundant subsystems, there may be some error in the subsystem mass estimate.

Only the power and avionics subsystems of each stage are given the possibility of using full subsystem redundancy. These two subsystems are among the leading causes of unreliability for launch vehicles [1], [28]. Full subsystem redundancy may not be applicable for some subsystems, such as the structure subsystem. However, if a design engineer decides to include the option of using redundancy on additional subsystems, this methodology can easily incorporate that capability.

3.4.3 Uncertainty Analysis

Uncertainty exists from using historical data to provide reliability estimates for new components and subsystems which will be operating in a different flight environment. However, by using Monte Carlo simulation, a range of reliability estimates can be used to calculate the system level reliability.

Triangular distributions are used in place of single failure rates for each individual reliability calculation. For example, the power subsystem will rely upon a range of λ values in Equation 3-10 to calculate its reliability estimate. Figure 3-27 illustrates how the component and subsystem reliability computations are combined with uncertainty analysis for the S-IVB stage of the Saturn V. Triangular distributions replace the deterministic failure rates in Figure 3-27 and the stage and vehicle reliability is calculated using Monte Carlo Simulation. The ranges for each reliability estimate are based on historical failure rates from various references [23], [1], [28], [46], [63] and listed in Appendix A. The ranges for the failure rates were selected by using engineering judgment.

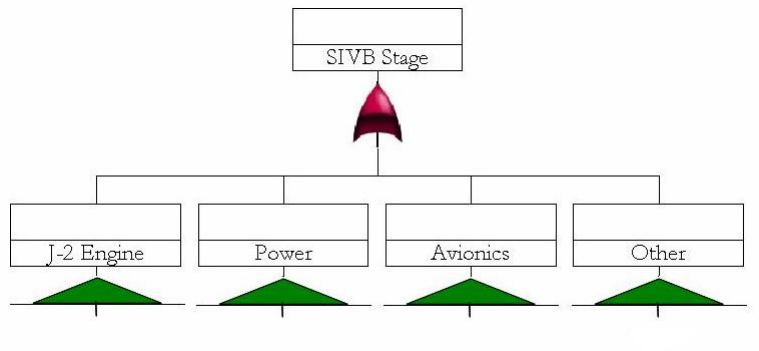

Figure 3-27: SIVB Reliability Calculation with Uncertainty Analysis.

The subsystem and component level reliability estimates are combined into their respective stages and the stages are combined into the system level reliability estimate. The system reliability estimate is determined by using a 70 percent certainty value from the Monte Carlo Simulation, which denotes that 70 percent of the values generated will be above this value. The 70 percent certainty value is an assumption and can be easily modified in this methodology.

The system reliability estimate will combine the different subsystem and component reliability estimates using fault trees. The process of how the subsystem and component reliabilities are combined into their respective stages is the focus of the next section.

3.4.4 System Reliability Calculation

Each subsystem and component reliability is combined into a stage reliability estimate using Equation 3-18. An illustration of the S-II stage is shown in Figure 3-28. Uncertainty analysis is always included but is not directly illustrated in Figure 3-28. The application of this methodology focuses on the propulsion, power, and avionics subsystems. Therefore, the other subsystems on each stage can be combined into the "other" event shown in Figure 3-28. If other subsystems were to receive more attention, then another gate could be added to the fault tree and the subsystem would be separated from the "other" event.

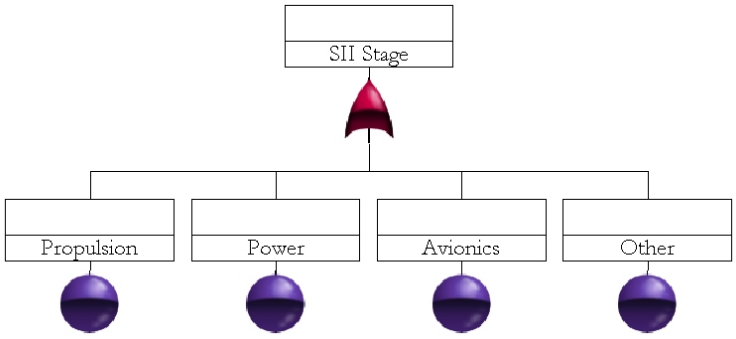

Figure 3-28: SII Stage Representation with No Subsystem Redundancy.

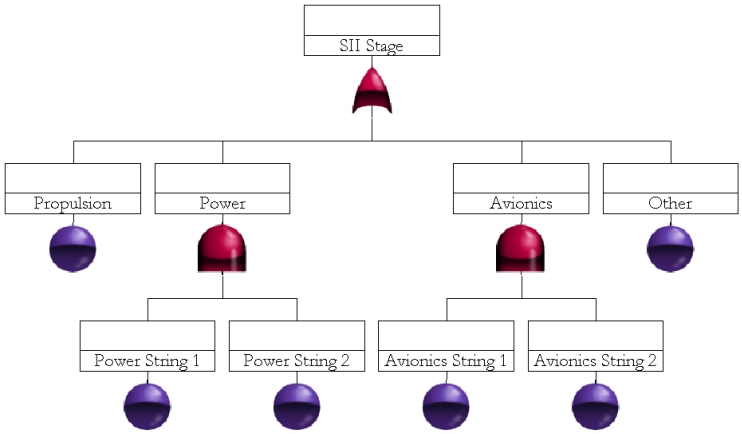

Figure 3-29: SII Stage Representation with Power and Avionics Redundancy.

The stage fault tree will vary depending upon the options selected by the design

engineer. If the design engineer prefers to study the effects of including dual redundancy for both the power and avionics subsystems, then the fault tree for the S-II stage would look like Figure 3-29.

As mentioned in Section 3.4.1, the propulsion subsystem is modeled by combining the total engine reliability with the rest of the components in the propulsion subsystem. Therefore, the propulsion subsystem will also change depending on whether engine out capability is used. If engine out capability is included on a stage, then Figure 3-26 is used to calculate the total engine reliability. If there is no engine out capability on a stage, then Equation 3-18 can be used to calculate the total engine reliability.

The system reliability for both the Saturn V and the CaLV is calculated using the reliability estimates for each stage in a series configuration, as illustrated by the fault tree in Figure 3-30. Equation 3-18 can be used for this top level calculation.

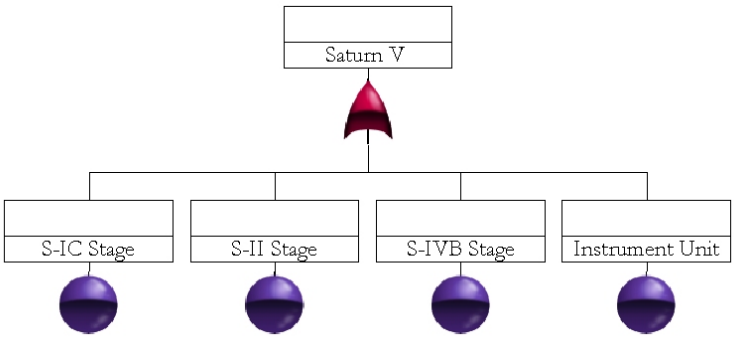

Figure 3-30: Saturn V Reliability Calculation.

3.4.4.1 Baseline Reliability Estimates

The reliability estimates for the S-II and S-IVB stages are listed in Tables 3-8 and 3-9. Appendix A contains the remaining reliability estimates for the Saturn V, including the S-IC stage and the Instrument Unit. The failure rates can be determined from the reliability estimates by knowing the baseline operating time and using Equation 3-10.

Table 3-8: S-II Subsystem Reliability Estimates.

S-II Subsystem	Reliability	MFBF
Structures	0.99832	595
Total Engines	0.95111	21
Main Propulsion System	0.97679	43
Guidance, Navigation, and Control	0.99458	185
Separation	0.99926	1351
Electrical Power & Distribution	0.95778	24
Command, Control & Data Handling	0.99997	33333
Environmental Control and Life Support	0.99626	268
Range Safety	0.99984	6250
Total	**0.87952**	**8.3**

Table 3-9: S-IVB Subsystem Reliability Estimates.

S-IVB Subsystem	Reliability	MFBF
Structures	0.99989	909
Liquid Rocket Engine	0.98800	83.3
Main Propulsion System	0.98276	58
Guidance, Navigation, and Control	0.98000	50
Separation	0.99996	25000
Electrical Power & Distribution	0.96100	26
Command, Control & Data Handling	0.99978	4546
Environmental Control and Life Support	0.99917	1205
Range Safety	0.99968	3125
Total	**0.91305**	**11.5**

The power and avionics subsystems, highlighted in red in Tables 3-8 and 3-9, can be improved by using a form of subsystem redundancy. The total engine reliability, also highlighted in red in Tables 3-8 and 3-9, can be improved by using engine out. For the application of this methodology, the reliability of the remaining subsystems and components in Tables 3-8 and 3-9 (i.e. the non-red subsystems and components) cannot be improved by the design variables. As mentioned earlier, the methodology is constructed so that studying the effects of improving the reliability of subsystems besides the power, avionics, and propulsion disciplines can be easily incorporated.

The baseline CaLV subsystem reliability estimates are listed in Table 3-10. The reliability estimates for the booster stage are from ESAS [66]. The EDS subsystem reliability estimates are determined from examination of historical references [23], [1], [28], [46], [63] and engineering judgment. As with the Saturn V launch vehicle, only the total engine, power, and avionics reliability can be improved for the Cargo Launch Vehicle in the present application.

Table 3-10: CaLV Baseline Reliability Estimates.

Booster	**Reliability**	**MFBF**
SSME	0.9935	154
RSRB	0.9993	1370
Shroud	0.9997	3096
Power	0.9998	6250
Other	0.9996	2500
Total	**0.992**	**124**
EDS	**Reliability**	**MFBF**
J-2S	0.996	250
Power	0.995	200
Avionics	0.999	1000
Other	0.9999	10000
Total	**0.989**	**86**

The Saturn V and Cargo Launch Vehicle reliability will be calculated using the models and techniques developed in the preceding sections. This reliability value is the maximum value possible for a particular launch vehicle design. However, there will be a reliability growth period for those launch vehicles as demonstrated by the Atlas launch vehicle in Figure 3-20. The Delta and Titan launch vehicles also underwent reliability growth periods, as will be seen in the next section. The next section will explain how to combine the launch vehicle reliability growth with the system level reliability estimates.

3.4.5 Reliability Growth Model

The reliability growth model used in this dissertation combines the Duane model from Equation 3-20 with historical data to calculate the growth rate parameter alpha (α). The historical growth of the Atlas launch vehicle was shown in Figure 3-20. The Delta and Titan launch vehicles are also used to forecast the reliability growth of the Saturn V and Cargo Launch Vehicle and their data can be found in Appendix D [41], [21], [89].

The growth rate parameter in Equation 3-20, α, is determined by fitting a power curve in the form of the Duane model to each data set. Table 3-11 lists the resulting growth rate parameter from the Atlas, Delta, and Titan data sets.

Table 3-11: Growth Rate Parameter.

Launch Vehicle	α
Atlas	0.2006
Delta	0.0669
Titan	0.0570

The growth rate parameters listed in Table 3-11 are lower than the growth rate parameters quoted in literature [16], [89]. According to the literature, a value of 0.2 means "[c]orrective action is taken for important failure modes." [16] The Atlas launch vehicle is an example of this scenario. A value greater than 0.4 shows "[t]here is a program dedicated to failure elimination." Thus, while this methodology will use the growth rate parameters from historical research, higher growth rate parameters may be more appropriate considering the effort put forth toward correcting design flaws. However, if little corrective action is required to improve launch vehicle reliability, such as when there is heritage behind a launch vehicle design, then low values of α may be appropriate as in the case of the Delta and Titan launch vehicles.

The result of the system reliability analysis is the estimated plateau launch vehicle

reliability for that particular configuration. However, the initial launch vehicle reliability and the required number of flights to reach the final reliability are unknown. One of these parameters must be determined to complete the reliability growth analysis.

When reviewing historical launch vehicle data, the number of flights to reach the plateau reliability value varies significantly. When considering the Atlas program, Figure 3-20, over 100 flights were required before the Atlas reliability reached a plateau. However, the plateau reliability of both the Titan and Delta launch vehicle families was achieved with fewer flights. In Figure D-1, approximately 40 flights were required before the Titan launch vehicle reached a plateau reliability. The Delta launch vehicle reached plateau reliability in approximately 20 flights, as seen in Figure D-2. The Apollo engineers predicted the Saturn V would reach plateau reliability in 15 to 20 flights [58]. The Exploration System Architecture Study predicted an air-start SSME would reach a reliability plateau after the fifth flight while a new liquid oxygen and liquid methane engine developed for the lunar lander would require 19 flights to reach a plateau value [66].

The initial reliability value can be used instead of the number of flights to complete the reliability growth analysis. Johnson & et al. use launch vehicle heritage to predict an initial reliability value [42]. However, this value is predicted based upon baseline launch vehicle configurations and does not vary if the configuration changes. It is assumed in this methodology that different launch vehicle configurations will experience the same growth rate as predicted by the Duane model; therefore, using a single initial reliability value as discussed in Reference [42] would result in each configuration having the exact same reliability growth curve. Therefore, the number of flights is varied to illustrate the reliability growth of the optimal launch vehicle configurations.

Due to the different growth rate parameters listed in Table 3-11, two reliability

growth figures are presented for both the Saturn V and the CaLV. While the methodology's primary goals are to demonstrate how the final launch vehicle reliability can be increased with different design choices and to determine the cost of using those design variables, reliability growth can also be incorporated to reveal additional information about the launch vehicles.

3.4.6 Reliability Summary

The individual reliability values are calculated at the subsystem level for the majority of the launch vehicle. Engine reliability is calculated at the component level because engines are a significant driver of system reliability. After the individual reliabilities have been calculated using Equation 3-10 with triangular distributions for the failure rate λ, the individual reliabilities are combined into stage reliability values using fault trees. The stage reliability values are then combined with another fault tree to calculate the system level reliability.

Engine out modeling requires its own development because of the additional burn time that occurs when an engine fails. Stochastic petri nets provide the best method for incorporating the additional burn time, but the effect is also captured by the fault tree model shown in Figure 3-26. If engine out is not used on a vehicle, then Equation 3-18 can be used to calculate the total engine reliability.

Two types of full subsystem redundancy (i.e. a one out of two subsystem configuration) are also included for study within this methodology. The first type is susceptible to common cause failure because identical sets of components are used for subsystem redundancy. For the case of functional redundancy, the second type of full subsystem redundancy, an assumption is made that this redundancy type is not susceptible to common cause failure.

Using subsystem redundancy and engine out will increase the reliability of a launch

vehicle. Additionally, a higher thrust-to-weight ratio will also benefit system reliability by reducing the burn time of the launch vehicle. While these options are beneficial for system reliability, the effects on cost must still be determined.

3.5 Cost Analysis

Cost estimation is important since resources are limited and finding the most cost effective method to meet the mission objectives is one step for ensuring program success. This section will review the different cost categories, various cost estimating techniques, and present a rationale for the cost analysis used in this methodology.

The Life-Cycle Cost (LCC) of a vehicle is defined by the NASA systems engineering handbook [62] as "the total of the direct, indirect, recurring, nonrecurring, and other related costs incurred, or estimated to be incurred in the design, development, production, operation, maintenance, support, and retirement over its planned life span."

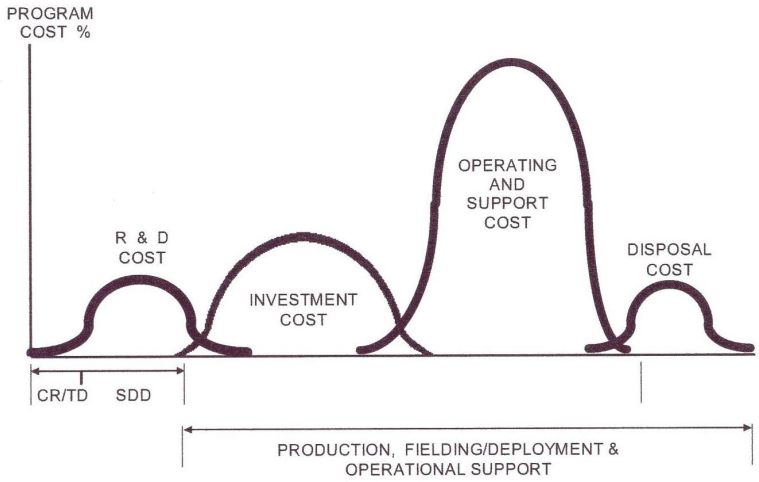

Figure 3-31: DoD LCC Categories [15].

The Department of Defense (DoD) uses Figure 3-31 to illustrate the different LCC categories [15]. The "R & D" cost in Figure 3-31 refers to research and development cost. Research and development cost are the costs associated with the beginning of the program until vehicle production begins. This area encompasses all of the

costs associated with initial vehicle designs and trade studies along with any final technology development that is required to enable the vehicle's operation. All final design and configuration management is covered under the research and development cost. The research and development cost in Figure 3-31 also includes the prototype production along with all testing and evaluation that occurs at each level of the design. The research and development cost category is equivalent to the Design, Development, Testing and Evaluation (DDT&E) cost that will be used later as one part of the cost metric.

The investment cost category in Figure 3-31 is the cost associated with production throughout the life of the program. In this methodology and Reference [62], these costs are referred to as production costs, which are any costs associated with manufacturing the flight hardware.

The operations and support cost is incurred once the program is operating and includes all sustaining engineering. Other operations costs include the costs required for operating the vehicle and its maintenance, along with the costs for the support systems needed for vehicle operation. Within the operations and support category, costs can be split into two areas: recurring and non-recurring. The non-recurring costs include any costs associated with having space flight capability, such as the costs associated with the technicians that must be kept on staff regardless of whether the vehicle is flying. A recurring operations cost is the cost of fuel for a launch vehicle. For reusable vehicles such as tanks, aircraft, and even the Space Transportation System, the operations and support cost can be the largest driver of LCC, as seen in Figure 3-31.

The final category in Figure 3-31 is the disposal cost. This cost represents the costs associated with the end of the vehicle's life. These costs could include recovery and permanent dismantling of the vehicle or the propellant cost to boost a satellite into a disposal orbit.

The summation of the DDT&E, production, operations and support, and disposal cost results in a life-cycle cost. To calculate the LCC, a variety of techniques can be used and a few of them are discussed in the next section.

3.5.1 Cost Calculation Techniques

Three methods for calculating cost are (1) using parametric cost models, (2) analogous systems, and (3) grass-roots techniques [62]. The NASA Systems Engineering Handbook recommends using different techniques for different phases of the program. As the system becomes more defined, higher fidelity techniques can be used to calculate the system cost.

Parametric cost models are recommended for the early stages of program development because little information is known about the design and the goal is to determine the significant parameters that drive cost. An example of a parametric cost model is a Cost Estimating Relationship (CERs). CERs are based on historical data and correlate an independent variable to the cost of an item using regression. An example CER is shown in Equation 3-24. The cost of an engine is calculated by raising the mass of the engine to a power and multiplying it by a coefficient. Equation 3-24 is an example equation and is not used in this dissertation.

$$Cost_{engine} = 1.85 * M_{engine}^{0.8} \tag{3-24}$$

Parametric cost models are useful in trade studies when rapid estimates of system cost are needed. CERs provide quick cost estimates and reveal the sensitivity of the system cost to changes in the design variables. For the space industry, dry mass is the primary independent variable in a cost estimating relationship. Figure 3-32 illustrates how the engine cost changes as a function of engine thrust when using parametric cost modeling. By using parametric cost models during conceptual design, engineers can determine which parameters need more focus during the detailed design phase.

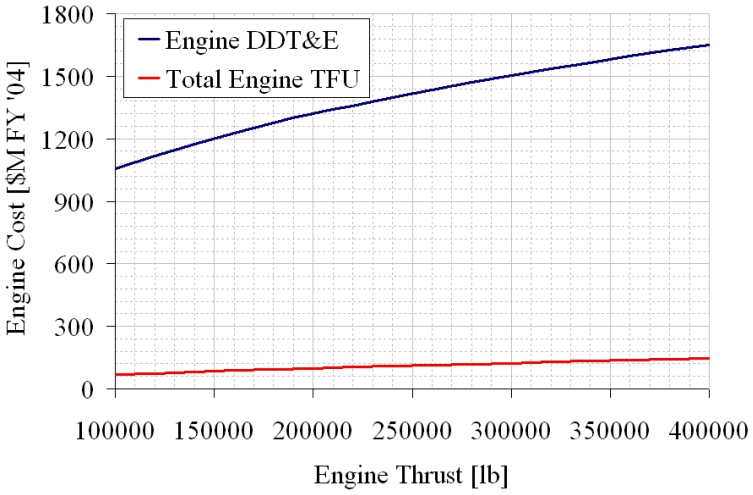

Figure 3-32: Engine Costs as a function of Engine Thrust.

Creating cost estimates through analogy requires experience and engineering judgment. When using analogies, cost estimates are created by finding similar characteristics between an existing vehicle and the current vehicle design. The use of engineering judgment and experience will allow the engineer to increase or decrease the cost estimate based on the differences between the current design and the previously created vehicle.

Grass-roots cost analysis is a higher fidelity method for cost estimation compared to parametric cost models and analogous systems. Grass-roots techniques rely on the engineering group responsible for an item to produce the item's cost estimate [62]. This technique is a higher fidelity method because the cost relies upon the engineers who are directly involved with creating the subsystem and all of its parts to provide a cost estimate. A disadvantage of grass-roots cost analysis is the method is labor-intensive and time consuming because the cost of each part, component, and subsystem must be estimated [62]. Therefore, a grass-roots technique is not conducive for use in rapid trade studies where the component or subsystem will change rapidly as different vehicle configurations are evaluated.

Parametric cost models are used for application of this methodology. One goal of

this methodology is to determine the important parameters that need additional focus during the next design phase. Therefore, rapid cost estimates are needed, which can be provided with parametric cost models. Additionally, parametric cost models are traceable and the CERs' assumptions can be exposed to the decision maker. Finally, by using parametric cost models, different vehicle configurations are compared in the same manner, as opposed to other cost techniques which may be influenced by the engineer responsible for preparing the cost estimate. The parametric cost models used in this methodology are the focus of the next section.

3.5.2 Calculating Cost for Space Applications

Within the space community, there are a number of tools used for parametric cost analysis. Cost tools include TRANSCOST and NAFCOM, SEER, PRICE, SOCM, and an Advanced Missions Cost Model [64], [8], [62]. The cost estimation tools cited are primarily used for calculating the DDT&E and production costs of a space vehicle. The exception is TRANSCOST, which calculates operations costs with additional CERs.

Operations and support costs are also evaluated using the Architectural Assessment Tool - enhanced (AATe) [100] and the Conceptual Operations Manpower Estimating Tool/Operations Cost Model (COMET)/(OCM) [64]. COMET/OCM was developed by the Marshall Space Flight Center (MSFC) and relies upon STS and Expendable Launch Vehicle (ELV) operations data. COMET assesses manpower requirements for the launch vehicle and OCM applies a labor rate and other factors to calculate an operations cost [64]. AATe is built upon the STS database and uses system characteristics to produce an overall operations cost for reusable vehicles.

3.6 Current Cost Estimation

The cost tool used in this dissertation is the NASA/Air Force Costing Model (NAFCOM). NAFCOM uses CERs to calculate cost by using dry mass as the primary independent variable [65]. NAFCOM also allows the user to select analogous systems to tailor the CER based upon the similarity between the current vehicle design and historical space systems. For example, a user may decide to include only the vehicles from the Apollo era for their cost estimates. An example of the NAFCOM tool is shown in Figure 3-33.

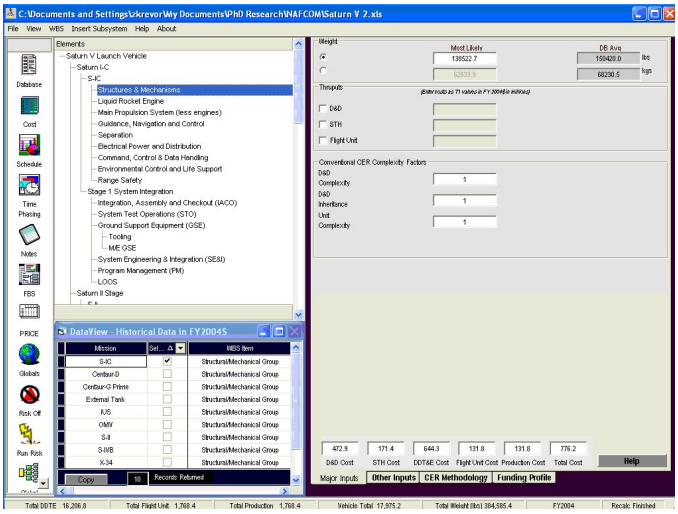

Figure 3-33: NAFCOM Visual Example.

Once the performance disciplines have calculated the subsystem masses of the launch vehicle, the CERs from NAFCOM will be used to calculate the DDT&E and production cost. Each item listed in the WBS in Appendix E will have an associated cost estimate. The summation of these subsystem costs will result in the vehicle DDT&E and Theoretical First Unit (TFU) cost. The total production cost is calculated by multiplying the number of flights by the TFU cost. The DDT&E plus production cost is equivalent to the "R & D" plus the "Investment" cost in Figure 3-31 and is used in the system optimization as the cost metric. Equation 3-25 is the formula for calculating the cost metric. The number of flights is set to twelve for both

the Saturn V and Cargo Launch Vehicle (CaLV) application.

$$CostMetric = DDT\&E + No.Flights * TFU \tag{3-25}$$

The operations and support costs along with the disposal costs are not included within the cost metric for this methodology. It is assumed that the disposal costs are not greatly affected by changing the configuration of a launch vehicle. The operations costs for launch vehicles are difficult to determine because the private space industry guards this data closely. AATe and COMET/OCM primarily rely upon the Space Transportation System (STS) database to produce their operations cost estimates. Thus, calculating operations costs with a database heavily influenced by the STS may lead to inaccurate answers.

This methodology was created with the flexibility to easily make additional enhancements. Therefore, an operations cost model that can discriminate between launch vehicle concepts based on their characteristics could be added. The operations cost would be included in Equation 3-25 and the complete life-cycle would be evaluated. Methodology enhancements are discussed in Section 3.10.

The time value of money is not considered because schedule is not an integral part of this methodology. The development schedule could be important because certain vehicle designs have a larger development cost to save resources later in the program. Thus, the first flight of a vehicle could be delayed if the budget is constraining the initial development. However, additional resources could be used to alter the development schedule. Therefore, eliminating a configuration because of its schedule may not be appropriate due to the initial assumptions.

A first order examination of the development schedule is presented for the Saturn V and CaLV applications. The DDT&E plus the TFU cost is spread over eight years to represent the cost incurred until after the first flight. A beta distribution is used to spread the development costs over the time period in accordance with

NASA guidelines [65], [62]. The probability density function for a beta distribution is shown in Equation 3-26. The significant parameters are p and q, which define the distribution. $B(p,q)$ is the beta function and is defined in Equation 3-27.

$$f(x) = \frac{1}{B(p,q)} x^{p-1}(1-x)^{q-1}, 0 \leq x \leq 1, p > 0, q > 0 \tag{3-26}$$

$$B(p,q) = \int_0^1 x^{p-1} dx = \frac{\Gamma(p)\Gamma(q)}{\Gamma(p+q)} \tag{3-27}$$

When spreading the development costs over a time period, assumptions are made about when the majority of the resources are used. NASA typically employs a 60 percent profile, which means 60 percent of the total costs are used during the first half of the defined time period [62]. In other words, 60 percent of the costs are spent within the first four years of development for an eight year development program. The beta distribution in Equation 3-26 can be defined with the shape parameters p and q to match the assumptions about the development schedule. However, NASA has created a cost calculator for use in determining how the development cost is spread over a given time period [8]. Table 3-12 lists a comparison of the cost fraction for different cost profiles.

Table 3-12: Development Cost Comparison.

Development Year	**Cost Fraction 40%**	**Cost Fraction Constant**	**Cost Fraction 60%**	**Cost Fraction 70%**
1	0.011	0.125	0.050	0.083
2	0.075	0.250	0.188	0.272
3	0.209	0.375	0.385	0.495
4	0.400	0.500	0.600	0.700
5	0.615	0.625	0.791	0.857
6	0.812	0.750	0.925	0.953
7	0.950	0.875	0.989	0.994
8	1.000	1.000	1.000	1.000

In Table 3-12, the cost fraction is the percentage of the total development cost spent by the current year. For example, 40 percent of the total cost is spent by year four when assuming a 40 percent profile (column two). The cost fraction is used to determine a year by year profile of the resources required to satisfy the total development. The constant cost fraction means the development cost is spread evenly over the eight year time period.

Another important result calculated using the beta distribution to spread development cost is the peak year funding. The peak year funding illustrates the maximum cost incurred in a single year by the program development. The maximum cost may be significant when exploring a complete budget profile. NASA's budget is approximately 17 billion dollars per year and the budget must be apportioned to account for the peak funding years of a program's development. The peak year funding values are presented for the Saturn V and CaLV in the results section.

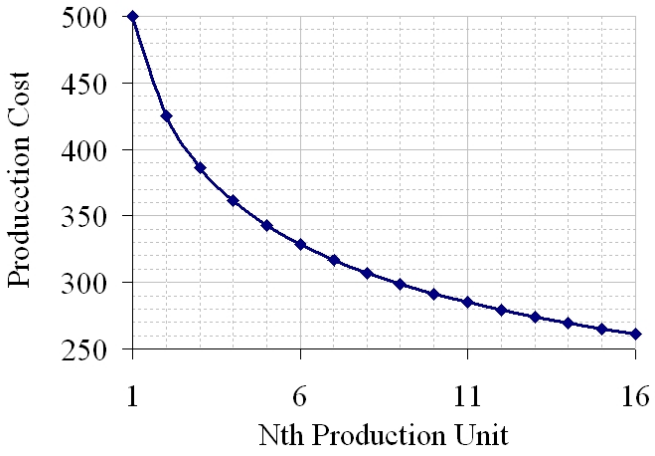

Figure 3-34: Learning Curve Example.

Additionally, a learning curve is not applied to the vehicle production costs. A learning curve is a manufacturing concept where the production cost of a vehicle decreases as more vehicles are created [65]. An example of a learning curve is shown in Figure 3-34. The goal of this methodology is to determine the optimum design characteristics for a balance of reliability and cost. The learning curve would be

an assumption on top of the costs calculated in this process and may affect the final results. The future work section will discuss how a learning curve could be incorporated into this methodology.

3.6.1 Cost and Redundancy

The cost model treats the subsystem redundancy strategies differently. Table 3-13 is a notional example that compares the cost of using a one out of two configuration to provide full subsystem redundancy. When a launch vehicle configuration does not include subsystem redundancy, only the baseline subsystem cost estimates are included in the system cost. Using two identical sets of components to provide redundancy is referred to as identical components in Table 3-13. When two identical sets of components are used to provide full subsystem redundancy, no additional DDT&E cost is required for developing an identical second unit. However, the production cost will double because two units are needed.

Table 3-13: Full Subsystem Redundancy Notional Cost Comparison.

Redundancy Type	**DDT&E [$M FY '04]**	**Total TFU [$M FY '04]**
None	1	1
Identical Components	1	2
Functional	2	2

When functional redundancy is used, two different sets of components are created; therefore, the DDT&E cost of each set of components must be included in the cost estimate, as listed in Table 3-13. For example, batteries from two different manufacturers are developed and thus the DDT&E of each battery must be included. It is assumed in this methodology that because the batteries are required to perform the same task, the development cost of two subsystems is equal to double the DDT&E cost of a single subsystem, as listed in Table 3-13. Furthermore, the production cost

for both strings is assumed to equal two times the single subsystem production cost.

3.6.2 Uncertainty Analysis

NAFCOM has the capability of including uncertainty analysis within its cost analysis. Both the mass estimates and CERs are based upon regression analysis of historical databases of space vehicles and error exists because historical data is used to forecast the masses of a new vehicle. Therefore, margins are used on the mass estimates to account for the MER errors while a distribution is assumed for the CERs to incorporate the cost model uncertainty.

To build a distribution around the CER, a minimum, maximum, and most likely mass estimate are required. In the application of the methodology to the Saturn V and Cargo Launch Vehicle, the minimum value is the original subsystem mass estimate from the MER. The most likely estimate adds a 15 percent margin to the baseline while the maximum estimate is a 30 percent margin on the original subsystem mass calculation. Figure 3-35 illustrates the mass margin assumption.

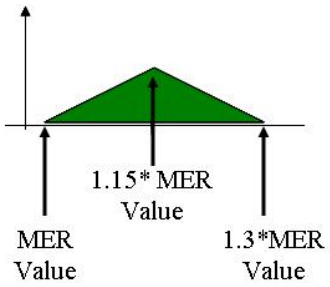

Figure 3-35: Mass Margin.

Using these three mass estimates, a distribution is built around each subsystem CER. Based on NAFCOM, each subsystem CER uses a lognormal distribution for the uncertainty analysis. The standard deviation is calculated from the range of subsystem masses and then multiplied by a factor to account for the specific CERs used in the cost analysis. The standard deviation multiplier depends upon the NAFCOM

analogies selected and will be constant as long as the analogies do not change. Figure 3-36 illustrates the complete process for using uncertainty with the cost analysis.

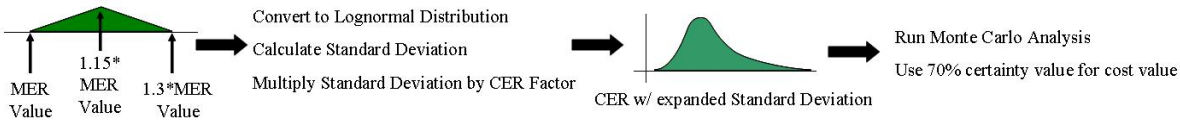

Figure 3-36: Cost Uncertainty Analysis.

For the single value needed in the objective function for optimization, a 70 percent certainty value is used. For the cost discipline, 70 percent of the calculated costs will be lower than this value. The 70 percent estimate is an assumption and can be changed easily depending upon the engineer's preference. The results will also show the range of cost and reliability estimates based upon the 10 and 90 percent confidence bounds.

3.6.3 Summary of Cost Estimation

The cost metric in this methodology is the DDT&E plus the total production cost for the launch vehicle, as shown in Equation 3-25. The operations cost was not included due to a lack of data, but this methodology is capable of finding the parameters that are the leading factors for system cost and reliability of a launch vehicle. Additionally, once operations costs become available, these costs can be incorporated into the process outlined in this dissertation.

Uncertainty analysis is also included within the cost estimate. Margin is included on the mass estimates, which are the basis for the lognormal distribution used in place of a deterministic CER. The standard deviation is calculated from the three mass estimates and multiplied by a factor determined from the analogous systems selected for calculating the deterministic cost estimate. The cost analysis process was outlined in Figure 3-36. Cost analysis is included in the optimization scheme, which is used to find the best design configuration for a specific weighting of system

reliability and cost. Optimization is the subject of the next section.

3.7 Optimization

Optimization is the practice of determining the best combination of design variables to meet an objective function. Examples of objective functions include maximizing the reliability of a vehicle or minimizing its life-cycle cost. An objective function that uses multiple figures of merit, such as cost and reliability, is referred to as an Overall Evaluation Criterion (OEC) or a value function. Design variables are defined as variables that an engineer can control such as the length of a stage, the thrust level of an engine, or the number of crew on a vehicle. In summary, the goal of optimization is to determine the combination of design variables that best satisfies the objective function.

One advantage of using optimization is that bias can be removed from the design process [68]. Since optimization only uses the analysis results to calculate the objective function, one set of design variables is not favored over another. Another advantage of using optimization is automation. Optimization schemes are wrapped around a set of analysis modules to automate the complete process. Therefore, a user can select a set of design variables to change, along with an objective function, and run the optimization scheme with no further action. Optimization is also useful for complex problems with many design variables. Changing the design variables one setting at a time or using intuition to select settings of design variables will most likely lead to a sub-optimal answer. Though the problem may be complex, there are numerous optimization schemes to suit each problem.

There are disadvantages to using optimization. First, the analysis modules that calculate the objective function must be repeatable [68]. When analysis modules are not repeatable, such as when they are combined with Monte Carlo Simulation (MCS), the objective function may be skewed due to the varying result. Therefore, a

set of design variables may be the optimal set because they happen to have a favorable Monte Carlo run. Additionally, setting up an optimization scheme may require considerable effort. The proper inputs and outputs must be determined and linked between the analysis modules along with linking certain outputs to the objective function. A proper objective function must also be determined. The set of design variables must be established along with their ranges. A final disadvantage is that some optimization schemes require a smooth, continuous function. Thus, there is no single technique that a user can apply to an optimization problem to determine an answer. Each problem requires knowledge of optimization techniques and familiarity with the problem itself in order to decide which techniques are applicable. Even though optimization does have its disadvantages, the benefit of knowing which values of the design variables lead to an optimal solution greatly outweigh those drawbacks.

Optimization techniques can be split into two main categories: domain spanning and path building. Domain spanning techniques are optimization schemes that cover the entire design space. Typically, they are less efficient and do not guarantee finding the best objective function. However, domain spanning optimization techniques can handle both discrete and continuous variables along with discrete jumps in the objective function. These techniques do not require an initial guess but they do require boundaries for the design variables. Two examples of domain spanning techniques are a grid search and a Genetic Algorithm (GA) [68].

Path building techniques require an initial guess and use its previous history to find a solution [92]. In a smooth design space, these techniques can find an optimal solution quicker than domain spanning schemes. When used with objective functions that may have local solutions, or solutions that are specific to a certain range of design variables, path building techniques have difficulty moving beyond these local solutions. If a user believes there is only one solution, path building techniques may be more effective because they require less time due to their reliance on previous

history.

Optimization schemes can be decomposed further depending on whether or not they use gradients of the objective function. A series of schemes exist for zero, first, and second order techniques, which are named for how they rely upon the gradient of the objective function. A zero order technique does not rely upon gradient of the objective function to find the answer. Zero order methods are beneficial when discrete jumps exist for either the design variables or the objective function. An example of this optimization technique is called Powell's method [92].

Using the first or second derivative of the objective function can be beneficial because the use of the derivative can reduce the time required for the optimization scheme to find a solution. For example, by using a first order method, the derivative of the objective function can be used to determine the optimum level for the design variables in the current search direction. A new search direction is then selected based upon the algorithm and a new optimum solution is found. This is faster than zero order methods, which rely upon checking the objective function at a new point despite not knowing if that point is the optimum in the current direction. An example of a first order method is the Steepest Descent Method [92].

Second order methods are among the fastest optimization techniques because they create an estimate of the second derivative. Once this second derivative is known, these methods will find the optimal solution in a single step for a quadratic design space. Additional time is required to calculate the second derivative, but that time is offset by moving directly toward the minimum solution. One second order technique is called Sequential Quadratic Programming [68] and is used in engineering software programs such as MATLAB.

3.7.1 Genetic Algorithm

As mentioned earlier, one example of a domain spanning technique is called a Genetic Algorithm (GA). GAs are good techniques for large complex problems that have many design variables and discrete settings within those design variables. A GA "mimics natural selection over several generations" in order to find the minimum point of a function [68]. A Genetic Algorithm will be the optimization scheme used in this methodology to find the best combination of design variables based upon a given weighting of cost and reliability.

The GA optimization scheme loops through three main steps in order to solve the optimization problem. The GA process begins by initializing a population with random designs; each design is a set of design variables at a specific level. Continuous variables must be discretized at a resolution decided by the user. Each design is then evaluated for its objective function value. The lowest value is stored. The next generation of designs is selected using three biologically inspired sub-processes: reproduction, crossover, and mutation. The GA process is illustrated in Figure 3-37.

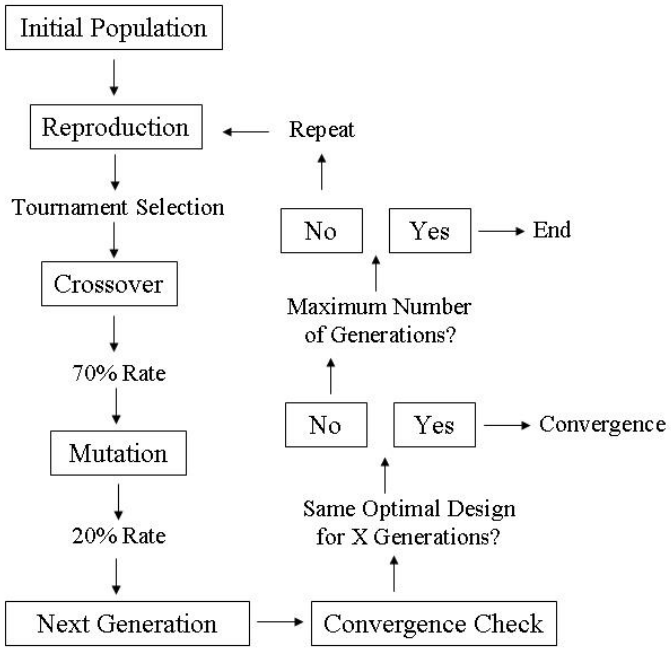

Figure 3-37: GA Process.

In reproduction, which may also be called replication, two different methods can be used. One method for replication is tournament selection. In this method, two or more different designs are selected at random. Each design is evaluated; the design with a lower function value moves forward to the next generation. This process is repeated until the next generation's population size is the same as the previous generations'. An original design is never eliminated during this selection; each design has an equal chance of being selected for a tournament, regardless of previous tournament history.

The next process in GA is crossover. Two different techniques for crossover can be used, but two-point crossover will be discussed. In two-point crossover, two designs are randomly selected for crossover. A random number generator is used to determine if crossover will occur; depending on the user's preferences, crossover may occur seventy-percent of the time. When crossover occurs, an input variable of the two designs is randomly selected [68]. The two designs will then switch their settings of that input variable. Another random number generator is then used to determine how many input variables are switched between the two designs. If a design is selected for crossover, it is removed from the current generation and cannot be selected again. If crossover does not occur, the designs move into the next population untouched.

The final GA sub-process is mutation. Mutation is used to move away from the local minimum in order to ensure global optimization. There is a scenario that all designs in a generation will have the same value for an input variable. In the first two sub-processes, a mechanism does not exist for changing a design variable; therefore, mutation is used to vary the setting of an input variable within a design. If a design is selected for mutation, then one design variable is changed. According to user preferences, a design may mutate twenty percent of the time [68]. After the design is checked for mutation, it moves into the next population.

As a result of stepping through the sub-processes, the next generation has been created. This generation now goes through the sub-processes again until the best

objective function is constant for a specific number of generations. This is one type of convergence criteria. Other convergence criteria include using a maximum number of objective function evaluations.

In this methodology, a genetic algorithm is used because the optimization problem has many design variables and may have multiple local solutions. Additionally, these design variables have a large number of settings, further increasing the dimensionality of the problem. A grid search would take too long because of the number of variables and their settings, while a path-building method cannot be used because of the multiple local solutions. Optimization techniques that rely upon the gradient cannot be used because of the discrete input variables in the design process.

3.7.2 Optimization Application

A genetic algorithm is used to determine the best combination of design variables for a given weighting of reliability and cost. These two metrics are combined in an OEC shown in Equation 3-28. The goal of the optimization is to maximize the OEC; the calculated reliability value is scaled by a maximum whereas the cost minimum is scaled by its calculated variable. The use of the reliability maximum and cost minimum is to ensure that the cost and reliability values have the same order of magnitude.

$$OEC = W_R \frac{R_{calc}}{R_{max}} + (1 - W_R) \frac{C_{min}}{C_{calc}} \tag{3-28}$$

The variable W_R in Equation 3-28 is the weighting on reliability and determines the weighting on cost. This weighting can be varied to find the maximum reliability, minimum cost, or any other specified point. The 'calc' subscript refers to the calculated value and the 'max' and 'min' subscripts are the baseline values for reliability and cost, respectively. The first two cases of the integrated model were conducted to find the maximum reliability and the minimum cost values. Once those values were

known, a range of weightings were used to force the OEC from reliability centric to cost centric.

3.8 Integrated Model

Once the performance, cost, and reliability models have been created, they can be integrated into one environment to study how cost and reliability are coupled for launch vehicles. A set of design variables will be used to change the launch vehicle configuration and examine the sensitivity of the design variables on the performance, reliability and cost metrics. This section will explain how the performance, cost, and reliability models are integrated into a single environment and reveal the design variables used in this methodology.

3.8.1 Design Process

Table 3-14 lists the design variables used for a generic launch vehicle in this methodology. If a three stage launch vehicle is studied, such as the Saturn V, then a set of design variables is added for the third stage. Engine out and the selections of full subsystem redundancy (i.e. a one out of two subsystem configuration) are binary choices. An example of full subsystem redundancy is when two power subsystems are included on a stage but only one is required. Subsystem redundancy does not refer to the propulsion subsystem since engine out is a separate variable choice.

While only one line per stage is shown in Table 3-14, subsystem redundancy can be used for multiple subsystems on a stage. The variable "subsystem redundancy type" in Table 3-14 is also a binary choice and refers to the option of using identical components or functional redundancy for subsystem redundancy. For example, full subsystem redundancy could be selected for the power subsystem and another choice is to use identical components to accomplish subsystem redundancy. As discussed in Section 3.6.1, using identical components is cheaper compared to functional redundancy.

Table 3-14: Generic Launch Vehicle Design Variables.

Design Variable
T/W Ratio Stage 1 T/W Ratio Stage 2
Number of Engines Stage 1 Number of Engines Stage 2
Engine Out (Yes/No) Stage 1 Engine Out (Yes/No) Stage 2
Full Subsystem Redundancy (Yes/No) Stage 1 Full Subsystem Redundancy (Yes/No) Stage 2
Subsystem Redundancy Type Stage 1 Subsystem Redundancy Type Stage 2

The design variables are used in an integrated environment illustrated by Figure 3-38. Figure 3-38 is the design structure matrix created by using this methodology. The discipline tools are listed in the lower right of Figure 3-38. A genetic algorithm is used to find the optimum combination of design variables for a given weighting of system reliability and cost.

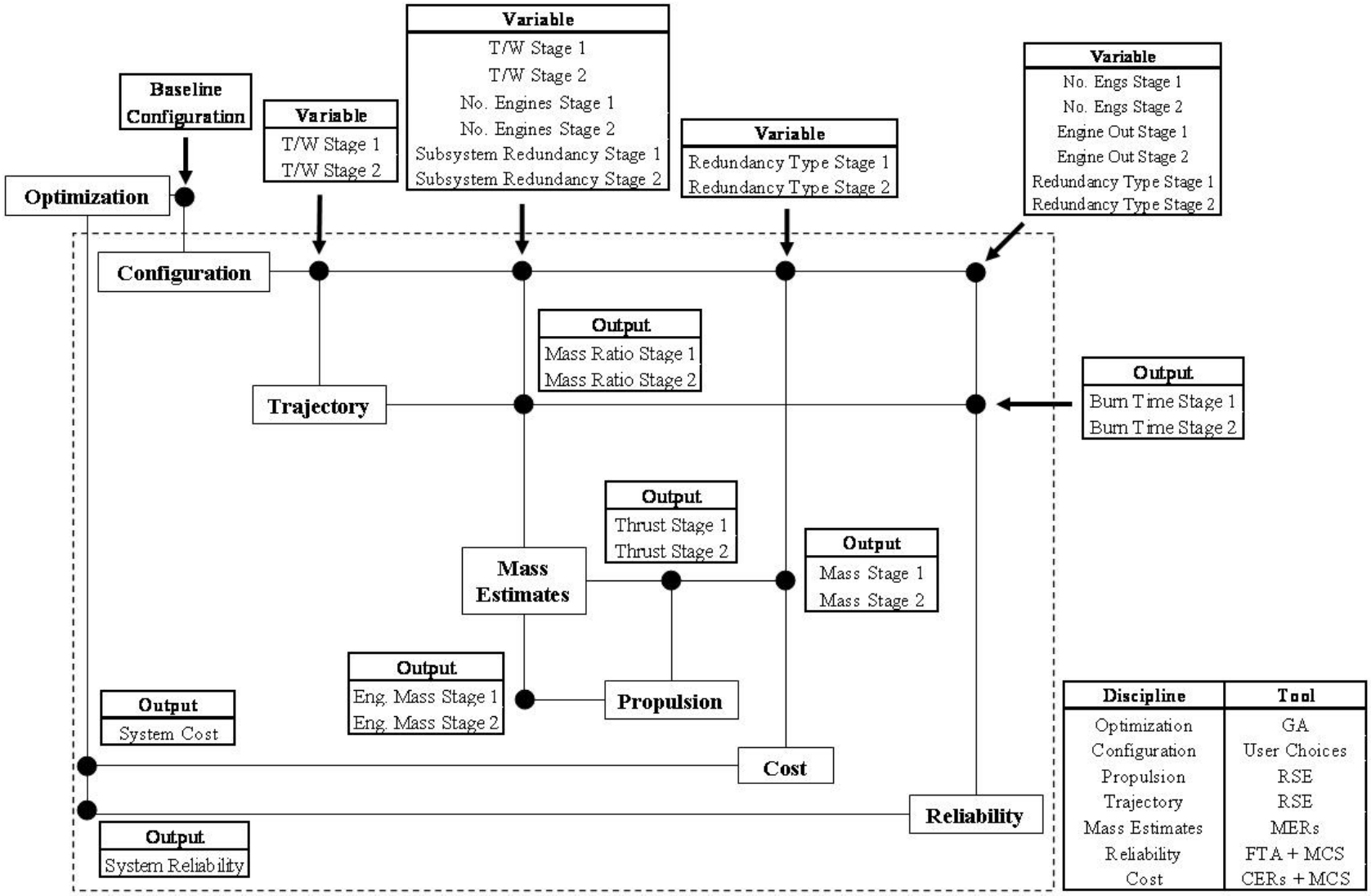

Figure 3-38: Methodology Design Structure Matrix.

In Figure 3-38, the thrust-to-weight ratio of each stage will determine the mass ratio of the respective stages. The mass estimates are completed by using the stage thrust-to-weight ratio, the mass ratio of each stage, and the number of engines per stage. Additionally, the mass of a subsystem may be doubled if full redundancy is selected for a particular subsystem. Since the engine mass depends on the engine thrust, as seen in Figure 3-7, the mass estimates and propulsion disciplines will iterate. The cost model then uses the mass estimates, along with the type of subsystem redundancy, if applicable, to calculate the design, development, testing and evaluation and theoretical first unit cost for each launch vehicle configuration. The cost metric is calculated using Equation 3-25 and the optimization scheme uses the result of Equation 3-25 as one half of its overall evaluation criterion.

The stage reliability estimate is calculated by using the number of engines, whether engine out is utilized, and the type, if any, of full subsystem redundancy. Additionally, the burn time is calculated in the trajectory discipline and used by the reliability analysis for the stage operating time. The stage reliability estimates are combined, as described in Section 3.4.4, to produce the system reliability estimate. This estimate is the other half of the overall evaluation criterion used by the genetic algorithm for optimization.

3.8.1.1 Design Variable Effects

Each design variable choice results in a different vehicle configuration with its own cost and reliability. The stage thrust-to-weight ratio will affect the burn time of the vehicle, the mass estimates, and the thrust level of each engine. The number of engines will affect the thrust level of the engine which then affects the mass estimates. Engine out also affects the mass estimates and thrust level because the stage is required to carry mass that is not performing any function. The use of subsystem redundancy will greatly affect the mass estimates since subsystem mass is doubled if subsystem

redundancy is included.

The cost calculation is affected by all design variables which affect the mass estimates. Additionally, cost is affected by the type of subsystem redundancy used on the vehicle.

Reliability is affected by the stage thrust-to-weight ratio because as the stage thrust-to-weight ratio increases, the operating time decreases. System reliability is also affected by the number of engines because as the engine count increases, total engine reliability decreases. Engine out can be used to increase total engine reliability and system reliability. Finally, using either type of full subsystem redundancy will improve the system reliability. Functional redundancy will have a greater system reliability benefit compared to using identical components for full subsystem redundancy.

3.8.1.2 Model Validation

When modeling a system, validation is important. The development of this methodology required validation due to the performance modeling and the use of response surface equations. The meta-models must be accurate so a design engineer has confidence in using the response surface equations to replace the higher fidelity analysis.

Validation of both the performance models and the RSEs will be shown in Chapter 4. Validation of the models for application to both the Saturn V and the CaLV is completed by comparing different subsystem masses of each vehicle. The Saturn V validation is completed using flight data whereas the CaLV validation is a comparison of analyses. The dry and gross masses are compared along with the trajectory curves. For the response surface equations, statistics such as the R^2 and $R^2 - adjusted$ are used along with a comparison of the predicted versus actual values in order to confirm that the meta-models are acceptable. The developed reliability models will also be validated by comparing the results to models created in RELEX and the stochastic

petri net framework.

Additional validation by analysis occurs when an optimized design point is compared to a design with the same input variables but using the higher fidelity analysis tools such as POST, REDTOP-2, SPN and NAFCOM. The comparison shows that the RSEs do a satisfactory job of approximating the analysis modules.

3.8.1.3 Integrated Model Summary

Table 3-14 listed the design variables for a generic launch vehicle and Figure 3-38 illustrated the design structure matrix for a generic launch vehicle. In the results section of both the Saturn V and Cargo Launch Vehicle applications, the specific design variables and DSM are shown.

The results of using the integrated environment shown in Figure 3-38 will lead to a better understanding of how launch vehicle reliability can be improved and the resulting cost of any reliability improvement. The integrated environment created by linking the performance, cost, and reliability disciplines will also lead to an understanding of the significant cost and reliability drivers of a launch vehicle. Chapter 4 will present the results of applying this methodology to the Saturn V and the Cargo Launch Vehicle. The significant factors of reliability and cost for the Saturn V and CaLV will be revealed along with a set of optimal configurations based on different system cost and reliability weightings.

3.9 Research Hypotheses

After creating this methodology, hypotheses are listed regarding the outcome of applying the present process. The hypotheses will be re-examined in Chapter 5.

- **Hypothesis 1:** No optimal launch vehicle can be determined but the trade between cost and reliability can be identified for selection by a decision maker.
- **Hypothesis 2:** Improvements can be made to the performance based launch

vehicle design processes reviewed earlier. Some of the slower discipline tools can be replaced with response surface equations to improve the speed of a function call. Reliability and cost modeling can be added to the process by using accepted techniques and developing models specific to launch vehicle design. These reliability models will be dynamic and change with different launch vehicle configurations.

- **Hypothesis 3:** Launch vehicle reliability can be increased by (1) reducing operating time, (2) adding engine out to increase total engine reliability, and (3) using full subsystem redundancy (i.e. one out two subsystems) for non-propulsion subsystems. However, both the degree of reliability improvement due to each strategy and the most cost effective reliability strategy may depend on the baseline launch vehicle configuration.

- **Hypothesis 4:** Launch vehicle gross mass may vary greatly when increasing system reliability but the absolute range is to be determined.

- **Hypothesis 5:** The range of launch vehicle system cost is expected to be large because cost is assumed to be a function of mass. The most cost effective method for increasing system reliability is unknown.

- **Hypothesis 6:** Uncertainty analysis should be included in the mass, cost, and reliability disciplines. This will result in a wide range of possible costs and reliability for each design concept.

3.10 Methodology Enhancements

While this methodology improves upon the launch vehicle design process, a few considerations are not included within the approach outlined in this chapter. The only metrics evaluated are development and production cost and system reliability. The Exploration Systems Architecture Study (ESAS) evaluated many other metrics; each

launch vehicle concept was analyzed for a mix of qualitative and quantitative Figures of Merit [66]. Additionally, the operations cost for each vehicle was considered during ESAS [66]. The possibility of including these additional features is discussed below.

3.10.1 Additional Metrics

The qualitative metrics, such as risk and extensibility, can still be evaluated by using discipline experts in the same method that was used for ESAS. While there will be many more configurations to evaluate, using general guidelines may be able to speed up the qualitative assessment for configurations whose design variables are very similar. As mentioned earlier, approaching an optimal solution from the infeasible region is a process commonly used in optimization and the same process may lead to configurations that were not previously considered.

Development risk is one of the biggest qualitative drivers and one reason that "clean-sheet" designs were not evaluated during ESAS. However, the possibility exists that some of the "clean-sheet" configurations could have similar characteristics to current launch vehicles. The new designs could be modified to include aspects of current launch vehicles without losing their effectiveness and reducing the development risk. For example, if the J-2S engine is being re-started, the possibility of re-starting the F-1 engine may be a consideration. Re-starting the F-1 production line could lead to less engines on the booster stage of the Cargo Launch Vehicle. Therefore, while risk is not considered in this methodology, the results may lead to a different configuration that can still be used with some design modifications.

Schedule is another metric that is not considered in detail within this methodology. Schedule is important because a requirement of the Vision for Space Exploration is to land on the Moon by the end of 2020 [6]. The CaLV is an enabling element of the Vision and its development schedule should be considered.

Schedule is a function of the characteristics of the launch vehicle. New development items, like engines, traditionally require longer development time compared to using existing hardware. However, the development time of certain areas could be reduced with additional resources. Therefore, to eliminate a configuration without examining its benefits because its development schedule was deemed too long may not be appropriate. It will be unknown if a configuration has significantly higher benefits compared to designs using existing hardware unless the configuration is evaluated. This methodology will provide the capability to evaluate the configurations eliminated due to schedule and examine the assumption that these configurations will not provide a significant advantage compared to the current concepts.

A quantitative metric that is not evaluated in this methodology is safety. Launch vehicle safety refers to the probability of loss of crew per mission. As a general trend, configurations that increase reliability will also increase safety. However, there are scenarios where uncertainty exists if increasing vehicle reliability will increase safety. Additionally, evaluating safety requires additional modeling capabilities beyond those used for reliability. How a component fails and the possibility for abort must be considered. One example of the additional complexities of calculating safety is increasing the stage-thrust-to-weight ratio. Increasing this ratio decreases the possibility for successful abort near the region of maximum dynamic pressure but vehicle operating time is reduced. Therefore, it is uncertain how the probability of loss of crew would change when the stage thrust-to-weight ratio is increased.

Safety would benefit the higher reliability configurations by giving them extra weight in the selection process. The safety metric could easily be added within the design process because this methodology was created with a goal of flexibility. Therefore, if a safety model that depends upon the different characteristics of a launch vehicle is created, it could be added to this methodology.

3.10.2 Operations Costs

Operations costs are a feature that should be included as this methodology evolves. The results presented will show the best configuration for a combination of the development and production cost. Without the operations cost, the full life-cycle is not included. As mentioned earlier, operations costs are difficult to model. Very little data exists about launch vehicle operations costs because the private industry protects these costs due to competition.

The various configurations presented in Chapter 4 will have widely varying mass estimates and thrust-to-weight ratios, which leads to wide ranges in liftoff thrust levels. A configuration that requires significant modifications of the existing infrastructure compared to the baseline design should be penalized by additional operations cost. For example, the gross mass of the maximum reliability configuration of the CaLV is 3,000,000 pounds heavier than the baseline CaLV. Any operations modifications for the baseline CaLV would require additional improvements to accommodate such a larger vehicle. Adding extra engines or another power subsystem would increase the processing time and this cost penalty should be accounted for when evaluating different configurations. An operations cost model that can be used in an integrated design environment would be an excellent enhancement to the process outlined in this dissertation. Additional enhancements, such as the cost of unreliability, are discussed in the future work section.

3.10.3 Methodology Limitations

There are some limitations when implementing the process outlined in this chapter. The exponential distribution is used as the governing failure distribution for all reliability analysis. One property of the exponential distribution is a failure rate that is constant with time. Thus, the different phases of flight, such as liftoff, tower clearance, area of maximum dynamic pressure, etc., are not considered in great detail. If more

detail is desired, such as a lower level analysis of engine reliability to analyze engine ignition, the Weibull distribution may be more appropriate for use as the governing failure distribution. The Weibull distribution was discussed in Section 3.3.2. The Weibull distribution allows an engineer to model the different phases of flight with varying failure rates. A varying failure rate could be useful when analyzing engine reliability; a degrading failure rate would result in a higher probability of failure for engine ignition compared to the steady operational phase.

If this methodology were applied to a reusable system, such as the next in-space human vehicle, then a Weibull distribution should be used because of the change in failure rate. The changing failure rate will model vehicle aging, which is more appropriate for reusable systems than a constant failure rate.

A conservative approach to the design of engine out configurations is another limitation of this methodology. An assumption is made to design the engine out configurations for the worst case scenario, which is failure during stage ignition. Therefore, an engine out design may be able to sustain two engine failures later in flight when some of the propellant has been burned. However, additional reliability credit is not considered for launch vehicles with this capability. Additionally, a configuration without engine out may be able to sustain a single engine failure later in flight but again, the additional reliability benefit is not considered.

Another limitation of this methodology is the fidelity of the cost discipline. The focus of this methodology is on developing the necessary reliability models for creating an integrated environment. The performance disciplines have been well developed due to the traditional focus on these areas throughout history. Thus, the fidelity of the cost discipline differs from the performance and reliability disciplines. In this methodology, cost is primarily a function of the dry mass of a vehicle. However, a composite structure may weigh less than an aluminum alloy but could cost more because of the higher manufacturing complexity of large composite elements. More

refined cost techniques and estimates are required before a decision maker can have full confidence in the absolute cost results.

A design option that was not considered was the engine cycle type, which leads to a different Isp. Adding engine cycle type would alter the original baseline design but the capability to study thousands of completely different concepts would be beneficial for launch vehicle design. However, creating response surface equations to replace the trajectory analysis will become more difficult with the inclusion of engine Isp. Furthermore, additional RSEs may be required to represent the propulsion discipline because the engine thrust-to-weight ratio will vary depending on cycle type.

CHAPTER IV

RESULTS

In this chapter, the results of applying the integrated performance, cost, and reliability methodology to the Saturn V and Cargo Launch Vehicle are presented. The Saturn V launch vehicle was selected for a demonstration problem since all of the necessary performance models could be verified by actual flight data. Additionally, reliability estimates existed for each of the subsystems and components required to calculate the system reliability.

The second problem selected for application of the methodology is the Cargo Launch Vehicle (CaLV) which was originally selected for the next lunar mission. The results will be compared to ESAS [66], which used existing engines for its final CaLV design.

A genetic algorithm was used to find a series of optimal designs using an overall evaluation criterion with varying weights on cost and reliability. The optimal designs show how the launch vehicle configuration changes from a cost centric to a reliability centric design. The number of function calls to find a converged solution varied from slightly over 1800 to slightly under 3200. However, with the use of response surface equations, only five seconds was required to evaluate a launch vehicle concept as compared to five minutes if the original propulsion and trajectory analysis modules were incorporated. The uncertainty analysis was the leading cause of evaluation time and strategies for reducing that time are discussed in the future work section.

The models created for the launch vehicle design process must be validated against a standard, which could be commercial software, other accepted models, or a baseline. The reliability modeling is validated by comparing the model development to the

commercial software package RELEX [75]. Stochastic Petri Nets were used to validate the engine out model in Section 3.4.1.2. The subsystem redundancy models with common cause failure are validated using RELEX. The cost model is NAFCOM; additional validation is unnecessary because NAFCOM is the cost model that NASA uses for manned missions. The performance models for the Saturn V are validated against historical references while the CaLV is validated using ESAS [66].

The propulsion and trajectory RSEs must be validated because they are replacing higher fidelity analysis modules. In addition to examining the statistical measures of merit, such as R^2, further RSE validation is completed by comparing off-design points to the true values. All of the model and RSE validation is completed within the first two subsections of the Saturn V and CaLV sections. By building confidence in the models used within the methodology, the results can be examined for trends as opposed to questioning their validity.

The results of both applications follow the validation section. This chapter illustrates how the total production and development cost will vary as different design variables are selected to increase system reliability. A graph will be used to show the optimal configurations based on different weightings of reliability and cost. A design engineer can use the results of applying this methodology to examine the system cost of increasing launch vehicle reliability and know which configurations lead to particular results.

4.1 Saturn V

The Saturn V launch vehicle was described in Section 2.2.1. For review, the Saturn V launch vehicle was a three stage launch vehicle with five engines on the S-IC stage, five engines on the S-II stage, and a single engine on the S-IVB stage. One important note is that the engines on the S-II and S-IVB stage were the same; therefore, all Saturn V configurations presented in this section will use the same engine for the

second and third stage. The mission objectives and trajectory constraints are listed in Appendix I.

The Saturn V design variables are listed in Table 4-1. For the Saturn V application, the only subsystems with the option of using full subsystem redundancy (i.e. a one of two subsystem redundancy configuration) were the power and avionics subsystems. As mentioned earlier in Section 3.4.2, other subsystems could have been studied with additional reliability models. Since the S-II and the S-IVB stages use the same engine, only the S-II stage determines the thrust of the engine and the option of selecting the S-IVB thrust-to-weight ratio is not included. Iteration is used to match the S-IVB thrust-to-weight ratio with the correct mass ratio.

Table 4-1: Saturn V Design Variables.

Design Variable	**Minimum**	**Maximum**	**Type**
S-IC T/W Ratio	1.1	1.3	Continuous
S-II T/W Ratio	0.65	1.0	Continuous
No. of Engines S-IC	4	7	Discrete
No. of Engines S-II	4	7	Discrete
No. of Engines S-IVB	1	4	Discrete
Engine Out S-IC	Yes	No	Discrete
Engine Out S-II	Yes	No	Discrete
Engine Out S-IVB	Yes	No	Discrete
Full Power Redundancy S-IC	Yes	No	Discrete
Full Avionics Redundancy S-IC	Yes	No	Discrete
Full Power Redundancy S-II	Yes	No	Discrete
Full Avionics Redundancy S-II	Yes	No	Discrete
Full Power Redundancy S-IVB	Yes	No	Discrete
Full Avionics Redundancy S-IVB	Yes	No	Discrete
Power Redundancy Type S-IC	Identical Components	Functional	Discrete
Avionics Redundancy Type S-IC	Identical Components	Functional	Discrete
Power Redundancy Type S-II	Identical Components	Functional	Discrete
Avionics Redundancy Type S-II	Identical Components	Functional	Discrete
Power Redundancy Type S-IVB	Identical Components	Functional	Discrete
Avionics Redundancy Type S-IVB	Identical Components	Functional	Discrete

The design structure matrix for the Saturn V is shown in Figure 4-1. Figure 4-1 is very similar to Figure 3-38 except vehicle specific design variables are used.

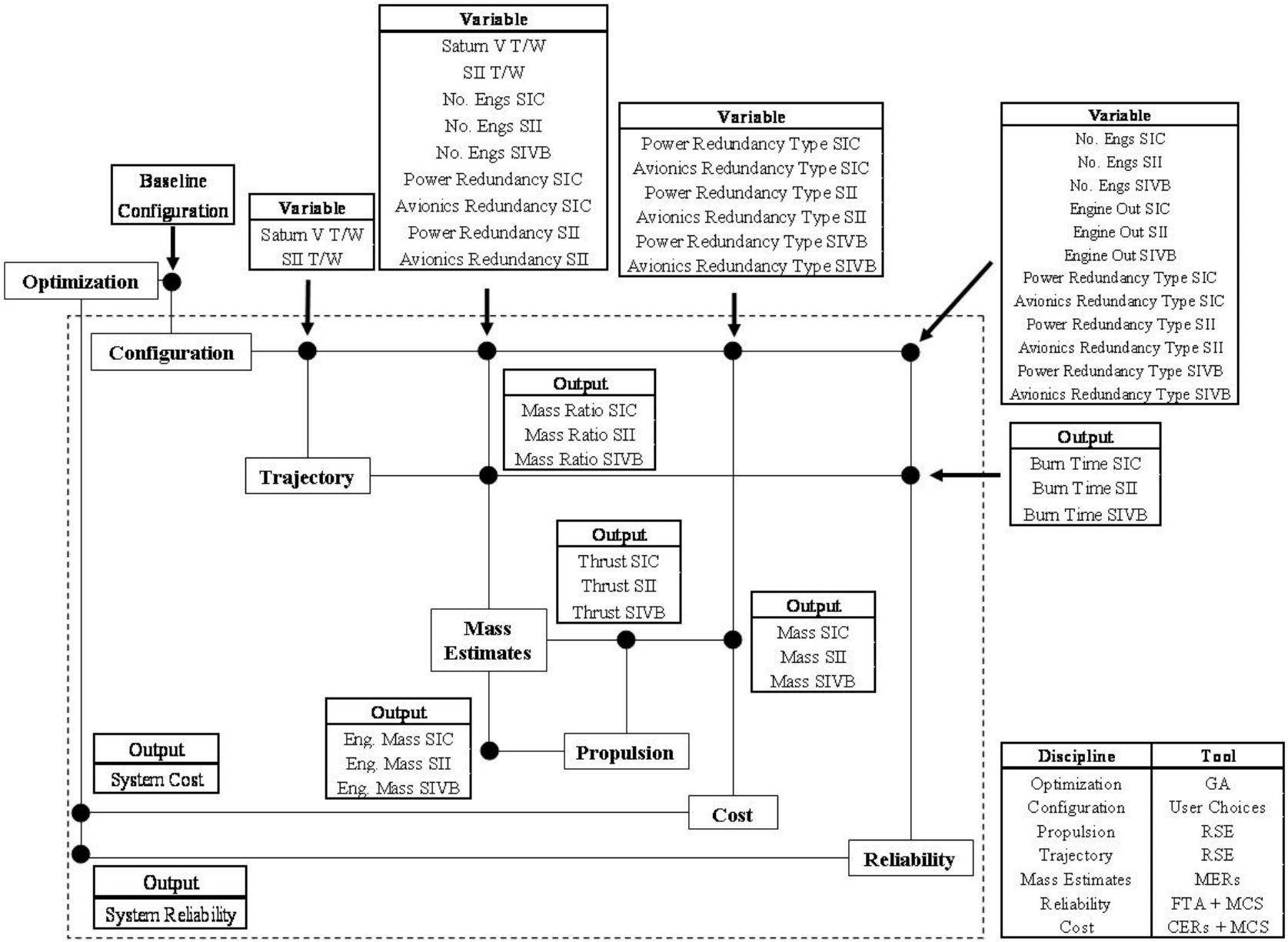

Figure 4-1: Saturn V Design Structure Matrix.

4.1.1 Model Validation

4.1.1.1 Reliability Validation

The reliability models in the present application are validated with the commercial software RELEX [75]. As expected, there is no significant difference between the RELEX calculation and the analysis used in the integrated model. For any calculations in series, such as when functional redundancy is selected for a subsystem, Equation 3-18 is used to calculate the reliability. Since the calculation is simple, no validation is shown; the analysis in the integrated model was cross-checked by hand to ensure the validity of the calculation. When using full subsystem redundancy (i.e. a one out two subsystem redundancy configuration) with identical components, common cause failure is included in the calculations; the validation of this redundancy model is listed in Table 4-2. The β value is equal to 0.1 and the component reliability is 0.98. The RELEX model for this system is shown in Appendix B.

Table 4-2: Reliability Validation for Component Redundancy.

Calculation	**RELEX**	**Model**	**% Difference**
Reliability	0.9977	0.9977	0.00
MFBF	430.41	430.29	0.03

The engine out failure model shown in Figure 3-26 is validated by using a model created in the stochastic petri net framework. Table 3-6 shows good agreement between the engine out model with uncertainty and the stochastic petri net model. Equation 3-18 is used to complete the stage and system reliability calculations; these computations are also cross-checked by hand to ensure the correct calculation.

4.1.1.2 Performance Validation

The performance models also need to be validated. Both the mass estimates and the trajectory optimization are compared to historical references. The masses are

calculated with MERs [78] and compared to historical data in Table 4-3 [95]. Table 4-3 and Table 4-4 show good agreement between the MERs and the historical data.

Table 4-3: Dry Mass Comparison for Saturn V Stages[lb].

Stage	Reference	MERs	% Difference
S-IVB	27307	27504	0.07
S-II	97375	97492	0.12
S-IC	287451	287579	0.04

Table 4-4: Gross Mass Comparison for Saturn V Stages[lb].

Stage	Reference	MERs	% Difference
S-IVB	264709	263838	0.33
S-II	1081781	1088195	0.59
S-IC	5030911	5090577	1.19
S-V	6486333	6551541	1.01

The POST validation is completed by comparing a model to a historical reference. Since POST performs a trajectory optimization, there are a few differences between the modeled trajectory and the actual performance. Table I-1 in Appendix I lists the trajectory assumptions used for the Saturn V in the POST analysis.

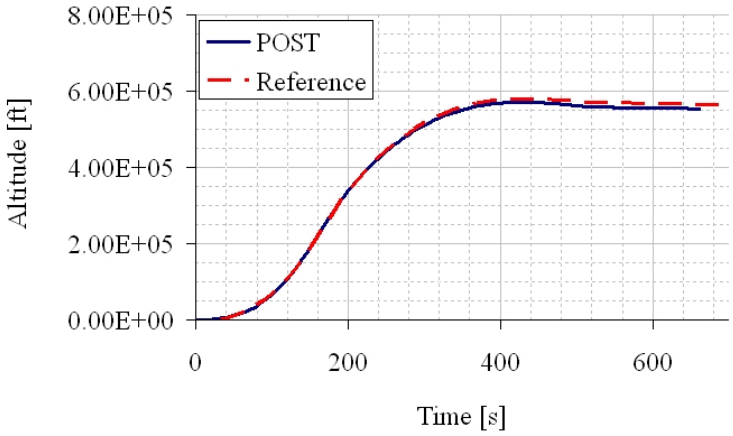

Figure 4-2: Trajectory Comparison for the Saturn V.

The Saturn V flight manual is used as a reference for the data values in Figures 4-2 - 4-4 [61]. Figure 4-2 illustrates the trajectory using an altitude versus time plot. Figure 4-3 is a comparison of the inertial velocity as a function of time for the Saturn V. These plots show good agreement, with special attention paid to the bends in the curve at each staging point. The first staging point is where the largest error occurs between the reference and the model. However, the error at this point is less than 5 percent and the rest of Figure 4-3 matches well.

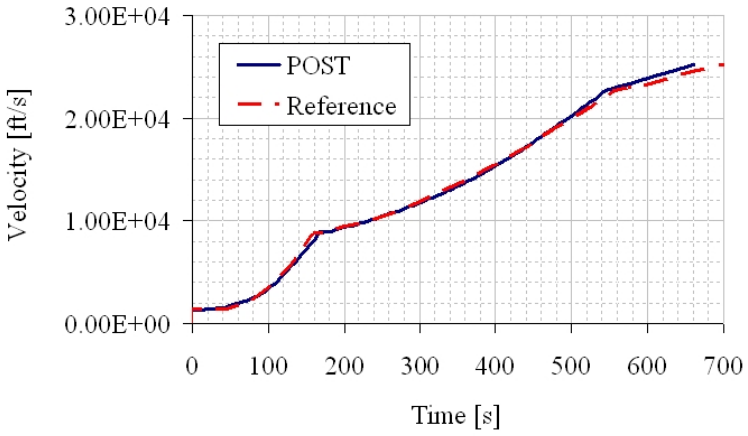

Figure 4-3: Inertial Velocity Comparison for the Saturn V.

In Figure 4-4, there is a difference between the curve generated from the historical data and the curve from POST. The most likely source of error is from comparing a trajectory optimization to the actual Saturn V flight. When examining Figure 4-4, the first dip is caused by the center engine shutdown of the F-1 on the S-IC stage. The reference has the engine shut down occurring later in time at approximately 170 seconds whereas the optimal trajectory has a center engine shutdown at approximately 160 seconds.

The second acceleration peak is different because the Saturn V vehicles in Figure 4-4 are staging on the same final conditions. Since the POST model shuts down the center engine earlier than the actual Saturn V, the POST model will burn for a longer period of time. This explains the difference in the first staging point along with why

the acceleration peak is higher at the end of the S-IC burn. The opposite is happening with regard to the S-II stage. The acceleration matches well until center engine cut-off; then the acceleration plots diverge. In this scenario, the center engine for the POST model is burning for a longer period of time compared to the reference data, reaching a higher acceleration peak for the S-II stage. Additionally, the reference data appears to have a different thrust profile because the thrust-to-weight ratio is different at S-II center engine shutdown. The difference in thrust profile carries over to the S-IVB stage where the acceleration plots match the trend, but not the values.

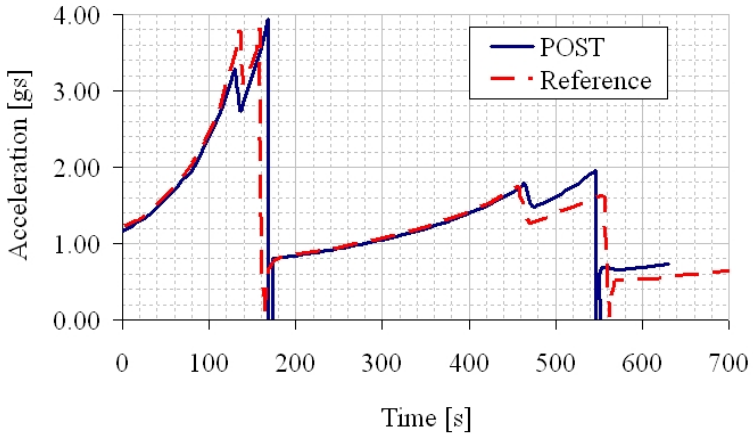

Figure 4-4: Acceleration Comparison for the Saturn V.

The mass ratio and burn time are slightly different when comparing the POST model and the flight data from the Saturn V. POST is optimizing a trajectory for minimum propellant mass, which is why these differences are occurring. The optimized solution uses slightly less propellant and can reach the final velocity conditions in slightly less time. However, the overall POST results match well with the actual flight data and the trajectory discipline will be based on POST.

4.1.2 RSE Validation

When using response surface equations, additional validation beyond examining the goodness of fit statistics is recommended to provide full confidence that the RSE can

be used in place of the analysis module. RSEs are used in both the propulsion and trajectory discipline to accelerate the process and streamline the methodology. An RSE was created for the propulsion discipline to generate the J-2 engine thrust-to-weight (vacuum) ratio as a function of the engine thrust. The data values from the RSE fit are listed in Table F-7 in Appendix F.

Table F-7 in Appendix F lists a comparison of the REDTOP-2 results with the values calculated from the RSE using off-design points. Off-design points are data points that were not used to create the original RSE. The errors are small and within an acceptable range to justify the use of an RSE to approximate the propulsion discipline.

A series of response surface equations were generated to replace POST. Two RSEs were created for each stage; the independent variable was the stage thrust-to-weight ratio. The dependent variables of the two trajectory RSEs were the stage mass ratio and the stage burn time. The statistics of the POST RSEs are listed in Appendix F.

Table F-8 in Appendix F lists three points for each stage of the Saturn V that were not used in the original RSE fit. The mass ratio fit is very good, with little error on the stages. The burn time has a little error, specifically for the S-IC stage; however, the burn time error is never larger than a few seconds.

4.1.3 Saturn V Results

Figure 4-5 illustrates how the reliability of the Saturn V launch vehicle could change by using different settings of the design variables in Table 4-1. Additionally, Figure 4-5 illustrates the range of system costs that would be required to increase the Saturn V reliability. The Saturn V baseline design is illustrated with the circle in Figure 4-5.

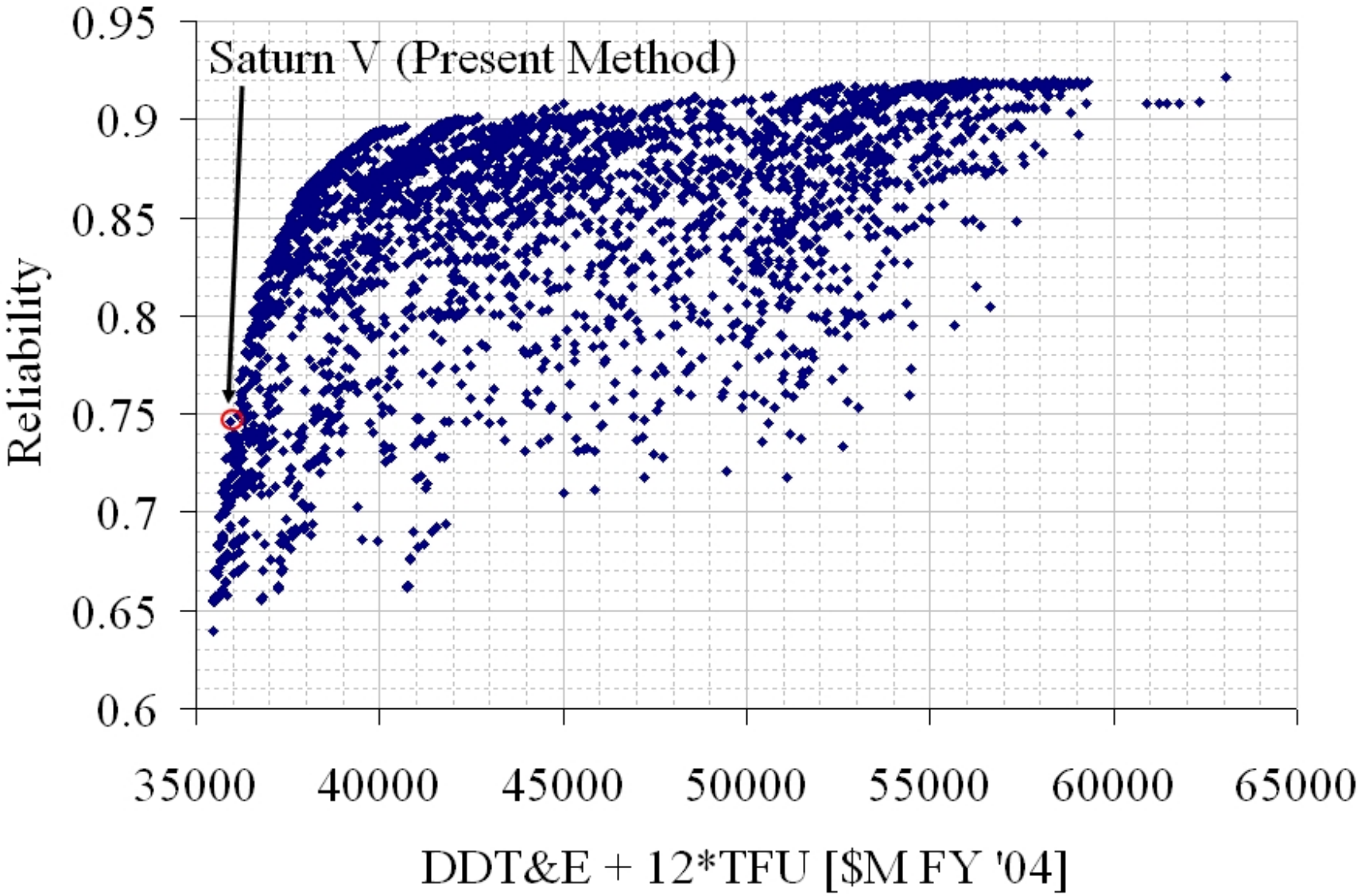

Figure 4-5: System Cost versus Reliability for the Saturn V.

Figure 4-6 illustrates the same results as Figure 4-5 except mean flights between failure is the metric along the y-axis instead of reliability. Examining Figure 4-6 shows that the MFBF of the Saturn V could have been reduced from 3.94 to 8.05 for an additional 2.7 billion dollars [FY '04]. The decrease in MFBF is 104 percent while the cost increase is 7.6 percent.

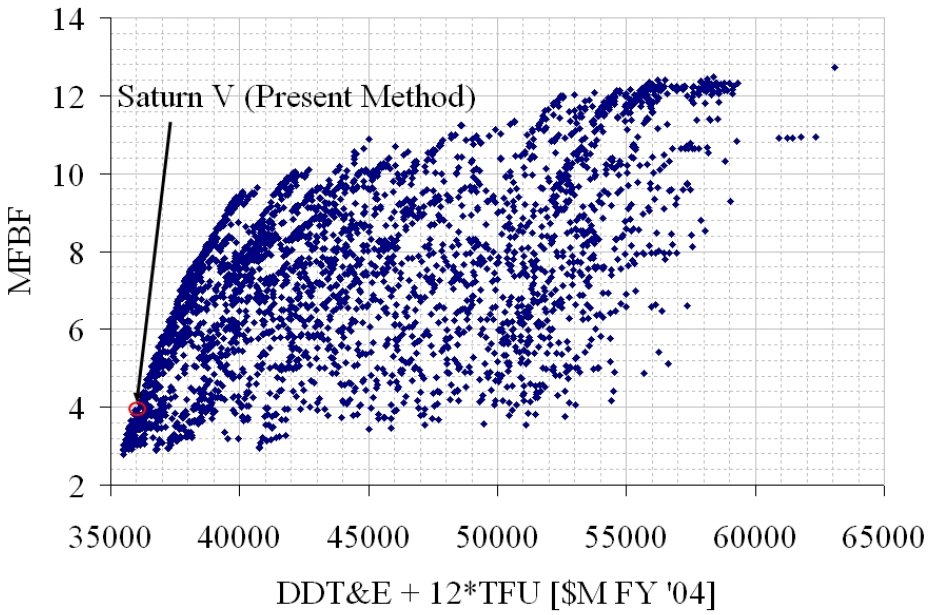

Figure 4-6: System Cost versus MFBF for the Saturn V.

4.1.4 Optimal Configurations

A pareto frontier is shown in Figure 4-7. A pareto frontier is the boundary created by finding all of the design configurations that have the maximum reliability for a specific cost. To the right of the pareto frontier are all the possible design configurations while the left side represents the infeasible area. The Saturn V is identified in Figure 4-7 with a circle.

Table 4-5 lists the design variable settings used to produce the results in Figure 4-7. The abbreviation "IC" refers to the use of identical components for subsystem redundancy, while "F" is used to denote functional redundancy. Cost and reliability

both increase when examining the vehicle designs from left to right across Table 4-5. A more detailed mass comparison of the minimum cost configuration, "Design 6", and the maximum reliability configuration can be found in Table H-1. A more detailed cost comparison of the three mentioned designs is listed in Table G-1. The trajectory plots for the minimum cost configuration, design six, and the maximum reliability configuration can be found in Appendix I.

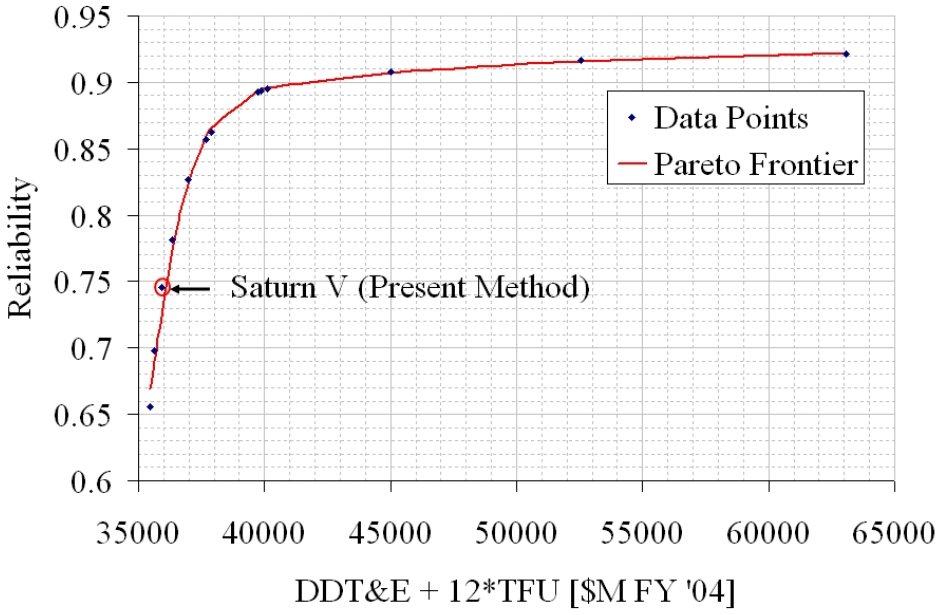

Figure 4-7: Saturn V Pareto Frontier.

Table 4-5: Design Variable Settings for the Saturn V Pareto Frontier.

Parameter	**Min. Cost**	**Design 2**	**Design 3**	**Design 4**	**Design 5**	**Design 6**	**Design 7**	**Design 8**	**Design 9**	**Design 10**	**Design 11**	**Max. Rel.**	**Saturn V Baseline**
Cost [$M FY '04]	35473	35619	36339	36952	37701	37889	39738	39881	40110	44998	52548	63070	35939
Reliability	0.6555	0.6976	0.7814	0.8271	0.8571	0.8627	0.8924	0.8936	0.8950	0.9082	0.9167	0.9215	0.7460
S-IC T/W Ratio	1.129	1.129	1.129	1.129	1.129	1.157	1.186	1.186	1.186	1.243	1.243	1.300	1.160
S-II T/W Ratio	0.70	0.75	0.80	0.80	0.80	0.85	1.00	1.00	1.00	1.00	1.00	1.00	0.75
No. of Engines S-IC	5	5	5	5	5	5	4	4	4	4	4	4	5
Engine Out S-IC	No	No	No	No	No	No	No	No	No	No	No	Yes	No
No. of Engines S-II	7	6	5	6	5	5	4	4	4	4	4	4	5
Engine Out S-II	No	No	No	Yes	Yes	Yes	Yes	Yes	Yes	Yes	Yes	Yes	No
No. of Engines S-IVB	1	1	1	1	1	1	1	1	1	1	1	2	1
Engine Out S-IVB	No	No	No	No	No	No	No	No	No	No	No	Yes	No
Power Redundancy S-IC	None	None	None	None	IC	IC	IC	F	F	F	F	F	None
Avionics Redundancy S-IC	None	None	None	None	None	None	None	None	None	None	IC	F	None
Power Redundancy S-II	None	None	IC	IC	IC	IC	F	F	F	F	F	F	None
Avionics Redundancy S-II	None	None	None	None	None	None	None	None	None	IC	IC	F	None
Power Redundancy S-IVB	None	None	IC	IC	IC	IC	IC	IC	F	F	F	F	None
Avionics Redundancy S-IVB	None	None	None	None	None	None	None	None	None	F	F	F	None

4.1.5 Reliability Results

By examining Table 4-5, a variety of different trends are revealed. The stage thrust-to-weight ratio of both the S-IC and S-II increases as greater emphasis is placed on system reliability. This trend is expected since increasing the stage thrust-to-weight ratio decreases the stage operating time. Additionally, the number of engines on each stage decreases as system reliability increases. This occurs because reducing the number of engines eliminates an additional component with the possibility of failure. An exception occurs when engine out is included on the second stage; the number of engines increases but only to accommodate the extra engine used in the engine out scenario.

The first type of redundancy used on the Saturn V is when full power subsystem redundancy (i.e. a one of out two power subsystem configuration) is selected for both the S-II and S-IVB stages on "Design 3" in Table 4-5. Identical components are used to provide the full power subsystem redundancy with a one out of two subsystem configuration and this reliability strategy is selected before engine out is utilized.

Table 4-6: Design 3 Reliability Importance.

Reliability Strategy	**System Reliability**	**System Cost [$M FY '04]**
None (Baseline)	0.7393	35880
Power Red. S-II	0.7577	36095
Power Red. S-IVB	0.7622	36147
Power Red. S-II & SIVB	0.7814	36339
EO S-II	0.8027	36907

Table 4-6 lists why the power subsystem redundancy is selected before engine out is chosen. Using "Design 3" without any reliability strategies as a baseline (i.e. "Design 3" without any type of redundancy), the cost of using engine out on the S-II stage is too high compared to using power subsystem redundancy in a one out of two

configuration with identical components. While the reliability benefit of using power subsystem redundancy is smaller compared to using engine out on the S-II stage, the cost of using power subsystem redundancy is also less compared to the cost of employing engine out on the S-II stage.

In Table 4-5, engine out is not included on the S-IC or the S-IVB stage until the maximum reliability configuration is found. Table 4-7 uses design three from Table 4-6 as a baseline to compare the benefits of adding engine out to each stage. For the S-IVB stage, adding an extra engine to increase system reliability does not justify the extra cost. Likewise, adding an extra engine to the S-IVB increases the mass of the entire launch vehicle, as seen in Table 3-2. As seen in Table A-1, the S-IC engine reliability is very high; therefore, engine out on the S-IC stage does not provide a large enough reliability benefit to justify the additional cost.

Table 4-7: Design 3 Stage Engine Out Comparison.

Reliability Strategy	**System Reliability**	**System Cost [$M FY '04]**
None (Baseline)	0.7393	35880
EO S-IC	0.7898	37177
EO S-II	0.8027	36907
EO S-IVB	0.7934	37083

The maximum reliability configuration uses the least amount of engines for the S-IC and S-II stages, along with engine out for all three stages of the Saturn V. The thrust-to-weight ratio of both the S-IC and S-II stage are at the maximum values; as thrust-to-weight ratio increases, the stage burn time will decrease. Additionally, functional redundancy is included for every subsystem because since it is assumed that functional redundancy is not susceptible to common cause failure.

4.1.6 Cost Results

The minimum cost configuration in Table 4-5 uses low stage thrust-to-weight ratios, no engine out, and no type of subsystem redundancy. Adding any subsystem redundancy adds mass which is not required to meet the mission objectives. Additionally, engine out capability also adds mass that is not necessary to satisfy the mission constraints for the Saturn V. Since cost is calculated from mass, any unneeded mass becomes a cost burden.

Table 4-8 lists a comparison between the minimum cost configuration from Table 4-5 and designs that are changed by a single parameter. For example, the design in row two of Table 4-8 is the same as the minimum cost configuration listed in Table 4-5 except the S-IC thrust-to-weight ratio is changed from 1.129 to 1.1.

Table 4-8: Minimum Cost Comparison.

Parameter Changed	**New Value**	**System Cost [$M FY '04]**	**System Reliability**
None	Min. Cost	35473	0.6555
S-IC T/W	1.1	35474	0.6547
S-IC T/W	1.15	35484	0.6560
S-II T/W	0.65	35474	0.6547
S-II T/W	0.75	35484	0.6560
S-IC No. Engs.	6	35483	0.6553
S-IC No. Engs.	4	35485	0.6557
S-II No. Engs.	6	35597	0.6837

Table 4-8 shows that increasing and decreasing the S-IC and S-II thrust-to-weight ratio leads to configurations with higher system costs. Decreasing the stage thrust-to-weight ratio will increase the dry mass of the launch vehicle because of the higher trajectory losses, as discussed in Section 3.1.6. A higher dry mass can lead to a higher system cost.

Engine costs are a primary driver of stage cost, as shown in Figure 4-8 for the S-II stage. Avionics are also a leading factor of stage cost but the avionics mass is

not as sensitive to changes in the design variables, unless subsystem redundancy is employed. Increasing the stage thrust-to-weight ratio will lead to a higher system cost because of an increasing engine cost. The engine thrust increases as the stage thrust-to-weight ratio increases; a higher engine thrust leads to a higher engine cost as seen in Figure 3-32. Table 4-9 lists a comparison of engine costs for the design configurations listed in Table 4-8.

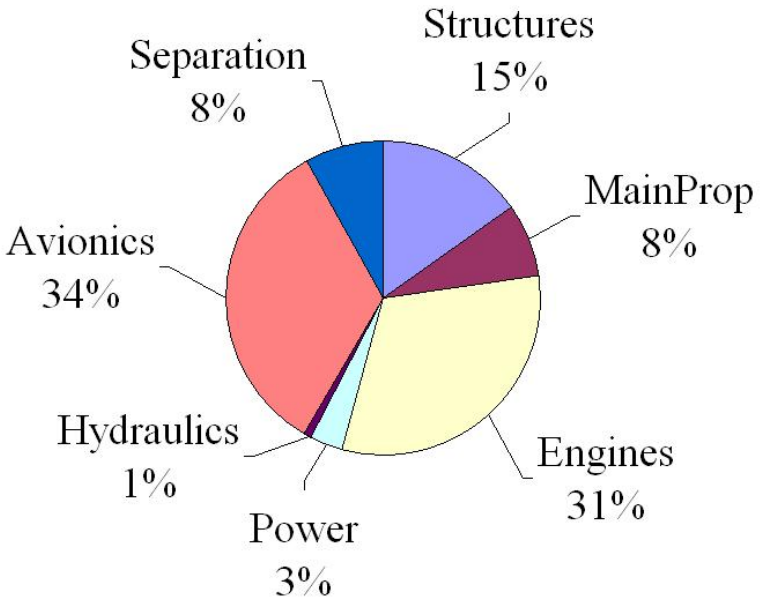

Figure 4-8: S-II DDT&E Cost Breakdown.

Table 4-9: Engine Cost Comparison for Minimum Cost Configurations [$M FY '04].

Row Number	**Parameter Changed**	**New Value**	**S-IC Eng. DDT&E**	**S-IC Eng. TFU**	**S-II Eng. DDT&E**	**S-II Eng. TFU**
1	None	Min. Cost	1094	69	923	57
2	S-IC T/W	1.1	1090	69	923	57
3	S-IC T/W	1.15	1097	70	923	57
4	S-II T/W	0.65	1099	70	907	55
5	S-II T/W	0.75	1090	69	938	58
6	S-IC No. Engs	6	1035	79	923	57
7	S-IC No. Engs	4	1172	58	923	57
8	S-II No. Engs	6	1096	69	968	51

The results listed in Table 4-9 show how the engine costs vary at design points near the minimum cost configuration. When the S-II engine DDT&E is reduced by lowering the S-II thrust-to-weight ratio, row four in Table 4-9, the extra propellant mass required for the S-II stage has a cascade effect on the S-IC stage and the engine costs of the S-IC stage increase. When six engines are used on the S-IC stage, row six in Table 4-9, the DDT&E cost is reduced but the total engine TFU cost is higher than the minimum cost configuration. Therefore, over a campaign of twelve flights, the difference in TFU cost will account for the difference in DDT&E cost.

The minimum cost configuration will change if the number of campaign flights is changed. Figure 4-9 shows two other design configurations that could be the minimum cost configuration if the number of campaign flights changes. Design two could be the minimum cost configuration if 16 flights are used in the campaign while design three could be the minimum cost configuration if the campaign has only one flight.

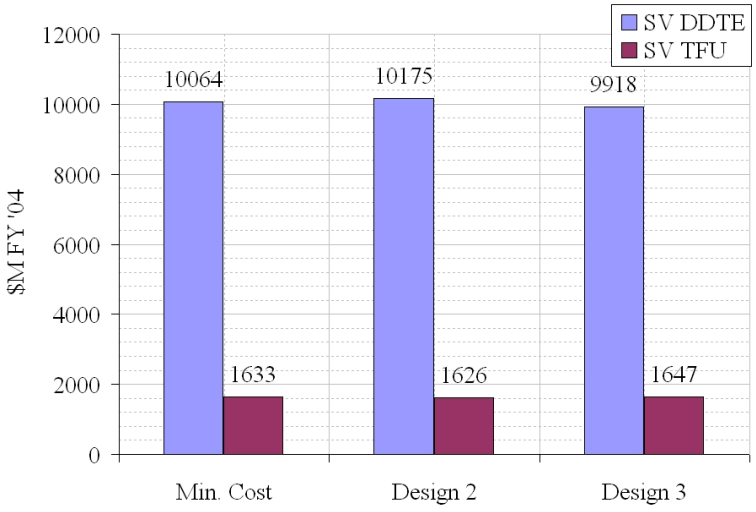

Figure 4-9: Alternative Design Cost Comparison.

Schedule considerations are presented using the cost fractions listed in Table 3-12. An eight year development is assumed; the distributed cost is the development (DDT&E) cost plus the first unit (TFU) cost. A detailed cost profile for the designs

listed in Table 4-5 can be found in Table J-1 - Table J-4 of Appendix J. The different tables in Appendix J correspond to various assumptions about the development schedule. Figure 4-10 illustrates the peak year funding for each of the designs listed in Table 4-5.

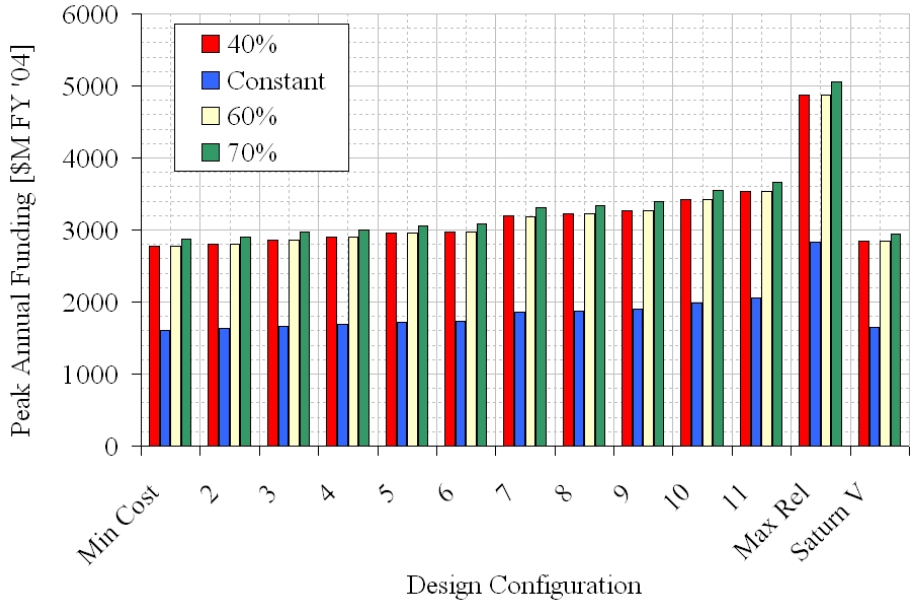

Figure 4-10: Optimal Configuration Peak Funding Comparison.

In Figure 4-10, the large difference in peak funding occurs when a constant development spread is used. The constant development spread means that each year will require a constant amount of resources to complete program development. When using the other spread assumptions, the peak funding values are relatively close for each design. However, the peak funding differs across the whole range of optimal configurations. While the schedule results are a first order analysis, a decision maker could use Figure 4-10 to examine if any designs should be eliminated because of peak funding concerns.

Table 4-10 lists a detailed peak funding comparison of the design configurations in Figure 4-10. Comparing the Saturn V baseline with design five in Table 4-10 reveals the Saturn V MFBF could have been increased significantly for little additional peak

funding cost. The increase in cost would have been approximately three percent across the different distributions while the MFBF would have increased by 78 percent. A comparison of design four with the Saturn V baseline reveals the MFBF could have been increased by 47 percent for a peak funding increase of two percent.

Table 4-10: Peak Funding Comparison.

Design Config.	**40 Percent Assumption**	**Constant Assumption**	**60 Percent Assumption**	**70 Percent Assumption**	**Reliability**	**MFBF**
Min. Cost	2772	1612	2771	2876	0.6555	2.90
2	2801	1628	2800	2905	0.6976	3.31
3	2860	1663	2859	2967	0.7814	4.58
4	2898	1685	2897	3006	0.8271	5.78
5	2953	1717	2952	3063	0.8571	7.00
6	2972	1728	2971	3082	0.8627	7.28
7	3190	1855	3189	3309	0.8924	9.29
8	3219	1872	3218	3339	0.8936	9.40
9	3272	1902	3271	3394	0.8950	9.52
10	3425	1991	3423	3552	0.9082	10.89
11	3537	2056	3535	3668	0.9167	12.01
Max Rel.	4878	2836	4876	5060	0.9215	12.74
Saturn V	2844	1654	2843	2950	0.7460	3.94

4.1.7 Additional Results

Uncertainty analysis is included on the pareto frontier in Figure 4-11 by using the 10 percent and 90 percent confidence bands. A 90 percent confidence band means that the 90 percent of the reliability estimates are above this value while 90 percent of the cost results are below this value.

In Figure 4-11, the uncertainty bands are very wide. The uncertainty ranges are reflective of historical reliability and cost estimates at the time of the Saturn V design. Therefore, with very little data available, the range of possible results should be very wide. The minimum cost configuration has a range of nearly 18 billion dollars [FY '04] (+/- 25%) and a reliability range between 0.62 and 0.72 (+/- 8%). The maximum reliability configuration has a cost range of nearly 25 billion dollars (+/- 20%) while the reliability range is between 0.89 and 0.94 (+/- 5%).

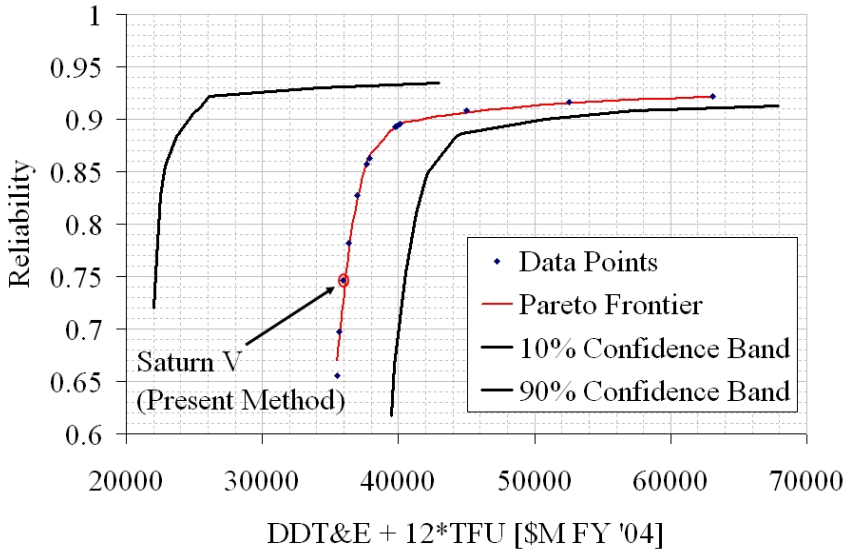

Figure 4-11: Pareto Frontier with Uncertainty.

The sensitivity of the common cause failure parameter, β, is examined in this section. Changing β will only affect the reliability calculation of each design configuration. As β increases, the system reliability benefit of using engine out and identical components to provide full subsystem redundancy (i.e. a one out of two subsystem redundancy configuration) is reduced. Reducing or eliminating β, as seen in Figure 3-15, will increase the system reliability benefit of using identical components for redundancy. Functional redundancy is unaffected by β because it is assumed that functional redundancy is not affected by common cause failure.

Table 4-11 lists how system reliability varies with changes in β for "Design 3", "Design 6" and the maximum reliability launch vehicle design from Table 4-5. The minimum cost configuration and "Design 2" do not use any redundancy so their reliability is unaffected by variations in β.

In Table 4-11, the reliability values are slightly different compared to the baseline calculations. The differences are not large enough to change the optimal configurations shown in Figure 4-7. However, only another study outside the scope of this dissertation would prove this hypothesis.

Table 4-11: β Sensitivity Study.

Design	β **= 0.1 (Base)**	β **= 0.0**	β **= 0.2**	**Cost [$M FY '04]**
Design 3	0.7814	0.7858	0.7773	36339
Design 6	0.8627	0.8694	0.8559	37889
Max. Rel.	0.9215	0.9237	0.9193	63070

4.1.8 Results Summary

The pareto frontier illustrated in Figure 4-7 shows that the Saturn V reliability could have been increased by nearly 15 percent for an additional 1.76 billion dollars [FY '04] (5% cost increase). The increase in reliability corresponds to an increase from 3.94 to 7.0 in the mean flights between failure. The significant parameters are the stage thrust-to-weight ratio, the number of engines, and the use of power redundancy in a one out of two configuration with identical components. Increasing the stage thrust-to-weight ratio increased the burn time while reducing the number of engines eliminated another possibility for component failure. These results are in contrast to previous studies that minimized the thrust-to-weight ratio to minimize dry mass as a surrogate for system cost.

Engine out was only important for the S-II stage; the system reliability benefit of using engine out on the S-IC and S-IVB stage did not warrant its inclusion unless a maximum reliability configuration was desired. Using identical components for power subsystem redundancy provided a system reliability increase for minimal increase in system cost. By altering the original configuration of the Saturn V, a lower cost design could have been utilized. With respect to system reliability, the Saturn V reliability could have been increased significantly with little additional cost.

With Figure 4-7 illustrating that significant improvements in Saturn V reliability were possible for little additional cost, the question arises about why these improvements were not implemented. There are a few reasons that the Apollo engineers may

not have altered the Saturn V configuration to increase its reliability. One reason was contracts were already created for specific engines early in the design phase because of President Kennedy's time constraint [57]. Another reason for not improving the Saturn V reliability with configuration changes during the conceptual design phase may have been because of the uncertainty regarding the final results from each discipline. As noted earlier in Section 2.2.1, uncertainty about the final mass of the payload led to the addition of an extra engine on the S-IC stage. Another reason for not improving Saturn V reliability may have been the infancy of the reliability discipline. While the traditional aerospace disciplines, such as aerodynamics and propulsion, had years of research to draw upon, the reliability discipline was still emerging during the Apollo era. Fault trees were not introduced until the early 1960s and Petri Nets were not developed until Dr. Petri's dissertation in 1962 [87]. Therefore, due to Apollo era capability and the contracts for set engines, the Saturn V did not undergo any configuration changes to increase its reliability.

4.1.9 Optimal Design Point Validation

Design six from Table 4-5 is validated by using the higher fidelity tools to check that the values produced from the integrated environment are correct. In Table 4-12, the reliability discipline is validated by using the stochastic petri nets. Since only the S-II stage from design six uses engine out capability, the S-II engine reliability is the only propulsion subsystem included in Table 4-12. The other reliability calculations use the series and parallel formulas from Section 3.3 and were previously validated.

The parameter values from POST and REDTOP-2 are compared with the calculations from the response surface equations used in the methodology. The mass calculations are compared using the POST mass ratio estimates and the RSE mass ratio values. Table 4-12 lists the comparison for each design tool, the values, and the percentage difference. All cost units are in millions of dollars [FY '04] and the masses

are in pounds.

Table 4-12 shows good agreement between the parameters calculated using the higher fidelity analysis tools and the response surface equations. There is minimal error in the burn time of the S-IC stage, but the absolute burn time does not vary by more than six seconds (3.7% of the total S-IC burn time). Furthermore, the total Saturn V burn time does not vary by more than ten seconds, which is only 1.7 percent of the total burn time. The difference in Saturn V reliability is less than one percent.

Table 4-12: Optimal Design Validation.

Discipline	**Tool**	**Tool**	**Check**
Trajectory	**POST**	**RSE**	**% Diff.**
S-IC Mass Ratio	3.505	3.495	0.26
S-II Mass Ratio	2.866	2.852	0.50
S-IVB Mass Ratio	1.223	1.224	0.08
S-IC Burn Time	167	161	3.88
S-II Burn Time	326	324	0.46
S-IVB Mass Ratio	91	93	2.02
Propulsion	**REDTOP-2**	**RSE**	**% Diff.**
$T/W_{eng.}$	73.34	73.44	0.13
Weights	**POST**	**RSE**	**% Diff.**
S-IC Dry Mass	304782	301908	0.94
S-IC Gross Mass	5341405	5372003	1.09
S-II Dry Mass	112365	111663	0.62
S-II Gross Mass	1139278	1129129	0.89
S-IVB Dry Mass	33116	33051	0.20
S-IVB Gross Mass	276656	276800	0.05
Saturn V Gross Mass	6947534	6878127	1.00
Reliability	**SPN**	**Model**	**% Diff.**
S-II Total Engine Unreliability	0.0227	0.0226	0.10
S-II Propulsion Reliability	0.9774	0.9774	0.002
Saturn V Reliability	0.8627	0.8627	0.002

4.1.10 Saturn V Reliability Growth

The pareto frontier illustrated in Figure 4-7 shows the plateau launch vehicle reliability for the design configurations listed in Table 4-5. The designs in Table 4-5 can be expected to experience some reliability growth before reaching their plateau.

To estimate the reliability growth, the Duane model has been used to calculate the growth rate parameter from the Atlas and Delta launch vehicles. A historical review of launch vehicle reliability provides the number of flights required to reach the plateau reliability. Three designs from Table 4-5 are selected for comparison; the minimum cost configuration, design six, and the maximum reliability configuration. A summary of those designs is listed in Table 4-13.

Table 4-13: Saturn V Reliability Growth Configurations.

Design Description	**Plateau Reliability**	**DDT&E [$M FY '04]**	**TFU [$M FY '04]**
Min. Cost	0.6555	10064	1633
Design 6	0.8627	10810	1748
Max. Rel.	0.9215	17655	2869

Figure 4-12 and Figure 4-13 illustrate the reliability growth for each of the designs in Table 4-13. As mentioned earlier, two different growth rate parameters are used based upon the Atlas, Figure 4-12, and Delta, Figure 4-13, launch vehicles. Additionally, it is assumed in Figure 4-12 and Figure 4-13 that ten flights are required to reach the plateau reliability. The first flight includes the development cost and first unit cost while the second flight adds another vehicle production cost.

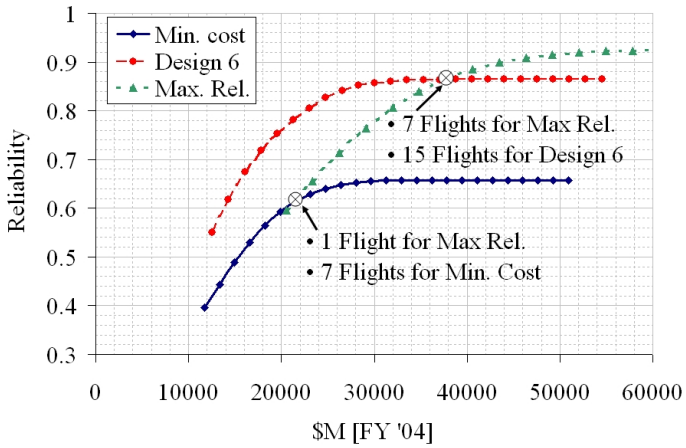

Figure 4-12: Saturn V Reliability Growth with $\alpha = 0.2006$ [Atlas].

In Figure 4-12, the maximum reliability configuration costs the highest initially and does not provide a large reliability benefit until much later in the campaign. Design six has a higher initial reliability and provides a better reliability value compared to the minimum cost configuration.

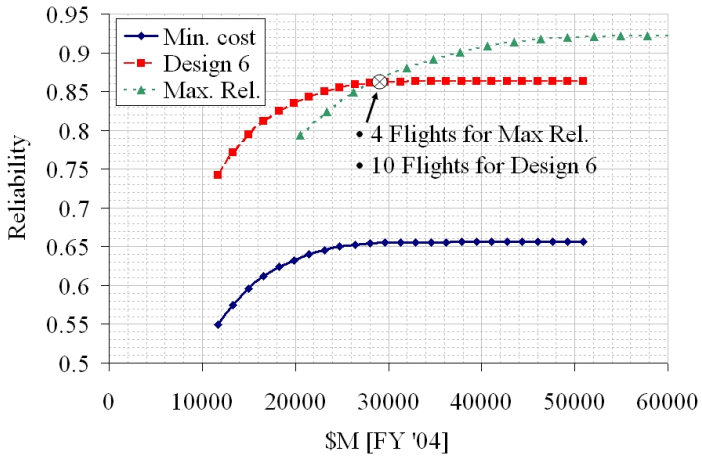

Figure 4-13: Saturn V Reliability Growth with $\alpha = 0.0669$ [Delta].

Figure 4-13 illustrates the reliability growth of the same three launch vehicle designs using the growth rate parameter derived from the Delta launch vehicle. Design six has a higher reliability for the same cost as the minimum cost configuration. The maximum reliability configuration also provides a better value compared to the minimum cost configuration once the 20 billion dollar [FY '04] threshold is reached.

Other reliability growth models can be incorporated into this methodology. The methodology will predict a final reliability value based on the design choices used in the integrated environment. The cost estimates are already completed by using the integrated environment so a different reliability growth model can use those cost values. Thus, more information is provided to assist with selecting the optimal launch vehicle design based upon its cost and reliability.

4.2 Cargo Launch Vehicle

The results of applying the methodology to the Cargo Launch Vehicle described in the Exploration System Architecture Study [66] and Section 2.2.3 are presented in this section. The specific design variables used in the CaLV application are listed in Table 4-14. As with the Saturn V, the only subsystems given the option of full subsystem redundancy (i.e. a one out of two subsystem configuration) are the avionics and power subsystems. The CaLV application requires less design variables compared to the Saturn V because the CaLV has one less stage.

Table 4-14: CaLV Design Variables.

Design Variable	**Minimum**	**Maximum**	**Type**
CaLV T/W Ratio	1.38	1.5	Continuous
EDS T/W Ratio	0.4	1.1	Continuous
No. of Engines Boos.	2	7	Discrete
No. of Engines EDS	1	4	Discrete
Engine Out Boos.	Yes	No	Discrete
Engine Out EDS	Yes	No	Discrete
Full Power Redundancy Boos.	Yes	No	Discrete
Full Avionics Redundancy Boos.	Yes	No	Discrete
Full Power Redundancy EDS	Yes	No	Discrete
Full Avionics Redundancy EDS	Yes	No	Discrete
Power Redundancy Type Boos.	Identical Components	Functional	Discrete
Avionics Redundancy Type Boos.	Identical Components	Functional	Discrete
Power Redundancy Type EDS	Identical Components	Functional	Discrete
Avionics Redundancy Type EDS	Identical Components	Functional	Discrete

The CaLV application uses the same design process illustrated in Figure 3-38. Figure 4-14 shows the CaLV specific design structure matrix.

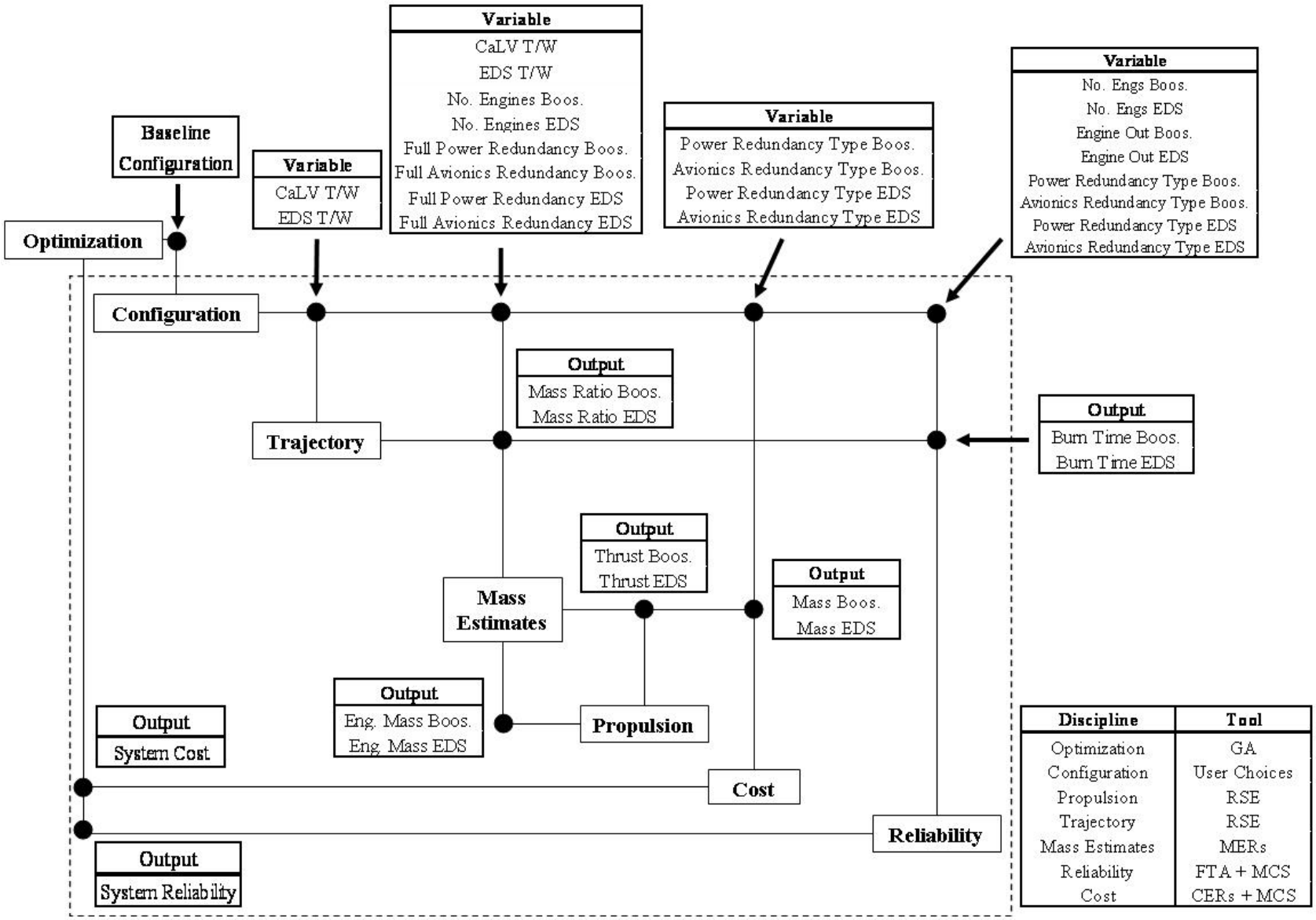

Figure 4-14: CaLV Design Structure Matrix.

4.2.1 CaLV Model Validation

The reliability modeling used in this section is very similar to the modeling used for the Saturn V application and a repeat of the validation shown in Section 4.1.1.1 is unnecessary.

For the cost analysis, the Solid Rocket Boosters were assumed to cost 450 million dollars [FY '04] for the DDT&E and 120 million dollars [FY '04] in total TFU. These values are based on the work completed by Young [98] for verifying the performance of the CLV.

4.2.1.1 Performance Modeling

The performance models are built upon the work completed by Young and et al. [99] The mass validation is listed in Table 4-15. There is good agreement between the CaLV model created by Young and et al. [99] and the model used in ESAS [66]. The work breakdown structure listed in Table E-2 shows the validation in more detail by comparing subsystem mass estimates.

Table 4-15: CaLV Mass Comparison Between ESAS and Young [lb].

Booster	**ESAS**	**MERs**	**% Difference**
Dry Mass	194997	194563	0.22
Gross Mass	2428061	2442803	0.61
EDS	**ESAS**	**MERs**	**% Difference**
Dry Mass	42645	42528	0.27
Gross Mass	640171	650816	1.66
CaLV	**ESAS**	**MERs**	**% Difference**
Gross Mass	6393975	6408445	0.23

The trajectory models were also built upon the work completed by Young and et al. [99] As with the Saturn V, POST is used for the trajectory optimization of the CaLV and the results are compared to ESAS [66]. Appendix I lists the requirements and assumptions for the trajectory analysis. Figure 4-15 shows a comparison between

the trajectory curve from ESAS [66] and the trajectory curve produced by Young and et al. [99]. There is a little error between the curves but the trends and slopes are similar.

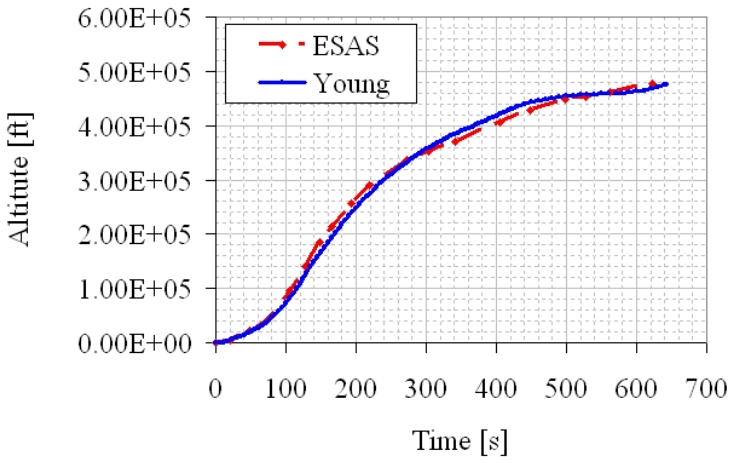

Figure 4-15: Trajectory Comparison for CaLV.

Figure 4-16 is the comparison of the inertial velocity. The main discrepancy in Figure 4-16 is from the staging point of the booster; the staging point occurs a little bit earlier for ESAS when compared to the Young model. The error may result from not having all of the ESAS assumptions and information incorporated in the model.

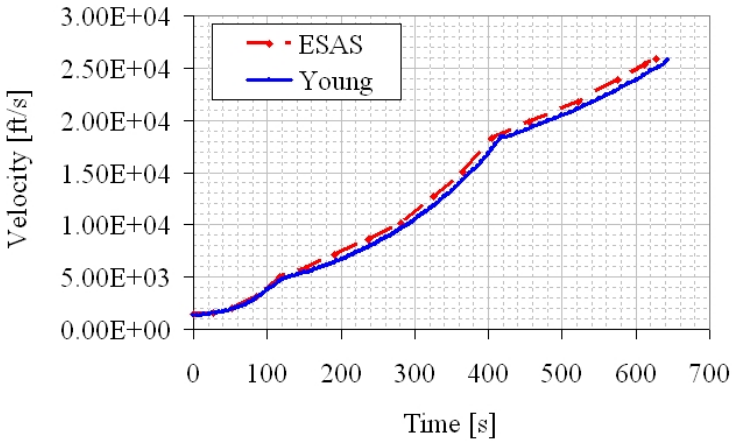

Figure 4-16: Inertial Velocity Comparison for CaLV.

Figure 4-17 is a comparison of the acceleration profiles of the Young and the

ESAS models. There is a small discrepancy in Figure 4-17 and this error may lead to the discrepancies seen in the previous two figures. The exact thrust profile and staging condition of the Solid Rocket Boosters may be unknown, which could cause the discrepancy seen in Figure 4-17. The general trend in Figure 4-17 is virtually identical, but the acceleration changes occur at different points in time.

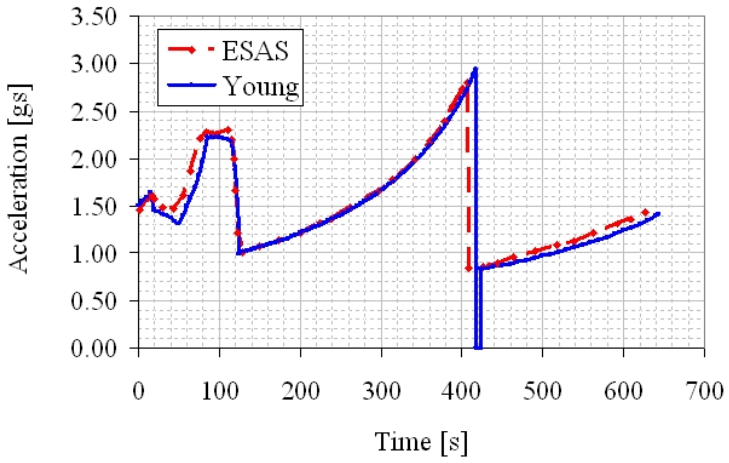

Figure 4-17: Acceleration Comparison for CaLV.

The early differences in the acceleration profile cascade to the later points; the booster in the Young model stages later when compared to the ESAS analysis but the SRB acceleration profile also changed later for the Young model. Furthermore, the peak acceleration of the Young model is slightly higher when compared to the ESAS model. In Figure 4-17, the general trends are close and both plots include the acceleration rise around 100 seconds.

4.2.2 CaLV RSE Validation

The Cargo Launch Vehicle application also relies upon response surface equations. The previous propulsion RSE from the Saturn V application was used along with a lower thrust RSE to calculate the J-2S engine thrust-to-weight ratio based upon the J-2S thrust. Table F-13 in Appendix F lists all of the RSE statistics, such as R^2 and $R^2 - adjusted$, for the propulsion RSE. Also in Appendix F is a comparison between

using REDTOP-2 and the propulsion RSE to calculate the engine thrust-to-weight ratio based on data not included in the original RSE fit.

As with the Saturn V application, a series of trajectory RSEs are used to calculate the stage mass ratio based upon the stage thrust-to-weight ratio. Another two response surface equations are used to calculate the burn time of the booster and the EDS stage based upon the stage thrust-to-weight ratio.

The RSE fit statistics for the mass ratio and burn time are listed in Table F-9 through Table F-12 in Appendix F. Table F-14 of Appendix F lists a comparison of the burn time and mass ratio when using POST and the RSE for points not used in the original fit. There is a little error in the Earth Departure Stage burn time, but the absolute error is small compared to the total trajectory time.

4.2.3 CaLV Results

The Cargo Launch Vehicle results are illustrated in Figure 4-18. One reason that the final CaLV design was selected in ESAS was because it used existing engines. Since the true costs of the ESAS CaLV have not been published, a series of data points are created to represent the ESAS CaLV based upon a percentage of predicted engine DDT&E cost. In Figure 4-18, the left most data point is the ESAS CaLV design that does not incur any engine DDT&E costs. The engine DDT&E cost percentage is applied to the engines on both the booster and Earth Departure Stage. Five different cost values are presented for the ESAS CaLV design in Figure 4-18 which represent increasing the engine DDT&E cost by 25 percent. The right most data point in the series of ESAS CaLV data points represents a CaLV design that incurs 100 percent of the predicted engine DDT&E cost.

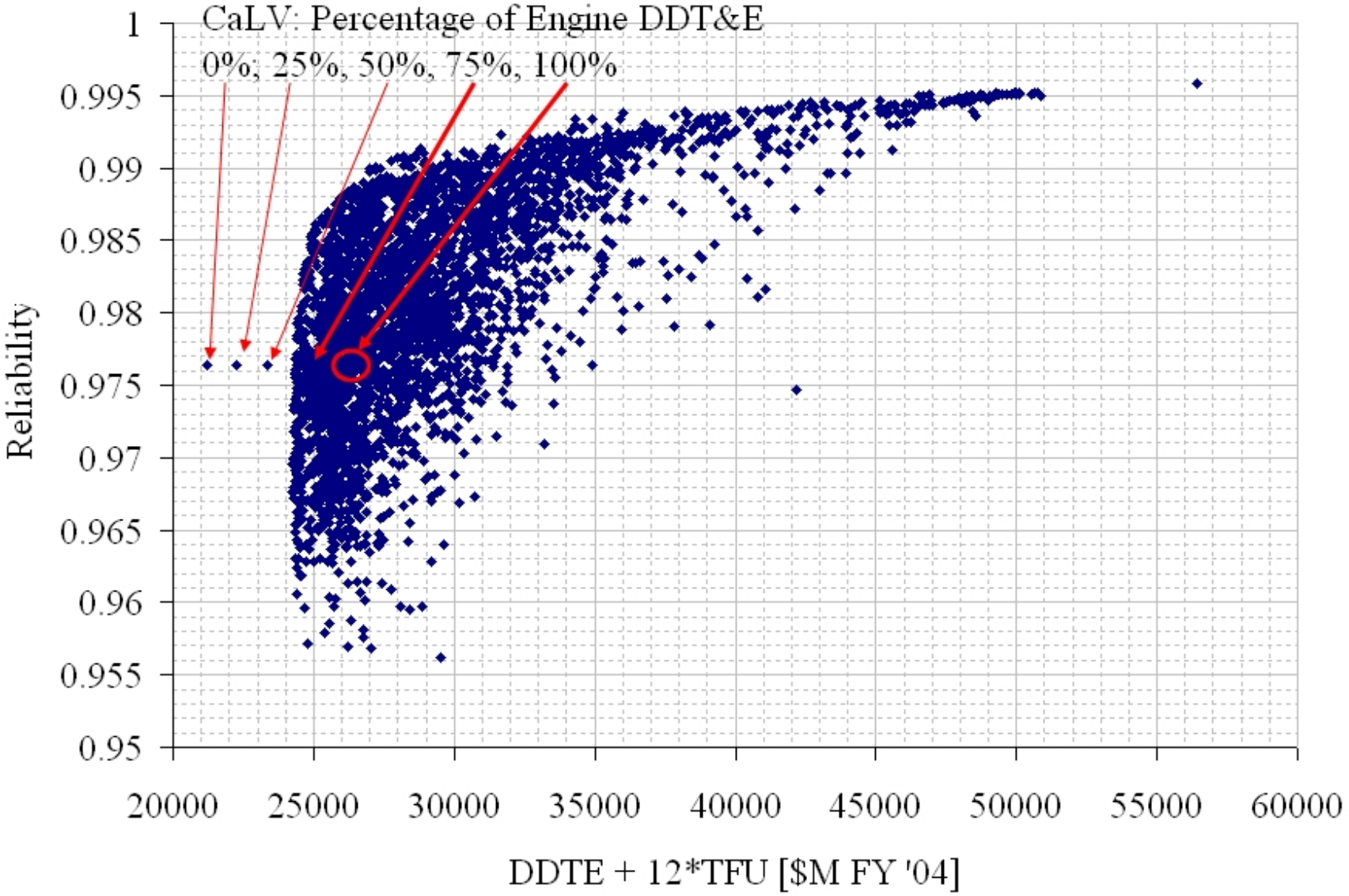

Figure 4-18: CaLV Design Space.

Figure 4-18 shows that if the full engine DDT&E cost is paid, then the CaLV is a sub-optimal design for the two metrics used in this methodology. There are different configurations of the CaLV that will result in a lower cost launch vehicle or a design with higher reliability for the same cost. The break-even point is at the 75% cost level for engine DDT&E; if greater than 75% of the engine DDT&E costs are paid for, then a different CaLV configuration should be selected.

Figure 4-19 illustrates the same results as Figure 4-18, except the mean flights between failure is the y-axis metric. The MFBF of the CaLV design can be increased significantly for an additional 28 percent in system cost if the CaLV program does not pay for any engine DDT&E costs. The CaLV MFBF can be increased from 42.4 to 99.2 for an additional 5.8 billion dollars [FY '04] if the CaLV program does not pay for engine DDT&E.

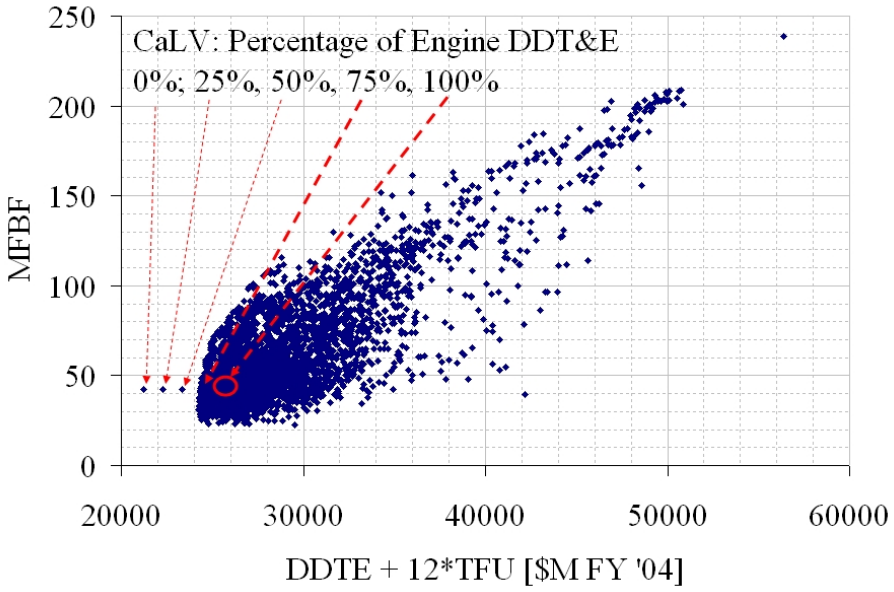

Figure 4-19: CaLV Cost versus MFBF.

4.2.4 CaLV Optimal Configurations

Figure 4-20 illustrates the pareto frontier for the Cargo Launch Vehicle. The data points in Figure 4-20 represent the maximum reliability configurations for a specific

cost value. The CaLV from ESAS is shown by the series of five data points representing the percentage of engine DDT&E cost incurred in the design. Figure 4-20 reinforces that a different CaLV design may be more appropriate if the engine DDT&E costs are greater than 75 percent of the total predicted value.

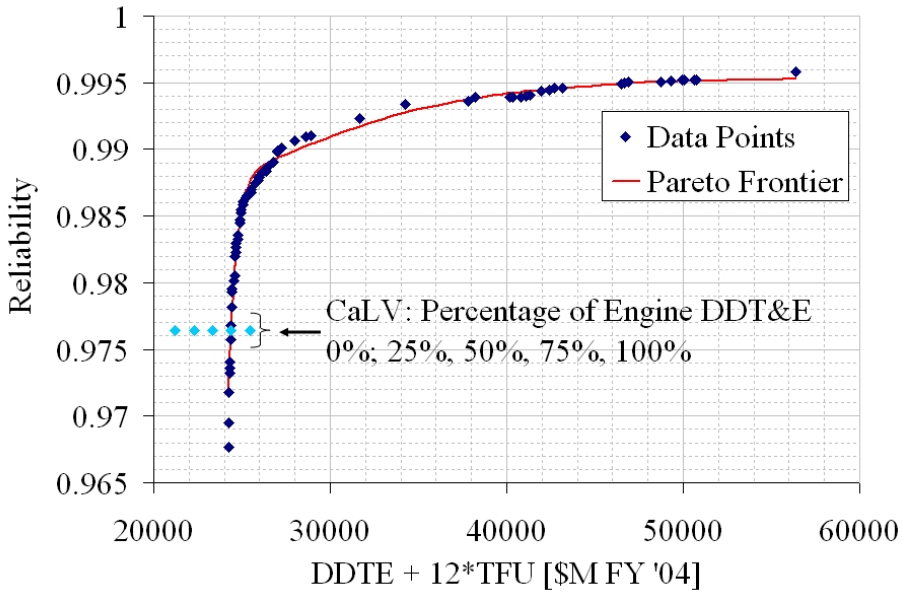

Figure 4-20: CaLV Pareto Frontier.

A sample of the design points shown in Figure 4-20 are listed in Table 4-16. As with the Saturn V results, the abbreviation "IC" refers to using identical components for subsystem redundancy, while "F" is used to denote functional redundancy. Cost and reliability both increase when examining the launch vehicle designs from left to right across Table 4-16. Table H-2 lists a more detailed mass comparison of the minimum cost configuration, "Design 9", and the maximum reliability configuration from Table 4-16. A more detailed cost comparison for the three previously mentioned configurations can be found in Table G-3. The trajectory plots for the minimum cost configuration, design nine, and the maximum reliability configuration can be found in Appendix I.

Table 4-16: Design Variable Settings for the CaLV Pareto Frontier.

Parameter	**Min. Cost**	**Design 2**	**Design 3**	**Design 4**	**Design 5**	**Design 6**	**Design 7**	**Design 8**	**Design 9**	**Design 10**	**Design 11**	**Max. Rel.**	**CaLV Base 75% Eng. Cost**
Cost [$M FY '04]	24253	24263	24287	24570	24786	25067	25924	26004	27008	38213	42412	56403	24384
Reliability	0.9676	0.9695	0.9733	0.9805	0.9836	0.9861	0.9879	0.9879	0.9899	0.9939	0.9945	0.9958	0.9764
CaLV T/W Ratio	1.414	1.414	1.414	1.431	1.431	1.431	1.431	1.431	1.431	1.380	1.500	1.500	1.38
EDS T/W Ratio	0.540	0.587	0.587	0.633	0.633	0.633	0.633	0.680	0.727	1.007	1.100	1.100	0.84
No. of Engines Boos.	4	4	4	3	3	2	2	2	2	2	3	2	5
Engine Out Boos.	No	No	No	No	No	No	No	No	No	Yes	Yes	Yes	No
No. of Engines EDS	4	4	3	2	1	1	1	1	1	1	3	2	2
Engine Out EDS	No	No	No	No	No	No	No	No	No	No	Yes	Yes	No
Power Redundancy Boos.	None	None	None	None	None	None	None	IC	IC	IC	F	F	None
Avionics Redundancy Boos.	None	None	None	None	None	None	None	None	None	None	IC	F	None
Power Redundancy EDS	None	None	None	None	None	None	IC	None	IC	IC	IC	F	None
Avionics Redundancy EDS	None	None	None	None	None	None	None	None	None	None	F	F	None

4.2.5 CaLV Reliability Results

The maximum reliability configuration listed in Table 4-16 is expected. The design relies upon the highest stage thrust-to-weight ratio, uses engine out with the least amount of engines, and also includes functional redundancy for the subsystems. Increasing the stage thrust-to-weight ratio decreases the launch vehicle operating time which then increases the system reliability.

Engine out is not used on the configurations in Table 4-16 until there is more focus on system reliability. When using engine out capability, the thrust level of the engines is equivalent to a different design that has one less engine on its stage. However, the design with engine out is carrying unnecessary mass, so the thrust level of a stage with engine out capability will be higher compared to a design with no engine out capability and one less engine. The value of using engine out to boost system reliability is not large enough to justify the increase in system cost. Furthermore, the baseline reliability estimates for the booster and Earth Departure Stage, as listed in Table 3-10, are much higher compared to the Saturn V launch vehicle. Therefore, using engine out on the CaLV does not provide as large of a reliability benefit as the Saturn V launch vehicle. From Table 4-16, the bigger system reliability benefit comes from reducing the operating time through increasing the stage thrust-to-weight ratio and reducing the number of engines.

Table 4-17 lists a comparison of changing different design variables to increase system reliability. In Table 4-17 the abbreviation "EO" refers to engine out capability and "IC" refers to using identical components to provide full subsystem redundancy. The baseline for these trades is "Design 2" in Table 4-16.

While using engine out on both the booster and EDS stage does provide a large system reliability benefit, Table 4-17 shows that a comparable reliability benefit can be gained by reducing the number of engines for a lower system cost. The results listed in Table 4-17 also reveal the engine out on the EDS is more beneficial compared to engine

Table 4-17: CaLV Design 2 Reliability Trade Study.

Reliability Strategy	**Parameter Value**	**System Reliability**	**System Cost [$M FY '04]**
None	Design 3	0.9695	24263
Boos. T/W	1.45	0.9703	24398
EDS T/W	0.7	0.9729	24714
No. Engs. Boos.	3	0.9719	24331
No. Engs. EDS	3	0.9733	24287
EO Boos.	Yes	0.9758	26960
EO EDS	Yes	0.9791	25577
Boos. Power	IC	0.9709	25004
EDS Power	IC	0.9715	25123

out on the booster stage. The EDS is required to perform the trans-lunar injection burn, which adds significant burn time to its total operating time. Additionally, the EDS engine has a lower reliability value, so providing engine out capability will also enhance its total engine reliability. However, the reliability benefit of using engine out does not provide the same value as reducing the number of engines, as seen in Table 4-16.

Neither power nor avionics subsystem redundancy is included on any of the optimal designs in Table 4-16 until there is greater emphasis on system reliability. The reliability estimates for these subsystems are initially high, as seen in Table 3-10, and therefore the cost of adding redundancy with a one out of two configuration for these subsystems does not justify the increase in system reliability. Table 4-17 also showed that adding an additional power subsystem provided a lower system reliability increase compared to reducing the number of engines or increasing the thrust-to-weight ratio of the EDS stage. The cost of adding an additional power subsystem was higher compared to the other reliability options. Functional redundancy is not included on any designs because the system reliability benefit is not large enough to justify the additional cost.

4.2.6 CaLV Cost Results

The minimum cost configuration in Table 4-16 uses multiple engines without engine out capability on both stages, and neither power nor avionics subsystem redundancy. As discussed in Section 4.1.6, adding mass that is not required to complete the mission objectives will add unnecessary cost. Therefore, since engine out capability and additional subsystems for redundancy are unneeded mass, they are not included on the minimum cost configuration.

The stage thrust-to-weight ratio is determined by balancing the engine costs and minimizing the dry mass. Increasing the stage thrust-to-weight ratio will lower the propellant mass, which lowers the required structure and tank mass. However, engine thrust increases with an increasing thrust-to-weight ratio which also increases system cost. Selecting the number of engines on each stage is also based upon the same reasoning. The engine DDT&E cost decreases as the engine thrust decreases, which can be accomplished by using more engines to provide the required thrust. However, there is a balance because too many engines will increase the total TFU cost. Table 4-18 shows how changing the stage thrust-to-weight ratio and the number of engines per stage will increase the system cost from the minimum cost configuration.

Table 4-18: CaLV Minimum Cost Comparison.

Parameter Changed	**New Value**	**System Cost [$M FY '04]**	**System Reliability**
None	Min. Cost	24253	0.9695
Boos. T/W	1.38	24466	0.9669
Boos. T/W	1.45	24375	0.9703
EDS T/W	0.45	24710	0.9631
EDS T/W	0.70	24714	0.9729
Boos. No. Engs	5	24265	0.9653
Boos. No. Engs	3	24308	0.9719
EDS No. Engs	3	24287	0.9733

Table 4-18 reveals the balance between finding a low engine thrust and a stage

thrust-to-weight ratio that does not excessively increase the structure and tank mass. The engine costs are the primary cost driver for both stages. Figure 4-21 and Figure 4-22 show the percentage contribution to DDT&E and TFU cost by subsystem, respectively.

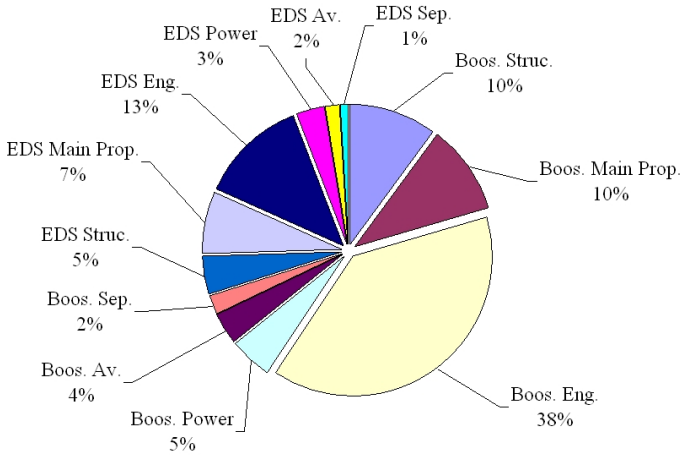

Figure 4-21: CaLV DDT&E Subsystem Cost Percentage.

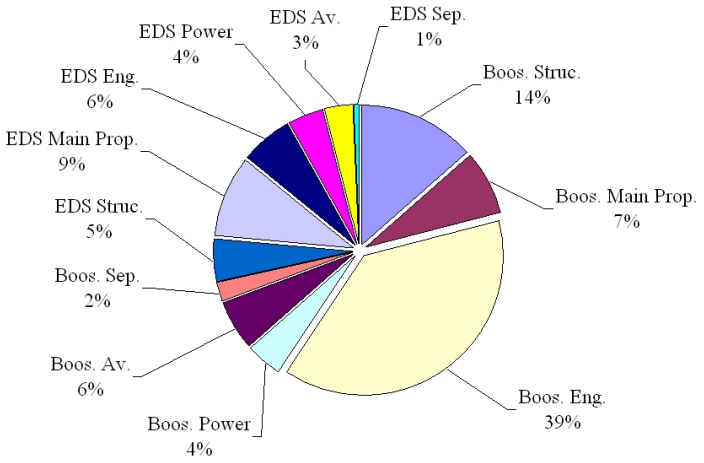

Figure 4-22: CaLV TFU Subsystem Cost Percentage.

Table 4-19 compares the booster and EDS engine costs of each configuration listed in Table 4-18 to demonstrate how the engine costs increase; the engine costs are larger because of a higher DDT&E, total TFU cost, or both.

Table 4-19: Engine Cost Comparison for CaLV Minimum Cost Configurations [$M FY '04].

Row Number	Parameter Changed	New Value	Boos. Eng. DDT&E	Boos. Eng. TFU	EDS Eng. DDT&E	EDS Eng. TFU
1	None	Min. Cost	1767	290	585	48
2	Boos. T/W	1.38	1769	290	585	48
3	Boos. T/W	1.45	1794	298	585	48
4	EDS T/W	0.45	1831	308	558	44
5	EDS T/W	0.70	1749	285	635	55
6	Boos. No. Engs.	5	1625	314	585	48
7	Boos. No. Engs.	3	1969	262	585	48
8	EDS No. Engs.	3	1767	290	643	42

Using five engines on the booster stage, row six in Table 4-19, reduces the engine DDT&E cost compared to the minimum cost configuration. However, the difference in total engine TFU cost between the minimum cost configuration and the design listed on row six in Table 4-19 is large enough to overcome the difference in engine DDT&E cost.

Using a lower booster thrust-to-weight ratio, row two in Table 4-19, nearly leads to a lower engine DDT&E cost. The mass increase on the configuration in row two from the extra propellant is the reason why its engines are so large. Additionally, the other subsystems masses on the configuration listed in row two are larger because of the higher propellant mass and will lead to a higher system cost.

Increasing the EDS thrust-to-weight ratio, row five in Table 4-19, and decreasing the number of engines on the EDS, row eight in Table 4-19, causes the same effect on system cost. The engine thrust increases which increases the system cost. Decreasing the EDS thrust-to-weight ratio, row four in Table 4-19, also increases the propellant mass of the EDS. A cascade effect then occurs on the booster stage and the booster must increase its engine thrust to maintain a constant thrust-to-weight ratio.

As with the Saturn V, the number of flights in the campaign had an effect on the minimum cost configuration. Figure 4-23 illustrates two other designs that could have

been the minimum cost configuration if the number of flights were different. If ten flights were used in a campaign, then design two in Figure 4-23 would have been the minimum cost configuration. If the number of campaign flights was 20, then design three would have been the minimum cost configuration.

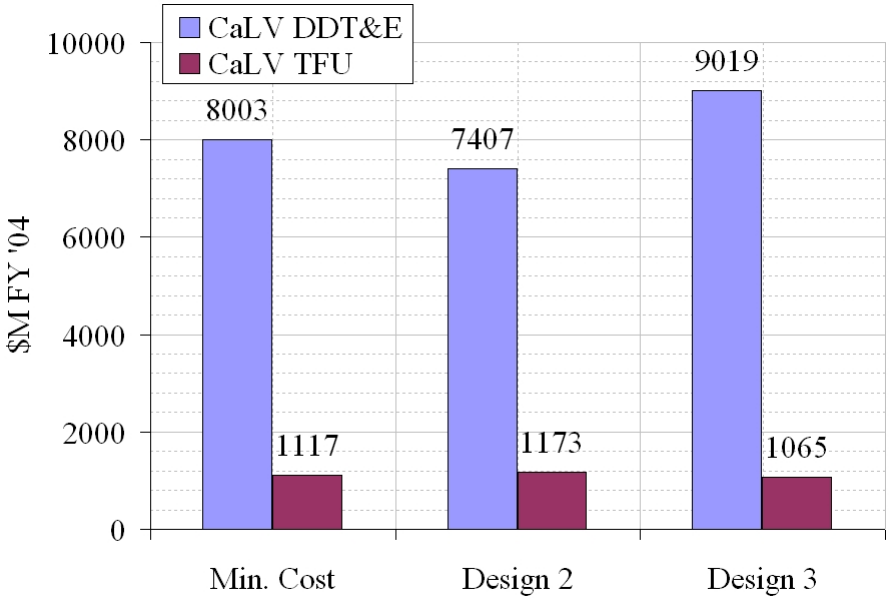

Figure 4-23: CaLV Minimum Cost Configurations.

A set of development cost profiles for the optimal CaLV configurations listed in Table 4-16 are listed in Table J-5 - Table J-8 of Appendix J. As with the Saturn V results, each table corresponds to a different distribution assumption. The peak funding requirements for each design are illustrated in Figure 4-24.

When a constant funding profile is used in Figure 4-24, the peak year funding is significantly lower compared to the maximum funding value using the other distribution assumptions. However, this level of funding must be maintained throughout the program development which may constrain other programs within NASA. The other assumption values result in similar peak funding values within each design. However, the peak funding does vary by design, which is expected because the cost results have a wide range.

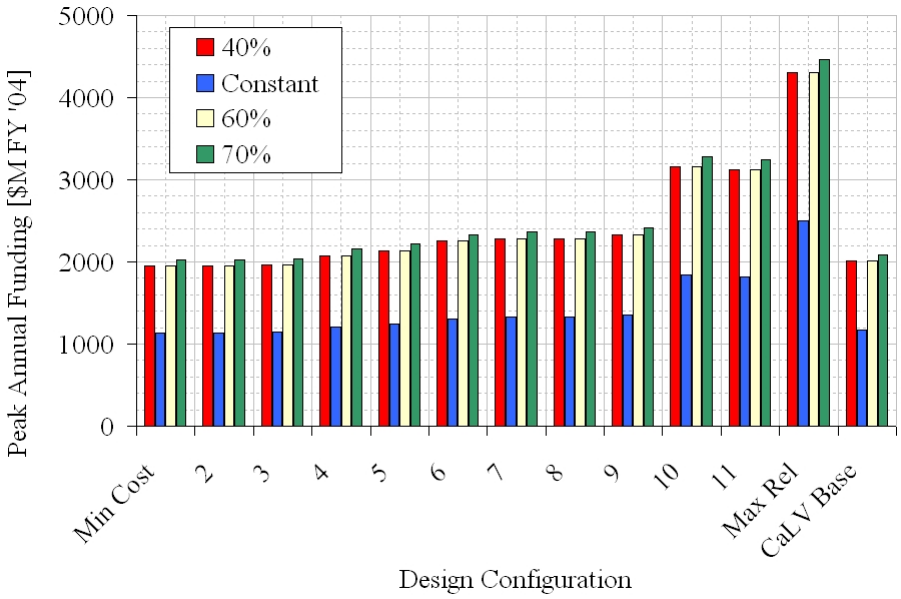

Figure 4-24: CaLV Optimal Configuration Peak Funding Comparison.

Table 4-20: CaLV Peak Funding Comparison.

Design Config.	**40 Percent Assumption**	**Constant Assumption**	**60 Percent Assumption**	**70 Percent Assumption**	**Reliability**	**MFBF**
Min. Cost	1951	1135	1951	2024	0.9676	30.91
2	1952	1135	1951	2024	0.9695	32.80
3	1968	1144	1968	2042	0.9733	37.39
4	2077	1208	2077	2155	0.9805	51.24
5	2135	1241	2134	2214	0.9836	60.82
6	2251	1309	2251	2335	0.9861	71.75
7	2277	1324	2276	2361	0.9879	82.59
8	2281	1326	2281	2366	0.9879	82.62
9	2325	1352	2324	2411	0.9899	99.15
10	3164	1840	3163	3282	0.9939	163.29
11	3123	1816	3122	3240	0.9945	180.26
Max Rel.	4305	2503	4303	4465	0.9958	238.56
CaLV	2009	1168	2008	2084	0.9764	42.37

Table 4-20 lists a detailed peak funding comparison of the optimal configurations listed in Table 4-16. By comparing design six with the CaLV baseline, Table 4-20 reveals the CaLV MFBF could be increased by 70 percent for an approximate increase of twelve percent in peak funding across the different distribution assumptions. By comparing design four with the CaLV baseline, a peak funding increase of six percent

could increase the MFBF by 44 percent. The CaLV baseline listed in Table 4-20 assumes the concept incurs the full engine development cost.

4.2.7 CaLV Additional Results

Figure 4-25 illustrates the range of possible cost and reliability values around the pareto frontier using the 10 percent and 90 percent confidence bands. The 10 percent band is shorter because the minimum cost configuration will have a higher reliability and the maximum reliability configuration will have a lower system cost. There is a wide range of cost estimates for the maximum reliability configuration; the absolute width is approximately 14 billion dollars [FY '04] (+/- 15%). The absolute cost range is significantly smaller for the lower reliability configurations with the width equal to approximately 6 billion dollars [FY '04] (+/- 11%) for the minimum cost configuration. The reliability estimates also change significantly; the mean flights between failure varies between 197 and 343 (+/- 31%) for the maximum reliability configuration and 25.83 and 46.94 (+/- 34%) for the minimum cost configuration.

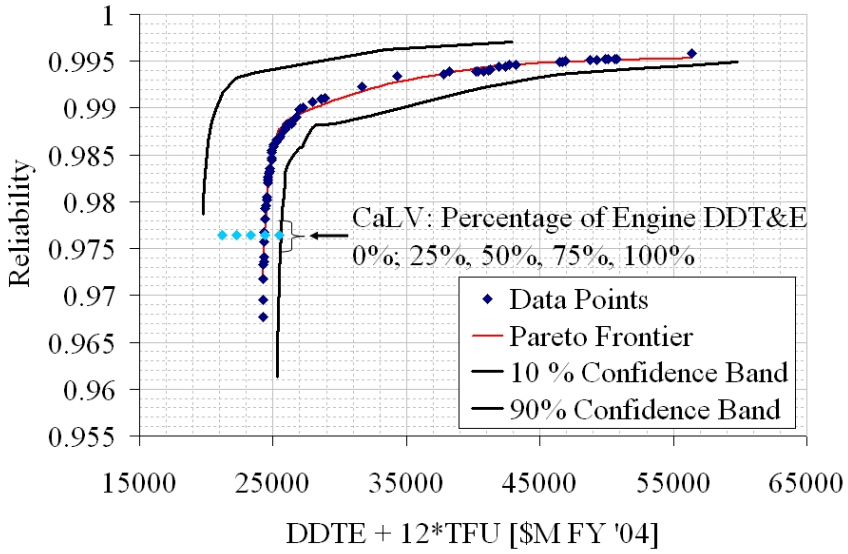

Figure 4-25: CaLV Pareto Frontier with Uncertainty.

The sensitivity of the β parameter in the common cause failure calculation is

examined in Table 4-21. Varying the β parameter does not have as large of an effect on system reliability compared to the results in the Saturn V section. The baseline subsystem and component reliability estimates of the CaLV are higher than the Saturn V, which makes the final reliability estimate of the CaLV less sensitive to changes in the common cause failure assumption.

Table 4-21: CaLV β Sensitivity Study.

Design	β **= 0.1 (Base)**	β **= 0.0**	β **= 0.2**	**Cost [$M FY '04]**
Design 9	0.9899	0.9902	0.9896	27008
Design 11	0.9945	0.9950	0.9939	42412
Max. Rel.	0.9958	0.9962	0.9954	56403

4.2.8 CaLV Results Summary

The CaLV demonstrates great potential for increasing its system reliability without incurring a large increase in system cost. The results in Figure 4-20 showed that the reliability of the CaLV could be increased by an additional percent for zero increase in system cost if the CaLV program incurs the entire engine DDT&E cost. Though the additional percent increase in reliability appears low, this increase corresponds to a 70 percent increase in the CaLV mean flights between failure metric. Even if the CaLV will incur no engine DDT&E cost, the MFBF can be increased from 42 to 99 with an additional 5.8 billion dollars [FY '04].

Additionally, if the CaLV incurs 75 percent or more of the predicted engine DDT&E cost, selecting an alternative configuration may reduce the system cost. A configuration with four engines on both the booster and EDS stages has a lower system cost, but also a lower system reliability. Figure 4-20 shows the results of using an integrated environment to perform rapid trade studies between reliability and cost. This additional information could be very useful in guiding a decision maker about which configurations deserve further study in the next design phase.

While the CaLV is still in conceptual design phase, configuration changes to improve its reliability appear unlikely. One reason is due to the constraint of using existing engines. Assumptions were made about the cost of modifying the SSME and re-starting the J-2S production line that result in the selection of the baseline CaLV as the heavy lift launch vehicle for lunar operations. Additionally, assumptions were made regarding the development risk of a new engine program that eliminated thousands of alternative configurations from quantitative evaluation. However, as seen in the cost results presented earlier, the allocation of resources can be altered to enable the development of a configuration that requires new engines. Therefore, by quantitatively evaluating alternative configurations as demonstrated in this dissertation, additional information can be generated that may prompt a review of the initial assumptions.

4.2.9 CaLV Optimal Design Point Validation

Design nine from Table 4-16 is used as a baseline for comparison between the higher fidelity analysis tools and the response surface equations used in this methodology. Since design nine does not use engine out capability, the reliability validation from the stochastic petri net tool is unnecessary.

Table 4-22 compares the results of the higher fidelity analysis tools and results of using the RSEs. The EDS burn time has some error, which is expected since the EDS burn time fit was not as good as the other RSE fits. However, the absolute error is small and the difference in system reliability when using the true burn time is 0.04 percent. The rest of the comparisons listed in Table 4-22 show good agreement between the results of the higher fidelity analysis and the results of the response surface equations.

Table 4-22: CaLV Design Nine Validation.

Discipline	**Tool**	**Tool**	**Check**
Trajectory	**POST**	**RSE**	**% Diff.**
Boos. Mass Ratio	3.514	3.506	0.22
EDS Mass Ratio	1.695	1.690	0.27
Boos. Burn Time	396	395	0.15
EDS Mass Ratio	257	249	3.25
Propulsion	**REDTOP-2**	**RSE**	**% Diff.**
EDS $T/W_{eng.}$	78.36	78.68	0.41
Weights	**POST**	**RSE**	**% Diff.**
Boos. Dry Mass	209222	207193	0.97
EDS Gross Mass	2467648	2447477	0.82
Boos. Dry Mass	41259	41152	0.26
EDS Gross Mass	554735	552478	0.41
CaLV Gross Mass	6436104	6413675	0.35

4.2.10 CaLV Reliability Growth

The reliability growth for the minimum cost configuration, design nine, and the maximum reliability configuration in Table 4-16 are compared using the same approach demonstrated in the Saturn V results. Table 4-23 lists a summary of these configurations.

Table 4-23: CaLV Reliability Growth Configurations.

Design Description	**Plateau Reliability**	**DDT&E [$M FY '04]**	**TFU [$M FY '04]**
Min. Cost	0.9676	8003	1117
Design 9	0.9899	9634	1178
Max. Rel.	0.9958	17428	2594

Figure 4-26 and Figure 4-27 illustrate the reliability growth results using the Atlas and Delta growth rate parameters, respectively. The required number of flights to reach the plateau reliability is ten in these two figures.

In Figure 4-26, the minimum cost configuration provides the best reliability value because this configuration completes the twelve flight campaign for less cost and

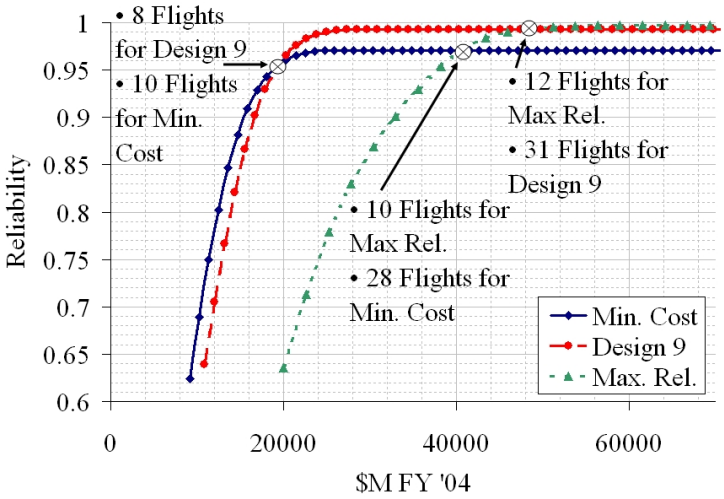

Figure 4-26: CaLV Reliability Growth with $\alpha = 0.2006$ [Atlas].

almost identical reliability as design nine. The maximum reliability configuration does not provide a high enough reliability benefit for the required costs to be considered for a final design solution when using the present growth rate and flight number assumptions.

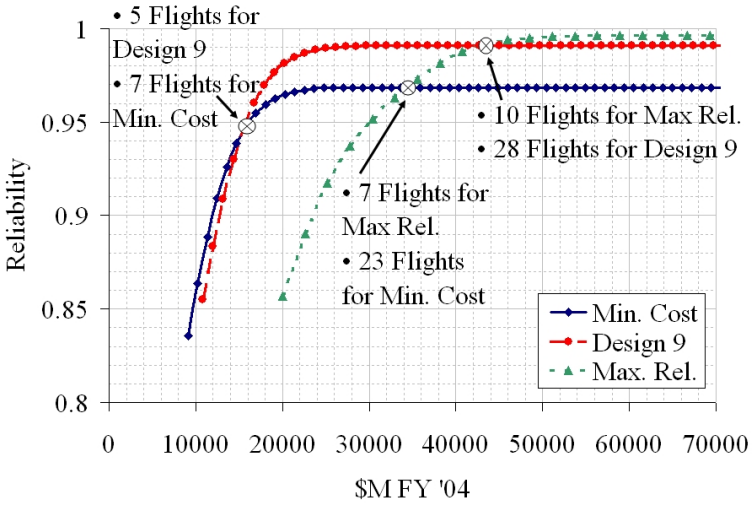

Figure 4-27: CaLV Reliability Growth with $\alpha = 0.0669$ [Delta].

The best design solution in Figure 4-27 is not as clear compared to Figure 4-26. If the 20 billion dollar [FY '04] threshold is crossed in Figure 4-27, then design nine may be the best design given the current assumptions about growth rate and campaign

flight number. As seen earlier, the maximum reliability configuration does not provide a high enough reliability benefit for the required resources to be considered as a final design solution.

When comparing the reliability growth figures, the minimum cost configuration consistently provides the best reliability value. Given these assumptions the maximum reliability configuration costs too much to be considered. For a full system study, the reliability growth of all optimal designs should be studied to increase the information available to a decision maker. This information may be important because the best configuration in Figure 4-20 may not be the optimal configuration when reliability growth is included.

This dissertation demonstrated one approach for reliability growth and compared three optimal configurations. A different reliability growth model may predict that the minimum cost configuration does not provide the best reliability value, but with this methodology, a new reliability growth model is easily incorporated.

CHAPTER V

CONCLUSION AND FUTURE WORK

5.1 Conclusion

The methodology in this dissertation can be used to create an integrated environment to evaluate the system cost and reliability of a launch vehicle. New information about each launch vehicle was created by using the methodology outlined in this dissertation. This information should assist decision makers when selecting a final vehicle configuration during conceptual design. Additionally, the design process created in this dissertation can rapidly evaluate thousands of launch vehicle configurations allowing the quantitative evaluation of alternative configurations.

The design environment was created by using performance and cost discipline tools accepted by the space community. The reliability modeling was developed specifically for use in launch vehicle design and the primary historical causes of unreliability were captured.

Hypothesis one was confirmed by the pareto frontiers illustrated in both the Saturn V and CaLV results' sections. The pareto frontiers showed that a single optimal configuration for cost and reliability could not be created. However, based upon a decision maker's preference, an optimal configuration can be found for a specific weighting of cost and reliability.

Hypothesis two was verified because improvements were made in the efficiency of the launch vehicle design process. The reliability models in this dissertation dynamically updated as the configuration varied; this was important for demonstrating that reliability modeling can be included in an integrated design environment. The design process was improved because thousands of configurations can be evaluated in

a matter of hours.

The best method for improving launch vehicle reliability depended on the type of launch vehicle, as postulated in hypothesis three in Section 3.9. For the Saturn V, using engine out on the S-II stage was one of the first choices for increasing reliability while attempting to minimize cost. However, reducing the number of engines and increasing the stage thrust-to-weight ratios proved to be better values for increasing the reliability of the Cargo Launch Vehicle. Subsystem redundancy, whether through identical components or functional redundancy, was not as effective for increasing system reliability while minimizing cost.

As shown in Figure 4-6 and Figure 4-19, the reliability of each launch vehicle increased significantly by using the different reliability strategies, as postulated in hypothesis three. There was a 330 percent increase in the mean flights between failure between the minimum cost Saturn V configuration and the maximum reliability Saturn V configuration. The Cargo Launch Vehicle had a 670 percent increase in the mean flights between failure from the minimum cost configuration to the maximum reliability configuration.

There were significant variations in gross mass between the minimum cost configuration and the maximum reliability configuration, as postulated by hypothesis four. For the Saturn V, as listed in Table H-1, the range of mass was nearly 3,000,000 pounds. The difference in CaLV mass was just over 1,000,000 pounds, as seen in Table H-2.

For both the Saturn V and the Cargo Launch Vehicle, the cost range was also large, as postulated by hypothesis five. The absolute range was on the order of 30 billion dollars [FY '04] for the Saturn V and 25 billion dollars for the CaLV [FY '04]. Additionally, the relative increases were close to 100 percent between the minimum cost configurations and the maximum reliability configurations.

Hypothesis six proposed that uncertainty analysis could be applied within the

mass, cost, and reliability disciplines to provide more information about each launch vehicle. Figure 4-11 and Figure 4-25 revealed the possible ranges of both reliability and cost for the optimal Saturn V and CaLV configurations. Additionally, multiple references were found that could be used to provide future uncertainty ranges.

The results from applying this methodology to the Saturn V revealed that the Saturn V launch vehicle had great potential to increase its reliability without significant increases in additional resources. Figure 4-7 showed the range of optimal configurations that could have been used to increase the Saturn V reliability and the potential system cost. Table 4-5 listed the specifications of each design shown in Figure 4-7 in greater detail.

The mean flights between failure of the Saturn V could have been increased by 78 percent for an additional 1.76 billion dollars [FY '04]. Engine out capability was important for the S-II stage but not as important for the other two stages. Additionally, reducing the operating time by increasing the stage thrust-to-weight ratio provided a large system reliability benefit without a significant increase in system cost.

Figure 4-18 illustrated how the reliability of the Cargo Launch Vehicle could be improved along with resulting system cost. The cost of the CaLV from the Exploration System Architecture Study is also included in Figure 4-18 as a series of designs that depend upon the amount of engine DDT&E cost incurred. Figure 4-20 showed that if the total engine DDT&E cost exceeds 75 percent, then a different configuration should be considered.

While engine out is often mentioned as a solution for increasing launch vehicle reliability, the configurations listed in Table 4-16 showed that a better solution for increasing reliability would be to reduce the number of engines. Reducing the number of engines provides a reliability increase for lower costs compared to using engine out capability. Reducing the operating time by increasing the stage thrust-to-weight ratio

may also be a good solution for increasing system reliability while trying to minimize system cost.

Figure 4-20 showed there is justification for bringing multiple launch vehicle configurations forward to the detail design phase. If the assumptions regarding the use of existing engines change during the detail design phase, other configurations may provide higher launch vehicle reliability for a similar cost.

It is acknowledged that development risk has not been considered. The risk of developing a new engine is much higher compared to the risk of modifying an existing engine. However, modifying an existing engine to work in a new environment has its own challenges [9]. Therefore, while risk has not been considered, the possibility exists that the assumptions regarding the risk of modifying an existing engine may be aggressive and additional configurations should be brought forward to the detail design phase to keep the trade space open.

The Saturn V and CaLV have significant differences in system reliability. One reason for the difference in the baseline reliability estimates may be due to launch vehicle heritage. The Saturn V had little heritage to build upon while the CaLV is a derived vehicle. The CaLV uses modified Shuttle hardware with the accumulated experience of over 100 flights. This experience may provide engineers with greater confidence in their launch vehicle designs. Another reason for the differences in reliability estimate could be the growth of the reliability discipline. Current reliability analysis methods are much more advanced compared to the Apollo era. Therefore, more physics based reliability analysis can be completed instead of relying upon conservative approaches such as large safety margins. The advancement of the reliability disciplines has been accompanied by the large increase in available data as hundreds of different launch vehicles have flown since the Apollo era. With the increase of quantitative data, reliability estimates can be improved based upon actual flight experience. While the Saturn V reliability estimate appears conservative, future CaLV

launches should demonstrate an improvement in the accuracy of reliability analysis.

The flexibility of this methodology was also demonstrated in this dissertation by applying the methodology to two different launch vehicles. The Saturn V was a three stage launch vehicle and required additional design variables to study the trade space. The inclusion of the Solid Rocket Boosters on the CaLV make closing the vehicle design more challenging compared to a launch vehicle with only two stages. Yet, the methodology was applied to both cases and new information was generated in the results section of both applications.

First order development schedule results were also presented. Assumptions were made to create the funding profile over an eight year development. Careful consideration should be given to development schedule because the results vary based upon the underlying assumptions. Figure 4-10 illustrates the mean flights between failure of the Saturn V could have been increased by 78 percent for an increase in 3 percent in peak year funding using a 60 percent distribution assumption. The comparison is between design five in Figure 4-10 and the baseline Saturn V. The CaLV results, illustrated in Figure 4-24, showed that the mean flights between failure could be increased by 70 percent for an additional 250 million dollars [FY '04] (12 percent) in peak funding by switching to design six and assuming a 60 percent distribution assumption. This comparison was made assuming the CaLV incurs the full engine development cost.

By examining the schedule results in the Saturn V and CaLV applications, the complete NASA budget profile over the defined time period should be considered before eliminating any design options. A configuration that demonstrates significant improvement over the baseline design may require a different resource allocation to fit within the year to year budget. The improved configuration might not have been discovered if it was eliminated without evaluating its quantitative system metrics.

The process outlined in this methodology can be used to perform integrated launch vehicle design and study thousands of configurations within a few hours. Cost and

reliability are coupled through the performance of the launch vehicle and the results show the sensitivity of cost to increases in system reliability. While life-cycle cost is not included in this process, the methodology was created with enough flexibility to easily add an operations cost model when one becomes available. Additionally, if safety modeling was completed, this metric could be added to study how safety and cost are coupled.

This methodology satisfied all of its objectives and created a process for linking cost and reliability for launch vehicle design. New information about the cost of reliability has been created for both the Saturn V and Cargo Launch Vehicle. Using the figures created by the application of this methodology, a decision maker will have additional information about a launch vehicle that was not available prior to the completion of this dissertation. More informed decisions should lead to fewer design changes later in the program where design changes have a higher system cost compared to revisions made during the conceptual design phase. The primary goals of the dissertation have been satisfied and the approach created in this dissertation is another tool that can be used to aid the launch vehicle selection process during conceptual design.

5.2 Future Work

There are a few improvements that could be made to this methodology to completely link reliability and life-cycle cost. The first area that needs to be addressed is the operations cost. Operations cost data is very difficult to acquire and that is the reason operations analysis was not addressed. However, by obtaining data on the shuttle, more detailed data on the Saturn V, and data from the ESAS study, a foundation could be established for creating an operations model for integration with this methodology. Subsystem redundancy is added with only a mass and extra development cost penalty but the operations impact would magnify the penalty of using

redundancy. If this methodology was used on a reusable launch vehicle that flies a campaign of four flights a year for twenty years, then the cost of having to check dual and triple redundant systems would add up quickly. In conjunction with developing an operations cost model, another model for upgrading component reliability is needed.

The cost of increasing component reliability is not considered due to a lack of data. However, a trade exists between the use of fully redundant subsystems and whether to increase component reliability. Quantifying the increase of component reliability will rely upon obtaining additional data, but an engineer with access to testing data could develop the required model. The cost and reliability models could be modified to include the capability to study increasing component reliability. This methodology would benefit from using industry data about increasing component reliability to add another design option for increasing system reliability.

Learning curve affects were not included in this methodology. A learning curve could be applied to calculate the cost of each production vehicle based upon the original first unit value. Then the cost metric would become the summation of these production costs and the total development cost.

Another discipline to add is safety. As mentioned earlier, safety requires consideration of how a component/subsystem/stage will fail and how an abort can be performed. Yet, the methodology is flexible enough to include safety once the modeling capability is created. The complexity of the safety model will determine how much, if any, the time required for the design process will increase.

The cost of unreliability was not considered during this methodology. If a launch vehicle fails in today's environment, there is time lost due to an investigation into root causes and to the design alterations once a solution is found. For example, the Space Transportation System did not fly for two years after the Columbia accident but NASA had to pay to keep its space flight capability operational. The cost of

unreliability would further benefit increased reliability systems because the cost could be distributed using the mean flights between failure for each concept. Therefore, configurations with a higher mean flights between failure estimate would have a lower cost per flight.

First order development cost profiles were presented in this dissertation. Future enhancements could improve upon the development schedule results with additional study and detail. However, because the development cost profile is sensitive to the underlying assumptions, schedule should not be used as the sole metric for evaluating launch vehicle configurations.

The Weibull distribution should be considered for future enhancements of this methodology. A Weibull distribution may provide additional detail about the operational phases of a launch vehicle. Additionally, by using a varying failure rate, cost and reliability could be coupled for the conceptual design of the next in-space human element.

The methodology focused exclusively on space hardware. However, software and human reliability also deserve future consideration. An implicit assumption was made that configuration changes will not affect human or software reliability, but a more rigorous analysis may prove differently. Human reliability analysis may be coupled with operations analysis as varying the number of components on a vehicle could change the human reliability contribution as the processing time gets longer. Additionally, more software is required as the number of components increases; therefore, the software reliability may degrade with additional subsystems.

While the design time for evaluating thousands of alternative launch vehicle configurations only requires a few hours, improvements could be made to speed up this process. The cause for a five second evaluation time per design is due to the uncertainty analysis. However, there are techniques that can perform uncertainty analysis faster than Monte Carlo simulation, as described by McCormick [53]. Using one of

these techniques, such as Discrete Probability Optimal Matching Distribution, could decrease the cycle time for evaluating a single launch vehicle design and lead to a faster design process.

APPENDIX A

S-IC SUBSYSTEM RELIABILITY AND RELIABILITY UNCERTAINTY RANGES

Table A-1: S-IC Subsystem Reliability Estimates.

S-IC Subsystem	**Reliability**	**MFBF**
Structures	0.0.9976	416.6
Propulsion System (Engines Only)	0.995	200
Feed System	0.99	100
Guidance, Navigation, and Control	0.99	100
Separation	0.999988	83333.3
Electrical Power & Distribution	0.999997	333333.3
Range Safety	0.999999	1000000
Total	**0.975**	**40**
Instrument Unit	0.972	35.7

Table A-2: Saturn V MCS Reliability Ranges.

Subsystem	**Minimum**	**Maximum**	**Distribution**
F-1 Reliability	0.9995	0.9999	Triangular
S-IC Power	0.956	0.9999	Triangular
S-IC Avionics	0.98	0.9999	Triangular
S-IC Other	0.99	0.9999	Triangular
J-2 Reliability	0.955	0.999	Triangular
S-II Power	0.956	0.999	Triangular
S-II Avionics	0.98	0.999	Triangular
S-II Other	0.99	0.9999	Triangular
S-IVB Power	0.956	0.999	Triangular
S-IVB Avionics	0.98	0.999	Triangular
S-IVB Other	0.97	0.9999	Triangular
Catastrophic Percentage	0.2	0.4	Uniform

Table A-3: CaLV MCS Reliability Ranges.

Subsystem	**Minimum**	**Maximum**	**Distribution**
SSME Reliability	0.995	0.9999	Triangular
Boos. Power	0.9957	0.99999	Triangular
Boos. Avionics	0.99957	0.99999	Triangular
Boos. Other	0.999	0.99999	Triangular
J-2S Reliability	0.995	0.9999	Triangular
EDS Power	0.9957	0.9999	Triangular
EDS Avionics	0.99957	0.9999	Triangular
EDS Other	0.999	0.99999	Triangular
Catastrophic Percentage	0.2	0.4	Uniform

APPENDIX B

RELIABILITY MODEL VALIDATION

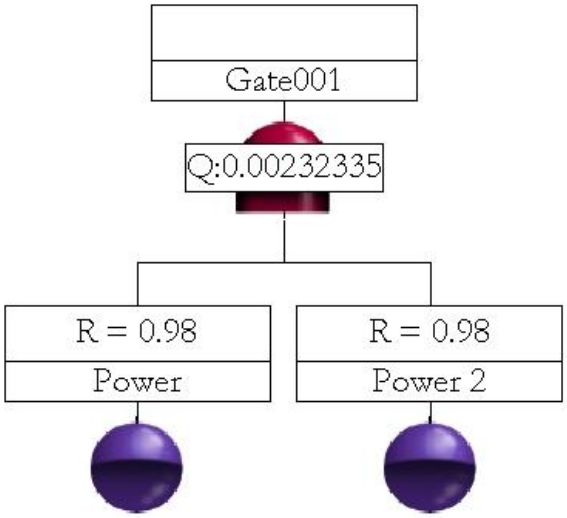

Figure B-1: RELEX Component Redundancy Model.

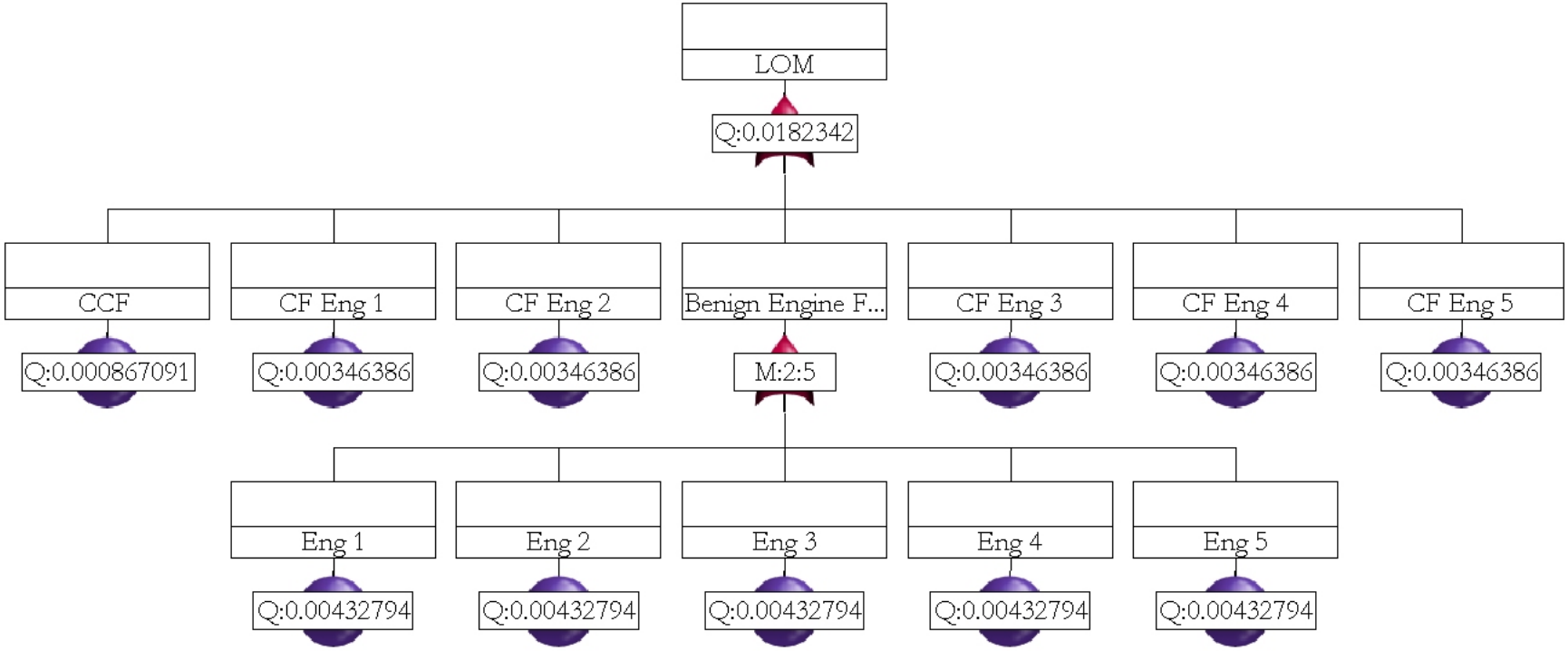

Figure B-2: RELEX Engine Out Failure Model.

APPENDIX C

RELIABILITY TECHNIQUE COMPARISON

Table C-1 lists a comparison of the different reliability analysis methods. Table C-1 also lists a comparison between the baseline S-II propulsion subsystem and using engine out on the S-II. The baseline configuration in Table C-1 and on the S-II was a five engine configuration in series. The J-2 reliability was equal to 0.988. The units are per mission; for example, 94.4% reliability per mission for the S-II baseline and 4.3 missions until Saturn V failure as shown under the MTTF column. The initials "E.O." denote a five engine configuration with engine out capability; thus, only four engines are needed to complete the mission.

The first line lists the single J-2 engine reliability and the MTTF. The baseline S-II stage is the second line without including MCS. This line is calculated using Equation 3-14. Uncertainty analysis is incorporated on the third line in Table C-1 and the last line of Table C-1. As discussed in the previous section, a triangular distribution is assumed for the J-2 engine reliability. Once MCS is included, the baseline Saturn V is severely degraded because the minimum value for J-2 reliability in the uncertainty analysis is 0.96.

Table C-1: Analysis Comparison for 5 Engine Configuration with Engine Out (E.O.).

Line Number	**Reliability Model**	**S-II Propulsion Reliability**	**S-II Propulsion MFBF**	**Saturn V Reliability**	**Saturn V MFBF**
1	Single Engine	0.9880	83.3	N/A	N/A
2	Baseline (no MCS)	0.9414	17.1	0.768	4.30
3	Baseline (MCS)	0.8308	5.91	0.677	3.10
4	FT (E.O.)	0.9993	1363.9	0.815	5.40
5	FT + CCF (E.O.)	0.9985	684.0	0.814	5.38
6	FT + CCF + CF (E.O.)	0.9818	54.85	0.801	5.01
7	FT + CCF + CF w/MCS (E.O.)	0.9745	39.7	0.795	4.87
8	SPN Longer Burn Time (E.O.)	0.9743	38.8	0.794	4.86
9	SPN Increase Failure Rate (E.O.)	0.9668	30.1	0.788	4.72

An engine out scenario is calculated on the fourth line of Table C-1 without including CCF or using the catastrophic engine failure model. Equation 3-17 is used for this calculation. Using engine out raises the Saturn V reliability. However, CCF decreases the propulsion subsystem reliability as listed on the fifth line of Table C-1. This calculation was completed by combining Equation 3-17 with Equation 3-16 [54]. The Saturn V reliability does not change very much from the initial engine out calculation on line four. This occurs because there are many other subsystems in this calculation and some of them are significant drivers of system reliability.

The sixth line incorporates the catastrophic failure model shown in Figure 3-23 and the reliability of the propulsion subsystem decreases. The effect on the Saturn V MTTF is small compared to the fault tree model in line four. Line seven incorporates the effects of uncertainty analysis with the catastrophic engine failure model. Line seven is the model used in this methodology.

The next two lines are the reliability analysis completed with the SPN model shown in Figure 3-25. Line eight is a SPN model that incorporates the effects of modeling the additional burn time in the reliability analysis. There is a decrease in the propulsion subsystem compared to the full catastrophic model, but the effect of the Saturn V is small. The SPN model on line nine increased the J-2 engine failure rate by an order of magnitude after a benign engine failure occurred. The MTTF of the degraded J-2 is 8.3 missions.

APPENDIX D

RELIABILITY GROWTH DATA

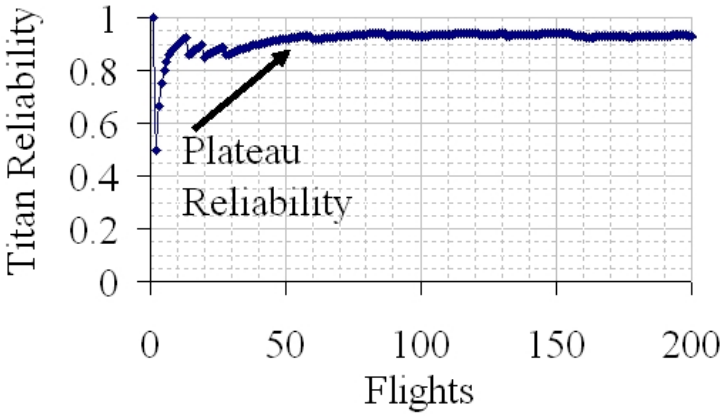

Figure D-1: Titan Launch Vehicle Reliability Growth.

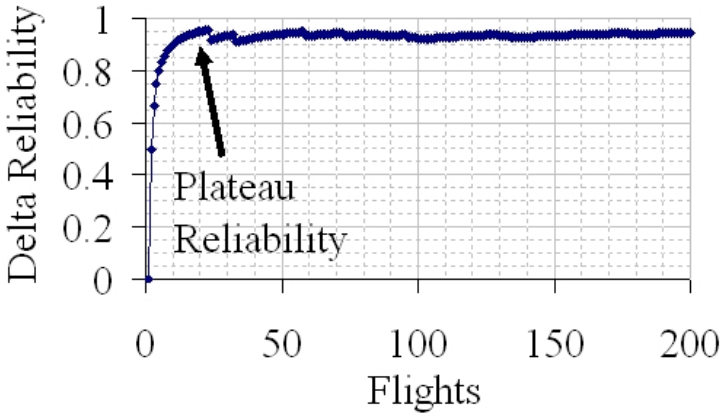

Figure D-2: Delta Launch Vehicle Reliability Growth.

APPENDIX E

VEHICLE WBS

Table E-1: Saturn V WBS.

Subsystem	Reference Mass [lb]	Mass Estimate [lb]	% Diff.
S-IC Stage			
Structures	142162	142450	0.2
Main Prop.	47020	45062	4.16
Engines	92490	93347	0.93
Power	947	973	2.77
Avionics	3457	3417	1.15
Separation	1375	2331	69.51
Total Dry	**287451**	**287579**	**0.04**
Total Gross	**5030911**	**5090577**	**1.19**
S-II Stage			
Structures	62169	62379	0.34
Main Prop.	10217	10282	4.36
Engines	15925	15873	0.32
Power	817	897	2.96
Avionics	4432	4310	2.74
Separation	3761	3750	0.12
Total Dry	**97375**	**97492**	**0.12**
Total Gross	**1081781**	**1089583**	**0.72**
S-IVB Stage			
Structures	13686	13648	0.28
Main Prop.	2986	2886	4.02
Engines	3185	3175	0.32
Power	2157	2181	1.10
Avionics	2522	2601	3.11
Separation	2699	3034	12.42
Total Dry	**27235**	**27504**	**0.99**
Total Gross	**264709**	**262694**	**0.76**
Total SV Gross	**6551541**	**6486333**	**1.01**

Table E-2: CaLV WBS.

Subsystem	**Reference Mass [lb]**	**Mass Estimate [lb]**	**% Diff.**
Booster Stage			
Structures	116599	116771	0.56
Main Prop.	23065	21099	36.5
Engines	34950	34950	0.00
Power	4726	4730	3.33
Avionics	670	715	6.69
Growth	14986	15375	2.59
EDS Stage			
Structures	24026	24040	0.06
Main Prop.	5358	5352	0.11
Engines	7291	7290	0.01
Power	1833	1817	0.88
Avionics	431	430	0.15
Growth	3583	3599	0.45

APPENDIX F

RSE VALIDATION

Table F-1: Saturn V SIC Mass Ratio RSE Data.

Indpt. Var.	**Saturn V T/W**
Minimum	**Maximum**
1.1	1.3
Fit	**Statistics**
R^2	0.991
$R^2 - adj$	0.983

Table F-2: Saturn V SIC Burn Time RSE Data.

Indpt. Var.	**Saturn V T/W**
Minimum	**Maximum**
1.1	1.3
Fit	**Statistics**
R^2	0.999
$R^2 - adj$	0.999

Table F-3: Saturn V SII Mass Ratio RSE Data.

Indpt. Var.	**SII T/W**
Minimum	**Maximum**
0.65	1.25
Fit	**Statistics**
R^2	0.998
$R^2 - adj$	0.997

Table F-4: Saturn V SII Burn Time RSE Data.

Indpt. Var.	**SII T/W**
Minimum	**Maximum**
0.65	1.25
Fit	**Statistics**
R^2	0.999
$R^2 - adj$	0.999

Table F-5: Saturn V SIVB Mass Ratio RSE Data.

Indpt. Var.	**SIVB T/W**
Minimum	**Maximum**
0.4	1.25
Fit	**Statistics**
R^2	0.997
$R^2 - adj$	0.997

Table F-6: Saturn V SIVB Burn Time RSE Data.

Indpt. Var.	**SIVB T/W**
Minimum	**Maximum**
0.4	1.25
Fit	**Statistics**
R^2	0.999
$R^2 - adj$	0.999

Table F-7: Saturn V T/W_{eng} RSE Validation.

Thrust Level [lb]	**REDTOP-2**	**RSE**	**% Difference**
225000	72.136	72.398	0.363
245000	72.670	72.606	0.088
265000	72.716	72.821	0.145
285000	72.916	73.037	0.166
305000	73.124	73.248	0.170
325000	73.313	73.450	0.187
345000	73.735	73.636	0.135
365000	73.894	73.801	0.126
385000	74.039	73.940	0.133
405000	74.174	74.048	0.170

Table F-8: Saturn V Mass Ratio & Burn Time RSE Validation.

SIC T/W	**POST MR**	**RSE MR**	**% Error**	**POST BT[s]**	**RSE BT[s]**	**% Error-**
1.125	3.539	3.539	0.01	170	166	2.41
1.225	3.426	3.434	0.24	155	151	2.79
1.275	3.425	3.437	0.34	148	146	1.27
SII T/W	**POST MR**	**RSE MR**	**% Error**	**POST BT[s]**	**RSE BT[s]**	**% Error-**
0.675	2.975	2.976	0.04	418	418	0.04
0.825	2.863	2.863	0.01	336	335	0.22
0.975	2.819	2.815	0.11	282	281	0.48
SII T/W	**POST MR**	**RSE MR**	**% Error**	**POST BT[s]**	**RSE BT[s]**	**% Error-**
0.625	1.223	1.225	0.17	124	125	0.93
0.875	1.222	1.224	0.15	88	88	0.26
1.075	1.222	1.224	0.15	72	73	1.96

Table F-9: CaLV Booster Mass Ratio RSE Data.

Indpt. Var.	**CaLV T/W**
Minimum	**Maximum**
1.38	1.5
Fit	**Statistics**
R^2	0.999
$R^2 - adj$	0.998

Table F-10: CaLV Booster Burn Time RSE Data.

Indpt. Var.	**CaLV T/W**
Minimum	**Maximum**
1.38	1.5
Fit	**Statistics**
R^2	0.995
$R^2 - adj$	0.993

Table F-11: CaLV EDS Mass Ratio RSE Data.

Indpt. Var.	**EDS T/W**
Minimum	**Maximum**
0.4	1.1
Fit	**Statistics**
R^2	0.994
$R^2 - adj$	0.991

Table F-12: CaLV EDS Burn Time RSE Data.

Indpt. Var.	**EDS T/W**
Minimum	**Maximum**
0.4	1.1
Fit	**Statistics**
R^2	0.997
$R^2 - adj$	0.996

Table F-13: CaLV T/W_{eng} RSE Validation.

Thrust Level [lbs]	**REDTOP-2**	**RSE**	**% Difference**
105000	69.05	69.27	0.312
115000	69.43	69.64	0.294
125000	69.81	69.97	0.231
135000	70.15	70.27	0.180
145000	70.45	70.55	0.140
165000	71.21	71.04	0.246
175000	71.21	71.26	0.064
185000	71.42	71.46	0.055
195000	71.86	71.66	0.272

Table F-14: CaLV Mass Ratio & Burn Time RSE Validation.

CaLV T/W	**POST MR**	**RSE MR**	**% Error**	**POST BT[s]**	**RSE BT[s]**	**% Error-**
1.395	3.642	3.638	0.11	422	425	0.67
1.445	3.472	3.470	0.05	384	385	0.23
1.495	3.414	3.400	0.42	347	347	0.83
EDS T/W	**POST MR**	**RSE MR**	**% Error**	**POST BT[s]**	**RSE BT[s]**	**% Error-**
0.475	1.764	1.779	0.82	416	423	1.64
0.625	1.702	1.702	0.04	304	295	2.97
0.975	1.680	1.668	0.75	190	196	2.90

APPENDIX G

COST TABLES

Table G-1: Saturn V Design Configuration Cost Comparison [$M FY '04].

Subsystem Element	**Min. Cost**	**Design 6 Cost**	**Max Rel. Cost**	**Min. Cost**	**Design 6 Cost**	**Max Rel. Cost**
S-IC Stage	**DDT&E**	**DDT&E**	**DDT&E**	**TFU**	**TFU**	**TFU**
Structures	693	708	883	141	144	189
Main Prop.	516	535	817	89	93	145
Single Engine	1094	1114	1495	17	17	29
Power	87	85	283	10	20	37
Avionics	1289	1296	2761	190	191	410
Separation	19	19	25	5	5	7
Total	**5127**	**5205**	**823**	**683**	**855**	**1447**
S-II Stage	**DDT&E**	**DDT&E**	**DDT&E**	**TFU**	**TFU**	**TFU**
Structures	135	138	153	43	44	50
Main Prop.	280	366	492	40	53	73
Single Engine	922	1171	1489	10	14	21
Power	85	84	236	11	21	31
Avionics	1567	1612	2573	267	274	443
Separation	32	36	46	4	5	7
Total	**4210**	**4747**	**6954**	**688**	**750**	**1114**
S-IVB Stage	**DDT&E**	**DDT&E**	**DDT&E**	**TFU**	**TFU**	**TFU**
Structures	70	72	80	8	8	10
Main Prop.	135	212	478	7	11	27
Engines	0	0	0	9	14	21
Power	143	142	487	2	4	7
Avionics	101	104	229	36	37	84
Separation	28	31	48	3	4	8
Total	**725**	**857**	**2018**	**121**	**143**	**308**
Saturn V	**10064**	**10810**	**17655**	**1633**	**1748**	**2869**

Table G-2: CaLV SRB Assumption.

Element	**Cost**
SRB DDT&E	450
SRB TFU	120

Table G-3: CaLV Design Configuration Cost Comparison [$M FY '04].

Subsystem Element	**Min. Cost**	**Design 9 Cost**	**Max Rel. Cost**	**Min. Cost**	**Design 9 Cost**	**Max Rel. Cost**
Boos. Stage	**DDT&E**	**DDT&E**	**DDT&E**	**TFU**	**TFU**	**TFU**
Structures	477	471	580	103	101	132
Main Prop.	467	469	1116	57	57	141
Single Engine	1767	2301	4030	73	114	294
Power	230	246	667	32	35	105
Avionics	176	170	701	43	86	222
Separation	94	94	149	18	17	32
Total	**5611**	**6566**	**12684**	**689**	**708**	**1641**
EDS Stage	**DDT&E**	**DDT&E**	**DDT&E**	**TFU**	**TFU**	**TFU**
Structures	207	207	223	38	38	41
Main Prop.	329	403	991	70	88	241
Single Engine	585	1017	1237	12	31	45
Power	150	165	370	30	34	80
Avionics	72	76	239	26	57	115
Separation	40	41	56	5	5	8
Total	**1903**	**2630**	**4294**	**304**	**376**	**833**
CaLV	**7965**	**10850**	**17428**	**1112**	**1205**	**2594**

APPENDIX H

MASS TABLES

Table H-1: Saturn V Design Mass Comparison.

Subsystem Element	**Min. Cost Mass [lb.]**	**Design 6 Mass [lb.]**	**Max Rel. Mass [lb.]**
S-IC Stage			
Structures	144228	148811	219148
Main Prop.	44516	47236	98566
Total Engines	92453	98103	204706
Power	972	1875	4187
Avionics	3417	3438	7390
Separation	2346	2446	4000
Total Dry Mass	**287932**	**301908**	**537996**
S-II Stage			
Structures	62424	64706	81110
Main Prop.	9103	14467	24086
Total Engines	14193	22033	38614
Power	885	1758	2885
Avionics	4290	4403	7159
Separation	3636	4295	6154
Total Dry Mass	**94531**	**111663**	**160008**
S-IVB Stage			
Structures	13338	14046	18065
Main Prop.	1812	4032	16783
Total Engines	2027	4406	19307
Power	2142	4257	9490
Avionics	2564	2662	5939
Separation	2714	3646	8629
Total Dry	**24597**	**33051**	**78214**
Saturn V GLOW	**6646164**	**6878139**	**9581353**

Table H-2: CaLV Design Mass Comparison.

Subsystem Element	**Min. Cost Mass [lb.]**	**Design 9 Mass [lb.]**	**Max Rel. Mass [lb.]**
Boos. Stage			
Structures	118108	116728	169951
Main Prop.	25206	26029	119762
Total Engines	41518	42821	185309
Power	4855	8755	18903
Avionics	695	712	3590
Separation	11879	12148	24914
Total Dry Mass	**202260**	**207193**	**522428**
EDS Stage			
Structures	23975	24040	27602
Main Prop.	3070	4188	15958
Total Engines	4682	6307	22728
Power	1767	3264	5062
Avionics	370	417	1570
Separation	2685	2936	4618
Total Dry Mass	**36549**	**41152**	**77538**
CaLV GLOW	**6443663**	**6413668**	**7843252**

APPENDIX I

TRAJECTORY AND ENGINE DATA

Table I-1: Saturn V POST Assumptions.

Parameter	**Value**
Max. Q [psf]	780
Max. Accel [gs]	4.0
TLI δV [ft/s]	10900
Final Velocity [ft/s]	25622
Perigee Altitude [nmi]	90
Apogee Altitude [nmi]	97
Lunar Payload [lb]	100932

Table I-2: CaLV POST Assumptions.

Parameter	**Value**
Max. Q [psf]	620
Max. Accel [gs]	3.85
TLI δV [ft/s]	10334
Final Velocity [ft/s]	25707
Perigee Altitude [nmi]	16.2
Perigee Altitude [nmi]	86.4
Lunar Payload [lb]	160112

Table I-3: Engine Characteristics.

Parameter	**J-2**	**J-2S**	**F1**	**SSME**
Thrust [psf]	230000	274500	1740134	512410
Isp_{vac} [s]	425	452	304	452
T/W_{eng}	72.5	75.3	94.1	67.2
Reliability	0.988	0.998	0.999	0.9987
DDT&E [$M FY '04]	1015	629	1044	923
TFU [$M FY '04]	12	23	16	56

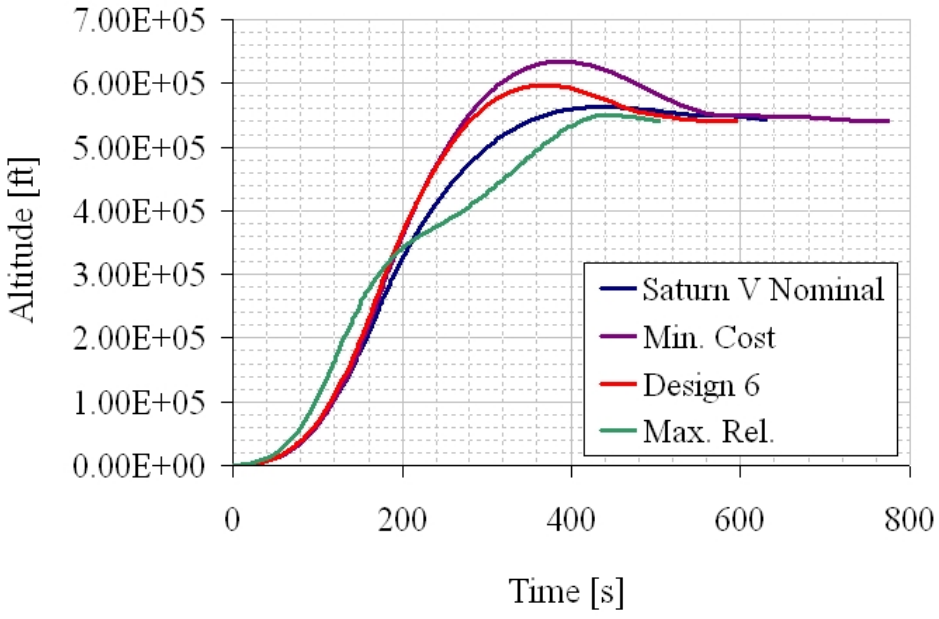

Figure I-1: Trajectory Results for Saturn V Configurations.

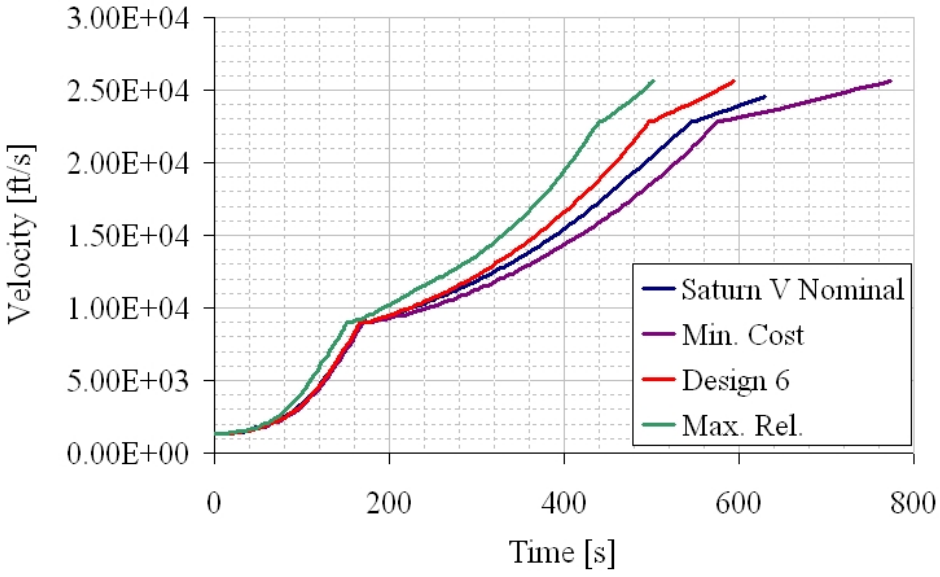

Figure I-2: Velocity Comparison for Saturn V Configurations.

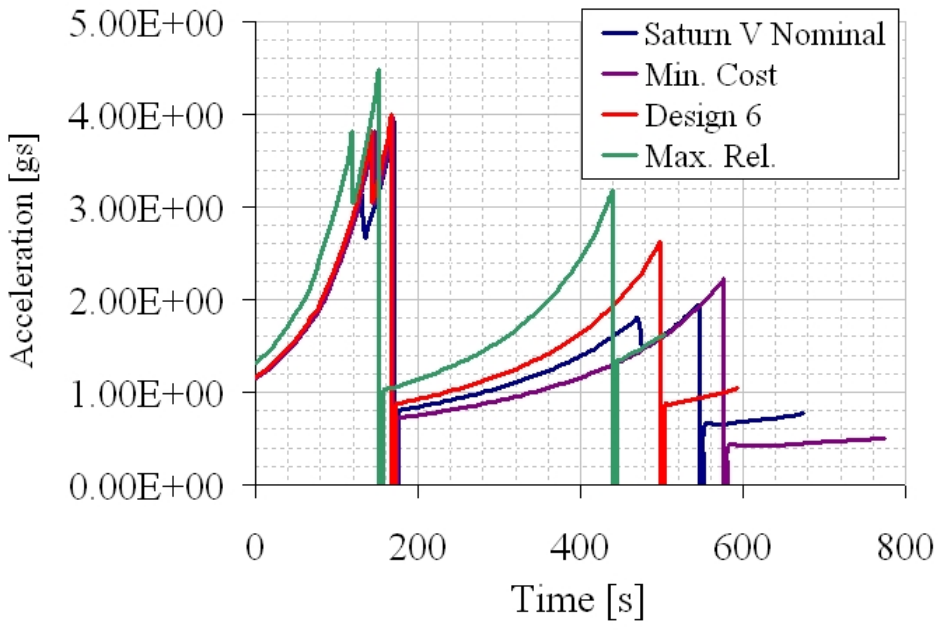

Figure I-3: Acceleration Comparison for Saturn V Configurations.

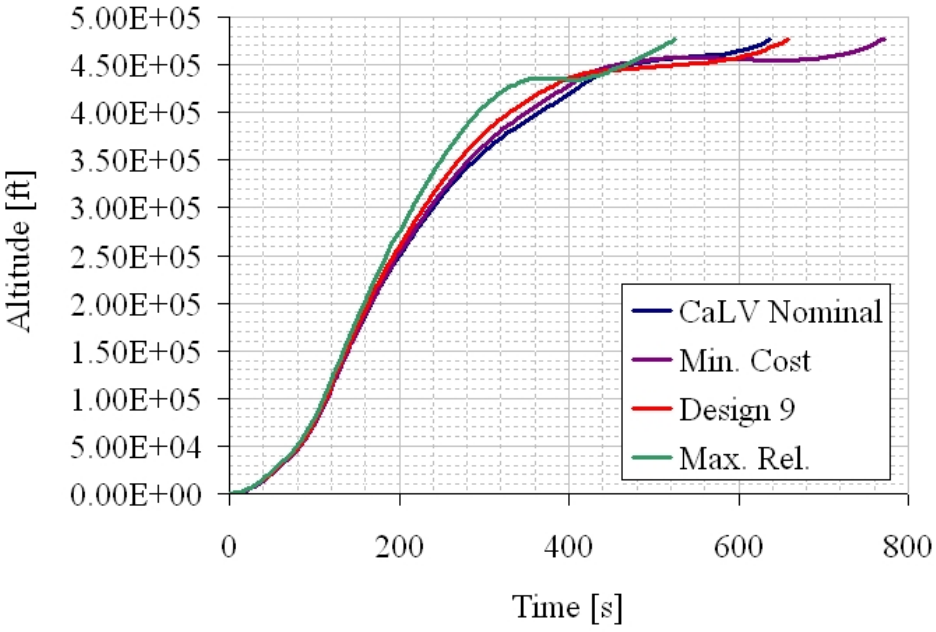

Figure I-4: Trajectory Results for Optimal CaLV Configurations.

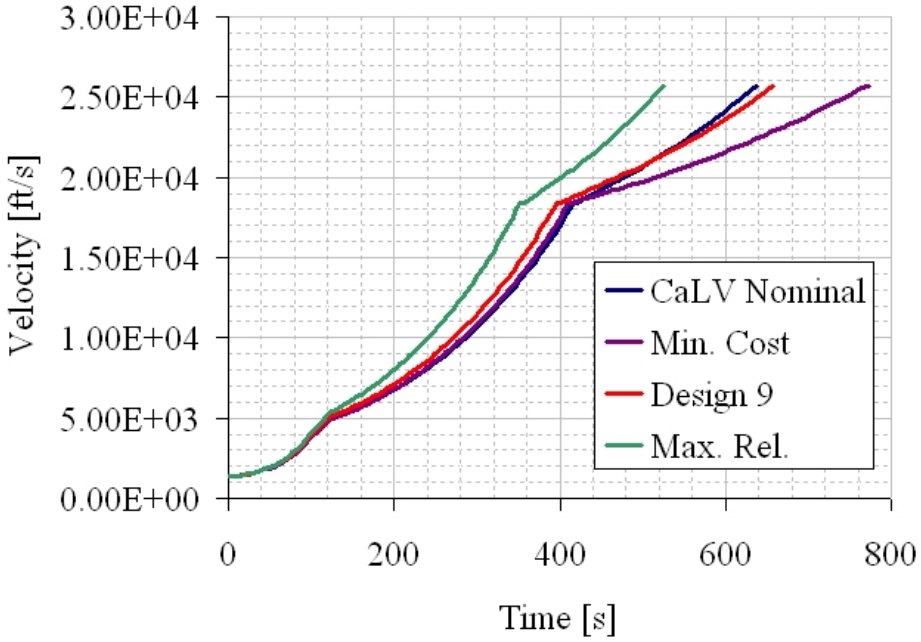

Figure I-5: Velocity Comparison for Optimal CaLV Configurations.

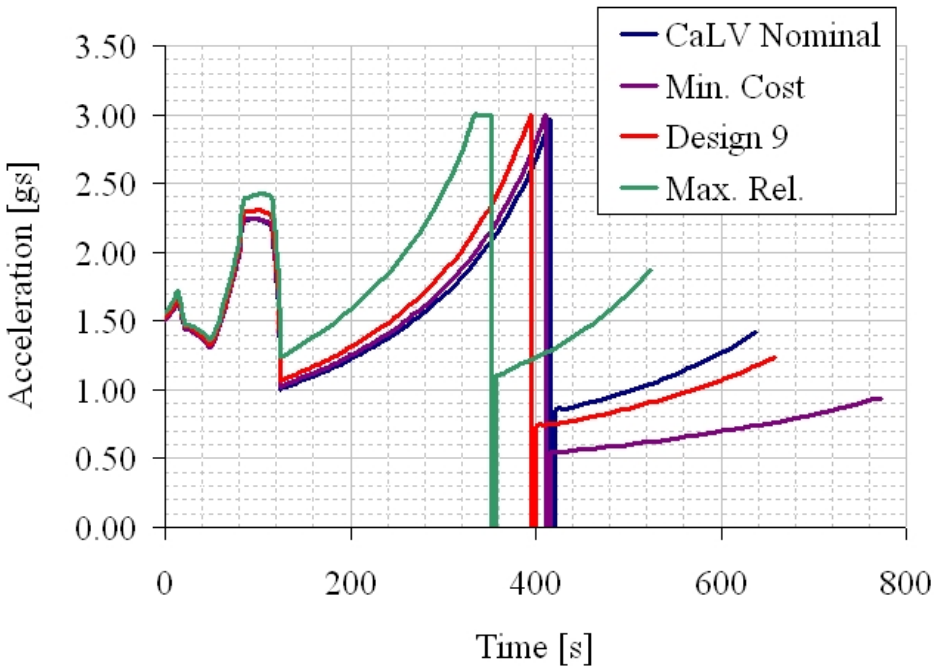

Figure I-6: Acceleration Comparison for Optimal CaLV Configurations.

APPENDIX J

DEVELOPMENT COST PROFILES

Table J-1: Saturn V Development Cost Profile with 40 Percent Assumption [$M FY '04].

Parameter	**Min. Cost**	**Design 2**	**Design 3**	**Design 4**	**Design 5**	**Design 6**	**Design 7**	**Design 8**	**Design 9**	**Design 10**	**Design 11**	**Max. Rel.**	**Saturn V Baseline**
Development Year	**Annual Cost**	**Annual Cost**	**Annual Cost**	**Annual Cost**	**Annual Cost**	**Annual Cost**	**Annual Cost**	**Annual Cost**	**Annual Cost**	**Annual Cost**	**Annual Cost**	**Annual Cost**	**Annual Cost**
1	142	143	146	148	151	152	163	165	167	175	181	250	146
2	825	834	851	863	879	885	950	958	974	1019	1053	1452	847
3	1728	1746	1783	1806	1841	1852	1988	2007	2039	2134	2204	3040	1773
4	2463	2488	2541	2574	2624	2640	2834	2860	2907	3042	3142	4333	2527
5	2772	2801	2860	2898	2953	2972	3190	3219	3272	3425	3537	4878	2844
6	2540	2566	2621	2655	2706	2723	2923	2950	2998	3138	3241	4470	2606
7	1779	1798	1836	1860	1896	1907	2048	2066	2100	2198	2270	3131	1826
8	645	651	665	674	687	691	742	749	761	796	822	1134	661

Table J-2: Saturn V Development Cost Profile with Constant Assumption [$M FY '04].

Parameter	**Min. Cost**	**Design 2**	**Design 3**	**Design 4**	**Design 5**	**Design 6**	**Design 7**	**Design 8**	**Design 9**	**Design 10**	**Design 11**	**Max. Rel.**	**Saturn V Baseline**
Development Year	**Annual Cost**	**Annual Cost**	**Annual Cost**	**Annual Cost**	**Annual Cost**	**Annual Cost**	**Annual Cost**	**Annual Cost**	**Annual Cost**	**Annual Cost**	**Annual Cost**	**Annual Cost**	**Annual Cost**
1	1612	1628	1663	1685	1717	1728	1855	1872	1902	1991	2056	2836	1654
2	1612	1628	1663	1685	1717	1728	1855	1872	1902	1991	2056	2836	1654
3	1612	1628	1663	1685	1717	1728	1855	1872	1902	1991	2056	2836	1654
4	1612	1628	1663	1685	1717	1728	1855	1872	1902	1991	2056	2836	1654
5	1612	1628	1663	1685	1717	1728	1855	1872	1902	1991	2056	2836	1654
6	1612	1628	1663	1685	1717	1728	1855	1872	1902	1991	2056	2836	1654
7	1612	1628	1663	1685	1717	1728	1855	1872	1902	1991	2056	2836	1654
8	1612	1628	1663	1685	1717	1728	1855	1872	1902	1991	2056	2836	1654

Table J-3: Saturn V Development Cost Profile with 60 Percent Assumption [$M FY '04].

Parameter	**Min. Cost**	**Design 2**	**Design 3**	**Design 4**	**Design 5**	**Design 6**	**Design 7**	**Design 8**	**Design 9**	**Design 10**	**Design 11**	**Max. Rel.**	**Saturn V Baseline**
Development Year	**Annual Cost**	**Annual Cost**	**Annual Cost**	**Annual Cost**	**Annual Cost**	**Annual Cost**	**Annual Cost**	**Annual Cost**	**Annual Cost**	**Annual Cost**	**Annual Cost**	**Annual Cost**	**Annual Cost**
1	639	645	659	668	681	685	735	742	754	789	815	1124	655
2	1784	1802	1841	1865	1900	1912	2053	2072	2105	2204	2276	3139	1830
3	2543	2569	2623	2658	2709	2725	2926	2953	3001	3141	3243	4474	2608
4	2771	2800	2859	2897	2952	2971	3189	3218	3271	3423	3535	4876	2843
5	2459	2485	2537	2571	2620	2636	2830	2856	2902	3038	3137	4327	2523
6	1727	1744	1781	1805	1839	1851	1987	2005	2038	2133	2203	3038	1771
7	827	835	853	864	881	886	952	960	976	1021	1055	1455	848
8	145	147	150	152	155	156	167	169	171	179	185	256	149

Table J-4: Saturn V Development Cost Profile with 70 Percent Assumption [$M FY '04].

Profile	**Min. Cost**	**Design 2**	**Design 3**	**Design 4**	**Design 5**	**Design 6**	**Design 7**	**Design 8**	**Design 9**	**Design 10**	**Design 11**	**Max. Rel.**	**Saturn V Baseline**
Development Year	**Annual Cost**	**Annual Cost**	**Annual Cost**	**Annual Cost**	**Annual Cost**	**Annual Cost**	**Annual Cost**	**Annual Cost**	**Annual Cost**	**Annual Cost**	**Annual Cost**	**Annual Cost**	**Annual Cost**
1	1070	1081	1104	1119	1140	1147	1232	1243	1263	1322	1365	1883	1098
2	2437	2462	2514	2547	2596	2612	2805	2830	2876	3010	3109	4288	2500
3	2876	2905	2623	2658	2709	2725	2926	2953	3001	3141	3243	4474	2608
4	2643	2671	2859	2897	2952	2971	3189	3218	3271	3423	3535	4876	2843
5	2024	2045	2537	2571	2620	2636	2830	2856	2902	3038	3137	4327	2523
6	1238	1251	1781	1805	1839	1851	1987	2005	2038	2133	2203	3038	1771
7	529	534	853	864	881	886	952	960	976	1021	1055	1455	848
8	77	78	150	152	155	156	167	169	171	179	185	256	149

Table J-5: CaLV Development Cost Profile with 40 Percent Assumption [$M FY '04].

Parameter	Min. Cost	Design 2	Design 3	Design 4	Design 5	Design 6	Design 7	Design 8	Design 9	Design 10	Design 11	Max. Rel.	CaLV Baseline
Development Year	Annual Cost	Annual Cost	Annual Cost	Annual Cost	Annual Cost	Annual Cost	Annual Cost	Annual Cost	Annual Cost	Annual Cost	Annual Cost	Annual Cost	Annual Cost
1	100	100	101	106	109	115	116	117	119	162	160	220	103
2	581	581	586	618	635	670	678	679	692	942	930	1281	598
3	1216	1216	1227	1295	1331	1403	1419	1422	1449	1972	1947	2683	1252
4	1734	1734	1749	1845	1897	2000	2022	2027	2065	2811	2775	3824	1785
5	1951	1952	1968	2077	2135	2251	2277	2281	2325	3164	3123	4305	2009
6	1788	1788	1804	1903	1956	2063	2086	2090	2130	2899	2862	3944	1841
7	1253	1253	1263	1333	1370	1445	1461	1464	1492	2031	2005	2763	1289
8	454	454	458	483	496	524	529	531	541	736	726	1001	467

Table J-6: CaLV Development Cost Profile with Constant Assumption [$M FY '04].

Parameter	Min. Cost	Design 2	Design 3	Design 4	Design 5	Design 6	Design 7	Design 8	Design 9	Design 10	Design 11	Max. Rel.	CaLV Baseline
Development Year	Annual Cost	Annual Cost	Annual Cost	Annual Cost	Annual Cost	Annual Cost	Annual Cost	Annual Cost	Annual Cost	Annual Cost	Annual Cost	Annual Cost	Annual Cost
1	1135	1135	1144	1208	1241	1309	1324	1326	1352	1840	1816	2503	1168
2	1135	1135	1144	1208	1241	1309	1324	1326	1352	1840	1816	2503	1168
3	1135	1135	1144	1208	1241	1309	1324	1326	1352	1840	1816	2503	1168
4	1135	1135	1144	1208	1241	1309	1324	1326	1352	1840	1816	2503	1168
5	1135	1135	1144	1208	1241	1309	1324	1326	1352	1840	1816	2503	1168
6	1135	1135	1144	1208	1241	1309	1324	1326	1352	1840	1816	2503	1168
7	1135	1135	1144	1208	1241	1309	1324	1326	1352	1840	1816	2503	1168
8	1135	1135	1144	1208	1241	1309	1324	1326	1352	1840	1816	2503	1168

Table J-7: CaLV Development Cost Profile with 60 Percent Assumption [$M FY '04].

Parameter	**Min. Cost**	**Design 2**	**Design 3**	**Design 4**	**Design 5**	**Design 6**	**Design 7**	**Design 8**	**Design 9**	**Design 10**	**Design 11**	**Max. Rel.**	**CaLV Baseline**
Development Year	**Annual Cost**	**Annual Cost**	**Annual Cost**	**Annual Cost**	**Annual Cost**	**Annual Cost**	**Annual Cost**	**Annual Cost**	**Annual Cost**	**Annual Cost**	**Annual Cost**	**Annual Cost**	**Annual Cost**
1	450	450	454	479	492	519	525	526	536	729	720	992	463
2	1256	1256	1267	1337	1374	1449	1465	1468	1496	2036	2010	2770	1293
3	1790	1790	1805	1905	1958	2065	2088	2092	2132	2902	2865	3948	1842
4	1951	1951	1968	2077	2134	2251	2276	2281	2324	3163	3122	4303	2008
5	1731	1731	1746	1843	1894	1997	2019	2024	2062	2807	2771	3818	1782
6	1215	1215	1226	1294	1330	1402	1418	1421	1448	1970	1945	2681	1251
7	582	582	587	620	637	671	679	680	693	944	932	1284	599
8	102	102	103	109	112	118	119	120	122	166	164	226	105

Table J-8: CaLV Development Cost Profile with 70 Percent Assumption [$M FY '04].

Profile	**Min. Cost**	**Design 2**	**Design 3**	**Design 4**	**Design 5**	**Design 6**	**Design 7**	**Design 8**	**Design 9**	**Design 10**	**Design 11**	**Max. Rel.**	**CaLV Baseline**
Development Year	**Annual Cost**	**Annual Cost**	**Annual Cost**	**Annual Cost**	**Annual Cost**	**Annual Cost**	**Annual Cost**	**Annual Cost**	**Annual Cost**	**Annual Cost**	**Annual Cost**	**Annual Cost**	**Annual Cost**
1	753	753	760	802	824	869	879	881	898	1221	1206	1662	776
2	1715	1715	1730	1826	1877	1979	2001	2005	2044	2781	2746	3784	1766
3	2024	2024	2042	2155	2214	2335	2361	2366	2411	3282	3240	4465	2084
4	1861	1861	1877	1981	2036	2147	2171	2175	2217	3017	2978	4104	1915
5	1425	1425	1437	1517	1559	1644	1662	1666	1698	2310	2281	3143	1467
6	871	871	879	928	953	1005	1017	1019	1038	1413	1395	1922	897
7	372	372	375	396	407	429	434	435	443	603	596	821	383
8	54	54	55	58	60	63	64	64	65	88	87	120	56

REFERENCES

[1] Allen, B., "Historical reliability of U.S. launch vehicles," AIAA, Joint Propulsion Conference and Exhibit, 8 July 2001.

[2] "Apollo 13." http://en.wikipedia.org/wiki/Apollo_13, Accessed 2 Mar. 2007.

[3] Blair, J. and et al., "Launch vehicle design process: Characterization, technical integration, and lessons learned," tech. rep., May 2001.

[4] Braun, R. D. and et al., "Use of the collaborative optimization architecture for launch vehicle design," AIAA, NASA, and ISSMO, Symposium on Multidisciplinary Analysis and Optimization, 6th, AIAA, Inc., Sep. 1996.

[5] Braun, W., *Apollo: Expeditions to the Moon*, ch. Saturn the Giant. NASA, 1975.

[6] Bush, G., "President bush announces new vision for space exploration program." http://www.whitehouse.gov/news/releases/2004/01/20040114-3.html, Accessed on July 26th, 2006.

[7] Coit, D. and Smith, A., "Reliability optimization of series-parallel systems using a genetic algorithm," *IEEE Transactions on Reliability*, no. 0018-9529, 1996.

[8] "Cost estimating website." http://www1.jsc.nasa.gov/bu2/index.htm, Accessed 14 July 2006.

[9] Cowing, K., "Nasa encounters possible problems with crew launch vehicle design." http://www.spaceref.com/news/viewnews.html?id=1087, 17 Jan. 2006.

[10] "Degrees of freedom(statistics)." http://en.wikipedia.org/wiki/Degrees_of_freedom_%28statistics%29, Accessed 2 Feb. 2007.

[11] Department of Defense, *Military Handbook: Reliability Growth Management*, mil-hdbk-189 ed., Feb. 1981.

[12] Department of Defense, *Military Standard: Procedures for Performing a Failure Mode, Effects and Criticality Analysis*, mil-std-1629a ed., Nov. 1980.

[13] Dieter, G., *Engineering Design: A Materials and Processing Approach*. Boston, MA: McGraw-Hill Higher Education, 2000.

[14] "Systems engineering fundamentals." Department of Defense, Jan. 2001.

[15] "Defense acquisition guidebook." Department of Defense, Dec. 2004.

[16] Dodson, B. and Nolan, D., *Reliability Engineering Handbook*. New York: Marcel Dekker, Inc., 1999.

[17] Duane, J., "Learning curve approach to reliability monitoring," *IEEE Transactions on Aerospace*, vol. 2, pp. 563–566, 1964.

[18] Everhart, K. and et al., "Systems engineering "toolbox" for design-oriented engineers," Tech. Rep. Reference Publication 1358, NASA, Dec. 1994.

[19] "Falcon overview." http://www.spacex.com/, Accessed 14 July 2006.

[20] Fortescue, P. and et al., eds., *Spacecraft Systems Engineering*. West Sussex, England: John Wiley & Sons, Inc., 2003.

[21] Fragola, J., "Atlas launch vehicle reliability data.".

[22] Fragola, J., "Risk management in US manned spacecraft: From Apollo to Alpha and beyond," ESA, Product Assurance Symposium and Software Product Assurance Workshop, Mar. 1996.

[23] Fragola, J. and et al., "Probabilistic risk assessment of the Space Shuttle," Tech. Rep. N95-26398, Science Applications International Corporation, New York, NY 28 Feb. 1995.

[24] Fragola, J. and Collins, E., "Risk forecasting using heritage-based surrogate data," Annual Reliability and Maintainability Symposium, IEEE, 26-29, Jan. 2004.

[25] Fragola, J. and et al., "A risk evaluation approach for safety in aerospace preliminary design," Annual Reliability and Maintainability Symposium, IEEE, 27-30, Jan. 2003.

[26] Fragola, J. and et al., "Reliability and crew safety assessment for solid rocket booster/j-2s based launch vehicle," Tech. Rep. SAICNY05-04-1F, SAIC, Apr. 2005.

[27] Fragola, J. and Putney, B.F., J., "Development of the risk oriented program optimization tool (ROPOT) for orbital space plane design concepts," Annual Reliability and Maintainability Symposium, IEEE, 26-29, Jan. 2004.

[28] Futron, *Design Reliability Comparison for SpaceX Falcon Vehicles*, Nov. 2004.

[29] Galloway, T. and et al., "GASP-general aviation synthesis program," Tech. Rep. NASA-CR-152303, NASA, Jan. 1978.

[30] Ganguli, R., "Survey of recent developments in rotorcraft design optimization," *Journal of Aircraft*, no. 0021-8669, 2004.

[31] Griffin, M. and French, J., *Space Vehicle Design*. Blacksburg, VA: AIAA, 2nd ed., 2004.

[32] Hale, F., *Introduction to Space Flight*. New Jersey: Prentice Hall, Inc., 1994.

[33] Hamaker, J., *But What Will It Cost? The History of NASA Cost Estimating*. NASA, 1994.

[34] Hammond, W., *Space Transportation: A Systems Approach to Analysis and Design*. Reston, VA: AIAA, Inc., 1999.

[35] Hayter, A., *Probability and Statistics*. Pacific Grove, CA: Duxbury, 2002.

[36] Hershkowitz and et al., "Apollo technical manual," Tech. Rep. Z65-11545, NASA, 15 Oct. 1963.

[37] Huang, Z. and et. al, "Key reliability drivers of liquid propulsion engines and a reliability model for sensitivity analysis," The Boeing Company, Rocketdyne Propulsion & Power, 41st AIAA Joint Propulsion Conference & Exhibit, 10 Jul. 2005.

[38] Humble, R. and et al., eds., *Space Propulsion Analysis and Design*. Reston, VA: McGraw-Hill Companies, Inc., 1995.

[39] International Atomic Energy Agency, Vienna, *Procedures for Conducting Probabilistic Safety Assessment of Nuclear Power Plants (Level 1)*, 2002.

[40] "Technology for affordability: A report on the activities of working groups - integrated product/process development (ippd), simplified contracting, and dual-use manufacturing." The National Center for Advanced Technologies (NCAT), Jan. 1994.

[41] Isakowitz, S. and et al., *International Reference Guide to Space Launch Systems*. Reston, VA: AIAA., 2004.

[42] Johnson, V. and et al., "A hierarchical model for estimating the early reliability of complex systems," *IEEE Transactions on Reliability*, no. 0018-9529, 2005.

[43] Kennedy, J., "Special message to the congress on urgent national needs." http://www.jfklibrary.org/Historical+Resources/Archives/Reference+Desk/Speeches/JFK/Urgent+National+Needs+Page+4.htm, Accessed on July 26th, 2006.

[44] Kroo, I. A. and et al., "Multidisciplinary optimization methods for aircraft preliminary design," AIAA/USAF/ISSMO Symposium on Multidisciplinary Analysis and Optimization, 5th, AIAA, Inc., Sep. 1994.

[45] Kumamoto, H. and Henley, E., *Probabilistic Risk Assessment and Management for Engineers and Scientists*. New York: The Institute of Electrical and Electronics Engineers, Inc., 1993.

[46] Lee, S. S., "Reliability drivers for advanced space vehicles," Master's thesis, Georgia Institute of Technology, 2001.

[47] Leemis, L., *Reliability: Probabilistic Models and Statistical Methods*. Englewood Cliffs, NJ: Prentice-Hall, Inc., 1995.

[48] Lewis, E., *Introduction to Reliability Engineering*. New York, NY: John Wiley & Sons, Inc., 1994.

[49] Lipson, C. and Sheth, N., *Statistical Design and Analysis of Engineering Experiments*. San Francisco, CA: McGraw-Hill Book Company, 1973.

[50] Liu, T. and Chiou, S., "The application of petri nets to failure analysis," *Reliability Engineering and System Safety*, pp. 129–142, Aug. 1997.

[51] Mavris, D., "Advanced design methods 1." SST III, Georgia Institute of Technology, Fall Semester, 2001.

[52] McCormick, D., *Distributed Uncertainty Analysis Techniques for Conceptual Launch Vehicle Design*. PhD thesis, Georgia Institute of Technology, 2001.

[53] McMasters, J. and Cummings, R., "Airplane design-past, present, and future," *Journal of Aircraft*, no. 0021-8669, 2002.

[54] Modarres, M., *What Every Engineer Should Know About Reliability and Risk Analysis*. New York: Marcel Dekker, Inc., 1993.

[55] Monell, D. and et al., "Multidisciplinary analysis for future launch systems using NASA's advanced engineering environment (AEE)," 16th AIAA Computational Fluid Dynamics Conference, AIAA, Inc., 23-26, Jun. 2003.

[56] Moore, A. and et al., "Determination of optimal launch vehicle technology investment strategies during conceptual design," AIAA, NASA, and ISSMO, Symposium on Multidisciplinary Analysis and Optimization, 6th, AIAA, Inc., Sep. 1996.

[57] Murray, C. and Box, C., *Apollo: The Race to the Moon*. New York, NY: Simon & Schuster Inc., 2000.

[58] NASA, Washington D.C., *Manned Lunar Landing Program Mode Comparison*, 30 Jul. 1962.

[59] NASA, Washington, D.C., *Apollo Saturn 504 Mission Reliability Analysis Appendix C*, 1965.

[60] NASA, Washington D.C., *Report of the Space Task Group, 1969*, 1969.

[61] NASA, Marshall Space Flight Center, *Saturn V Flight Manual*, 25 June 1971.

[62] NASA, Washington, D.C., *Systems Engineering Handbook*, Jun. 1995.

[63] NASA, Hampton, VA, *General Aviation Aircraft Reliability Study*, Feb. 2001.

[64] NASA, Washington, D.C., *2004 NASA Cost Estimating Handbook*, 2004.

[65] NASA, Washington D.C., *Cost Estimating Handbook*, 2004.

[66] NASA, Washington, D.C., *Exploration Systems Architecture Study*, Nov. 2005.

[67] Olds, J., *Multidisciplinary Design Techniques Applied to Conceptual Aerospace Vehicle Design*. PhD thesis, North Carolina State University, 1993.

[68] Olds, J., "Advanced design methods 2." SST III, Georgia Institute of Technology, Spring Semester, 2002.

[69] Painton, L. and Campbell, J., "Genetic algorithms in optimization of system reliability," *IEEE Transactions on Reliability*, no. 0018-9529, 1995.

[70] Pate-Cornell, E. and Dillon, R., "Probabilistic risk analysis for the nasa space shuttle: a brief history and current work," *Reliability Engineering and System Safety*, pp. 345–352, Dec. 2001.

[71] Powell, R. and et. al, *Program to Optimize Simulated Trajectories (POST) Utilization Manual, Volume II, Version 5.2*. NASA Langley Research Center, Hampton, VA, Oct. 1997.

[72] Putney, B. Leading NASA Reliability Expert, E-mail to the author, 14 June 2006.

[73] Putney, B., "Personal interview," Mar. 2006.

[74] REDTOP-2, "Spaceworks engineering, inc.." http://www.sei.aero/.

[75] RELEX, "Relex software corporation." http://www.relex.com/.

[76] Rhodes, R. and et al., *Proposed Operability Design Requirements (TPMS)*. NASA, KSC, 2006.

[77] Rockwell International, *Advanced Transportation System Studies Alternate Propulsion Subsystem Concepts*, 1993.

[78] Rohrschneider, R., "Development of a mass estimating relationship database for launch vehicle conceptual design," Master's thesis, Georgia Institute of Technology, 2002.

[79] Rowell, L. and et al., "Multidisciplinary conceptual design optimization of space transportation systems," *Journal of Aircraft*, vol. 36, no. 1, 1999.

[80] Rowell, L. and Korte, J., "Launch vehicle design and optimization methods and priority for the advanced engineering environment," tech. rep., Oct. 2003.

[81] Saleh, J., "Senior space systems design II." Lecture, Georgia Institute of Technology, Spring Semester 2007.

[82] Saleh, J. and Marais, K., "Reliability: how much is it worth? beyond its estimation or prediction, the (net) present value of reliability," *Reliability Engineering and System Safety*, vol. 91, pp. 665–673, May 2005.

[83] Sandlin, D. and Davis, P., "A study of transonic aerodynamic analysis methods for use with a hypersonic aircraft synthesis code," Tech. Rep. N92-24803, NASA, May 1992.

[84] "Saturn v." http://en.wikipedia.org/wiki/Saturn_V, Accessed 10 Feb. 2007.

[85] "List of apollo missions." http://en.wikipedia.org/wiki/List_of_Apollo_missions, Accessed 20 Feb. 2007.

[86] Schrage, D., "Technology for rotorcraft affordability through integrated product/process development (ippd)," American Helicopter Society, 55th Annual Forum, May 1999.

[87] Schrage, D. and Volovoi, V., "Aerospace safety processes." ESM 215, Georgia Institute of Technology, Summer Semester, 2006.

[88] "STS-9." http://en.wikipedia.org/wiki/STS-9, Accessed 2 Mar. 2007.

[89] Smiljanic, R., "Systems engineering and integration." Lecture, National Institute of Aerospace, Hampton VA, May 2006.

[90] Stanley, D. and et al., "Conceptual design of a fully reusable manned launch system," *Journal of Spacecraft and Rockets*, vol. 29, no. 4, 1992.

[91] Unal, R. and et al., "Approximation model building and multidisciplinary design optimization using response surface methods," AIAA, NASA, and ISSMO, Symposium on Multidisciplinary Analysis and Optimization, 6th, AIAA, Inc., Sep. 1996.

[92] Vanderplaats, G., *Numerical Optimization Techniques for Engineering Design*. Colorado Springs, CO: Vanderplaats Research & Development., 2001.

[93] Volovoi, V., "Stochastic petri nets modeling using spn@." 2005.

[94] Wertz, J. and Larson, W., *Space Mission Analysis and Design*. Torrance, CA: Microcosm Press, 1999.

[95] Wilhite, A. E-mail to the author, 28 Sep. 2005.

[96] Williamson, R., "Developing the space shuttle." NASA SP-4407, May 2001.

[97] Young, D., *An Innovative Methodology for Allocating Reliability and Cost in a Lunar Exploration Architecture*. PhD thesis, Georgia Institute of Technology, May 2007.

[98] Young, D. and et. al, "Crew launch vehicle (CLV) independent performance evaluation," Georgia Institute of Technology, Space Systems Engineering Conference, Nov. 2005.

[99] Young, J. and et. al, "Architecture options for propellant re-supply of lunar exploration elements," Georgia Institute of Technology, AIAA Space 2006 Conference, Sep. 2006.

[100] Zapata, E. and Torres, A., "Space transportation operations cost modeling and the architectural assessment tool-enhanced," IAF, 50th International Astronautical Congress, Oct. 1999.

VITA

Zachary Clemetson Krevor was born on December 16, 1979 in New Haven, Connecticut. He attended grade school at Arundel Elementary and Central Middle School in San Carlos, California. Zachary graduated from Carlmont High School in June of 1997. In the fall of 1997, Zachary enrolled at the University of California-Los Angeles. Zachary graduated with a Bachelor of Science in December of 2001 and enrolled at the Georgia Institute of Technology in fall of 2002.

Zachary began his Georgia Tech career under the direction of Dr. Dimitri Mavris in the Aerospace Systems Design Laboratory. In the spring of his first year, Zachary was invited by Dr. John Olds to join the Space Systems Design Laboratory. One of Zachary's professors at UCLA, Dr. Todd Mosher, was a colleague of Dr. John Olds and Dr. Mosher provided a letter of reference for Zachary's admission to Georgia Tech. Zachary completed his Master's of Science under Dr. John Olds in December of 2004. The master's project was titled "A Case Study of the STS Indirect and Support Costs". Zachary completed his dissertation under the tutelage of Dr. Alan Wilhite. Zachary also completed internships at General Electric Aircraft Engines, NASA-Kennedy Space Center, and Blue Origin while at Georgia Tech. Zachary is a member of the American Institute of Aeronautics and Astronautics.